Characterisation of plasmid DNA complexes for application in genetic immunisation

A thesis submitted for the degree of Doctor of Philosophy

By

Arjun Dhanoya, MSc

Department of Biochemical Engineering

University College London

June, 2012

Acknowledgements

I would like to thank my primary supervisor Eli for her guidance, support and great enthusiasm throughout my project. In particular your open door policy and calm attitude when at times I have been stressed have been invaluable. Your guidance and advice on all things has helped me developed from a student to an enthusiastic mature researcher.

I would also like to thank my secondary supervisor Benny, who has been nothing short of fabulous for welcoming me into his department and allowing me to acquire various technical skills. Your guidance, opinion and technical advice has been indispensible for the project.

A special mention to Darren, Sally and Steven, who have been great in terms of providing me technical and personal advice. Darren, you have been like a big lab brother of mine who always has time for a chat on technical and random funny issues. Sally, you have been fantastic and always had time to offer help when needed. Steven, towards the end of my PhD you gave great technical advice and was fantastic company in the lab – the gossip was great!

I would also like to thank my family, in particular my mum whom I love so much and has always been supportive and been the bedrock of my life. My brothers Gaurav and Akash, and Raj, whose advice on life as a whole is a joy to hear.

Last but by no means least, a very special thanks to my fiancé Sheila. You have supported me throughout this project, bearing me whilst I have been stressed and impatient, and being with me every step of the way. I would not have made it through without you. I love you.

Abstract

Non-viral gene delivery into mammalian cells is widely used in bio-processing for the production of recombinant proteins as well as considered for clinical trials in gene therapy and vaccination. DNA can be delivered through various non-viral methods including polymers, lipids, peptides and entrapment within nanoparticles. Non-viral gene delivery often entails nucleic acids that are bound to a polymer or polycation to form a complex referred to as polyplexes. Various factors may affect the efficiency of polyplex uptake in mammalian cells. One factor is DNA topology, which is important from a regulatory perspective whereby FDA guidelines require the majority of plasmid DNA (pDNA) (>80%) to be in its supercoiled (SC) form. Therefore the motivation of this study was to investigate the impact of DNA topology on non-viral gene delivery.

In this study pDNA (6.8kb) was complexed with poly-$_L$-lysine (PLL) (MW, 9600) to form PLL/DNA polyplexes. pDNA of three topologies; SC, open circular (OC) and linear-pDNA were complexed with PLL. Biophysical analyses which included size, surface charge, DNA binding and nuclease resistance assays revealed topology dependent results. For example SC-pDNA polyplexes were smaller (<140nm); more efficiently packaged and displayed greater nuclease resistance than OC- and linear-pDNA polyplexes. DNA release from PLL was analysed although such experiments were not a time course study, rather a confirmatory assay to identify PLL-bound DNA.

Polyplex uptake in Chinese hamster ovary (CHO), HeLa and dendritic cells (DCs) were studied. Uptake was monitored by fluorescent confocal microscopy, flow cytometry and reporter gene expression assays. Regardless of cell type, complexes containing SC-pDNA displayed greater reporter gene expression than OC- and linear-pDNA polyplexes. In regards to CHO cells confocal image analysis revealed SC-pDNA polyplexes associated most

efficiently with host cell nuclei. SC-pDNA polyplexes were smaller and nuclease resistant than its counterparts which may facilitate uptake. Endocytic mechanisms of uptake were analysed in CHO cells. This is important as knowledge of polyplex uptake pathways could be exploited for future gene delivery studies.

Polyplex nuclear import was studied in regards to importin-7 (Imp7). Imp7 is key nuclear import receptor identified in previous studies, which was a preselected candidate. Gene expression studies along with qualitative and quantitative confocal microscopy analyses indicated possible exploitation of Imp7. However live cell imaging experiments showed co-localisation between DNA and nuclei fluorescence in Imp7 KD cells which suggests other routes of nuclear import may be employed.

Polyplex uptake in DCs was also studied as these are key sentinels of the immune system. SC-pDNA polyplexes displayed the most efficient uptake and gene expression profiles in DCs. Gene expression and ability to induce DC phenotypic changes was dependent on dosage and DNA topology. Therefore this study stresses the importance of DNA topology which impacts on the bio-processing of non-viral gene delivery products.

Table of Contents

List of Figures

List of Tables

Abbreviations

AIM2	Absent in melanoma 2
APCs	Antigen presenting cells
Amp	Ampicillin
APC	Allophycocyanin
BAC	Bacterial artificial chromosome
Back Imp7	back complemented KD cells with restored importin-7 function
CCVs	Clathrin coated vesicles
CD1a	Cluster of differentiation 1a
CD4	Cluster of differentiation 4
CHO cells	Chinese hamster ovary cells
Cl2	Clone 2
Cl4	Clone 4
CME	Clathrin mediated endocytosis
CMZ	Chlorpromazine hydrochloride
CTB	Cholera toxin subunit B
DAI	DNA-dependent activator of interferon-regulatory factors
DAPI	4',6-diamidino-2-phenylindole
DCs	Dendritic cells
DC-SIGN	Dendritic cell-specific intercellular adhesion molecule-3-grabbing non-integrin
DLS	Dynamic light scattering
DMEM	Delbecco's modified Eagle's medium
DMRIE	N-(2-Hydroxyethyl)-N,N-dimethyl-2,3-bis(tetradecyloxy)-1-propanaminium bromide
DOPE	Dioleoyl phosphotidylethanolamine
DOTAP	1,2-dioleoyl-3-(trimethylammonium) propane
DxR	*Discosoma corallimorpharian* DsRed

E.coli	*Escherichia coli*
EP	Electroporation
EtBr	Ethidium bromide
FCS	Foetal calf serum
FDA	U.S Food and Drug Administration
FITC	Fluorescein isothiocyanate
FRET	Fluorescence resonance energy transfer
gDNA	Genomic DNA
GAPDH	Glyceraldehyde 3-phosphate dehydrogenase
GG	Gene gun
GM-CSF	Granulocyte-macrophage colony-stimulating factor
HBBS	Hank's Buffered Salt Solution
HCS	High content screening
HIB	Hydrophobic interaction chromatography
HIV-I	Human immunodeficiency virus -I
HMGB	High mobility group box
IEC	Ion exchange chromatography
IFIT2	Interferon induced protein with tetratricopeptide repeats-2
IFNs	Interferons
IM	Intramuscular
Impα	Importin-α
Impβ	Importin-β
Imp7	Importin-7
IV	Intravenous
KD	Knockdown
LB	Luria Bertani
MCLs	Magnetic cationic liposomes

MEND	Multifunctional envelope-type nano device
MHC-I	Major histocompatibility complex class-I
MHC-II	Major histocompatibility complex class-II
NIR	Nuclear import receptor
NLS	Nuclear localisation signal
NPC	Nuclear pore complex
OC	Open circular
PAA	Poly(amidoamine)
PAMA	PEG-*block*poly(silamine) (PSAO)-*block*-poly{2-(N, N-dimethylamino)ethyl methacrylate]
PBS	Phosphate buffered saline
pDNA	Plasmid DNA
PE	Phycoerythrin
PEG	Polyethylene glycol
PEI	Polyethylenimine
PLL	Poly-$_{L}$-lysine
PMED	Particle mediated epidermal delivery
PRRs	Pathogen recognition receptors
PS	Penicillin:streptomycin
Q-PCR	Quantitative polymerase chain reaction
QDs	Quantum dots
RPMI	Roswell Park Memorial Institute media
RT	Reverse transfection
SC	Supercoiled
SDS	Sodium dodecyl sulphate
SEC	Size exclusion chromatography
SSC	Saline sodium citrate
STINGs	Stimulator of interferon genes

TBE	Tris-Borate EDTA
TLRs	Toll-like receptors
TOTO-3	TOTO®-3 iodide (642⁄660) dimeric cyanine stain
Tran	Transferrin
TT	Tetanus toxin
US	Ultrasound
Zeo	Zeomycin

Chapter 1. Introduction

1: Introduction

Genetic immunisation refers to the introduction of an engineered gene which encodes an antigen to immunise the host towards the respective encoded antigen (Tang *et al*, 1992). This is different to gene therapy which is defined as the employment of genetic material to treat a disease (Brown, 2004). Therefore genetic immunisation differs by aiming to trigger a specific immune response. Advantages include the bypassing of various purification steps and being economically viable. Consequently genetic immunisation methods are being explored in relation to the treatment of infectious diseases and cancer (Jones, 2008).

One specific strategy for genetic immunisation is the targeted delivery of genes to antigen presenting cells (APCs). This is done with the aim of inducing specific innate and adaptive immune responses that would otherwise be bypassed by conventional treatments. However delivery of genes to such specialised cells is dependent on many factors including; the nature of the gene vector, size of the delivery vehicle, the potential safety hazards posed by introducing a foreign vector within host cells and DNA cargo amongst others.

1.1 The importance of plasmid DNA technology

The introduction of plasmid DNA (pDNA) encoding antigenic sequences within host cells is an exciting venture which has generated great interest (Cooke *et al*, 2004; Dhama *et al*, 2008). Plasmids are circular forms of DNA which are frequently located within bacteria and replicate in an autonomous manner (Brown, 2001). There are many benefits offered by pDNA genetic immunisation. Plasmid DNA encoding the protein antigen of interest bypasses isolation and purification of pure proteins conventionally used as antigens. Expression of the encoded antigen can trigger an immune response to the protein antigen. This avoids the use of viral vectors and solvents that can potentially lead to insertional mutagenesis (Cooke *et al*,

2004). Additionally unlike conventional treatments pDNA is relatively simple to produce, manufacture can be scaled up, economically viable, stable and can be transported with no major issues unlike current vaccines which have hindered their impact upon global diseases (Dhama *et al*, 2008). In fact a cocktail of pDNA genes encoding various antigens can be administered to bolster immunity towards a range of diseases (Dhama *et al*, 2008). Such desirable characteristics has seen pDNA vaccines elevated to clinical trials (phase II) for diseases such as AIDS, rabies, and tuberculosis amongst others (Dhama *et al*, 2008; Cooke *et al*, 2004).

1.1.1 Characteristics of plasmids

Plasmids are sufficiently designed so as to allow optimal expression of the encoded antigen of interest which brings about the desired attributes mentioned previously. Plasmids employed for gene delivery consist of a eukaryotic promoter required to drive transcription and expression of the encoded gene (Babiuk *et al*, 2006; Brandsma, 2006). A poly-A tail in conjunction with an enhancer are present in order to allow sufficient translational expression (Brandsma, 2006; Liu, 2003). Importantly pDNA are designed to consist of antibiotic resistant genes (pre-requisite for such procedures) in order to allow distinction from non-transformed bacterial cells. To allow uptake to be monitored pDNA usually encode reporter genes whose expression within the target cell indicates successful uptake (Brandsma, 2006; Dhama *et al*, 2008). Reporter genes often include green fluorescent protein (GFP) or *lacZ*, a gene that encodes for β-galactosidase that can be detected via enzymatic assays. A bacterial replication site (Ori site) allows the propagation of plasmids, enabling such structures to replicate autonomously thereby increasing the intracellular concentration of the expressed gene. Plasmids also consist of sequences that are recognised by endonucleases which cleave the nucleic acid which allow insertion of a desired sequence for a target protein for instance.

1.1.2 Plasmid DNA topology

Plasmid DNA (pDNA) can exist in a variety of topological conformations which have important implications upon its application in biotechnology and biochemical engineering.

1.1.2.1 SC-pDNA

Plasmids usually confer to a natural supercoiled (SC) form in which the nucleic acid strands are coiled and twisted to form a dense intact structure (Figure 1.1). SC-plasmid DNA (SC-pDNA) can also display less compact forms whereby the unpaired nucleotide regions exist. Such forms may arise as a result of plasmid preparation and termed supercoiled denatured (Brown, 2001).

1.1.2.2 OC-pDNA

If the polynucleotide strands are nicked, the nucleic acid exhibits a more relaxed shape referred to as open circular (OC) (Brown, 2001; Cherng *et al*, 1999). OC-pDNA adopts conformations intermediate between those of SC and linear (see below) forms of pDNA. Interestingly OC-pDNA have been reported to exhibit similar sizes to those of SC-pDNA when bound to the polymer; poly((2-dimethylamino)ethyl methacrylate) (Cherng *et al*, 1999).

1.1.2.3 Linear-pDNA

Plasmids can also be cut at specific nucleotide sites through the recognition of nucleases which cleave both strands resulting in a linearized conformation; linear-pDNA. Linear-pDNA display more open and accessible conformations which may favour gene expression, but may also be prone to aggregation and exposure to nuclease attack (Anada *et al*, 2005).

The topological form of plasmids has important consequences for use in biotechnology. Conventional DNA uptake studies employ SC-pDNA which exhibiting a condensed shape

has been assumed to facilitate cellular uptake (Hsu and Uludag, 2008). The FDA (U.S Food and Drug Administration) requires that at least 80% of plasmid bulk product content for DNA vaccination should be in the SC conformation (Guidance for Industry: Considerations for Plasmid DNA Vaccines for Infectious Disease Indications – FDA, 2007). Few studies have analysed and systematically compared DNA of differing topologies in regards to gene delivery and ultimately vaccination, and so is a key area for consideration. Figure 1.1 displays the three major pDNA topologies.

Production of OC- and linear-pDNA can be confirmed by agarose gel electrophoresis. The different pDNA conformations display different sizes which can allow distinction by gel electrophoresis as mobility through the gel occurs on the basis of size. The condensed SC form is the smallest which facilitates migration through the gel, hence faster electrophoretic mobility. The linear form containing a double strand cut is larger and migrates slower, followed by OC-pDNA which migrates the slowest (Figure 1.1b).

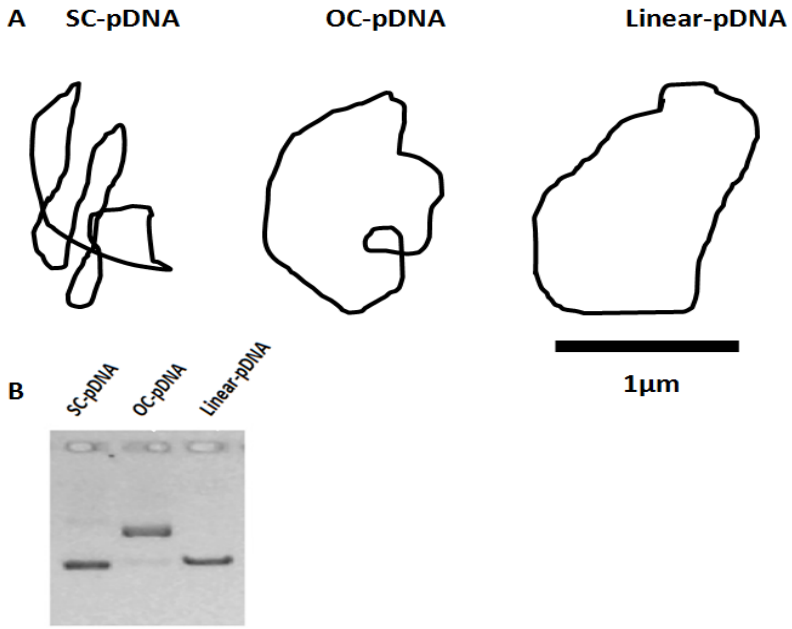

Figure 1.1: **The three major topological forms of pDNA**. Diagramatic representation of supercoiled (SC), open circular (OC) and linear-pDNA (A). Different pDNA conformations can be detected by agarose gel electrophoresis. This is due to different pDNA conformations displaying different electrophoretic mobilities. Electrophoretic diagram is cited from Remaut *et al*, (2006) (B).

1.2 Methodology of pDNA processing

Strategies for delivering new medicines can be brought about via non-viral methods such as recombinant pDNA in *Escherichia coli* (*E. coli*). As of 2011 naked pDNA or pDNA formulations constituted 18.7% of gene therapy clinical trials, demonstrating the growing importance of non-viral gene delivery strategies (The Journal of Gene Medicine Clinical Trial site, 2011). Bioprocess engineering of pDNA vaccines and the importance of upstream and downstream processing on productivity was reported previously (Hoare *et al*, 2005). Levy *et al*, (2000) stated the importance of pDNA processing and how maintenance of pDNA in its SC conformation is important for the attainment of pharmaceutical grade pDNA. A typical process diagram summarising the key aspects of pDNA processing is shown in Figure 1.2. Although the SC conformation is important for pharmaceutical grade DNA, other plasmid conformations such as linear-pDNA is important as it has a more open structure than the SC form which favours access for transcription factors to enable gene expression to occur. Furthermore very few studies have systematically compared plasmids of different DNA topologies in regards to biophysical characterisation, mammalian cell uptake and potential nuclear import.

1.2.1 Upstream processing of pDNA

Escherichia coli (*E. coli*) has often been employed as a vehicle to allow expression and propagation of pDNA. This is brought about by fermentation of cells (Figure 1.2). This is a key step in upstream processing in order to enhance the *E. coli* population and increase the quantity and quality of recombinant pDNA (Carnes *et al*, 2006; Ferreira *et al*, 2000; Lehajani *et al*, 1996: Yau *et al*, 2008). Studies have also stressed the need for the removal of contaminants. For example Shamlou (2003) identified increased genomic DNA (gDNA) impurities post fermentation, stressing the need to improve pDNA processing. In regards to clinical applications, FDA guidelines (2007) recommended that pDNA pharmaceutical

products should not exceed 100pg gDNA per dose. Studies have shown how factors such as host strain selection and DNA topology can affect pDNA processing and the amount of impurities (O'Kenedy *et al*, 2003; Yau *et al*, 2008; Carnes *et al*, 2006). For example host strain selection in upstream processing is important as certain strains have a greater specific growth rate than others. This has resulted in increased plasmid yields for certain strains than others which aids in bioreactor optimisation (Yau *et al*, 2008).

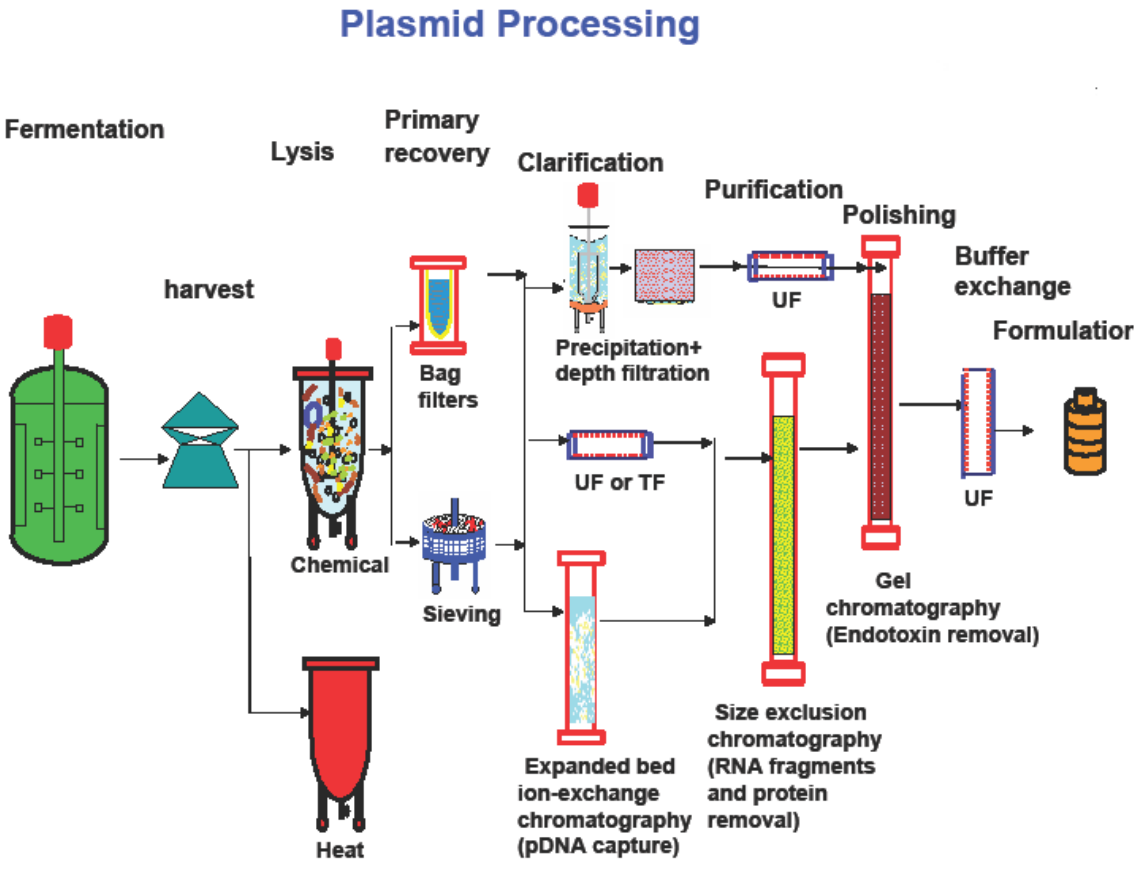

Figure 1.2: **Schematic of process options**. Schematic representation of pDNA processing stemming from upstream fermentation through to cell harvest, lysis filtration, ultrafiltration (UF) and further downstream chromatography steps prior to product formulation.

1.2.2 Downstream processing of pDNA

Downstream purification procedures are important in order to yield large amounts of stable pDNA (Stadler *et al*, 2004; Ferreira *et al*, 2000). These incorporate a variety of techniques to purify and increase the yield of therapeutically viable pDNA (Figure 1.2).

1.2.2.1 Lysis

Following fermentation downstream processing involves cleavage of cells (Ferreira *et al*, 2000). This is necessary for the secretion of cellular impurities including gDNA, RNA, and pDNA, which ultimately increases pDNA yields (Horn *et al*, 1995). Secretion is brought about by alkaline lysis, whereby cells previously suspended in neutral pH are then treated with alkaline detergent which lyses cells. Although this technique employs RNase to degrade impurities and is efficient on bench scale, such a method is unsuitable for large scale pDNA recovery due to the employment of RNase, which is considerably expensive (Ferreira *et al*, 2000). However even after alkaline lysis studies have reported that lysates often consisted of only 3% pDNA (Stadler *et al*, 2004). Alternative methods also include ultrafiltration (Theodossiou *et al*, 1997; Varley *et al*, 1999) and nucleases to remove gDNA and RNA contaminants (Monteiro *et al*, 1999; Chakrabarti *et al*, 1992).

1.2.2.2 Clarification and precipitation

Alkaline lysis results in a pDNA lysate containing cellular impurities which constitute a white flocculate. Removal of flocculate is important and is referred to as clarification and precipitation of pDNA (Hoare *et al*, 2005). Following alkaline lysis centrifugation is employed for removal of cellular impurities of the flocculate. Whilst this is suitable for small scale processing, it is not ideal for large scale recovery of pDNA (Blom *et al*, 2010). Filtration methods are often employed for flocculate removal, although filter clogging is an

issue which reduces yield. Sensitive and efficient removal of flocculate, so as to reduce release of any impurities have been discussed ranging from specific filter aids (Theodossiou *et al*, 1999), to the use of a pressure vessel used to separate flocculate from lysate (Przybylowski *et al*, 2007). A recent report discussed the use of an improved scalable method of alkaline lysis clarification. This involved the addition of ammonium hydrogen carbonate to the lysate which resulted in separation from the lysate (Blom *et al*, 2010). The benefits of this technique are that it is economically efficient as less time is spent on filtration. Therefore the need for specialised filters is reduced. When 5g *E. coli* was processed, 91% SC-pDNA content was recovered, although this decreased to <80% when scaled up to 940g highlighting the sensitivity of clarification pDNA recovery (Blom *et al*, 2010).

1.2.2.3 Ultrafiltration

Ultrafiltration (UF) is a form of membrane filtration in which hydrostatic pressure filters low molecular weight lysates through a permeable polymer membrane (van Reis and Zydney, 2007). UF often proceeds clarification steps and has been shown to be an effective tool in pDNA purification. Studies using UF found adsorption of lysates and led to <80% impurity removal (Kendall *et al*, 2002). Transmission through membrane pores is dependent on size and elongation characteristics of plasmids, which has allowed separation of different pDNA isoforms. SC-pDNA is smaller and is able to elongate and stretch allowing passage through membrane pores when induced with high filtration velocity (Latulippe and Zydney, 2011). However pressurised filtration can cause shearing and can jeopardise pDNA isoforms, thereby limiting pDNA yield.

1.2.2.4 Chromatographic purification

Chromatography is generally regarded as one of the most effective purification procedures for the attainment of pDNA suitable for therapeutic purposes (Stadler *et al*, 2004). The

advantage of such procedures is that chromatographic techniques exploit physiochemical attributes of pDNA which can potentially lead to primary eluents consisting of up to >80% pDNA (Stadler *et al*, 2004). However there are limitations to various chromatographic techniques (Table 1.1). For example ion exchange chromatography, which separates on the basis of charge, has been reported to retain RNA impurities (Sousa *et al*, 2008). This is a major limitation that can decrease pDNA yields. Other limitations include damage to pDNA which can alter conformation (Ferreira *et al*, 1999). However a recent study reported increased removal of cellular impurities through the use of boronate glass pore beads which were able to adsorb *E. coli* impurities such as RNA, LPS and cellular proteins (Gomes *et al*, 2010). Although improved pDNA yields have been reported, shearing and damage to pDNA throughout the processing procedure has reduced yields, highlighting the sensitivity and difficulty in attaining therapeutic viable pDNA. For example despite membrane filtration being an efficient tool in downstream pDNA purification, plasmids are susceptible to shearing and damage to the pDNA backbone (van Reis and Zydney, 2007). This emphasises the importance of pDNA yield for DNA vaccine production and attainment of pDNA in the correct topological form.

1.2.2.5 Formulation

Following purification pDNA products must undergo 0.22µm sterile filtration and meet various minimum requirements (Prather *et al*, 2003). According to Sagar *et al*, (2003), final pDNA product should consist approximately <1% total protein and <1% gDNA impurities. Although these parameters vary between regulatory bodies pDNA yield is still relatively low, which stresses the importance of optimal upstream and downstream pDNA processing to remove cellular impurities and enhance pDNA retention.

Downstream system	Function	Advantages	Disadvantages	References
Ion exchange chromatography	Separates components on the basis of charge and nucleic acid conformation.	Isolate different pDNA topologies.	Retention of impurities such as gDNA and RNA.	Huber, (1998) Sousa *et al*, (2008) Yamakawa *et al*, (1996)
Hydrophobic interaction chromatography	pDNA is separated on the basis of hydrophobic interaction.	Can separate larger pDNA with longer hydrophobic residues and hence different pDNA forms.	Technique employs toxic organic solvents which can damage pDNA.	Diogo *et al*, (2000) Stadler *et al*, (2004)
Size exclusion chromatography	Purification of pDNA on the basis of size.	Can filter out larger gDNA and RNA impurities.	Employs salts which can alter conformation of DNA.	Boles *et al*, (1990) Neidle, 1994 Ferreira *et al*, (1997) Ferreira *et al*, (1999)
Affinity chromatography	Use of an immobilised ligand to recognise antigen of interest.	Flexible procedure allowing multiple rounds of purification.	Specificity of ligand can limit processing.	Lowe *et al*, (2001)
Membrane filtration	Filters pDNA through polymeric membranes on the basis of size.	Filtration leads to pDNA viable for formulation prior to therapeutic use.	Cost of membrane is a limitation and it is difficult to filter larger pDNA vectors.	Kong *et al*, (2006) Hirasaki *et al*, (1995) van Reis and Zydney (2007)

Table 1.1: **Summary of the downstream processing techniques for pDNA.** Techniques range from a variety of chromatography processes to membrane filtration of pDNA

1.3 pDNA complexes and its use in non-viral gene delivery

Non-viral gene delivery into mammalian cells is widely used in the biotechnology industry for the production of recombinant proteins requiring post translational modifications as well as considered for clinical trials in gene therapy vaccination. Gene transfer through such means often entails delivery of nucleic acids that are bound to a cationic polymer (polycations) resulting in pDNA/polymer products, often referred to as polyplexes (Elouahabi and Ruysschaert 2005). In terms of cell therapy non-viral gene delivery has recently been found to treat spinal cord regeneration. DNA polyplexes transfected into endogenous cells have been identified to lead to the production of therapeutic molecules that stimulate long term tissue regeneration (Yao *et al*, 2012). There are numerous polycations which have been found to operate by binding and condensing pDNA which facilitates mammalian cell uptake (Tsai *et al*, 1999; Lee and Huang, 1996). Such polycations have been shown to condense pDNA into confined structures of approximately 100-200nm. These include that of polyethylenimine (PEI), poly-$_L$-lysine (PLL), poly(amidoamine) (PAAs) and dendrimers amongst others (Ko *et al*, 2009; Zhang *et al*, 2009; Hartmann *et al*, 2008; Tsai *et al*, 1999; Dutta *et al*, 2008).

1.3.1 Transient transfection

Transient transfection refers to the process of introducing foreign nucleic acids into host cells, often with the aim of expressing a desired protein product (Liu *et al*, 2008). The term 'transient transfection' is often used to describe non-viral gene delivery methods, for which it is often applied (Derouazi *et al*, 2004). In such cases the DNA is bound to a positively charged vector and gains cellular access via endocytosis (mechanism of cellular entry through membrane compartmentalisation). Transient transfection often leads to the short term expression of the reporter gene of interest, whereby the foreign DNA does not integrate

within the host chromosomal DNA. In terms of research, transient transfection is a widely used technique to safely and effectively deliver nucleic acids in a variety of cell types. It offers advantages including being a relatively simple and effective procedure, and has been applied in industry to maximise the production of recombinant proteins (Liu *et al*, 2008).

1.3.2 Reverse transfection

Transient transfection is often carried out on adherent cell lines to which the addition of the nucleic acid to a set of immobilised cells within culture media occurs. However many other cells, particularly key primary and immunological target cells are in suspension. Therefore to transfect suspended cells an alternative technique is required. Reverse transfection (RT) involves non-viral gene delivery through the immobilisation of DNA polyplexes to a cell adhesive surface, to which suspended cells are added (Bengali *et al*, 2009). RT offers many benefits over the conventional adherent cell transfection (bolus) technique as direct exposure of cells promotes internalisation and limits aggregation (Bailey *et al*, 2002; Shea *et al*, 1999). A study by Bengali *et al*, (2009), compared the conventional bolus and RT procedures, and did not find major variables. The amount of polyplexes that were cell associated was not significantly different. In addition the majority of polyplexes were often located in the media (bolus) or surface (RT), highlighting the limitations of transient transfection as a whole.

1.3.3 Labelling of DNA and polycation

To understand the mechanism of polyplex transfection and confirm uptake (defined as the intake of materials by a cell or tissue leading to its permanent or temporary retention) labelling as a means of tracking is essential. It is also crucial to consider whether labelling (either direct or indirectly) can affect the physiochemical properties of DNA polyplexes.

1.3.3.1 DNA labelling

Tracking the fate of transfected nucleic acids often involves labelling of some degree. This involves transfecting a plasmid encoding a reporter gene, in which the process depends on nuclear entry and gene expression, or staining procedures (or both). Nucleic acids can be fluorescently labelled both direct and indirectly allowing one to monitor the progress of uptake. Various methods of labelling are available which have been employed in the literature, and the key techniques will be reviewed in this present section.

1.3.3.1.1 Direct labelling

Labelling of nucleic acids allows one to follow the progress of uptake and identify the immediate fate of the DNA post transfection. Nucleic acids are often stained or tagged directly with fluorescent markers which can be traced by fluorescent confocal microscopy or flow cytometry. Direct labelling of nucleic acids is a relatively simple procedure which can be brought about by fluorescent intercalating dyes (Perry *et al*, 2008). An example of such fluorophores is the family of Dimeric Cyanine Nucleic Acid stains (Invitrogen) which are potent DNA intercalating agents. Advantages of such dyes are that they exhibit a high affinity for DNA with limited background fluorescence for unbound fluorophores (Perry *et al*, 2008). Additionally when bound to DNA such dyes are extremely stable and only fluorescence when interwoven between nucleic acid strands (Krishnamoorthy *et al*, 2002). Confirmation of successful staining can be deduced by fluorescence spectroscopy assays. Various studies have utilised such dyes to directly label DNA, particularly when analysing polyplex gene delivery (Krishnamoorthy *et al*, 2002; Srinivasan *et al*, 2009). One example is that of Perry *et al*, (2008) who employed an intercalating fluorescent stain and successfully monitored uptake of polyplexes within mammalian cells. The specific ability of the respective dye to intercalate (and fluoresce) between the DNA strands enabled characteristic analysis of the labelled

polycation/DNA complex, whereby direct labelling did not jeopardise key physiochemical attributes (size and surface charge).

1.3.3.1.2 Indirect labelling

Indirect labelling of transfected pDNA polyplexes has been successfully employed. For example DNA can be biotinylated and probed with a fluorescent avidin antibody. This provides a useful and sensitive detection system. Indirect labelling to monitor transfected pDNA polyplexes was reported by Wojda *et al*, (1999) whereby target biotinylation and streptavidin probing enabled PEI polyplexes to be followed by confocal microscopy. However a disadvantage of this particular labelling procedure is that it requires one to confirm that the target is successfully biotinylated. In the case of DNA this requires a Southern blot to confirm labelling was achieved (if any), which is laborious and a time consuming method prior to transfection.

1.3.3.2 Polycation labelling

Monitoring the cellular destiny of the nucleic acid through either direct or indirect labelling is essential, but it is equally important to investigate the fate of the polycation vector through fluorescent labelling. This is important in order to monitor and trace the path of the transfected polycation and whether it shares the same the fate as the nucleic acid or undergoes a different uptake mechanism. Godbey *et al*, (1999) previously reported successful fluorescent labelling of the polycation; PEI (polyethylenimine). These polycations consist of branched structures containing primary amine groups, which allow binding of fluorescent dyes via an ester linkage. For instance FITC-succinimidyl esters have been applied to bind and efficiently label such polycations with a reduction in background fluorescence. Such labelling has allowed research into the fate of transfected polyplexes (Godbey *et al*, 1999).

1.3.3.3 Cell labelling

Labelling of cells (either live or fixed) is important in terms of observing the transport of polyplexes through different cellular compartments. Labelling is often brought about via fluorescent tagging or staining. For example recent studies have labelled cells by fluorescent aptamers (Terazono *et al*, 2010). Aptamers are single stranded nucleic acids that interact and bind to a target sequence. Aptamer labelling is based on the addition of biotinylated single stranded DNA which binds to the target cell surface antigen. Fluorescent probe labelling is then brought about by the addition of streptavidin secondary molecules (Terazono *et al*, 2010). The benefits of this procedure are that labelling is highly efficient and quick. Furthermore alternative antibody labelling methods can lead to irreversible conjugation which in turn affects the function of the respective cell (Trickett and Kwan, 2003). Other labelling methods include fluorescent staining of whole cells as a means to provide a backdrop thereby highlighting passage of complexes or transfer through cells (Langevin *et al*, 2010).

1.3.4 Non-viral formulated gene delivery

1.3.4.1 Polymers

Polymers (or polycations) are polymeric structures harbouring positively charged residues that can be used to bind with nucleic acids (Hartmann *et al*, 2008). Binding to the negatively charged DNA occurs via electrostatic interaction. DNA is not only attached, but also condensed to a smaller conjugate due to the phosphate backbone being relaxed by the cationic polymer and coiling into a dense structure (Hartmann *et al*, 2008). The polymer/DNA complexes formed as a result are referred to as polyplexes, in which the positive charge induced upon the pDNA allows interaction and entry within the negatively charged cell membrane (Figure 1.3).

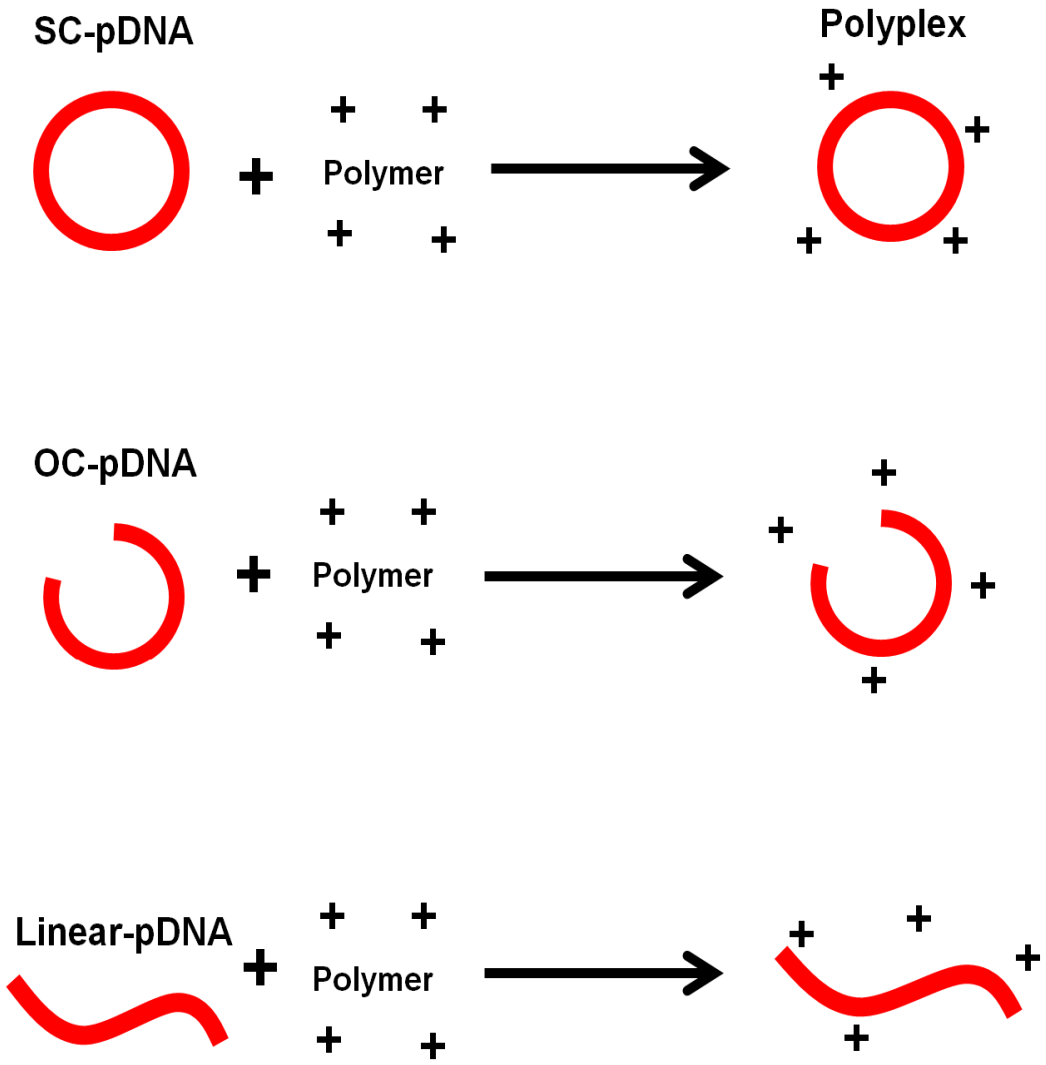

Figure 1.3: **Formation of DNA polyplexes**. The positively charged residues bind via electrostatic interactions with the negatively charged DNA phosphate backbone to produce a complex of net positive charge, which allows uptake into target cells. Polymers bind and condense DNA into smaller nanoparticles.

Various polymers and also lipid structures have been applied to deliver genes, each with advantages and disadvantages. In this section the key polycations are reviewed and how each one effectively delivers pDNA (summarised in Table 1.2).

Polymer	Structure	References
PLL	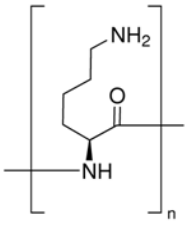	Lu *et al*, 2011. Diagram cited from Sigma-Aldrich®.
PEI	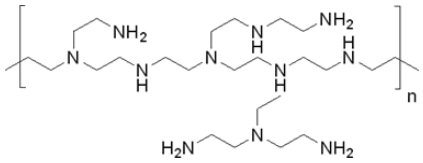	Hanzlikova *et al*, 2009. Diagram cited from Sigma-Aldrich®.
Dendrimers	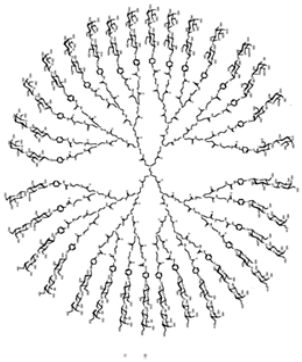	Dutta *et al*, 2008; Hartmann *et al*, 2008. Diagram cited from: Andre *et al*. 1999
MEND		Suzuki *et al*, 2008
Liposomes	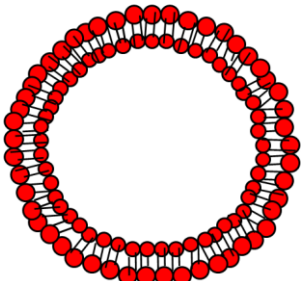	Perrie *et al*, 2001

Table 1.2: **Summary of the key non-viral gene delivery vehicles.** The polymers display a network of positively charged amine residues which facilitates binding with the negatively charged DNA backbone. Liposomes are lipid structures whose structures encapsulate the nucleic acid.

1.3.4.1.1 PLL

Poly-$_L$-lysine (PLL) is a widely used polycation DNA condensing agent which has been shown to be effective in inducing confined pDNA structures (Lee and Huang, 1996; Tsai *et al*, 1999). PLL harbours an extensive network of amide groups that facilitates pDNA binding (Table 1.2). Benefits offered by PLL include the ease and rapid ability by which it binds with DNA, allowing successful delivery of genes (Fu *et al*, 2011; von Erlach *et al*, 2011). The ability of PLL to effectively produce dense structures and impose a strong cationic charge has enabled successful encapsulation within lipid vectors (liposomes) (Lee and Huang, 1996). In order to analyse pDNA complexes in regards to gene delivery, the condensed PLL/DNA structures must be studied at great depth (Mann *et al*, 2008; Tsai *et al*, 1999). The study by Mann *et al*, (2008) showed how PLL-condensed plasmids conferred to rod-like structures which may have arisen through extensive plasmid coiling yielding monomolecular polyplexes. In terms of polymer length the authors observed how shorter PLL molecules produced more dense structures, whereby polyplex sizes of only 60nm were recorded (Mann *et al*, 2008). This is useful for gene delivery studies whereby specialised cells allow entry to smaller incoming cargo. Therefore the advantages of using PLL over other polymers include its ability to bind DNA through electrostatic interaction thereby condensing it (Luo and Saltzman, 2000). Further benefits of PLL over other polymer counterparts include its low cytotoxicity, cost, application to a wide range of cells and versatility whereby it can undergo chemical modification for tailor made transfection studies (Luo and Saltzman, 2000; Fu *et al*, 2011; von Erlach *et al*, 2011).

1.3.4.1.2 PEI

Polyethylenimine (PEI) is a popular polymer employed for non-viral gene delivery and functions similarly to that of PLL by facilitating cellular uptake (Neu *et al*, 2005; Ali and

Mooney, 2008; Hanzlikova *et al*, 2009). The PEI polycation exhibits a large extensive polymeric structure harbouring amide groups which contributes towards its overall cationic charge (which favours electrostatic binding with the negatively charged nucleic acid phosphate backbone) (Ali and Mooney, 2008). PEI not only condenses pDNA into confined forms but has been found to offer benefits such as providing protection from endosomal cleavage (major obstacle of non-viral gene delivery) and facilitating nuclear transport (Dunlap *et al*, 1997; Pollard *et al*, 1998). The structure and cationic charge of PEI is an advantage because following interaction with the negatively charged pDNA, bending of the usually rigid nucleic acid occurs leading to efficient DNA condensation and packaging, which ultimately enhances potential gene expression (Hartmann *et al*, 2008). This was reported previously whereby PEI/DNA was found to be efficiently transfected within smooth muscle cells (Hanzlikova *et al*, 2008). PEI also displays a low risk of cytotoxicity and reduced cost contributing towards its popularity within the field (Akhtar, 2006). However there are drawbacks, which primarily stems from its *in vivo* stability. Such complexes have been observed to be excluded from circulation leading to a build up of complexes within the reticuloendothelial (RE) organs (e.g liver) (Ko *et al*, 2009). The RE system refers to groups of cells of differing organs, capable of the uptake of nanoparticles (Brewer *et al*, 2012). Studies employing PEI have recorded modest transfection efficiencies (reporter gene expression). Excessive amounts of PEI have been reported to be quite cytotoxic which is in contrast to previous studies (Breuing *et al*, 2005). Although facilitating DNA packaging, the strong cationic charge of PEI may lead to association with non-specific components (Neu *et al*, 2005). A previous report addressed this issue by coating polyplexes with lipids which masks such excessive charges (Ko *et al*, 2009). Another issue is that PEI can exhibit a range of molecular weights and conformations which lends itself to being too polydisperse (Hartmann *et al*, 2008). This is an issue as such characteristics can affect the potency of the

cationic charge induced on pDNA and in turn greatly affects the degree of conjugation with the nucleic acid. In spite of such drawbacks, the simplicity, modest cost and ease by which it forms pDNA polyplexes (as highlighted in previous studies; Park *et al*, 2008; Hanzlikova *et al*, 2009; Ali and Mooney, 2008) continues to make it a predominant non-viral polymer gene delivery tool. PEI based systems were found to display sustained gene expression within the circulatory system, thus highlighting recent advances regarding the polymer (Ko *et al*, 2009).

1.3.4.1.3 MEND

Gene transfer can also take place through a multifunctional envelope-type nano device (MEND) (Suzuki *et al*, 2008; Kogure *et al*, 2004). This device consists of condensed pDNA coated with lipids to aid cellular integration in a manner similar to viral vectors (Khalil *et al*, 2006). Although MEND has recently been applied for non-viral gene transfer and displayed promising results, there are limitations. The formulated MEND/PLL/DNA complex displayed a large size that was not feasible for gene transfer (Khalil *et al*, 2006). This led to designs of a new form of MEND that would allow packaging of pDNA conjugates which does not compromise the size of the resulting complex. Condensed pDNA were further compacted within lipid bilayers and tagged with arginine residues to facilitate specific cellular recognition and entry (Suzuki *et al*, 2008) (Table 1.2). Mono-cationic detergents (MCDs) were employed to further condense pDNA thereby reducing the size of the complex. MCDs exhibit hydrophobic residues that have been found to depress pDNA (Khalil *et al*, 2004). The addition of the MCD condensed pDNA to a lipid envelope improved cellular entry via electrostatic interaction. In fact lipid coating of the nucleic acid significantly enhanced transfection in HeLa cells. Condensed pDNA complexes were found to be transfected into cells more efficiently than naked DNA and controls lacking a lipid coating did not enter cells. Therefore these studies stress the importance of both pDNA compaction and lipid coatings which greatly facilitates cellular recognition.

1.3.4.1.4 Dendrimers

Formulated gene transfer can also take place via dendrimers. Dendrimers are branched three dimensional components which offer the benefit of cellular networking and trafficking of DNA (Dutta *et al*, 2008) (Table 1.2). Dendrimers are of a relatively small size and their particular structure offers the advantage of avoiding degradation via the reticuloendothelial system (RES) (Dutta *et al*, 2008). Dendrimers harbour terminal amine residues which contribute towards a cationic charge (Tripathi *et al*, 2003). These polymers consist of large moieties of positively charged amino acids which interact with pDNA via hydrophobic electrostatic interactions in a more effective manner than fellow polycations (Zeng and Zimmerman, 1997). This may be due to the branched structure which aids in networking, allowing greater interaction with pDNA resulting in greater electrostatic binding that essentially eases the rigid phosphate backbone of pDNA (Lechardeur *et al*, 1999; Bielinska *et al*, 1997). Although cytotoxicity was reported previously (Bielinska *et al*, 1997), recent analysis highlighted improved safety issues (Zhang *et al*, 2007). Hydrophobic interaction allows dendrimers to bind and condense DNA efficiently into smaller conjugates. The condensed conjugates are then entrapped and bound within dendrosomes which serve as delivery vehicles (Dutta *et al*, 2008). Dendrosomes are advantageous because being vesicular they can act as transporters for the harboured dendrimer/pDNA polyplex. By containing the pDNA complex the desired therapeutic gene is shielded from intracellular nucleases (Perrie *et al*, 2001). Dendrimer/DNA complexes have also been found to stimulate T-helper cell responses indicating its ability to induce an immune response (Dutta *et al*, 2008). Dendrimers can also undergo modification in which the cationic charge may be masked which reduces non-specific binding and cytoxicity (Dutta *et al*, 2008). Despite encouraging results, dendrimers do fall short in terms of pDNA delivery to specific cellular compartments. Competition between negatively charged molecules and that of plasmids for binding upon the

polymer may lead to premature release (Perrie and Gregoriadis, 2000; Zelphati and Szoka, 1996).

1.3.4.1.5 PAA

Poly(amidoamines) (PAAs) are a form of dendrimer and have recently generated interest because unlike its polycation counterparts, methods have been devised that allow the design and construction of a more potent and defined pDNA polyplex. For instance PEI and PLL polymers are polydisperse and can also lead to aggregation (Tsai *et al*, 1999). Intricate alterations to the PAA sequence can lead to changes in the chemical orientation of amide groups. By doing this a more potent monodisperse system is constructed thereby reducing non specific binding, cytoxicity and aggregation (Hartmann *et al*, 2008). Modification of PAA amine groups minimises the negatively charged repulsions ever present on the DNA backbone, leading to a more relaxed nucleic acid structure that is susceptible to coiling (Bloomfield, 1996). Therefore PAA modification enhances DNA condensation and packaging. By producing such encouraging results the tailor-made polyplex method described may pave the way for future designs of non-viral gene delivery methods.

1.3.4.2 Lipids

A major drawback concerning pDNA delivery is susceptibility towards nuclease degradation (Lewis and Babiuk, 1999; Gregoriadis, 1998; Davis, *et al*, 1993). Such events restrict the amount of plasmid transferred to the nuclei, thereby reducing gene expression (Perrie *et al*, 2001). Various studies have analysed how pDNA may be delivered to target cells when encapsulated within cationic liposomes (Gregoriadis *et al*, 1997; Perrie *et al*, 2001) (Table 1.2). Liposomes are lipid complexes which allow attachment of nucleic acids through electrostatic binding (Perrie *et al*, 2001). Not only do liposome complexes shield the harboured pDNA from nucleases but such vehicles have been found to transport nucleic acids

to antigen presenting cells (APCs) thereby amplifying any potential immune response (Gregoriadis, 1998). The lipid content enables liposomes to be taken up via endocytosis by APCs within draining lymph nodes (Velinova *et al*, 1996). Liposomes have been identified to express encoded antigen and in doing so increasing the immune response (Gregoriadis, 1998).

1.3.4.2.1 Cationic liposomes

Lipid/DNA complexes are referred to as lipoplexes, which have been found to transport pDNA to target sites leading to efficient gene expression (Lee and Huang, 1996; Khalil *et al*, 2006). Electrostatic interactions allow the incorporation of negatively charged pDNA within cationic liposomes. Alternatively positively charged polyplexes can be encapsulated within anionic liposomes. Both methods have improved gene expression (Lee and Huang, 1996).

An important parameter to consider is lipid content with liposomes often containing specific lipids such as dioleoyl phosphotidylethanolamine (DOPE) or cholesterol. The application of DOPE is beneficial because it binds with fellow lipids which lead to the release of entrapped DNA when the pH decreases (Farhood *et al*, 1995). This is an advantage as many host cell degradative enzymes operate at an acidic pH. Therefore release of DNA avoids nuclease exposure. Cholesterol is required for stability and some reports have suggested a role for specific targeting (Allen and Chonn, 1987). The significance of liposomal constituents has been stressed in the literature and has been linked with improved pDNA uptake. Lipids such as 1,2-dioleoyl-3-(trimethylammonium) propane (DOTAP) seem to enhance pDNA incorporation. Perrie and co-workers (2001) injected mice with liposomes consisting of differing amounts of lipids. Antibody responses were recorded and were highest in models injected with either DOTAP or DOPE (Perrie *et al*, 2001). Therefore the design and

composition of such vesicles is important in entrapping, releasing the DNA, and also stimulating immune responses.

1.3.4.2.1.1 Application of cationic liposomes

Lipid content has been found to play a major role in gene delivery and studies have reported successful lipoplex gene transfer resulting in gene expression as well as inducing specific immune responses. For instance one study formulated a cationic liposome consisting of N-(2-Hydroxyethyl)-N,N-dimethyl-2,3-bis(tetradecyloxy)-1-propanaminium bromide (DMRIE) and DOPE (Margalith and Vilalta 2006). This lipoplex harboured an antigen which encoded a glycoprotein of rabies. Vaccine delivery and antigen expression was assessed by administering mice with either DMRIE/DOPE lipoplex formulations or standardised rabies vaccines. Results showed how mice treated with DMRIE/DOPE/pDNA vaccines displayed protective sustained antibody titres which lasted longer than control groups (Margalith and Vilalta, 2006). Results also included how a small dose of the DMRIE/DOPE/pDNA vaccine induced protective titres that were far beyond the standard threshold (responses quantified by a rapid fluorescence focus inhibition test – RFIT). This is beneficial as it is desirable to restrict the amount of cationic lipids administered to a minimal amount that can sustain protective responses, which lasted for up to 125 days (Margalith and Vilalta, 2006). However in comparison to fellow cationic liposome Vaxfectin™, the DMRIE/DOPE/pDNA vaccine was not as effective in inducing antibody responses.

1.3.4.2.1.2 Magnetofection

Although liposomes have been found to successfully deliver pDNA, there are drawbacks which include lack of potency (low gene expression and modest antibody responses) and non specific binding. However magnetic nanoparticles may significantly improve lipoplex uptake. Research by Ino *et al*, (2008) mentioned how the coupling of pDNA with magnetized

cationic liposomes led to effective complex uptake when induced with a magnetic force. The method, termed magnetofection has been analysed previously (Scherer *et al*, 2002; Gersting *et al*, 2004). Magnetofection occurs on the basis of a magnetic force which physically pulls and attracts the lipoplex towards the target cell. Ino and colleagues (2008) harnessed this method by constructing magnetic cationic liposomes (MCLs) which consisted of small magnetite molecules. MCLs can then be coupled to lipoplexes to form MCL/lipoplexes (Nagatani *et al*, 1998).

Reporter gene expression of MCL/lipoplexes was compared with that of non-magnetic lipoplexes. Magnetite molecules were mixed with the lipoplexes which allowed magnetite nanoparticle congregation on the surface of the desired cell (Shinkai *et al*, 1996). Uptake and gene expression was greater than non-magnetic controls. Furthermore optimal uptake was observed after only 5 minutes highlighting the swift delivery magnetofection has to offer The MCL/lipoplexes did not affect cell growth nor induce cytoxicity (Ino *et al*, 2008). In fact similar results were reported previously which employed lower MCL doses (Ito *et al*, 2004). Reports have identified successful gene expression and minimal safety issues regarding a wide range of cell types such as aortic endothelial cells (Ito *et al*, 2005) and mesenchymal stem cells (Shimizu *et al*, 2007).

1.3.4.2.1.3 Elastic liposomes

Elastic liposomes are dynamic structures that can penetrate and deliver pDNA through extreme barriers such as the transdermal skin barrier. Elastic liposomes are composed of phospholipids and ethanol which are responsible for its elastic tendencies (Manosroi *et al*, 2009). An advantage of these complexes is its stability whereby storage for as long as 8 weeks at temperatures as high of 45ºC did not hinder cellular uptake. (Manosroi *et al*, 2009).

An additional benefit is that the incorporation of ethanol enables free radicals to be mopped up, which are often the cause of DNA degradation (Evans *et al*, 2000).

Few studies have reported successful transdermal drug delivery due to the stratum corneum (SCM) barrier of the skin. With the incidence of skin diseases rising, drug formulations designed to penetrate such a barrier is in major demand. The employment of elastic liposomes may provide an answer as they facilitate delivery by penetrating the SCM, which increases the porosity of the skin (Manosroi *et al*, 2009). However drug delivery and gene expression through standard liposomes have not been as effective, leading to the design of a novel elastic form of cationic liposomes with the aim of bypassing rigid barriers. The components of elastic liposomes provide its elasticity by lowering the melting point which allows increased interaction. It is suggested ethanol may come into contact with fellow elastic components such as phospholipid head regions which enhances fluidity (Touitou *et al*, 2000). These beneficial characteristics along with the ability to extend the release of nucleic acids enable elastic liposomes to become effective gene delivery tools (Choi and Marbach, 2005). Elastic liposomes were found to enhance transdermal gene uptake, with gene expression being observed in viable epidermis and dermis (VED) (beyond SCM barrier) (Manosroi *et al*, 2009).

1.4 Mammalian cell targets and uptake

In order for pDNA to be used as a viable therapeutic product that requires delivery to target cells (regardless of polyplex or lipoplex formulation), mammalian cell uptake studies are crucial. For instance Chinese hamster Ovary (CHO) cells are employed for recombinant protein production and key primary immune cells are studied to trigger specific immune responses for the antigen of interest.

1.4.1 Chinese hamster ovary (CHO) cells

Non-viral methods have been tested within mammalian cells such as Chinese hamster ovary (CHO) cells, as these systems allow high protein expression and can be successfully scaled up in culture (Liu *et al*, 2008; Derouazi *et al*, 2004). Short term transient transfection of CHO cells using polyplexes has been reported to result in high protein yields (Schlaeger and Christensen, 1999; Reisinger *et al*, 2009) and successfully scaled up. CHO cells play a prominent role in the synthesis of recombinant proteins with production occurring through culture of either adherent or suspended cells (Wurm, 2004). Adherent CHO cells are those that can be transiently transfected and produce recombinant proteins. For instance adherent CHO cells have been successfully utilised to produce the drug; erythropoietin (Epogen, Amagen) (Wurm, 2004). However suspended CHO cell cultures are also very much the norm in regards to recombinant protein synthesis due to increased growth capacity. Therefore CHO cells are a key source of recombinant protein production.

1.4.2 Dendritic cells (DCs)

Dendritic cells (DCs) are key components of the immune system which function by binding and collecting antigens. Following recognition, DCs present the antigen of interest through selective surface markers termed major histocompatibility complex (MHC) class-I molecules. MHC is cell surface molecule which interacts with blood cells called T-cells and participates in antigen presentation. MHC molecules present antigens to T-cells which express receptors specific for the antigen of interest (Marieb, 2004). There are various classes of MHC molecules which present antigens to certain T-cells. For example MHC class-I molecules present antigens to T-cells expressing receptors specific for the cell surface marker CD8 (cluster of differentiation 8), these are referred to as CD8+ T lymphocytes (Marieb, 2004). In contrast MHC class-II molecules present antigens to T-cells expressing receptors specific for

CD4 (cluster of differentiation 4), which are termed CD4+ lymphocytes (Marieb, 2004). Following antigen presentation, T-cells become activated. When activated T-cells function by releasing small proteins referred to as cytokines which aid in the immune response (Ueno *et al*, 2011). Following antigen presentation T-cells differentiate into effector cells (Finkleman *et al*, 1996). DCs also function by presenting antigens to B cells, which release antibodies specific for the antigen of interest. It is these functions that researchers aim to exploit in the production of vaccines that target DCs and why they are referred to as antigen presenting cells (APCs). DCs are often located in peripheral tissues such as the skin whereby the likelihood of antigen interaction is highest (Banchereau *et al*, 2000). There are various types of DCs which can be classified according to their location; cutaneous DCs such as langerhan cells (LCs), the dermis DCs and macrophages (Valladeau and Saeland, 2005).

DCs are key sentinels of the immune system. They bridge both arms of immunity; the innate and adaptive response. The innate form of immunity refers to the immediate deployment of antimicrobial proteins and various cells as a means to prohibit foreign pathogen invasion. The adaptive arm of immunity is primed into response following exposure to a foreign antigen, which then specifically recognises and targets the foreign pathogen culminating in immunological memory for future attacks (Marieb, 2004). Therefore DCs are an ideal therapeutic target for polyplex gene delivery, and DNA vaccination.

1.4.2.1 Innate response

The innate arm of the immune system recognises foreign microbial agents, molecular pathogens and nucleic acids. This function is brought about via pathogen recognition receptors (PRRs) (Stevenson *et al*, 2010). An example of PRRs is toll-like receptors (TLRs) which are expressed on DCs and detect foreign DNA as well as other types of molecules (Stevenson *et al*, 2010). However DNA detection is not exclusive to TLRs. Takaoka *et al*,

(2007) reported that DNA-dependent activator of interferon-regulatory factors (DAI) recognises and binds DNA. Absent in melanoma 2 (AIM2) is another complex that detects DNA. It does this by recruiting a protein complex (AIM2 inflammasome) which stimulates caspase I, which functions by releasing the cytokine IL-1β (Fernandes-Alnemri *et al*, 2009). An alternative DNA detection pathway involves ribonucleic acid (RNA) polymerase III (RNA pol III) and retinoic acid-inducible gene I (RIG-I) (Stevenson *et al*, 2010). These two complexes work in partnership whereby RNA pol III transcribes the DNA to RNA which activates the RIG-I complex, which is involved in type I interferon production (Chiu *et al*, 2009). Interferons (IFN) are proteins produced in response to pathogen infection (Marieb, 2004). IFNs are proteins classed as cytokines which function by increasing viral or pathogen detection, by increasing antigen presentation to T-cells, which in turn enhances the immune response directed towards foreign antigen (Stevenson *et al*, 2010). Previous reports identified how stimulator of interferon genes (STING) performs as a DNA sensing agent of innate immunity (Ishikawa *et al*, 2009). Further PRR DNA detection systems also include high mobility group box (HMGB) (Yanai *et al*, 2009). This is summarised in Figure 1.4.

1.4.2.2 Adaptive response

The adaptive arm of immunity is involved in the activation of T-cells such as CD4+ T cells (Marieb, 2004). CD4+ T cells are white blood cells which are critical in maximising the immune response towards a foreign antigen by signalling the recruitment of antibodies specific for the antigen of interest (Marieb, 2004). If DNA vaccines are to be successful, then gene transfer must attract T-cell activity. Stevenson *et al*, (2010) stated that a successful DNA vaccine must incorporate sequences encoding for an adjuvant (pharmacological agent that amplifies an immune response). An example of a widely used adjuvant is tetanus toxin (TT) in which sequences derived from the adjuvant are encoded in the same vector as the antigen (Rice *et al*, 2008). The antigen fused adjuvant is presented to DCs, which express MHC-II

protein receptors which specifically recognise the adjuvant (Stevenson *et al*, 2010) (Figure 1.5). The MHC-II surface markers bind and present the DNA antigen which signals CD4+ T cells specific for the TT adjuvant. Such action primes the T cells to differentiate into effector cells to respond towards the presented DNA antigen (Stevenson *et al*, 2010).

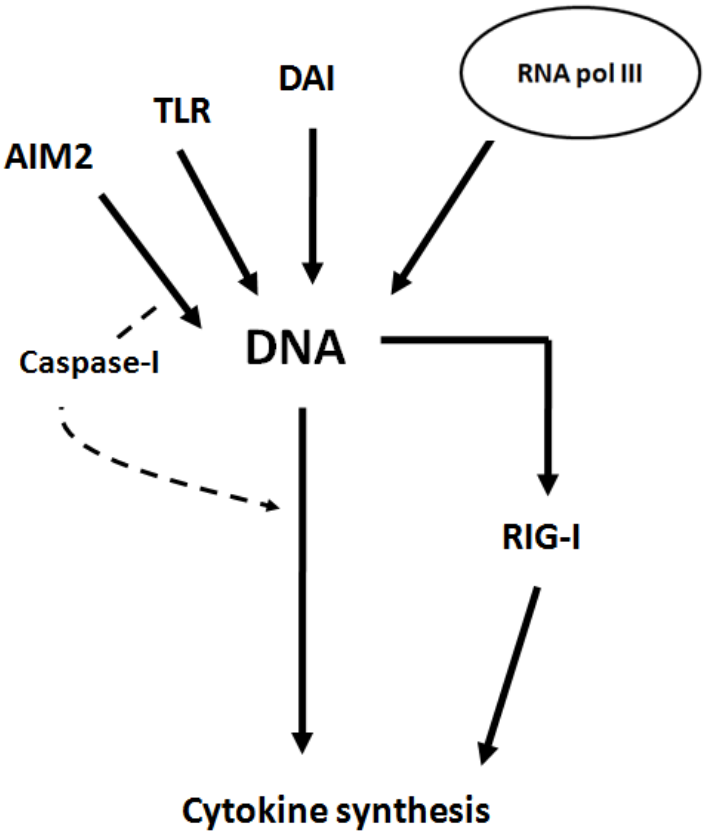

Figure 1.4: **Innate immune response leading to cytokine production.** Innate arm of immunity entails the activation of various DNA sensing agents, which ultimately culminates in cytokine synthesis as a means to direct an immune response towards DNA antigen.

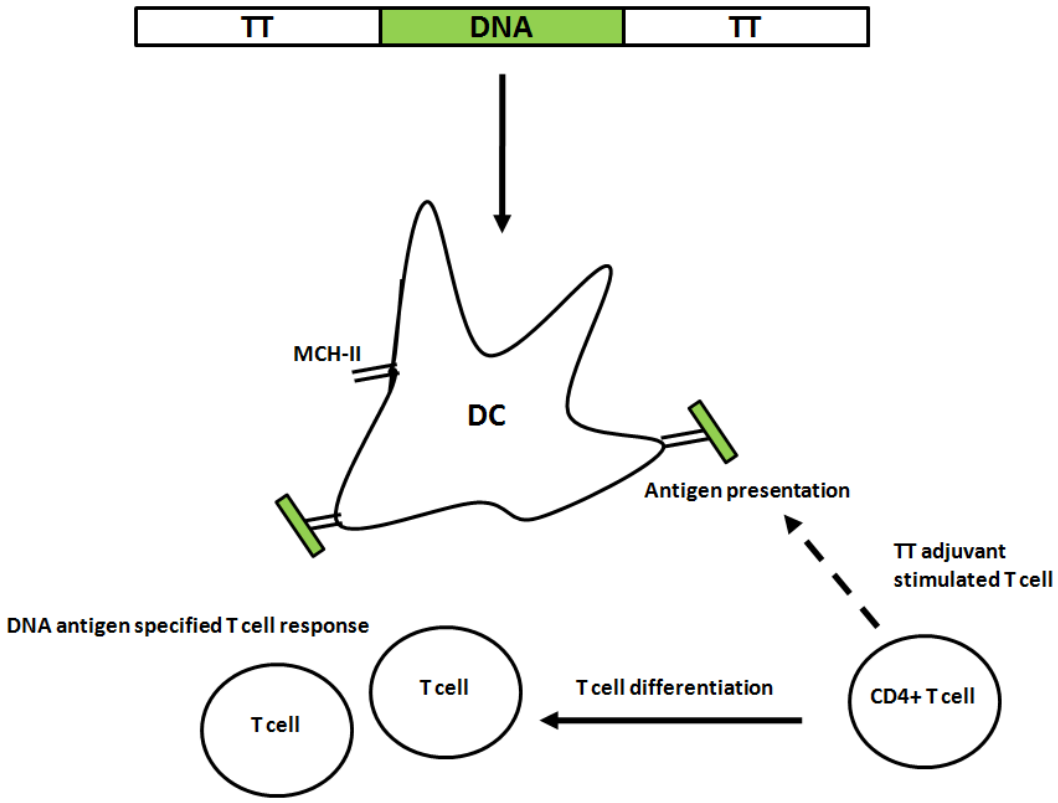

Figure 1.5: **Adaptive immune response leading to T cell differentiation which leads to antibody production.** Adaptive arm of immunity entails antigen presentation, enhanced via adjuvant sequences, which then attract adjuvant specific T cells to direct immunity towards the antigen of interest. TT refers to the adjuvant tetanus toxin.

1.4.2.3 Measuring activation of DC in regards to polyplex uptake

DCs are characteristic in that they express various cell surface markers such as MHC proteins and cluster of differentiation 1a (CD1a) which are all distinctive, but generally function by presenting foreign antigens. Interestingly studies have shown how exposure of DCs to chemical treatment and allergens alters DC surface marker expression leading to the activation of such cells (Hulette *et al*, 2002). Therefore DC surface marker expression is used as a predictor of the sensitization potential of a chemical (Hulette *et al*, 2002). Very few studies have actually focused upon the uptake of DNA polyplexes within DCs and whether uptake activates DCs. Therefore DC surface marker expression is a key indicator for cell activation.

1.4.3 Polyplex uptake within mammalian cells

1.4.3.1 Mechanism of polyplex uptake

The characterisation of pDNA complexes and their design, either as poly- or lipoplexes needs to be done with considerations towards the cellular uptake pathways in mind. After all, characterisation and design is based on the notion of delivering the encoded antigen to its intracellular target in order for its therapeutic function to take effect. However the plasma membrane poses a major obstacle towards such targets (Khalil *et al*, 2006). Endocytosis (cellular incorporation of foreign components) is widely regarded as the manner in which such vectors enter target cells (Khalil *et al*, 2006 and Zuhorn *et al*, 2002). Following endocytosis, the newly internalised (successful entry) molecules are entrapped within vesicle-like structures. These vesicles fuse with lysosomes which then degrade the internalised contents (Khalil *et al*, 2006). Therefore the design of novel polymer based gene delivery systems must enable endosomal release to avoid intracellular lysosomal degradation. In order to do so knowledge of the uptake mechanisms is necessary.

1.4.3.1.1 Endocytosis

Endocytosis refers to the process of internalisation of extracellular material within the cell and has been credited for polyplex uptake (Gould and Lippincott-Schwartz, 2009; Pinchon *et al*, 2010). Therefore polyplexes should be designed to maximise uptake through such mechanisms. Endocytosis can be subdivided into two main pathways; clathrin mediated endocytosis (CME) and clathrin independent pathways such as caveolae and macropinocytosis.

1.4.3.1.1.1 Clathrin mediated endocytosis (CME) pathway

The clathrin mediated endocytosis (CME) pathway is widely regarded as the predominant mechanism of polyplex cellular uptake (Takei and Haucke, 2001). The CME pathway is important as it oversees the continual supply of nutrients, growth factors and antigens. The transferrin loaded iron molecules that are essential for iron metabolism are internalised via CME (Khalil *et al*, 2006). Molecules taken up by the CME pathway are initially recognised by specific receptors. These receptors recognise certain ligands immobilised to the molecule of interest. Uptake leads to the build up of ligand/receptor complexes on coated pits of the membrane. These pits are made up of clathrin which form a polymeric structural lattice (Khalil *et al*, 2006). Subsequently such pits pinch off from the membrane forming clathrin coated vesicles (CCVs). The clathrin coating on these vesicles (containing ligand/receptor complexes) disintegrates leading to the formation of immature endosomes (vesicles containing foreign components) (Khalil *et al*, 2006). These endosomes come into contact with lysosomes which are characterised by a reduction in pH (approximately pH 5) whereby lysosomal enzymes degrade the vesicular contents. Therefore in terms of the CME pathway it is desirable to design a pDNA polyplex than can be incorporated within CCVs to maximise cellular entry but crucially enable endosomal release to avoid lysosomal degradation.

As mentioned previously aspects of both poly- and lipoplexes are designed to allow endosomal release thereby avoiding DNA degradation. In the case of lipoplexes, the pH sensitive lipid DOPE is often incorporated because at an acidic pH the lipid undergoes a conformational change which disrupts the membrane allowing release of the pDNA complex (Farhood *et al*, 1995). Lysosomal degradation is also overcome to some degree by PLL and PEI, whose structure allows it to become protonated (unlike other polymers) that ultimately results in osmotic damage to endosomes allowing the polyplex to be released. However this form of release is dependent on the type of polycation employed of which previous studies have mainly focused on PEI. Therefore a defined pH range for existing polycations needs to be applied. A more universal method could be employed for the variety of polycations available that would allow a defined pH range that could trigger endosomal release. This was postulated previously (Walker *et al*, 2005) whereby polyplexes were coated with a hydrophilic compound such as polyethylene glycol (PEG) to shield the true surface charge of the polyplex thereby reducing cytotoxicity, interaction with non specific targets and potential particle increase (Orgis *et al*, 1999; Ward *et al*, 2001 and Choi *et al*, 1998). This particular shielding is brought about via pH sensitive linkers (such as acetals and hydrozones, Tomlinson *et al*, 2003; Murthy *et al*, 2003 and Greenfield *et al*, 1990) or liposomes, which when in the circulatory system evades the true surface charge of the conjugate, but when incorporated within the endosomal system at an approximate pH of 5 hydrolytic cleavage occurs resulting in the liberation of the complex (Walker *et al*, 2005). This has been strongly correlated with increased gene expression within target cells. pH sensitive DNA complexes have been found to enter cells and display improved transfection efficiencies and reduction in non-specific target associations (Lehtinen *et al*, 2008). Such examples are intriguing as they effectively employ chemical linkers as pH toggles to allow the timed release of pDNA complexes.

1.4.3.1.1.2 Caveolae pathway

However there are alternative uptake pathways that avoid lysosomal contact such as the caveolae pathway. Caveolae are membrane bound vesicle-like structures that harbour large amounts of cholesterol (Khalil *et al*, 2006). Caveolae have been observed to uptake and incorporate foreign viruses. The first step of caveolae uptake involves association with the plasma membrane, in which the foreign cargo becomes encapsulated within a caveolae vesicle (Khalil *et al*, 2006). These vesicles interact with transport organelles termed; caveosomes which take up the newly internalised cargo under non-acidic conditions. This is an advantage as it avoids lysosomal degradation (Ferrari *et al*, 2003). Internalised cargo is then transported to the endoplasmic reticulum or golgi for processing. Therefore in regards to gene delivery it would seem polyplex uptake would be more appropriate through such mechanisms in order to avoid DNA damage and maximise gene expression (Khalil *et al*, 2006). Additional benefits of the caveolae pathway include uptake of molecules as large as 500nm (Rejman *et al*, 2004). However main drawbacks include that the process of uptake is very slow, the vesicles itself are very confined and the fluid volume for pDNA uptake is minute. Therefore the amount of pDNA incorporated and expressed is actually relatively low in comparison to the CME pathway (Schnitzer *et al*, 1994).

1.4.3.1.1.3 Macropinocytosis

An alternative CME independent pathway is macropinocytosis. This process entails the envagination of the plasma membrane to form large vesicles (Amyere *et al*, 2002). Macropinocytosis stems from the ruffling of the plasma membrane when cells are exposed to stimulators or growth factors (Khalil *et al*, 2006). Ruffling entails actin polymerisation which causes a thin outward extension from the membrane. This extension closes in to form a macropinosome, which are large vesicles enabling uptake in a non-specific manner (Conner

and Schmid, 2003). Macropinosomes are desirable gene transport targets as they avoid lysosomal degradation and being large (of up to 5µm) macropinosomes can harbour a large amount of pDNA complexes which could maximise potential gene expression (Khalil *et al*, 2006). Furthermore because macropinosomes are somewhat porous, they can allow efficient gene release into the cytosol (Khalil *et al*, 2006).

Despite the positive attributes drawbacks do include that uptake is dependent on the type of polymer employed. Goncalves *et al*, (2004) identified how macropinocytosis was hindered when the PLL was employed. Therefore the type of endocytic uptake mechanism is likely to depend on the choice of polycation. Additionally modest gene expression has been reported when nucleic acids have been taken up via macropinocytosis, which is why current polymers such as PLL and PEI are often applied as they are successfully internalised via the predominant CME or caveolae pathway.

1.4.3.1.2 Nuclear import of DNA complexes

1.4.3.1.2.1 Importin complex

If DNA polyplexes are to be employed for therapeutic purposes, then understanding the nuclear entry mechanisms are important. Few studies have reported detailed mechanisms of polyplex or naked DNA nuclear entry. While many reports focus on reporter gene expression as an end point parameter, the mechanisms leading directly to gene expression is important and understanding such processes can lead to improved yields.

Nuclear entry of DNA and other large macromolecular components involves many protein complexes working in tandem (Ao *et al*, 2007). Various transport proteins operate by hauling components to the nucleus. One example is importin-7 (Imp7) which is part of a large family of factors involved in the continuous shuttling of proteins between the cytoplasm and nucleus

(Fassati *et al*, 2003). Imp7 has been specifically implicated in the nuclear uptake of viral DNA; HIV-I (Zaitseva *et al*, 2009). Zaitseva and colleagues reported how knockdown (KD) of Imp7 reduced nuclear DNA accumulation and plasmid DNA gene expression. Nuclear DNA trafficking brought about by Imp7 KD was independent to that of RNA uptake (Zaitseva *et al*, 2009).

DNA nuclear import is summarised in Figure 1.6. Imp7 works in conjunction with various protein factors by binding to 3 key sites. Firstly the N-termini of Imp7 bind with the protein; Ran (related nuclear protein, which is GTPase dependent). Secondly Imp7 interacts with Ran ligands and finally with nucleoporins which constitute the nuclear pore complex (NPC) (Gorlich and Kutay, 1999). The first step of import involves binding of DNA to the nuclear import receptor in the cytoplasm (Figure 1.6). This complex then interacts with the NPC, through recognition of specific amino acid residues (Fassati *et al*, 2003). The NPC/DNA complex is then transported through the NPC pore facilitating entry into the nucleoplasm. Once the DNA is successfully transported, the complex segregates and is transported back to the cytosol to begin another import cycle (Fassati *et al*, 2003).

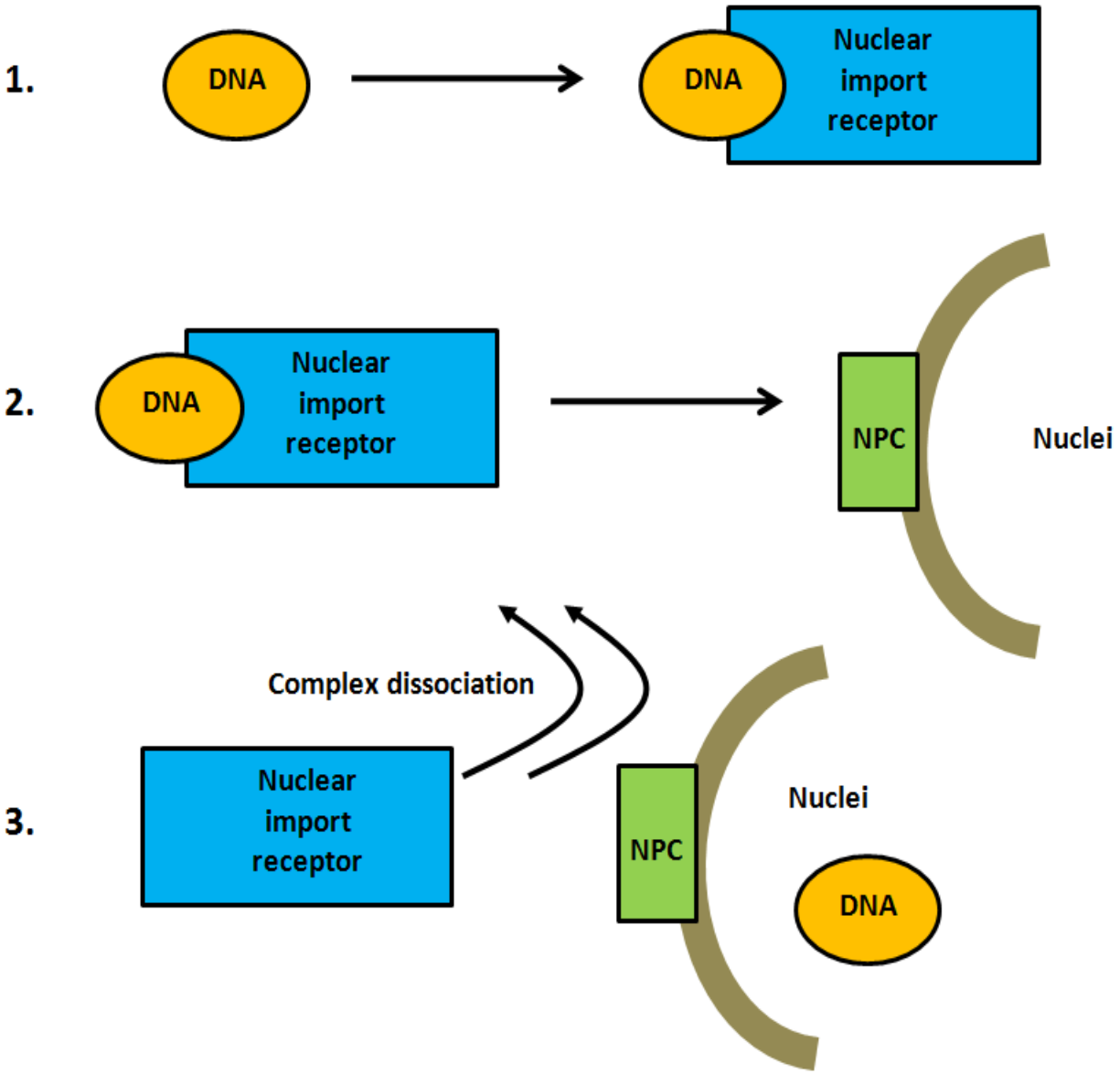

Figure 1.6: **Importin-7 (Imp7) mediated uptake of viral DNA.** Nuclear import receptor binds to its DNA cargo. The nuclear import receptor-DNA complex is then recognised by the NPC which grants passage through the nuclear pore.

1.4.3.1.2.2 NLS attachment

An alternative approach to enhance nuclear delivery of pDNA complexes is by physical attachment of nuclear localisation signal (NLS) peptides. NLSs are required to facilitate the nuclear entry of proteins and could favour pDNA nuclear entry (Paschal, 2002). NLS peptides facilitate nuclear entry by importin-mediated active transport (Zanta *et al*, 1999). NLSs are recognised by various importin proteins, in particular importin-α (Impα) which exhibits affinity for a sequence on the NLS. This interaction triggers the recruitment of importin-β (Impβ) which leads to the formation of a complex consisting of the polyplex/NLS conjugate combined with the importin proteins, which collectively are granted nuclear access via the NPC (Fernandez and Rice, 2009) (Figure 1.7). NLSs can be covalently attached to plasmids or with the polycations (Talsma *et al*, 2006). The use of NLS peptides to enhance nuclear entry of pDNA has been reported previously showing signs of promising results, but ultimately yielding insufficient gene expression (Pouton *et al*, 2007; Ciolina *et al*, 1999; Bremner *et al*, 2004; Nagasaki *et al*, 2003). In regards to clinical vaccination, incorporation of site specific ligands such as NLSs within DNA polyplexes can lead to improved gene expression which in turn can stimulate and increase immune response through T cell antigen presentation (Talsma *et al*, 2006). The application of NLSs to a wide range of structures is also appealing whereby a recent study covalently attached an NLS peptide to that of a pDNA intercalating agent and also those of liposomes (Zhang *et al*, 2009). Both poly- and lipoplexes were found to yield significantly improved gene expression than their respective controls by almost 3 fold (Zhang *et al*, 2009).

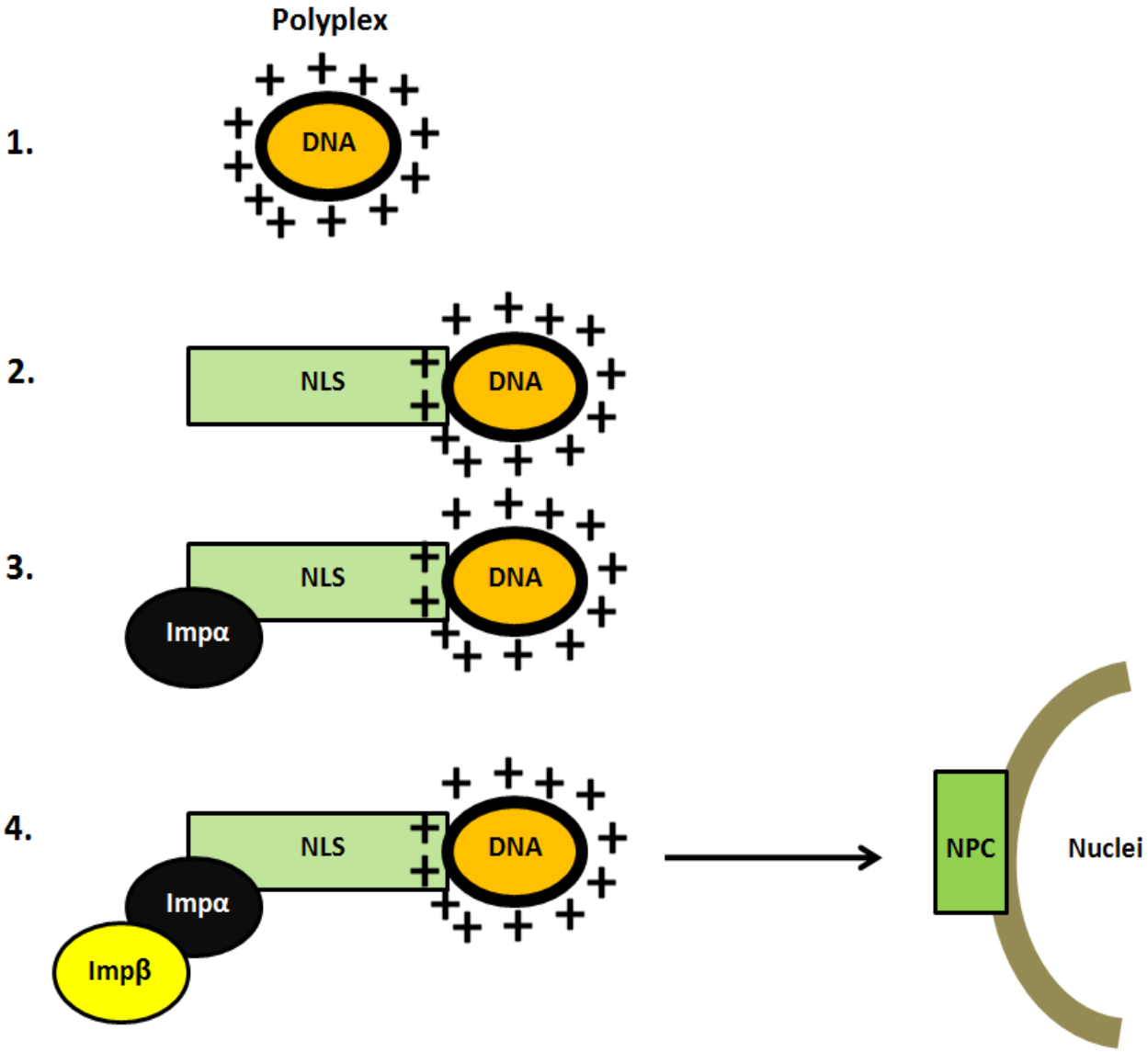

Figure 1.7: **Nuclear uptake of DNA polyplexes via NLS attachment.** The NLS peptide contains sequences that are recognised by Impα and Impβ which is then recognised by the NPC to allow nuclear passage.

1.5 Physical administration of DNA complexes

Physical administration of DNA is important in order to maximise cellular uptake and targeted delivery to achieve gene expression and desirable therapeutic effect.

1.5.1 Gene gun

Nucleic acid administration via gene gun (GG) (also commonly known as or particle mediated epidermal delivery, PMED) involves the coating of gold particles with pDNA and its direct delivery to the intracellular target by particle bombardment (Biewenga *et al*, 1997; Fuller *et al*, 2006). This method exploits small inert particles as delivery vehicles that can be accelerated to the point of facilitating cellular penetration through the epidermis (Fuller *et al*, 2006). The GG method contrasts to that of needle vaccinations in that it involves the direct *in vivo* entry of the DNA. Coated particles are in essence behaving like 'bullets' which are triggered and accelerated by to achieve cellular penetration (Biewenger *et al*, 1997). Electrical discharges or wavelength pulses have been successfully used as tools to 'fire' the particles towards target cells (Biewenga *et al*, 1997).

One of the first studies to apply GG delivery was that Klein *et al*, (1987) who suggested that the particle bombardment would result in penetration through the plant cell wall and enable pDNA delivery and expression. Soon application of GG to mammalian cells was successfully reported (Williams *et al*, 1991) and optimized further where such devices have since been applied in clinical trials (Fuller *et al*, 2006). The principle of GG delivery occurs on the basis of pDNA coated particle bombardment (usually upon the epidermis). Therefore its efficiency, optimisation and novel design are reliant on various physical boundaries (Sanford *et al*, 1993; Biewenga *et al*, 1997). The speed at which particles are fired towards the target is a major factor. This is because it is desirable to introduce pDNA coated particles at maximal speed to enable cellular entry, without jeopardising the structural integrity of the host cell membrane

(Biewenga *et al*, 1997). The physical characteristics of coated particles can dictate the speed at which it is delivered (Biewenga *et al*, 1997). Gold particles are often employed for GG delivery due to being non-toxic, exhibiting a suitable size and being unreactive, which all favour pDNA binding and cellular entry unlike other particle candidates (Russel *et al*, 1992; Fuller *et al*, 2006). Electrical discharge or changes in gas pressure have been successfully applied to enable particle bombardment (Biewenga *et al*, 1997). The latter has been applied more effectively for the delivery of particles at great velocities through inducing uniform pressure distribution. In gas pressure devices, the GG is composed of a chamber which houses the gas and confined by a form of membrane disk (Biewenga *et al*, 1997). When a specific amount of pressure is induced, the disk is broken resulting in a pulse that ripples through a neighbouring chamber that harbours a particle coated disk coated and such pressure applied forces the particles through the screen of the gun upon the exposed tissue (Sanford *et al*, 1993). Helium is often employed due to having a low density thereby facilitating greater acceleration (Takeichi *et al*, 1992).

The clinical efficiency of the GG method was reported, when compared with that of intramuscular (IM) injection. GG delivery of an encoded antigen vector was found to elicit $CD4^+$ T cells that reduced the development of diabetes within diabetic mouse models (Goudy *et al*, 2008). This was in stark contrast to IM administration whereby little or no effect was observed coupled with undesirable side effects (Tisch *et al*, 2001; Weaver Jr *et al*, 2001). In fact even when the amount of DNA introduced within mouse models was 100 times less than that loaded via IM delivery, expression was still vastly superior (Goudy *et al*, 2008). This indicates the potent penetration that GG can offer whereby particle loaded plasmids are transported to the cytoplasm thereby avoiding the intracellular membrane boundaries that often restrict gene delivery (Fuller *et al*, 2006). Additionally it was observed how GG delivery of the β cell autoantigen led to significant reduction of type 1 diabetes onset. In

contrast IM delivery of pDNA had no effect within 100% of treated mouse models developing type 1 diabetes.

1.5.2 DNA tattoo

DNA tattooing is an alternative form of nucleic acid administration which leads to effective introduction and subsequent expression of the gene of interest. DNA tattooing is an invasive technique entailing continuous perforating of the skin thereby causing immediate inflammation (Gopee *et al*, 2005). Although damage induced may not be quite applicable for immediate clinical trials, the wound generated recruits leukocytes, cells involved in cytokine secretion which is important for inducing specified immune responses (Pokorna *et al*, 2008). Unlike IM injection, tattooing entails pDNA delivery through a much greater surface area of the skin, thereby maximising the amount of cells likely to uptake DNA (Pokorna *et al*, 2008). DNA delivery via tattooing has actually been found to be more effective in terms of gene expression than that of IM delivery or GG (Sakurada *et al*, 2003; Baxby, 2002). The study carried out by Pokorna and colleagues is one of only a few publications to highlight how DNA tattooing induces greater innate and adaptive immune responses than counterpart procedures. In terms of adaptive responses, 100% of mice developed antibodies specific for the antigen delivered via tattooing, in comparison to 53% of mice administered via IM injection (Pokorna *et al*, 2008). Also antigen specific antibodies of those mice vaccinated via tattooing were up to 2000 times greater than injected models. Furthermore DNA tattooed mice generated antigen specific antibodies 16 times greater than their injected counterparts even in the presence of an adjuvant (Pokorna *et al*, 2008). In terms of innate responses Pokorna *et al*, (2008) reported an increase in IFN-γ cytokine levels in tattooed treated mice. Therefore such results indicate DNA tattooing as a useful procedure, albeit invasive, but effective in terms of inducing both innate and adaptive responses. It is suggested that tattooing induces a more robust immune response by possibly enhancing uptake of both non-

APCs and local APCs (through the large area of skin covered). The invasive nature of the procedure has been attributed towards recruiting local immune cells.

1.5.3 Needle injection

IM needle injection offers an alternative route towards stimulating host immune responses. IM needle vaccination involves the direct insertion of the respective nucleic acid. The purpose of such a procedure is that the nucleic acid encoding the antigen of interest interacts with APCs which via cross-presentation (Figure 1.5), are delivered to T cells (Belakova *et al*, 2007). Such a mechanism is an example of the adaptive response initiated by needle vaccinations which potentially leads to MHC-class II T cell response (Bivas-Benita *et al*, 2005).

Although the GG and DNA tattooing exhibit positive attributes, they do display various drawbacks such as the invasive nature posed and safety concerns. In light of this various studies have highlighted IM needle delivery as an effective gene vaccination tool. For instance Tanghe *et al*, (2000) compared the immunogenicity of mice when vaccinated via IM needle and epidermal GG. Immunogenic responses were greater in mice injected via IM needle vaccination unlike that of GG treated mice. Tanghe and co-workers (2000) found how mice treated via needle injections elicited a greater amount of antibodies than those of GG treated group.

1.5.4 Electroporation

An alternative method of DNA administration is electroporation (EP) which facilitates delivery through the induction of an electrical current at the site of administration. This leads to the formation of a porous membrane facilitating gene entry (Ulmer *et al*, 2006). EP has proven to be an effective manner in delivering nucleic acids, whereby small quantities of

even a microgram of DNA has led to detectable gene expression (Miao *et al*, 2001). This was highlighted in a previous study which observed improved antibody production and T-cell activity within primates as a result of EP mediated gene delivery (Otten *et al*, 2006). As mentioned in the Chapter, DNA vaccines have the potential to induce desirable innate and adaptive immune responses in the form of T-cell responses which was reported following EP mediated gene administration (Buchan *et al*, 2005). Thus the physical means by which pDNA enters the host cell is important, which stems from the porosity of the physical barrier (several microns), allowing safe passage of the nucleic acid.

1.6 Aims and Objectives

The aim of this work was to study non-viral gene delivery and how parameters such as DNA topology affect biophysical characteristics and uptake in mammalian cells. Non-viral gene delivery has generated interest in regards to recombinant protein production and treatment of various diseases. This is because unlike viral vector delivery, non-viral methods are considered safer (viral gene delivery systems can induce an immune response towards the vector), can be scaled up for manufacture and avoids issues such as potential insertional mutagenesis (mutation caused by the insertion of additional DNA within host organism). However unlike viral vectors, gene delivery via non-viral methods is relatively modest. Therefore understanding the parameters that affect DNA uptake is critical.

In terms of novelty the aim of this study was to analyse the impact of DNA topology on polyplex biophysical characteristics, mammalian cell uptake and potential nuclear import. This is important as very few studies have analysed this area which is important in regards to potential therapeutic applications. Furthermore the impact of DNA topology on polyplex uptake in variety of mammalian cells has not been reported particularly in dendritic cells which are key immune cells.

In this study a non-viral gene delivery system consisting of PLL complexed with a 6.8kb plasmid was formulated. Formation of PLL/DNA polyplexes are considered to display the suitable size and charge for successful gene delivery (Tsai *et al*, 1999). Therefore the application of DNA polyplexes has generated much interest. In this study uptake (defined as the intake of materials by a cell or tissue leading to its permanent or temporary retention) of PLL/DNA polyplexes was studied in three mammalian cell types; CHO cells, HeLa cells and DCs. DCs are of particular importance as they are key sentinels of the immune system and function by binding and collecting foreign antigens. Therefore one of the key goals of the project was to study polyplex uptake, gene expression (plasmid encoded *lacZ* [β-galactosidase] reporter gene) in all three cell types, and ability of polyplexes to alter DC phenotype.

The key objectives of this study included:

1. To formulate PLL/DNA polyplexes and analyse biophysical characteristics which included PLL/DNA surface charge, size, ability to evade nuclease degradation, ability of PLL to bind DNA, the effect of pDNA topology on biophysical characteristics and the impact of plasmid vector size.

2. To investigate the uptake of polyplexes within mammalian cells and whether biophysical characteristics impact on cellular uptake and reporter gene expression.

3. Report the mechanism of cellular uptake undertaken by DNA polyplexes. Nuclear import of DNA polyplexes which has important implications for gene delivery and potential therapeutic applications was addressed in this study.

4. Study whether uptake of polyplex DNA stimulates an anti-viral innate immune response, which is important for potential therapeutic applications.

This study combines biophysical analysis of PLL/DNA polyplexes with that of mammalian cell uptake studies to deduce if key parameters such as DNA vector topology have an effect on mammalian cell uptake. Knowledge of factors such as DNA vector topology, cellular uptake, mechanism of nuclear import, gene expression profiles, and the ability to induce innate anti-viral immune responses will aid in the design of improved non-viral gene delivery systems.

Chapter 2.
Materials and Methods

2: Materials and Methods

2.1 Plasmid DNA preparation

The plasmids; pSVβ (6.8kb) (Promega, Southampton, UK) is ampicillin resistant, pSELECT-NGFP-zeo (3.8kb) (InvivoGen, USA) is zeomycin resistant and pGEc47 (56.5kb) (Deutsche Sammlung von Mikroorganismen und Zellkulturen GmbH, Germany) is tetracycline resistant. Plasmids were transformed and propagated within *Eschericheria coli* (*E. coli*) DH5α cells. The pSVβ plasmid was selected as it is of a conventional size (6.8kb) for transfection studies and has been used in previous studies regarding PLL polyplex characterisation (Tsai *et al*, 1999). Plasmid maps are provided in Appendix I.

2.1.1 Culture medium and propagation of DH5α host cells

Luria Bertani (LB) medium (LB broth Lennox, Fisher Bioreagent, Loughborough, Leicestershire) was used for cell culturing along with Nutrient Agar CM0003 (Oxoid, Basingstoke, Hampshire) for the production of agar plates. The appropriate amount of antibiotics was added for selection of the desired plasmid (100µg/ml ampicillin, 25µg/ml zeomycin and 100µg/ml tetracycline). Cultures was grown overnight for approximately 16 hours at 37ºC within a rotary incubator at 250 rpm. In terms of pGEC47, cultures were grown for 36 hours. The cultures were then treated with glycerol (50% of total volume) which served as stocks and stored at -80ºC.

2.1.2 Plasmid DNA purification

Plasmids were routinely purified via Qiagen mini (small scale cultures) and maxi kits (large scale cultures) (Qiagen, Crawely, West Sussex). Plasmids were purified in accordance to the

manufacturer's protocol. Purified plasmids were analysed via agarose gel electrophoresis and quantified by a NanoDrop ND-1000 Spectrophotometer (NanoDrop Technologies).

2.1.3 Production of linear and nicked (open circular) plasmids

Purified supercoiled (SC) pDNA samples were both nicked and digested to generate open circular (OC) and linearised topologies. These samples were analysed upon a 1% agarose gel along with a naked untreated SC sample which served as a control. Restriction digestion was carried out using *PstI* and *Bam*HI enzymes (New England Biolabs). These enzymes were chosen as they cut at a single site upon the respective plasmid. Open circular (OC) forms were generated via the enzyme; Nt.*Bst*NBI as this catalyses a single strand break (New England Biolabs). Generation of both linear- and OC-pDNA was carried out in accordance to the manufacturer's instructions (New England Biolabs). Plasmids treated with the nicking enzyme were incubated at 55ºC for 1 hour while restriction digested samples were incubated at 37ºC for the same period. Following restriction digestion and nicking, enzymatic reactions were halted by heat treatment at 80°C for 20 minutes followed by purification of the DNA via chloroform-phenol extraction (Sigma). DNA was further purified via ethanol precipitation which entailed treatment of DNA with 2.5 volumes of 100% ethanol followed by 0.1 volume of 3M Sodium Acetate (Sigma) and incubation at -80°C for 1 hour. Samples were centrifuged on a bench top centrifuge for 20 minutes at maximum speed. DNA pellets were than washed with 70% ethanol and centrifuged for 10 minutes and DNA pellets were resuspended in endotoxin free TE buffer (10mM Tris-Cl, pH 8.0, 1Mm EDTA) (Qiagen).

2.2 Agarose gel electrophoresis

1% agarose gels were prepared by dissolving 1g of agarose (Sigma) in 100ml Tris-Borate EDTA (TBE) 10x concentrate (Sigma). This was then treated with 500µg/ml ethidium bromide (Sigma). Agarose gels were usually run at 100V and 100mA for 1 hour. DNA

samples were run alongside a TrackIt™ 1kb Plus DNA Ladder (Invitrogen). For analysis of the pGEc47 BAC, a BAC-Tracker™ Supercoiled DNA Ladder (Epicentre® Biotechnologies) was employed.

2.2.1 Southern blot analysis

Biotinylated DNA (see below) along with a biotinylated 2-Log DNA ladder (0.1-10 kb) (New England BioLabs), which served as a positive control, were run upon a 1% agarose gel for approximately 1 hour. The gel was then treated with 0.2M HCl (Sigma Aldrich) at room temperature for 10 minutes, after which the gel was then rinsed in double distilled water (ddH_2O), followed by three 15 minute period washes with 0.4M NaOH (Sigma Aldrich). A small cover tray was then submerged with 10x SSC (saline sodium citrate stock [300mM sodium citrate, pH 7.0, containing 1M sodium chloride]) (Sigma Aldrich) which acted as the transfer buffer. Filter paper soaked with transfer buffer was layered upon the tray and covered with plastic wrap, with the exception of an excision made in the shape of the gel thereby facilitating sole wick transfer through the gel. The gel was placed upon the excision site made and a 0.45µm nitrocellulose membrane (Protran BA-85, Whatman) cut to the size of the gel was placed directly above the gel and stacked with paper towels to facilitate transfer by the conventional wick procedure overnight. The following day the membrane was removed and rinsed briefly with ddH_2O and then cross linked within a CL-1000 ultraviolet cross linker (UVP). Subsequently the membrane was then blocked for at least an hour in 1% BSA/PBS followed by addition of streptavidin – horse radish peroxidase (Amersham Bioscience) for 15 minutes. Three 15 minute washes with PBS (phosphate buffered saline [137mM NaCl, 2.7mM KCl, 4.3mM Na_2HPO_4 and 1.47mM KH_2PO_4, pH 7.4]) was then followed by treatment with ECL reagent (Amersham ECL Plus™, GE healthcare). The membrane was then developed through autoradiography. For dot blots, biotinylated DNA was spotted

directly upon the membrane, which was then blocked, probed and processed as mentioned previously.

2.3 Production and characterisation of PLL/DNA polyplexes

Plasmids of differing topologies were bound with poly-$_L$-lysine hydrobromide (PLL) (Sigma) of molecular weight, 9600. This was in accordance to that of Tsai *et al*, (1999). A constant amount of DNA (20µg) was added to PLL, each of varying charge ratios. These samples were treated with 100µl 10mM HEPES buffer stock and made up to 1ml with Millipore filtered (0.2µm filter) water to form final concentration of 1mM HEPES buffer. Calculation of the amount of PLL which yields the desired charge ratio was deduced from Lollo *et al*, (2002). Individual aliquots of DNA and PLL of equal volume (500µl each dissolved in 1mM HEPES buffer) were prepared and then mixed. Once the nucleic acid was added to the condensing agent, samples were left at room temperature for 30 minutes. A smaller total volume of 100µl was used for polyplexes prior to the addition of cells for transfection.

2.3.1 Zeta Potentials measurements

The zeta potentials of the polyplexes were recorded via a Malvern Zetasizer Nanoseries instrument (Malvern Instruments, Malvern). A polystyrene standard (Malvern Instruments) was employed to calibrate the system. Following this 700µl of the PLL/DNA polyplex was loaded within the system and zeta potentials were recorded. The temperature was set to 25ºC, along with the dispersant cell viscosity (to which values for water were used). Also the instrument was set to allow a 5 minute incubation period prior to measurements in order to allow the desired temperature (25ºC) to be attained. Following this zeta potentials were recorded whereby an average of 5 readings were taken.

2.3.2 Dynamic light scattering (DLS) assays

Polyplex mean diameters were deduced by dynamic light scattering (DLS) measurements (90° angle scattering laser) via a Malvern Zetasizer Nanoseries instrument (Malvern Instruments, Malvern), whereby measurements were recorded at 25ºC. Prior to size measurements a low volume 45µl glass cuvette was rinsed with 70% ethanol and Millipore filtered water. The system was then blanked with 45µl Millipore filtered water (to reduce the particle count rate to less than 20kcps) followed by size measurements (nm) of which an average of ten readings were recorded.

2.3.3 DNA intercalating dye studies

2.3.3.1 Ethidium bromide assay – quantification of DNA condensation induced by PLL

Polyplexes were quantitatively analysed in terms of pDNA packaging and condensation via an ethidium bromide fluorescence assay. 10µg of polyplex DNA was treated with 2µg ethidium bromide and made up to a total volume of 200µl. These samples were loaded upon a standard 96 well plate along with a control consisting of 10µg of purified plasmid (corresponding to the respective topology) and 2µg ethidium bromide as mentioned previously. Samples were analysed via a Safire^2 plate reader at an emission wavelength of 591nm and excitation wavelength of 366nm (slit width of 20nm). Fluorescent values were expressed as a percentage of a naked DNA control

2.3.3.2 TOTO-3 fluorescence assay – quantification of DNA condensation induced by PLL

The dye; TOTO-3 (Dimeric Cyanine Nucleic Acid Stains – Invitrogen) was added to 10µg of polyplex DNA at a final concentration of 4µM and fluorescence was measured (excitation:

642nm and emission: 660nm). Fluorescent values were expressed as a percentage of a naked DNA control.

2.3.4 Ethidium bromide staining of DNA prior to PLL binding

In order to view the DNA that was eventually to be condensed by PLL, 20µg DNA was stained with 1µg ethidium bromide and then complexed with PLL as previously mentioned. Samples were analysed by electrophoresis using agarose gels without ethidium bromide for a short time period of only 10 minutes in order to view DNA complexed to PLL.

2.3.5 Release of PLL-bound pDNA

DNA was released from PLL by treating polyplex samples with 0.5% SDS (sodium dodecyl sulphate) (Sigma) and heating samples at 96°C for ten minutes. DNA was then precipitated with 70% ethanol.

2.3.6 Benzonase nuclease protection assay

In order to test the potential *in vivo* stability of polyplexes (of varying charge ratios), samples were treated with Benzonase nuclease (Novagen). 0.2µg polyplex DNA was treated with 50 units of the nuclease and incubated for 30 minutes at 37ºC. This was carried out in conjunction with suitable controls (naked untreated pDNA and an untreated polyplex). Within this 30 minute period at 5 minute intervals, samples were extracted and analysed via 1% agarose gel electrophoresis. The enzyme was inactivated via treatment with 100mM NaOH at 70°C for 30 minutes. DNA samples were extracted via precipitation with 70% ethanol.

2.4 Labelling of polyplexes

2.4.1 Fluorescent tagging of PLL

PLL was tagged with a fluorescent marker, Oregon Green 488, succinimidyl ester (Invitrogen) according to the protocol executed by Godbey *et al*, (1999). Unbound dye was removed by spin column purification in accordance to the manufacturer's protocol (Invitrogen). Successful tagging was confirmed by analysing the fluorescence of tagged PLL to that of unlabelled PLL via a safire^2 plate reader at an excitation wavelength of 488nm and an emission wavelength of 521nm (slit width of 20nm) in addition to the protocol provided by the manufacturer (Invitrogen).

2.4.2 Labelling of pDNA

Naked pDNA was directly biotinylated (Mirus Label IT tracker Intracellular Nucleic Acid Localization Kit) according to the manufacture's protocol. DNA was labelled at a 0.25:1 v:w ratio of reagent per µg of DNA. Free biotin was removed from the DNA via DNA ethanol precipitation with 70% ethanol according to the manufacture's protocol. Presence of biotinylated DNA was then confirmed through Southern Blot analysis. Plasmid DNA was alternatively labelled via the nucleic acid fluorescent stain; TOTO-3 (Dimeric Cyanine Nucleic Acid Stains – Invitrogen) at a final concentration of 4µM. The fluorescent stain exhibits excitation and emission spectra of 642 and 660nm respectively for analysis via confocal microscopy. To confirm successful TOTO-3 tagging, labelled polyplex fluorescence was measured by a safire^2 plate reader at the specific fluorophore spectra along with the appropriate controls which included naked TOTO-3 stained DNA, TOTO-3 labelled DNA/PLL complex, unlabelled naked DNA and unlabelled DNA/PLL complex. Additionally labelled TOTO-3 DNA was spotted onto PLL (labelled via Oregon Green tagging) coated coverslips which were subsequently mounted onto slides for confocal microscopy analysis.

PLL coated coverslips were prepared by treating coverlsips with 50µg/ml PLL for 30 minutes at room temperature. Coverslips were washed and then used for further analysis. Further confirmation of successful TOTO-3 DNA labelling entailed spotting TOTO-3 labelled DNA upon coverslips for a period of 10 minutes at room temperature and then treating such samples with a 50µl of Flow-Check Fluorophore beads (Beckman Coulter).

2.5 Mammalian cell culture

2.5.1 Chinese hamster ovary (CHO) cell culture

Chinese hamster ovary cells (CHO) which were adherent, were cultured in 5ml GIBCO® RPMI (Roswell Park Memorial Institute) Media 1640 (5% foetal calf serum [FCS] and 1% penicillin:streptomycin [PS]) (Invitrogen) in a 37°C, 5% CO_2 incubator. Prior to transfection media was aspirated and cells were washed with Hank's Buffered Salt Solution (HBSS) (Invitrogen) and then treated with 1x concentrate trypsin (2.5% trypsin which contains 25g/L trypsin and 8.5g/L NaCl) for 3 minutes at 37°C. Cells were then neutralised with media. From this a 10µl sample of cells was strained with Trypan Blue (Invitrogen) and counted. Approximately 1 x 10^6 CHO cells were seeded upon sterilised 22 x 22mm coverslips (VWR International), which were mounted within 6-well plates (Helena Biosciences) and incubated for approximately 41hours.

2.5.2 Generation of human monocyte-derived dendritic cells (DCs)

This study was approved by the joint University College London/University College London Hospitals National Health Service Trust Human Research Ethics Committee and written informed consent was obtained from all participants.

Monocyte-derived human dendritic cells (DCs) were initially produced via selection of $CD14^+$ cells. Human blood samples were treated with HBSS at a volume ratio of 1:0.5ml.

Samples were then extracted using heparinised syringes and transferred to tubes containing Lymphoprep (Axis-Shield). Samples were centrifuged at room temperature, 800xg for 20 minutes. Interface layer was removed and transferred to tubes containing HBSS. Samples were centrifuged at room temperature at 800xg for ten minutes. Supernatant was discarded and the cell pellet was dissolved in 5ml HBSS. This cell suspension was washed three times, with each wash step entailing; centrifuging at room temperature at 400xg for 5 minutes, discarding the supernatant and re-suspending in 5ml HBSS. After the third wash spin step, sample was re-suspended in cold MACS buffer (PBS, 10% FBS + 2mM EDTA) (400µl/100x10^6 cells). Anti-CD14 beads (Miltenyi Biotec) (50µl/100x10^6 cells) were added. Samples were incubated on ice for 30 minutes. Following this 10ml MACS buffer was added and samples were centrifuged at 400xg for 5 minutes at room temperature. Supernatant was discarded and re-suspended in 4ml cold MACS buffer. This was then passed through a sterile filter and collected. The filtered cell suspension was then was then passed through a MACS column which was attached to a pre-cooled MACS magnet. This was followed by the addition of MACS buffer (wash step). Collection of $CD14^+$ cells was achieved by adding 5ml cold MACS buffer and detaching column from the magnet. Sample was topped up with RPMI media 1640 and centrifuged at 400g for 5 minutes at room temperature. Supernatant was discarded and pellet re-suspended in DC differentiation media (RPMI, 10%FCS, GM-CSF [granulocyte-macrophage colony-stimulating factor] +IL4). Cells were seeded for 4 days at 37°C, 5% CO_2.

2.5.3 HeLa cells

HeLa cells were employed for importin-7 (Imp7) knock down (KD) studies. Control HeLa cells and Imp7 KD cells were kindly provided by Dr Ari Fassati (Wohl Virion Centre, UCL) in which KD was carried out previously (Zaitseva *et al*, 2009). Two controls were employed; HeLa cells containing an shRNA targeting the *Discosoma corallimorpharian* DsRed mRNA

(DxR) and HeLa cells that were back complemented with an Imp7 cDNA containing two silent mutations conferring resistance towards Imp7 gene silencing (Back Imp7). Two Imp7 KD clones were also employed; clone 2 (Cl2) and clone 4 (Cl4) (Zaitseva *et al*, 2009). HeLa cells were cultured in Delbecco's modified Eagle's medium (DMEM) (GIBCO®), with the addition of 10% FCS, 2mM glutamine and 1µg/ml puromycin at 37°C in 5% CO_2.

2.6 Mammalian cell uptake studies

2.6.1 Bolus transient transfection (for adherent cells)

Following seeding (48 hours), media was aspirated and replaced with fresh media lacking serum. Samples were left to incubate at room temperature for 10 minutes. 2µg of polyplex DNA (total DNA mass as deduced from nanodrop spectrophotometer analysis) was then added to the media and incubated at 37°C. Polyplexes were prepared at charge ratios of; +1.6 for SC- and OC-pDNA, and +5 for linear-pDNA. This particular charge ratio was selected due to recommendation by previous biophysical polyplex studies (Tsai *et al*, 1999). This particular charge ratio was also used for PEI polyplexes (Dunlap *et al*, 1997). Linear-pDNA required a higher charge ratio to satisfy a net positive charge necessary for transfection studies. Following the desired duration of transfection, samples were extracted and media aspirated. Cells were washed once with HBSS. Subsequently cells were treated with 1ml 3.8% paraformaldehyde and incubated for 15 minutes. This was followed by washing with PBS and the addition of 1ml 0.2% Triton-X (in PBS) for 10 minutes. In regards to confocal microscope analysis, coverslips were removed and mounted onto a microscope slide with DAPI mounting medium (Vectashield). In the case of transfected samples which were to be analysed by flow cytometry, samples were processed in BD FACS Calibur tubes (BD FACSCalibur) whereby washing steps entailed centrifugation at 1400rcf for 5 minutes.

2.6.2 Reverse transfection (for non-adherent cells)

Polyplexes were spotted (each spot contained either 2µg pDNA for confocal microscopy analysis or 20µg pDNA for gene expression studies) on PLL (50µg/ml) coated 22 x 22mm coverslips (VWR International) for 1 hour at room temperature in the dark. Subsequently cells were seeded (with the respective media, RPMI, DMEM or DC differentiation media) on the PLL coated coverslips and incubated at 37°C for the desired time. Following this cells were removed and processed as mentioned previously.

2.6.3 Gene expression analysis

Cells were seeded within 6-well plates (Helena Biosciences) for 48 hours to an approximate confluency of 80%. Subsequently cells were then transfected with polyplexes at the desired charge ratio for 48 hours. Following this period mammalian cells (CHO, DC or HeLa) were analysed for β-galactosidase expression to which the plasmid (pSVβ) encodes. Expression was detected using a colorigenic β-Gal Assay Kit (Invitrogen). The number of blue cells detected under a Ti-E light microscope (Nikon) connected with a Fi-1 CCD camera (Nikon), in 5 fields of view was expressed as a percentage of total cells.

2.6.4 Labelling of mammalian cells

Mammalian cells (CHO, HeLas and DCs) fixed to 22 x 22mm coverslips (VWR International) were stained following transfection with HCS CellMask™ Stains (Invitrogen) for a period of 30 minutes according to the manufacture's protocol. The stain displays excitation and emission spectra of 556 and 572nm respectively.

2.6.5 Intracellular tracking

To deduce uptake mechanisms, transfection experiments were repeated as previously mentioned, however this time incorporating specific endocytic markers. Transfected cells

were treated with a Rab5 antibody (Cell Signalling Technology) at a 1:100 dilution factor (10µg/ml) and incubated at 4°C overnight. The Rab5 antibody (source: rabbit) reactivity includes human, mouse, rat, hamster, and monkey. Cells were then washed three times with PBS and probed with the appropriate secondary fluorescent antibody; anti rabbit IgG (H+L), $F(ab')_2$ Fragment (Alexa Fluor® 488 conjugate) (Cell Signalling Technology) at a 1:100 dilution factor for 2 hours at room temperature protected from light. Rab5 is a marker for early endosomes particularly in the clathrin mediated endocytic (CME) pathway.

Alternative endocytic markers were also employed. Transfection experiments were repeated as before; however cells were treated with anti-caveolin-1 antibodies (reactivity includes mouse, rat, hamster, dog, human, Chinese hamster) (Abcam) at a dilution factor of 1:500 (20µg/ml) at 4°C overnight. Caveolin-1 antibody is a specific marker for the caveolae endocytic pathway. The following day cells were washed three times with PBS and treated with anti rabbit IgG (H+L) secondary FITC conjugated antibody (Abcam) at a dilution factor of 1:100 for 2 hours at room temperature protected from light.

2.6.6 Pathway inhibition experiments

In order to confirm the role of the CME pathway, the inhibitor; chlorpromazine hydrochloride (CMZ) (Sigma) was dissolved in RPMI media and applied to CHO cells at a final concentration of 10µg/ml for 2 hours at 37°C (Vercauteren *et al*, 2010) prior to transfection with polyplexes and probing of endocytic markers. CHO cells were also treated with 400µM genistein (Sigma) at 37°C for 2 hours (Vercauteren *et al*, 2010). Genistein is an inhibitor of the caveolae endocytic pathway. Samples were analysed by confocal microscopy or flow cytometry.

Control commercial endocytic markers were studied. Transferrin (Tran) (Invitrogen) and cholera toxin subunit B (CTB) (recombinant) (Invitrogen) were added to CHO cells (both at

10µg/ml each at 37°C for 20 minutes) according to Nagabhushana *et al*, (2010); Skretting *et al*, (1999), and the manufacturer's protocol. Dilutions and storage buffers of antibodies were made in PBS.

2.6.7 Confocal microscopy

2.6.7.1 Fixed cell analysis

A Leica SP2 confocal microscope (Division of Infection and Immunity, UCL) was used to view cells that were mounted on the appropriate slides. Fluorescence images were collected using a scan speed of 400 Hz and 8 frame averaging. Nuclei were detected using 4,6-diamidino-2-phenylindole (DAPI) (Vectashield) (excitation: 360nm, emission: 460nm). DNA was detected via TOTO-3 (Dimeric Cyanine Nucleic Acid Stains – Invitrogen) (excitation: 642nm, emission and emission: 660nm). DNA was also detected via Alexa Fluor 633 streptavidin (excitation: 632nm, emission: 647nm). PLL was detected via Oregon Green 488 (Invitrogen) (excitation: 488nm, emission 524nm) and cell labelling was detected by HCS CellMask™ (Invitrogen) (excitation: 556nm, emission: 572nm). To confirm whether polyplex uptake has occurred, images were taken as 3-D sections. Ten sections of each image, each of 0.2µm in thickness were taken. Mid section images were taken to confirm true polyplex uptake along with projection images of all slices (referred to as z-stack projection images).

2.6.7.2 Live cell imaging

HeLa cells were seeded (approximately $5x10^5$ cells per well) overnight on an 8 well chambered glass coverslip (Lab-Tek^{TM}) at 37°C. The following day the media was removed and replaced with RPMI 1640 (1x) media without phenol red (Invitrogen). Cells were treated with 5µg/ml Hoechst 34580 nuclear stain (Invitrogen) for 2 hours at 37°C. The coverslips

were then mounted upon a Leica SPE2 inverted microscope with sequential channel capture. The microscope chamber temperature was set at 37°C and fluorescently labelled polyplexes (containing 2µg DNA) were added to the cells and imaging was carried out immediately to monitor transient transfection in real time. Images were recorded every 2 minutes up to 1 hour. Slice-by-slice sectioned images of single cells were captured at a thickness of 0.2µm. A total of 10 image slices were taken at each time point. Each frame of the time lapse series was processed on ImageJ software.

2.6.7.3 Quantification of uptake

To quantify uptake approximately 30 cells from each slide were randomly selected under the DAPI filter and the number of cell associated polyplexes were counted and classified on the basis of their intracellular location (cell periphery, cytosol or nuclei of the respective cell) using ImageJ software and fluorescent co-localisation. If no fluorescent overlap between the polyplex and the CellMask™ occurs, complexes are defined as being at the cell periphery. If some overlap between the polyplex and the CellMask™ occurs, complexes are classified as located within the cytosol. Complete overlap between polyplex and nuclear stain is classified as nuclear association. The number of polyplexes within each cellular compartment was expressed as a percentage of the total number of polyplexes counted within the group of 30 cells. The number of cells (30) was selected as this was found to be statistically sufficient for quantification as recommended by previous studies (Akita *et al*, 2004; Chen *et al*, 2008). Each experiment was repeated in triplicate. Slides were blinded with regard to experimental condition before counting to reduce possible bias.

2.6.8 Flow cytometry

A FACS Calibur 2 flow cytometer was employed to analyse transfected CHO and DC populations of approximately $1x10^6$ cells. Transfected cells were suspended within 300µl PBS and stored at 4°C prior to analysis upon a FACS Calibur 2 flow cytometer.

2.7 Quantitative polymerase chain reaction (Q-PCR)

2.7.1 RNA extraction

HeLa cells (DxR control, Back Imp7, Cl2 and Cl4 Imp7 KD) were seeded in 6-well plates (approximately 1 x 10^6 cells per well) for 48 hours. Cells were transfected with polyplexes containing 20µg or 0.2µg pDNA for 4 hours (time required to stimulate anti-viral response). Following this cells were centrifuged (1400 rcf for 5 minutes) to attain pellets and RNA was extracted via an RNeasy Mini Kit (Qiagen) according the manufacturer's guide. All subsequent reactions were carried out in RNase free conditions.

2.7.2 Removal of DNA contaminants

Removal of DNA contaminants from purified RNA samples was achieved via a DNA-*free*™ Kit (Applied Biosystems). Protocol was carried out in accordance to the manufacturer. Purified RNA was stored at -80°C.

2.7.3 Reverse transcription (cDNA synthesis)

Production of the cDNA template was carried out via an Omniscript® Reverse Transcription Kit (Qiagen) according to the manufacturer's handbook. All subsequent reactions were carried out in DNase free conditions.

2.7.4 Taq man polymerase chain reaction

Q-PCR was performed in a final reaction volume of 25µl containing 1x PCR buffer including Taq man polymerase enzyme (Platinum® Quantitative PCR Super Mix-UDG w/ROX, Invitrogen) along with 7.5µM of each primer (forward, reverse and probe) according to the manufacturer's protocol. Primer sequences were as follows; GAPDH (glyceraldehyde 3-phosphate dehydrogenase) forward: 5'-GGCTGAGAACGGGAAGCTT-3, GAPDH reverse: 5'-AGGGATCTCGCTCGCTCGCTCGCTCCTGAA-3', GAPDH probe: 5'FAM-TCATCAATGGAAATCCCATCCCATCACCA-3' which was fluorescently labelled with 6-carboxyfluorescein (FAM, at a filter setting of 520nm). GAPDH is a housekeeping gene whose expression remains constant and was measured as a control. IFIT2 (interferon induced protein with tetratricopeptide repeats-2) was probed for expression. Along with the 1xPCR buffer, the 25µl was supplemented with IFIT2 mix (Applied Biosystems) which contained the IFIT2 forward, reverse and probes. The Q-PCR reaction was supplemented with 5µl cDNA and Millipore filtered water was added to the master mix (to compensate the final volume to 25µl). Q-PCR was performed on an Eppendorf MasterPlex. Cycle conditions included; 55°C for 2 minutes, 95°C for 10 minutes; 95°C for 15 seconds and 60°C for 1 minute for 40 cycles. Data attained via an Eppendorf MasterPlex was recorded as Ct (cycle threshold) values. The Ct value refers to the number of cycles required for the fluorescent signal to cross the threshold (beyond background fluorescence). Ct values are inversely proportional to the amount of target DNA sample present, hence high Ct values equate to low gene expression. Ct values were normalised against those of housekeeping genes whose expression remains constant (GAPDH). Ct values were normalized with those of the housekeeping gene GAPDH to yield delta Ct (dCt) values (dCt = IFIT2 Ct – GAPDH Ct).

2.8 DC phenotype measurements

Polyplexes containing 20µg of pDNA were reverse transfected into DCs (approximately 1.9 x10^6 cells per well). Two wells were used and designated for transfected cells and untransfected cells as a control. Cells were transfected for a period of 48 hours. After this cells were carefully transferred to a 5ml collection tube through gentle pipetting action in order to loosen attachment to the PLL coated coverslip. Cells were centrifuged at 1400rcf for 5 minutes and the supernatant was discarded. The pelleted DCs were then probed for β-galactosidase activity via an ImaGene Green™ C_{12}FDG *lacZ* Gene Expression Kit (Invitrogen) according to the manufacturer's protocol. Cells were centrifuged and resuspended in PBS, to which 100µl was aliquoted to tubes each containing 2µl antibodies for the following DC surface markers; IgG1, IgG2b, CD1a, DC-SIGN, CD11c, MHC-I, MHC-II, CD40, CD80, CD83 and CD86 (BD Pharmingen). Antibodies were fluorescently labelled with far red dyes phycoerythrin (PE) or allophycocyanin (APC) which do not overlay with the green fluorescence corresponding to β-galactosidase positive cells. Treatment of transfected and untransfected DCs with the antibodies entailed a 20 minute incubation period at room temperature in the dark. Cells were then centrifuged and resuspended in 300µl PBS and analysed by flow cytometry.

2.9 Statistical analysis

Student's t-test and one-way ANOVA were employed to deduce levels of statistical significance. Level of significance selected was $p = 0.05$. Bonferroni's Multiple Comparison's Test (GraphPad Prism) was used for statistical analysis for Q-PCR studies ($p = 0.05$).

Chapter 3. Characterisation of DNA polyplexes

3. Characterisation of DNA polyplexes

Non-viral gene delivery is increasingly becoming the focus of biotechnology industries as it avoids safety hazards brought about by viral delivery of DNA. Many studies have focused on the use of polymers as a means of gene delivery. Such polymers bind to DNA and condense it to form small nanoparticles that facilitate cellular uptake (Hartmann *et al*, 2008). Polymers are also referred to as polycations as they harbour an excess of positively charged residues which neutralises the negatively charged DNA backbone through electrostatic interaction. Such interaction results in the formation of polycation/DNA complexes – referred to as polyplexes.

In this study poly-$_L$-lysine (PLL), a widely used polymer was employed to bind with pDNA for potential non-viral gene delivery. Benefits offered by PLL include the ease and rapid ability by which it binds with pDNA, allowing successful delivery of genes (Fu *et al*, 2011; von Erlach *et al*, 2011). The current chapter focused on the biophysical characterisation of polyplexes such as the charge, size, degree of pDNA condensation induced by PLL and nuclease resistance of DNA polyplexes. Moreover the chapter addresses whether key factors such as DNA topology, ionic strength, charge ratio (ratio of PLL to pDNA) and plasmid size affect polyplex characterisation. Factors such as DNA topology are important from regulatory viewpoints (Guidance for Industry: Considerations for Plasmid DNA Vaccines for Infectious Disease Indications – FDA, 2007) and therefore characterisation of PLL/DNA polyplexes is critical in regards to understanding and optimising non-viral gene delivery strategies.

3.1 Preparation of different DNA topologies

Plasmids can display a variety of conformations. Plasmids often exhibit a natural supercoiled (SC) condensed structure. Alternatively pDNA can be cut (via restriction enzymes) at specific nucleotide sites to generate an uncoiled linear form (Anada *et al*, 2005). Plasmids can also have one strand nicked resulting in open circular (OC) forms (refer to Chapter 1, section 1.1.2). Therefore to study the effects of DNA topology on polyplex biophysical characteristics, linear and OC (as well as using SC) forms of the same plasmid (6.8kb) were generated. Restriction digestion (Figure 3.1a and 3.1b) and plasmid nicking (3.1c and 3.1d) were carried out via enzyme treatment as described in Chapter 2, section 2.1.3. Samples were analysed via agarose gel electrophoresis. Linearization and nicking of the plasmid occurred rapidly at less than 10 minutes. Production of OC- and linear-pDNA was confirmed by agarose gel electrophoresis whereby OC-, linear- and SC-pDNA have distinct electrophoretic mobilities (refer to Chapter 1, section 1.1.2). DNA migrates through the gel on the basis of size whereby the condensed SC form is the smallest which facilitates electrophoretic migration through the gel. The linear form containing a double strand cut is larger and migrates slower, followed by OC-pDNA which migrates the slowest (Figure 3.1e).

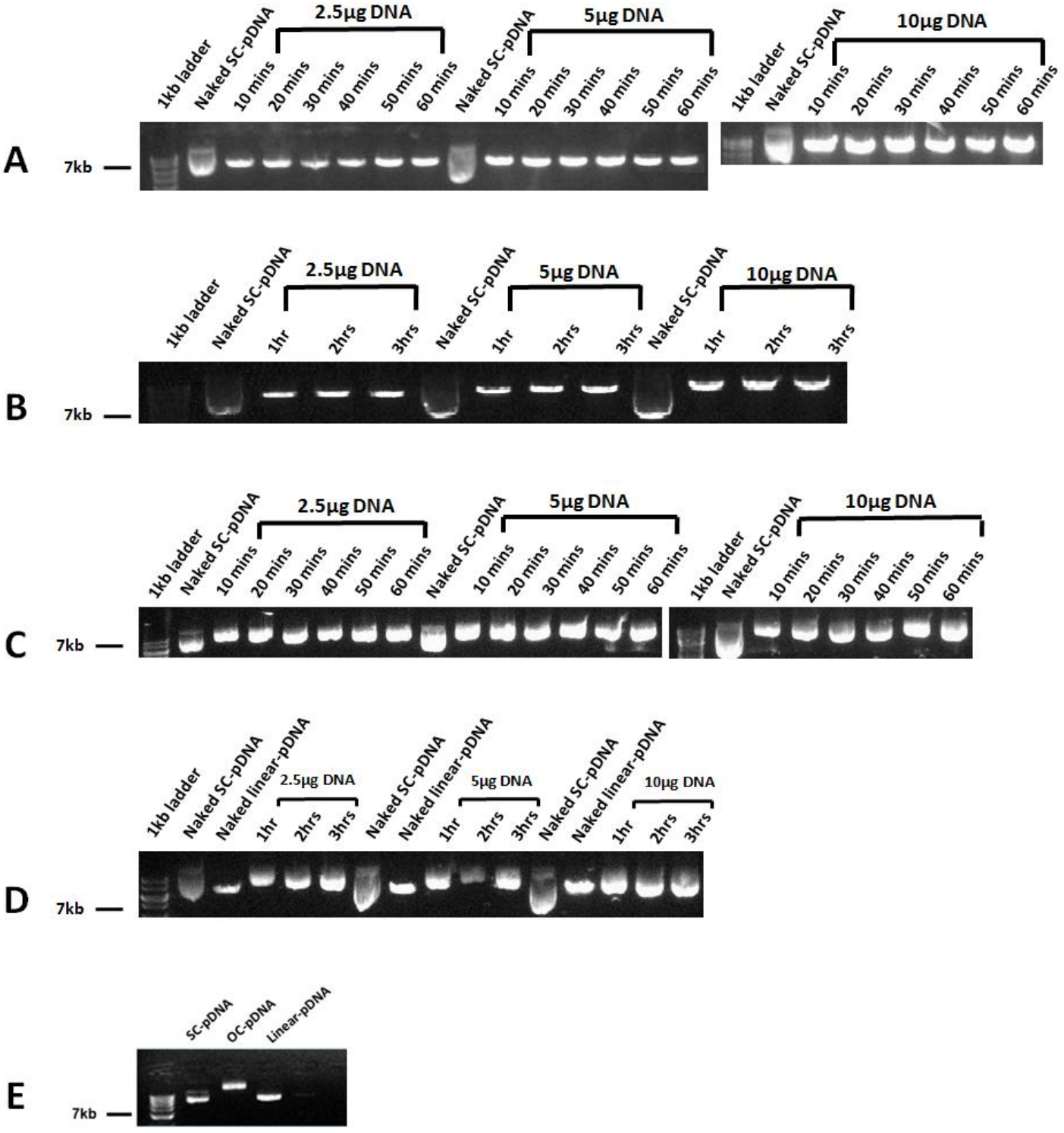

Figure 3.1: Restriction digestion and nicking of the pSVβ (6.8kb) plasmid. Assays were carried out in short and extended time courses. Restriction digestion (A-B) was carried out via the *PstI* enzyme and OC forms (C-D) were generated via Nt.*Bst*NBI. Electrophoretic mobilities corresponding to different DNA forms (E). The amount of enzymes used was 1 unit per µg of DNA as recommended by the manufacturer, New England Biolabs.

3.2 Confirmation of polyplex formation

Confirmatory assays are critical in order to identify successful complex formation. PLL and the respective nucleic acid (pSVβ, 6.8kb) form DNA polyplexes on the basis of electrostatic interactions. The present study focused on the interaction between the plasmid of varying topology (SC, OC or linear-pDNA) and that of PLL (molecular weight 9600).

3.2.1 Polyplex zeta potential measurements

Zeta potential studies enable a good method of characterising the surface charge of DNA polyplexes. This is important as surface charge is a key factor of non-viral gene delivery. The aim of this particular experiment was to measure zeta potentials of PLL/DNA polyplexes to confirm PLL interaction, and whether DNA topology affects this. A constant amount of pDNA (20µg) was added to varying amounts of PLL (2.67-66.67µg) in order to vary the PLL/DNA charge ratio. The charge ratio refers to the ratio of positively charged amine groups of PLL to that of the negatively charged phosphate groups of pDNA (high charge ratio values correspond to greater amounts of PLL and net positive charge). Formation of polyplexes is a rapid process that occurs almost instantaneously when cationic polymer and anionic phosphate groups interact (Hartmann *et al*, 2008). SC-pDNA showed an efficient charge neutralisation, losing its net negative charge with PLL at ratios of 0.6 or above (Figure 3.2). OC-pDNA required a slightly higher ratio of PLL (approximately +1) to neutralise the plasmid net negative potential. In contrast linear-pDNA complexes exhibited a more gradual conversion towards a net positive surface charge requiring a ratio of at least +2 to neutralise the overall negative charge.

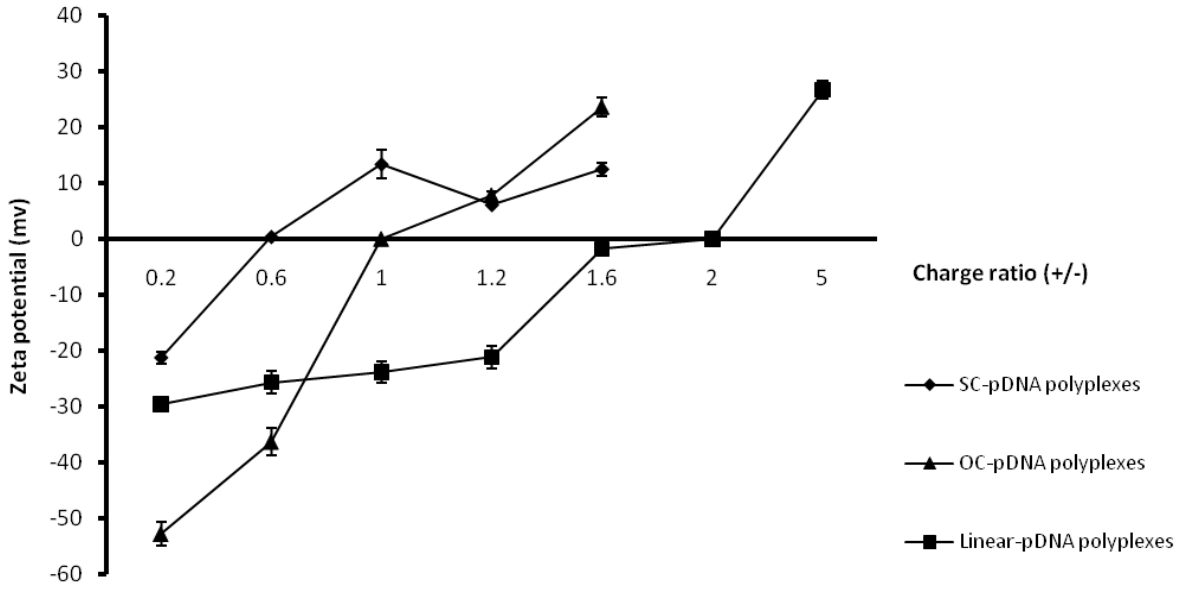

Figure 3.2: **Zeta potential measurements of DNA polyplexes**. The surface charge of SC-pDNA, OC-pDNA and linear-pDNA polyplexes made at different PLL/DNA ratios (1mM HEPES, pH 7.5), was estimated by measuring the particle zeta potentials as described in Chapter 2, section 2.3.1. The figure shows the mean and standard error (SE) of 5 replicate measurements. The experiment was repeated 3 times independently. One-way ANOVA was employed to deduce levels of statistical significance ($p < 0.05$) between complexes of differing DNA topologies.

3.2.2 Gel retardation and observation of DNA released from PLL

To further confirm successful polyplex formation, complexes were analysed by agarose gel electrophoresis. This experiment was selected as a change in surface charge, as detected in Figure 3.2, would be validated by electrophoretic analysis. The formation of polyplexes was associated with a decreased ability to bind ethidium bromide (EtBr) (due to PLL/DNA interaction restricting EtBr intercalation and fluorescence), and reduced electrophoretic migration (as a result of the change in zeta potential) (Figure 3.3a). Reduced EtBr staining appeared to occur at the same PLL/DNA ratio for all three topologies.

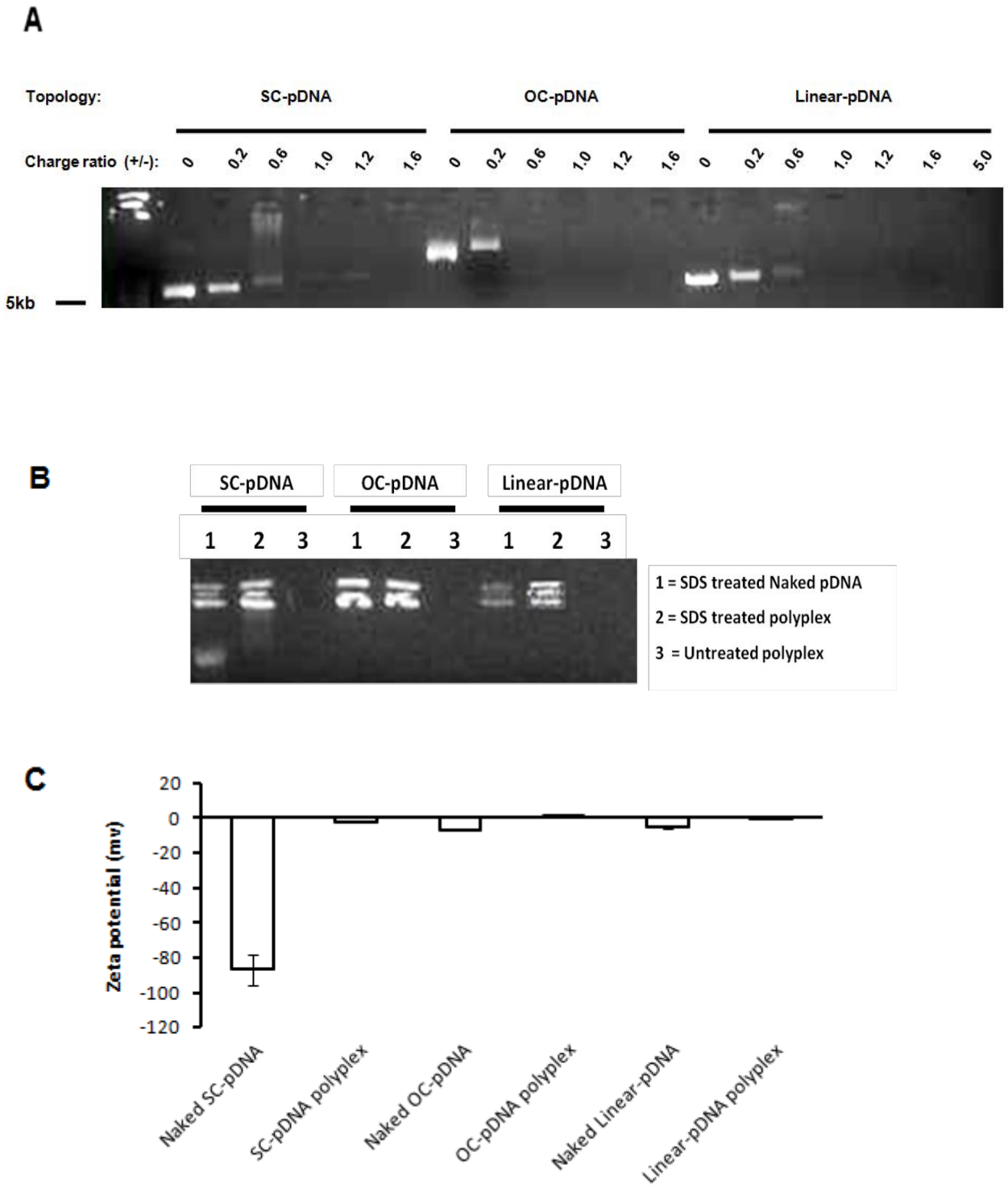

Figure 3.3: **Confirmation of polyplex formation and observation of PLL-bound DNA.** Agarose gel electrophoresis of DNA polyplexes (complexes prepared in 1mM HEPES, pH 7.5). (A). EtBr binding after SDS mediated removal of PLL (B). Surface charge measurements of SDS treated polyplexes and naked DNA controls (C). SC-pDNA, OC-pDNA and linear-pDNA polyplexes were formed at PLL/DNA charge ratios of +1.6 for SC-pDNA and OC-pDNA, and +5 for linear-pDNA. Figure 3.3c shows the mean and SE of 5 replicate measurements. The experiment was repeated 3 times independently. One-way ANOVA was employed to deduce levels of statistical significance ($p < 0.05$) between complexes of differing DNA topologies.

Although conventional gel electrophoresis is useful in confirming polyplex formation, electrophoretic detection of high charge ratio complexes is restricted (through lack of EtBr fluorescence). Therefore the aim of this particular experiment was to confirm the presence of DNA within complexes at high charge ratios. Polyplexes were treated with SDS detergent and boiled (96°C for 10 minutes), to remove the PLL. The removal of PLL restored the ability of pDNA of all topologies, to bind EtBr. Complete polymer removal did not occur as evident by the reduced electrophoretic mobilities (Figure 3.3b). Samples that were boiled with SDS underwent a DNA precipitation reaction to purify and isolate the liberated DNA as described in Chapter 2, section 2.3.5.

The zeta potentials of polyplexes treated with SDS were measured (Figure 3.3c). The zeta potentials of SDS treated polyplexes displayed an increased cationic charge than those of naked DNA controls, regardless of topology. This may be due to existing PLL binding and may account for the reduced electrophoretic mobility observed in Figure 3.3b.

3.2.3 Pre-staining with EtBr and electrophoretic identification of PLL-bound DNA

The experiment shown in Figure 3.3 tested the ability of PLL to exclude EtBr from polyplexes and the electrophoretic detection of DNA released from PLL. However it was important to detect DNA whilst complexed to PLL, which was the aim of this particular experiment. When EtBr was allowed to bind with DNA prior to polyplex formation, DNA (whose fluorescence is usually excluded as with the control preformed complexes) can be identified (Figure 3.4). Moreover polyplexes that were pre-stained with EtBr prior to formation seem to exhibit a greater cationic surface charge than that of polyplexes stained post formation resulting in differing electrophoretic velocities when the gel was stained with EtBr. This may be due to the positive charge of the ethidium exocyclic amines which are

important for electrostatic interaction (Nafisi *et al*, 2007). Furthermore EtBr binds to DNA and unwinds it, which in turn effects pDNA topology and hence a change in mobility (Neugebauer *et al*, 2007). The aim of Figure 3.4 was to confirm the presence of DNA in its complexed form with PLL and so electrophoresis was carried out for a short time period (10 minutes), after which the gel was stained to view complexed DNA (Chapter 2, section 2.3.4). This would account for the similar electrophoretic mobility observed for complexes stained post complexion.

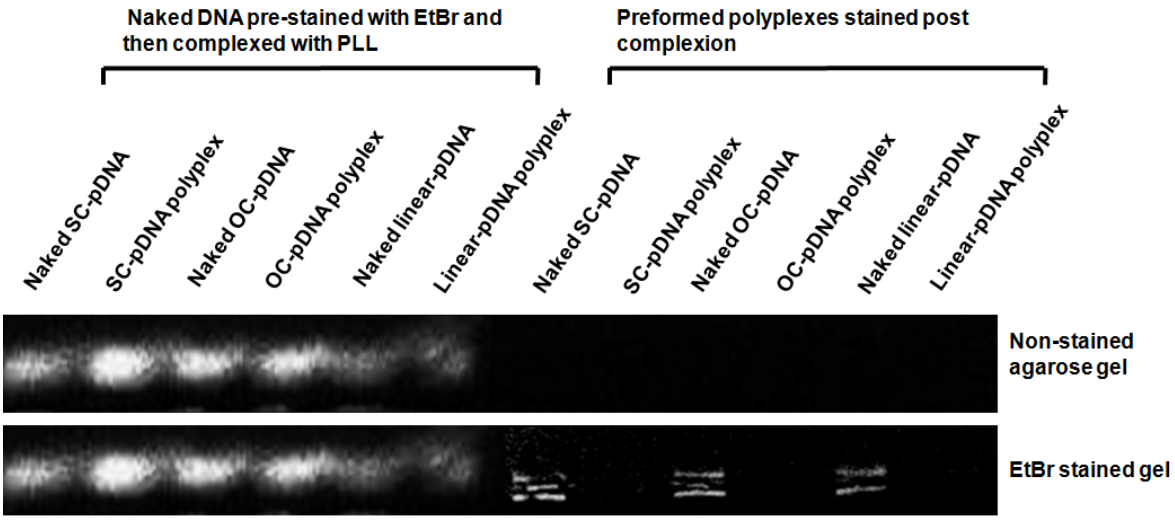

Figure 3.4: **Identification of PLL-bound DNA when pre-stained with ethidium bromide.** SC-pDNA, OC-pDNA and linear-pDNA polyplexes were formed at PLL/DNA charge ratios of +1.6 for SC-pDNA and OC-pDNA, and +5 for linear-pDNA, prior to the addition of EtBr. The fluorescence of the EtBr stained complexes was measured as described in Materials and Methods.

3.2.4 Size measurements of PLL/DNA polyplexes

Polyplex size is a key determinant of non-viral gene delivery. An experiment was carried out whereby polyplex size was estimated using dynamic light scattering (DLS). Complex mean diameters were recorded (Figure 3.5). Size was found to be topology dependent. At varying

charge ratios SC-pDNA polyplexes displayed mean diameters of up to 200nm. OC-pDNA polyplexes were larger, with sizes increasing with charge ratio. For SC- and OC-pDNA complexes the polydispersity index (PI) was 0.20-0.22 (narrow range of size characteristics of which a broad range corresponds to a PI value of 1); however that of linear-pDNA polyplexes was much higher for the Malvern instrument to read. Linear-pDNA complexes at the equivalent charge ratios displayed a much larger size and at a charge ratio of +5 exhibited a mean diameter of >1000nm. This may be due to the addition of excess polycation, which in turn increases aggregation. Therefore polyplex sizes were in the order (largest first) of Linear>OC>SC-pDNA polyplexes.

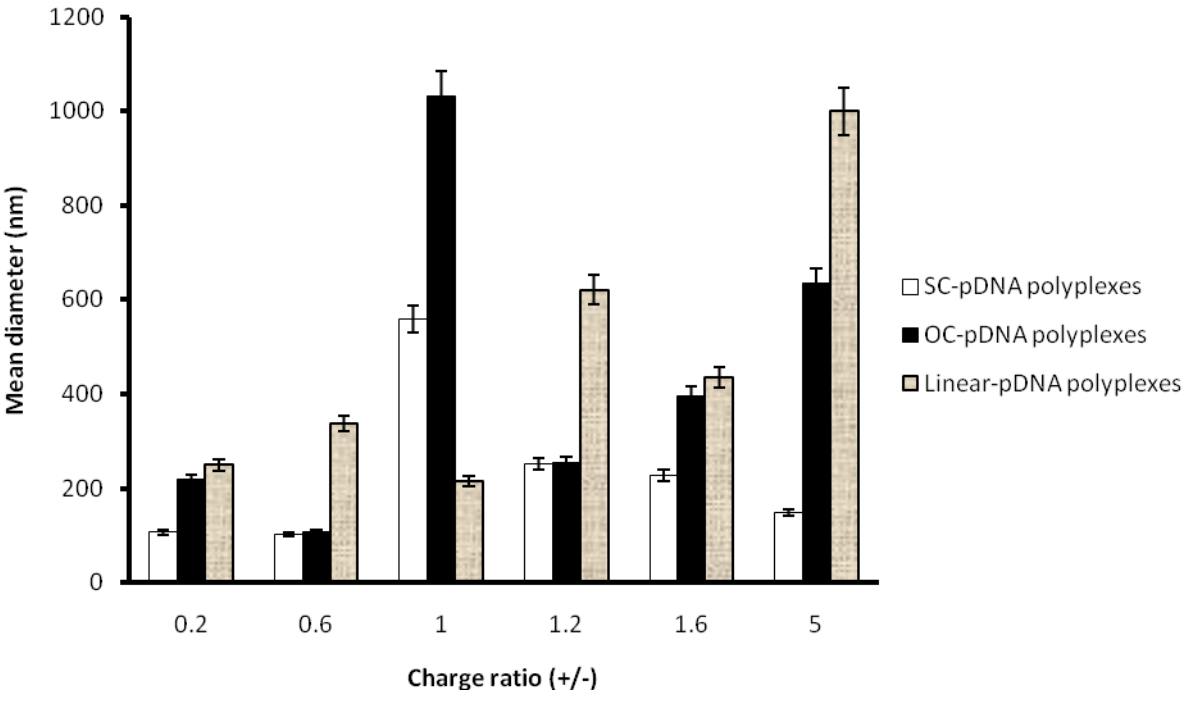

Figure 3.5: **Polyplex size measurements at varying charge ratios**. Polyplex (prepared in 1mM HEPES, pH 7.5) size measurements attained via dynamic light scattering (DLS). The figure shows the mean and SE for 10 readings. The figure shows the mean and SE of 5 replicate measurements. The experiment was repeated 3 times independently. One-way ANOVA was employed to deduce levels of statistical significance ($p < 0.05$) between complexes of differing DNA topologies.

3.2.5 Quantifying the degree of DNA condensation by PLL

Analysing the degree by which PLL condenses the nucleic acid is important in terms of observing the efficiency of the polymer to package the DNA cargo. Two fluorescent DNA intercalating agents were employed to stain the DNA; EtBr and TOTO-3.

3.2.5.1 EtBr fluorescence assays

EtBr is a fluorophore whose fluorescence is greatly enhanced when it is bound (i.e. intercalates) within DNA strands. Binding of PLL and the resulting DNA condensation restricts EtBr intercalation, and hence decrease fluorescence. Fluorescent values (which were expressed as a percentage of each DNA topology without PLL) for all three topological plasmid complexes decreased dramatically following the addition of PLL (Figure 3.6). At low ratios, SC-pDNA fluorescence is reduced most efficiently, followed by linear-pDNA, and then OC-pDNA. At higher charge ratios all forms of the plasmid severely restrict EtBr intercalation, although SC continues to give the lowest fluorescence. Usually pDNA exhibits a rigid structure owing to repulsions of the negatively charged phosphate backbone. However interaction with the positively charged PLL relaxes these repulsions resulting in the pDNA structure being able to bend and coil, which severely restricts DNA access for EtBr, especially in the case of SC-pDNA complexes (Hartmann *et al*, 2008). In regards to DNA topology, complexes containing SC-pDNA were most able to restrict EtBr fluorescence unlike that of OC- and linear-pDNA complexes. This may be attributed to the condensed nature of the supercoiled form along with PLL induced packaging of the DNA.

Although PLL condenses pDNA thereby reducing EtBr intercalation, such condensation could block interactions with external factors. However in many cases the DNA and polymer often dissociate in endosomes (vesicles which transport newly internalised materials). This occurs particularly within acidic conditions whereby enzymes operating at an acidic pH are

released by host cells to degrade foreign components. The advantages of polymers such as PLL is that they can become protonated at low pH and cause osmotic damage to the endosome allowing release of the DNA into the cytosol for subsequent nuclear import (Shim *et al*, 2011).

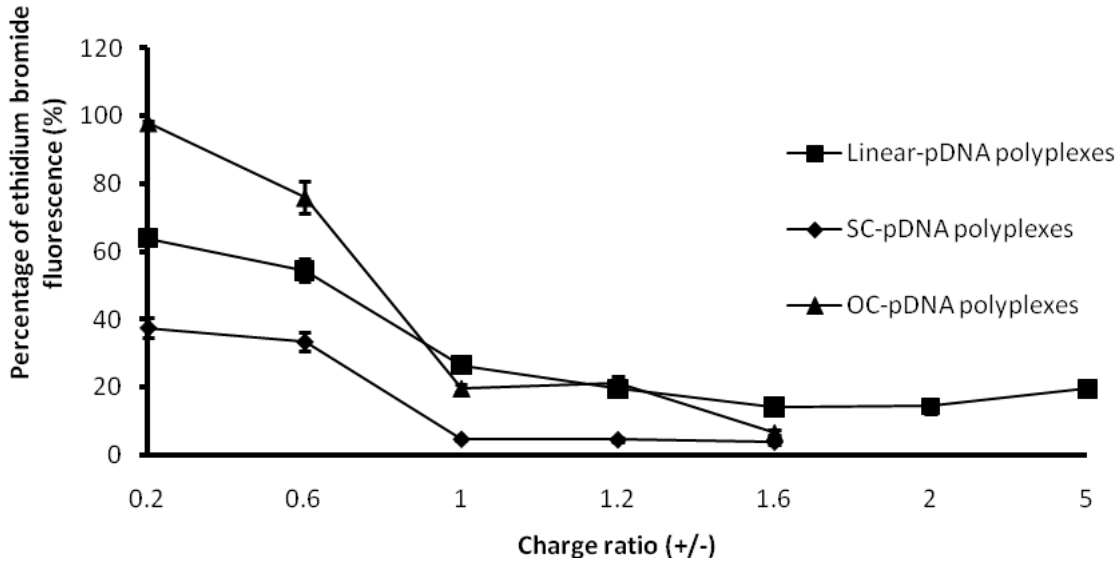

Figure 3.6: **Quantitative analysis of the ability of PLL to exclude ethidium bromide from DNA.** Ethidium bromide (EtBr) dependent fluorescence of PLL/DNA polyplexes of different topologies. The figure shows the mean and SE of 3 independent experiments. One-way ANOVA was employed to deduce levels of statistical significance ($p < 0.05$) between complexes of differing DNA topologies.

3.2.5.2 TOTO-3 Fluorescence assay

An alternative intercalating agent was also applied to polyplexes to measure fluorescence exclusion and hence the ability of PLL to condense the nucleic acid. The dye; TOTO-3 (Dimeric Cyanine Nucleic Acid Stains – Invitrogen) was added to the polyplexes at a final concentration of 4μM and fluorescence was recorded. Like EtBr, TOTO-3 fluoresces when interwoven between free nucleic acid strands. The percentage of dye fluorescence decreased

quite rapidly, particularly for polyplexes containing SC- and OC-pDNA at higher charge ratios (Figure 3.7). At a charge ratio of +1.2, polyplexes containing SC-pDNA displayed a TOTO-3 fluorescence of 33.4% (percentage of naked DNA control). However when the PLL concentration increased fluorescence was further reduced highlighting the efficient dye exclusion induced by PLL. A very similar pattern was observed for OC-pDNA complexes. In contrast linear-pDNA polyplexes were unable to effectively exclude fluorescence despite increased amounts of PLL. Although polyplexes were able to reduce TOTO-3 fluorescence, there is a discrepancy between Figures 3.6 and 3.7. TOTO-3 is a more sensitive and stable intercalating agent than EtBr by approximately 50 fold (Rey *et al*, 1992), which could account for the greater percentage of fluorescence detected.

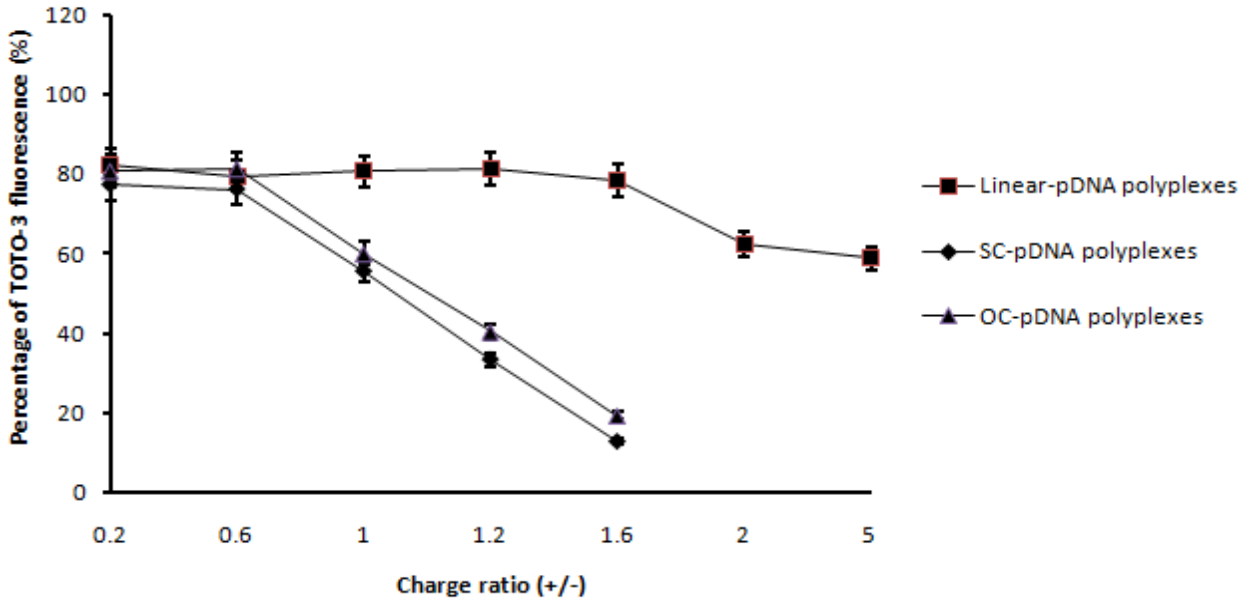

Figure 3.7: **Quantitative analysis of the ability of PLL to exclude TOTO-3 from DNA.** TOTO-3 fluorescent assay of polyplexes harbouring SC-, OC-, or linear-pDNA. Fluorescence was expressed as a percentage of a naked DNA control. The figure shows the mean and SE of 3 independent experiments. One-way ANOVA was employed to deduce levels of statistical significance ($p < 0.05$) between complexes of differing DNA topologies.

3.3 Polyplex robustness studies

3.3.1 Polyplex nuclease exposure

To test the stability of polyplexes to nucleases which are prevalent *in vivo*, samples were treated with bezonase nuclease. This nuclease was selected as it is employed for downstream removal of nucleic acids in recombinant protein production. 50 units of bezonase were employed as this has been previously found to degrade majority of DNA in cells (Grabski *et al*, 1999), and would therefore provide a measure of polyplex robustness. Polyplexes were exposed to the nuclease for a period of 30 minutes. At 5 minute intervals samples were extracted and analysed via agarose gel electrophoresis. Although in regards to SC-pDNA faint DNA bands at 5 minutes post exposure are present, nuclease treatment seemed to degrade the majority of DNA present (Figure 3.8). Little or no bands were observed for OC- and linear-pDNA complexes. As no bands were observed for treated and untreated samples, more sensitive detection methods were required to clarify whether nuclease degradation has occurred.

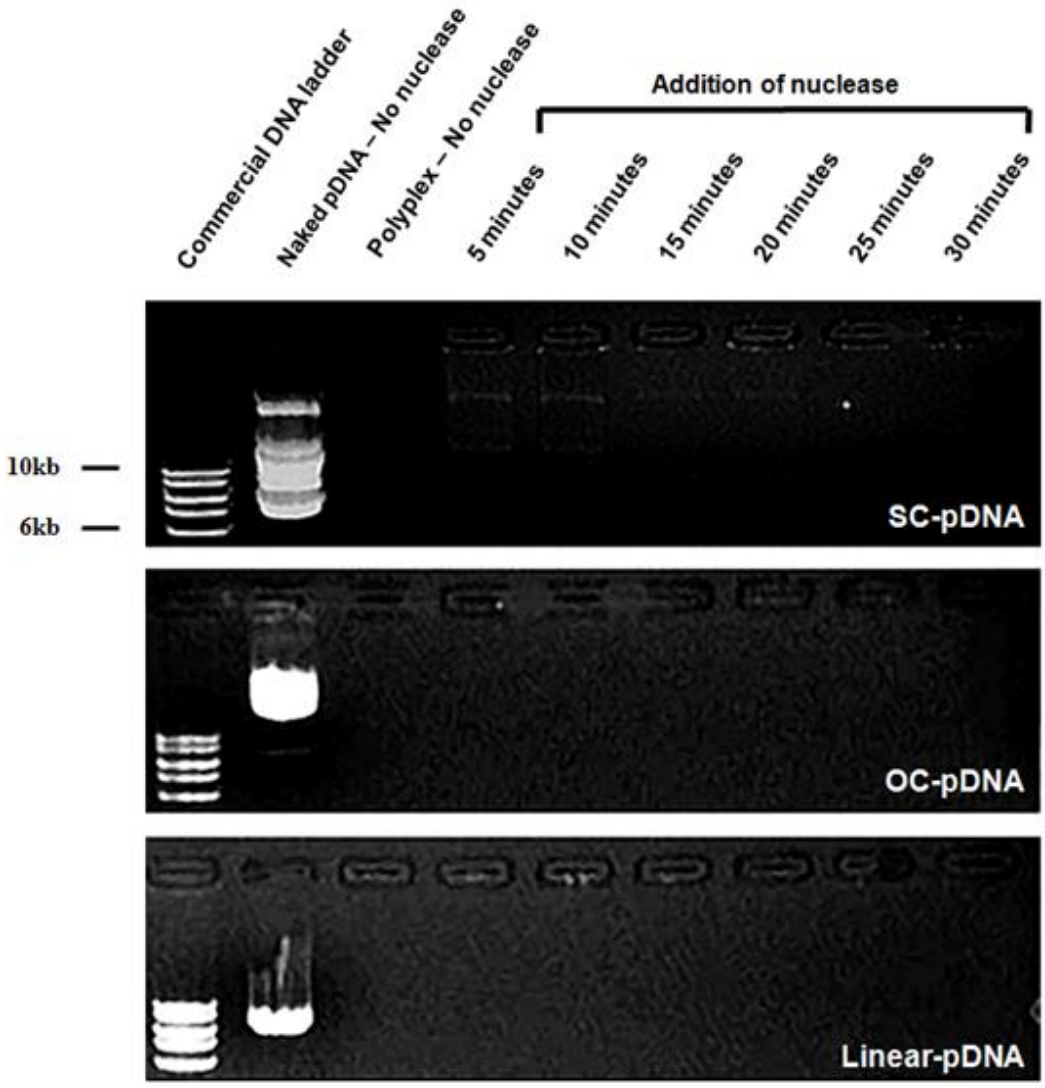

Figure 3.8: **Gel electrophoresis displaying polyplex exposure to bezonase nuclease**. Polyplexes (containing 2µg pDNA) exposed to 50 units of bezonase nuclease. Polyplexes were prepared at charge ratios of; +1.6 for SC- and OC-pDNA, and +5 for linear-pDNA.

3.3.2 Quantification of the remaining amount of DNA post nuclease exposure

The amount of DNA remaining post nuclease exposure was quantified and expressed as a percentage of an untreated DNA control. Figure 3.9 shows how the majority of the DNA that did remain after nuclease attack, comprised mainly of SC- and OC-pDNA while linear-pDNA polyplexes were susceptible to attack. Regardless of DNA topology the percentage of DNA remaining decreases by over 50% following 10 minutes of nuclease treatment. At 5 minutes post nuclease exposure, the percentage of SC- and OC-pDNA are approximately 30% of the untreated controls, which may correspond to the very faint bands observed in Figure 3.8. DNA was quantified by a NanoDrop ND-1000 Spectrophotometer (NanoDrop Technologies) as described in Chapter 2, section 2.1.2.

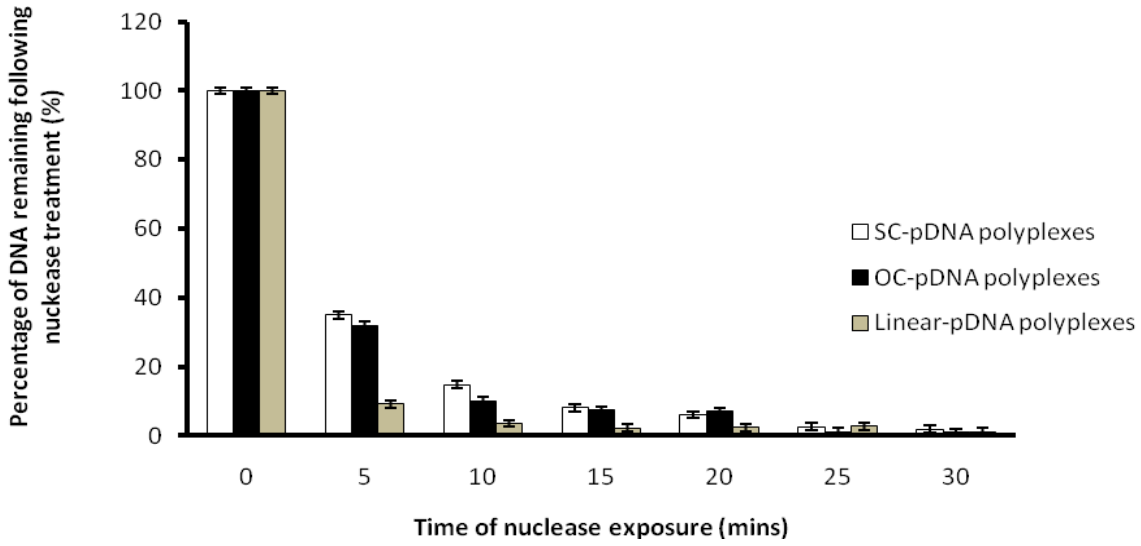

Figure 3.9: **Percentage of polyplex DNA remaining following nuclease exposure.** Polyplexes (containing 2µg pDNA) were prepared at charge ratios of; +1.6 for SC- and OC-pDNA, and +5 for linear-pDNA. The figure shows the mean and SE of 3 independent experiments. One-way ANOVA was employed to deduce levels of statistical significance ($p < 0.05$) between complexes of differing DNA topologies.

3.3.3 Naked DNA exposure to nuclease

As a control experiment naked pDNA (SC-, OC- and linear-pDNA) were exposed to the nuclease for the same time period and analysed via agarose gel electrophoresis. As shown, the nuclease completely degraded all forms of the plasmid, regardless of DNA topology, with little or no resistance towards degradation (Figure 3.10). This is shown by the lack of DNA bands in comparison to untreated controls. This may indicate the protective attributes PLL has to offer in terms of nuclease resistance.

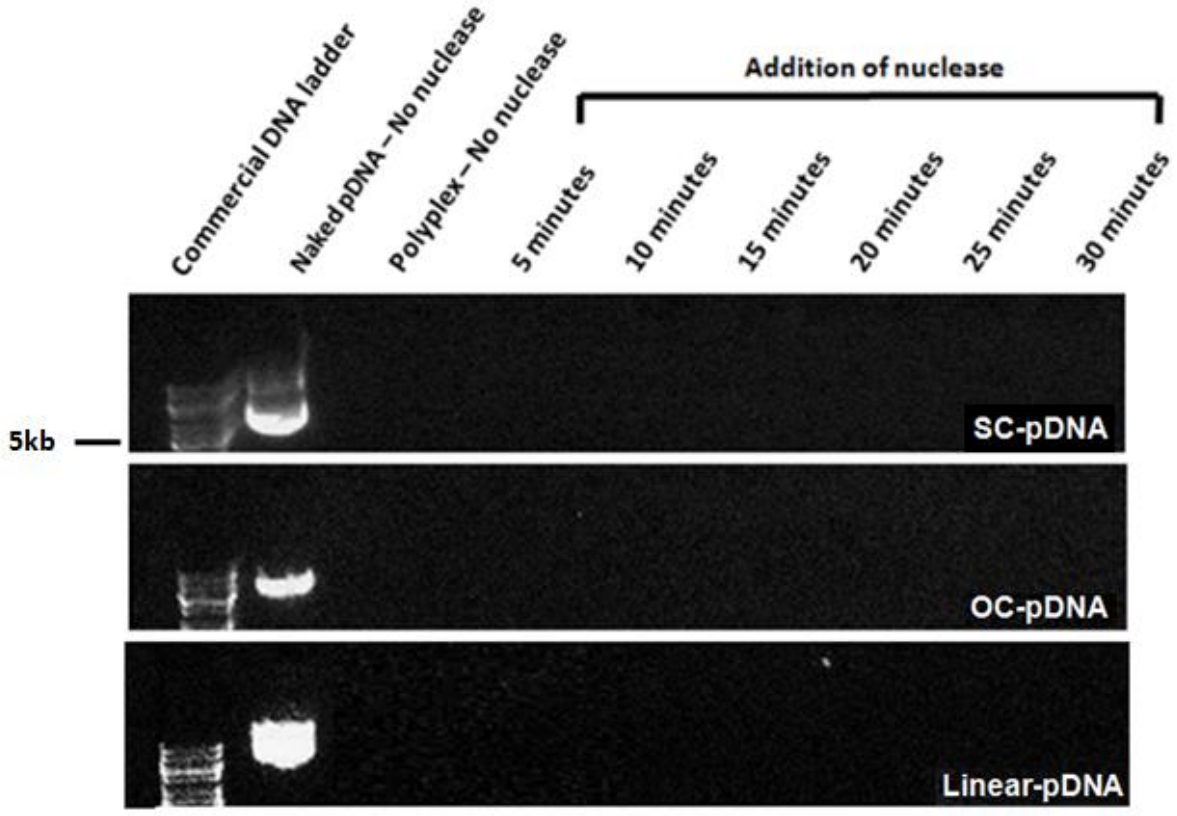

Figure 3.10: **Gel electrophoresis displaying naked pDNA exposure to bezonase nuclease.** Naked pDNA (2µg pDNA) exposure to 50 units of bezonase nuclease.

3.3.4 Southern blot analysis

Since polyplex formation inhibited EtBr staining, an alternative method of detecting DNA and monitoring nuclease degradation was used. Following nuclease treatment polyplex DNA was probed via Southern blot (Figure 3.11). DNA was biotinylated and probed by a streptavidin antibody (refer to Chapter 2, section 2.2.1). The strongest biotin signal corresponding to DNA was that of polyplexes containing SC-pDNA whereby the DNA signal was observed for up to 20 minutes post exposure. The probing of DNA allowed a more sensitive detection of the remaining amounts of nucleic acid. In contrast to Figure 3.8, the membrane blot showed how the polyplex DNA (SC-form) is cut into two fragments whose signal intensity decreases with time of enzyme exposure. Similar observations were found for OC-pDNA polyplexes and in line with Figure 3.9. Very weak DNA signals were identified for the linear form, suggesting it was much more susceptible towards nuclease degradation.

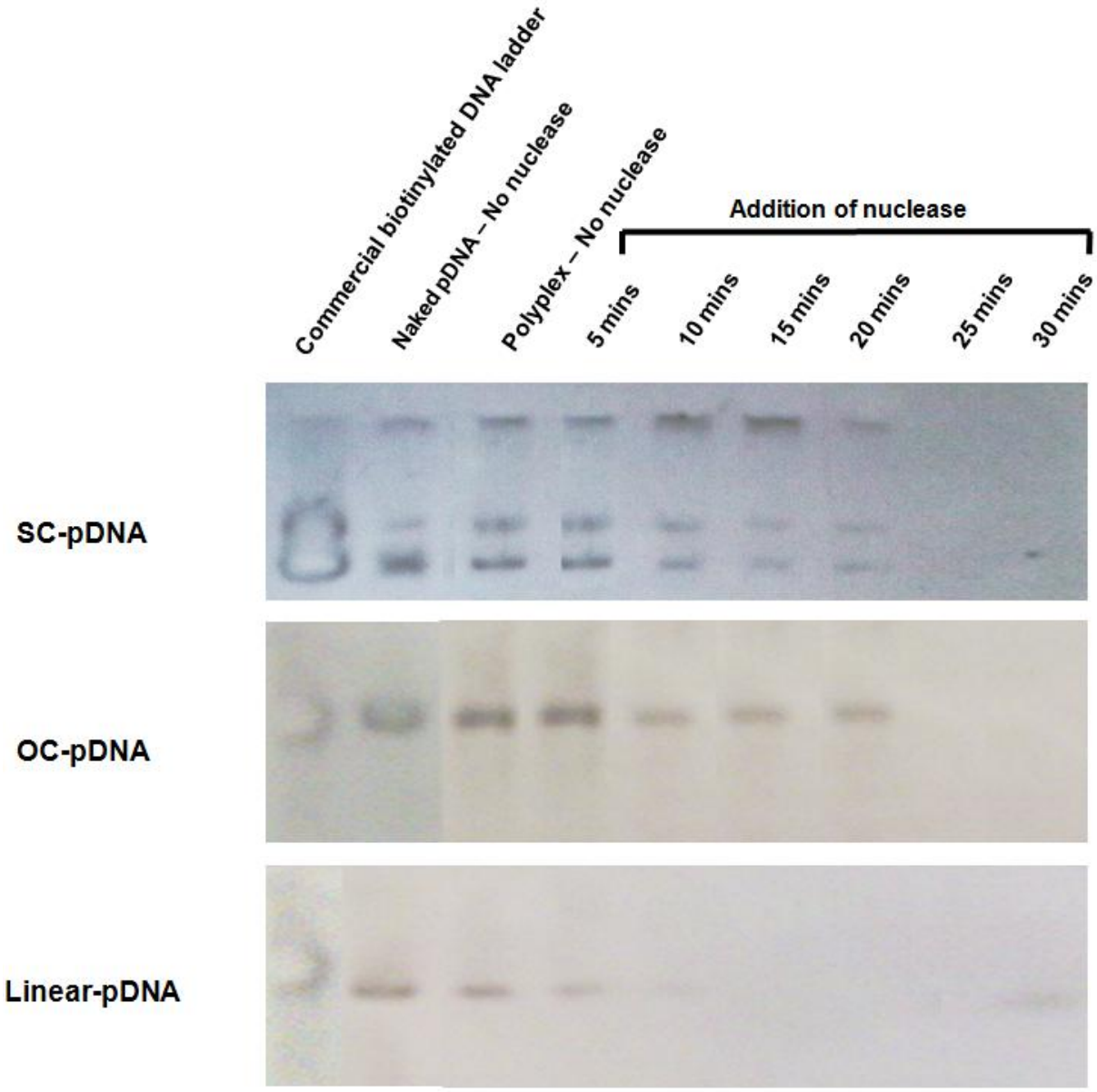

Figure 3.11: **Southern blot detection of polyplex DNA following nuclease exposure**. Polyplexes were prepared at charge ratios of; +1.6 for SC- and OC-pDNA, and +5 for linear-pDNA. Biotinylated DNA was probed by streptavidin-HRP antibody, and detected via chemiluminescence.

3.3.5 Gel electrophoresis of purified DNA post nuclease exposure

As an alternative approach to studying polyplex DNA post nuclease exposure, polyplexes were purified immediately after nuclease treatment using a commercial kit routinely employed for pDNA purification (Chapter 2, section 2.1.2). Purification involved the removal of proteins and other contaminants thereby isolating the desired DNA product. Purified nuclease treated polyplex DNA samples for all three topologies are shown in Figure 3.12. Faint DNA bands were observed for SC-pDNA polyplexes, whereas very little DNA was detected for that of OC- or linear-pDNA complexes.

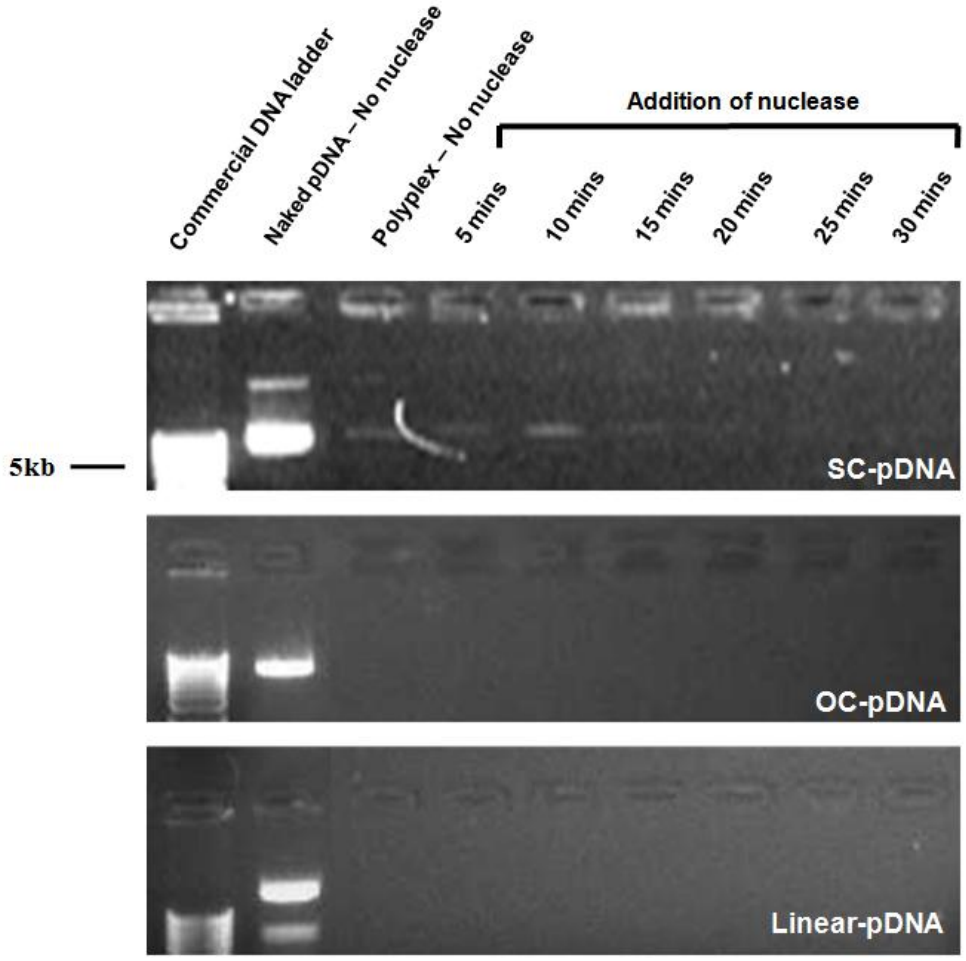

Figure 3.12: Agarose gel electrophoresis of nuclease treated polyplexes that subsequently underwent pDNA purification. Polyplexes were prepared at charge ratios of; +1.6 for SC- and OC-pDNA, and +5 for linear-pDNA.

3.3.6 Quantification of the amount of purified pDNA post nuclease exposure

The amount of purified DNA remaining following nuclease treatment was quantified and expressed as a percentage of naked DNA (same amount that was bound with PLL) that underwent the same purification process (Figure 3.13). Following both nuclease and purification (5 minutes post exposure) the majority of DNA was degraded. However SC-pDNA still constituted a large proportion of the DNA that did survive attack. There appeared to be approximately 9% of SC-pDNA remaining following exposure which was more than double the amount of OC- and linear-pDNA. The trend of stability is as follows: SC>OC>linear pDNA, which all severely decrease following 15 minutes post nuclease treatment which is consistent with the enzyme assay and Southern blot. The experiment of Figure 3.13 does suggest mini-prep purification does remove polymer bound DNA. Mini-prep purification entails spin columns which retain and purify plasmids. Unbound plasmids are larger in size than small polyplexes which may be lost during retention of larger DNA molecules. However it is clear that SC- or OC-pDNA when bound to PLL is much more resistant to nuclease attack than linear-pDNA. DNA was quantified by a NanoDrop ND-1000 Spectrophotometer (NanoDrop Technologies) as described in Chapter 2, section 2.1.2.

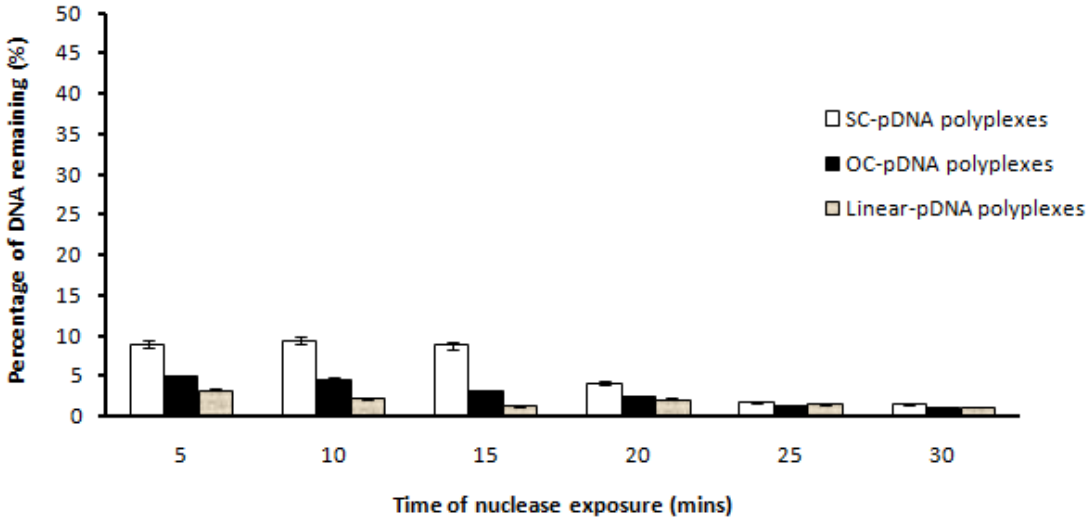

Figure 3.13: **Quantification of purified DNA post nuclease treatment.** Polyplexes were prepared at charge ratios of; +1.6 for SC- and OC-pDNA, and +5 for linear-pDNA. The figure shows the mean and SE of 3 independent experiments. One-way ANOVA was employed to deduce levels of statistical significance ($p < 0.05$) between complexes of differing DNA topologies.

3.4 Effect of ionic strength on polyplex formation and biophysical characterisation

Ionic strength can have a major impact on the biophysical characteristics of DNA polyplexes. The presence of salts can disrupt the PLL/DNA interaction thereby potentially perturbing the transport of DNA cargo and hence ultimately gene expression. Therefore the aim of the following sets of experiments was to study the effects of high ionic strength on polyplex formation and characterisation. To mimic the cellular ionic environment polyplexes were prepared in 150mM NaCl and also in PBS (phosphate buffered saline). Characteristic analysis such as size, zeta potential and DNA condensation studies were carried out and compared to polyplexes prepared in low salt solutions. Polyplexes containing either SC-, OC-

or linear-pDNA were prepared and analysed at charge ratios of +1.6 (for SC- and OC-pDNA) and +5 (for linear-pDNA) respectively.

3.4.1 The effect on polyplex size when formed in high salt concentration buffer

Previous studies have reported that high ionic strength impacts on polyplex size (Jeong *et al*, 2011). To investigate whether this was true of the present study, the diameter of polyplexes was estimated using DLS. As shown in Figure 3.14 size is topology dependent. SC-pDNA polyplexes were the smallest (mean diameter of <140nm). OC-pDNA polyplexes were larger at just over 300nm, while linear-pDNA complexes had diameters of approximately 840nm. When formed in high ionic strength solutions, polyplex sizes increased dramatically, presumably the presence of salts causes aggregation to the PLL/DNA interaction. However it is clear when made up in 1mM HEPES (pH 7.5) polyplexes consisting of SC-pDNA seem well equipped for cellular entry, an observation consistent with previous data (Tsai *et al*, 1999). This may be due to the pre-existing dense structure of SC-pDNA which when bound to PLL, is condensed further to a much more confined form.

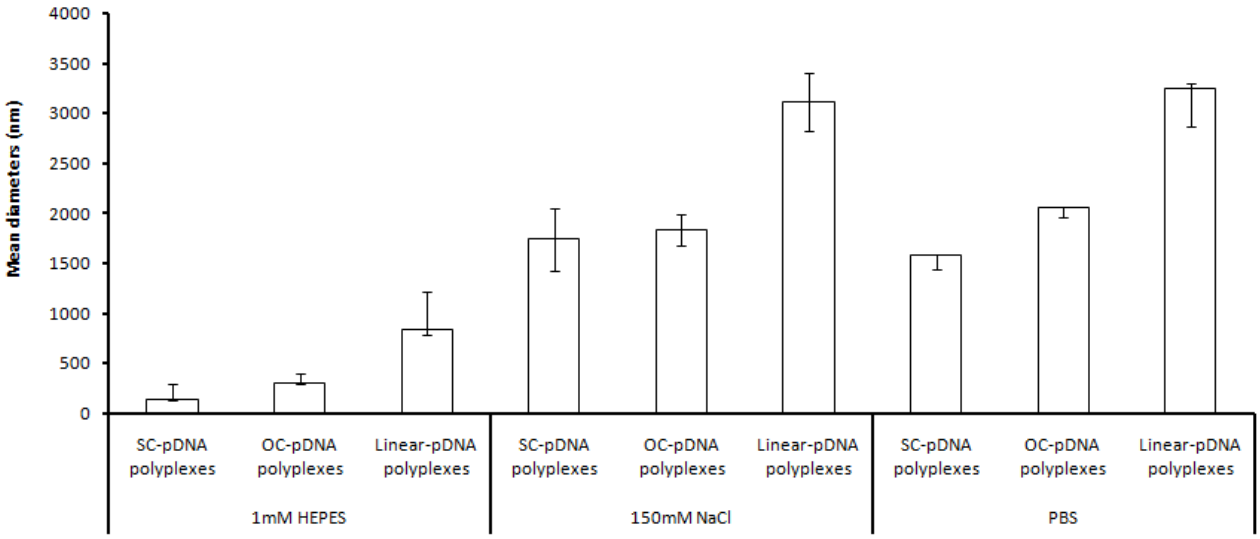

Figure 3.14: **The effect of high ionic strength on polyplex size.** Polyplexes were prepared in either 1mM HEPES, 150mM NaCl and PBS (pH 7.5). The polyplexes had PLL/DNA ratios of +1.6 for SC-pDNA and OC-pDNA, and +5 for linear-pDNA respectively. Points represent mean and SE for 10 readings. The experiment was repeated 3 times independently. One-way ANOVA was employed to deduce levels of statistical significance ($p < 0.05$) between complexes of differing DNA topologies produced in different buffers.

3.4.2 Impact on polyplex surface charge when formulated in high salt concentration buffer

Zeta potential studies provide a good technique for characterising the surface charge of non-viral gene delivery systems. Surface charge is a key parameter in determining gene delivery. The zeta potential of complexes produced in various buffers was measured (Figure 3.15). An additional control was added whereby complexes were produced in 0.2µm filtered water. These complexes along with those prepared in 1mM HEPES displayed cationic surface charges. However the zeta potential of complexes prepared in either 150mM NaCl or PBS is significantly reduced to a more neutral surface charge suggesting PLL/DNA interaction is

perturbed by the presence of salts causing a relaxation of the strong cationic charge induced by PLL.

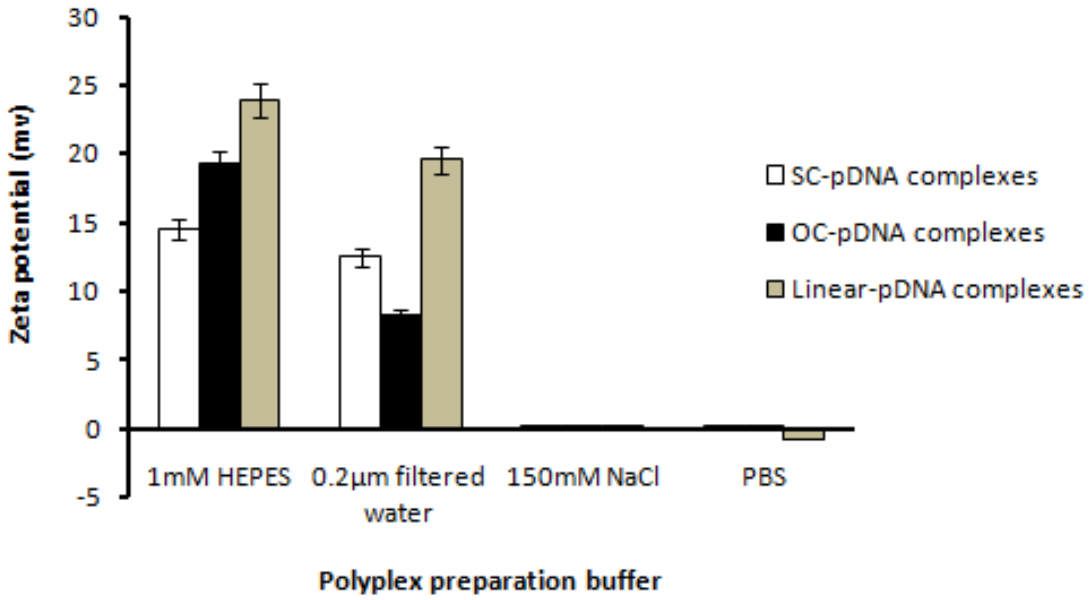

Figure 3.15: **The effect of high ionic strength on polyplex surface charge.** Polyplexes were prepared at charge ratios of; +1.6 for SC- and OC-pDNA, and +5 for linear-pDNA. The figure shows the mean and the SE of 5 replicate measurements. The experiment was repeated 3 times independently. One-way ANOVA was employed to deduce levels of statistical significance ($p < 0.05$) between complexes of differing DNA topologies produced in different buffers.

3.4.3 The effect of ionic strength on DNA condensation by PLL

Results from Figures 3.14 and 3.15 suggest the presence of salts did impact on the biophysical characteristics of DNA polyplexes, particularly at the vesicular ionic environment (150mM NaCl). Both surface charge and sizes were disrupted indicating the presence of salts perturbs PLL/DNA electrostatic interaction. To gain further insight into this, DNA condensation by PLL was studied by an EtBr assay (Figure 3.16). EtBr fluorescence is

reduced most effectively for polyplexes containing SC-pDNA in a topology dependent manner when prepared in low salt concentrated buffer, as shown previously (Figure 3.6). OC-pDNA complexes display similar exclusion profiles, while complexes containing linear-pDNA are least effective in restricting EtBr intercalation, and therefore are more accessible. However EtBr fluorescence rises over 5 fold for SC- and OC-pDNA complexes made up in 150mM NaCl. Similar observations were noted for complexes made up in PBS. Such results strongly suggest the presence of salts does disrupt PLL/DNA interactions leading to a decrease in PLL induced DNA condensation.

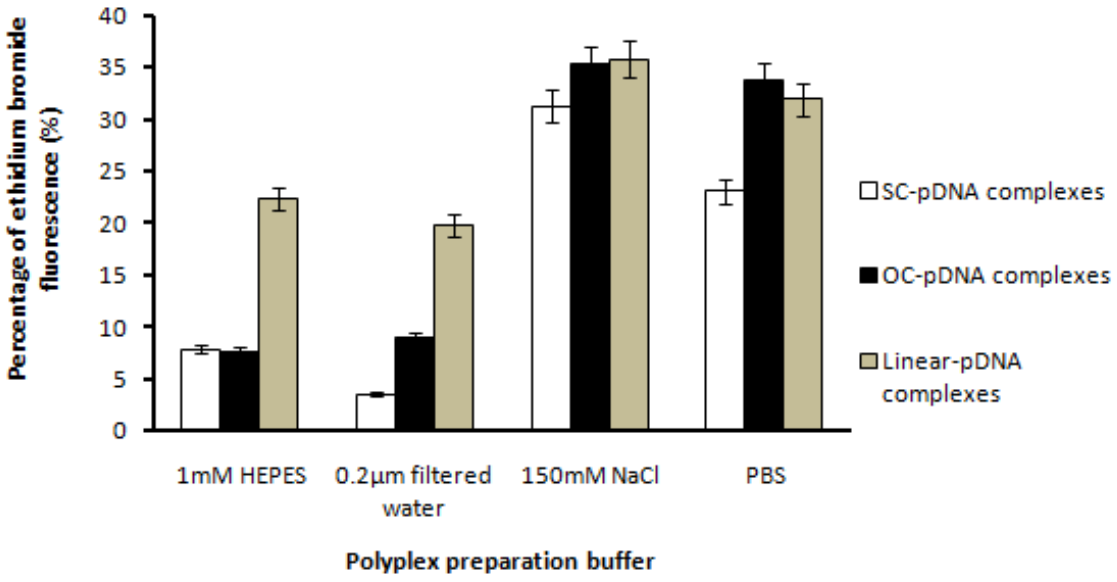

Figure 3.16: **The effect of high ionic strength on the ability of polyplexes to restrict ethidium bromide fluorescence.** Polyplexes were prepared at charge ratios of; +1.6 for SC- and OC-pDNA, and +5 for linear-pDNA. The figure shows the mean and SE of 3 independent experiments. One-way ANOVA was employed to deduce levels of statistical significance ($p < 0.05$) between complexes of differing DNA topologies produced in different buffers.

3.4.4 Electrophoretic analysis of DNA and polyplex formulations

As shown previously both size and surface charge are affected when the ionic strength is increased. Moreover the ability to restrict EtBr fluorescence is reduced and so to further analyse the effect of ionic strength on the physical characteristics of polyplexes, samples were analysed via gel electrophoresis (Figure 3.17). Both electrophoretic mobility and EtBr fluorescence is reduced which is in line with Figure 3.3a. Despite polyplexes produced in high salt concentrations and displaying a relatively neutral charge, the ability to reduce EtBr fluorescence seems to be independent of charge as shown in the gel. Although, when polyplexes are formulated in 150mM NaCl and PBS, fluorescence is observed (situated in the well as a result of the change in charge) which is in line with Figure 3.16. Additionally the corresponding formulations seemed to have virtually no effect on electrophoretic mobility or ability to stain naked uncomplexed DNA (Figure 3.17b).

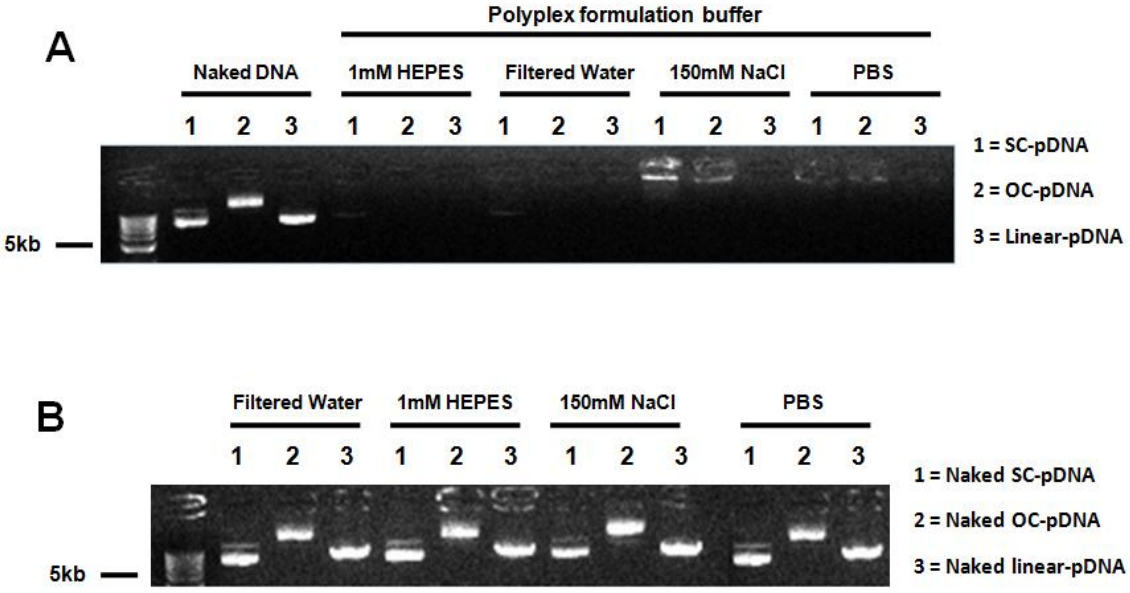

Figure 3.17: **Electrophoretic analysis of polyplexes and naked pDNA formulated in differing buffers.** Electrophoretic analysis of polyplexes (A) and naked DNA (B) in different formulation buffers. Polyplexes were prepared at charge ratios of; +1.6 for SC- and OC-pDNA, and +5 for linear-pDNA.

3.5 The effect of plasmid DNA size on polyplex formation and characterisation

Plasmid DNA size is a key factor that can affect polyplex formation and various physical attributes required for non-viral gene delivery. Plasmid size is a key area of interest in regards to gene therapy and vaccination. Large plasmids (>30kb) offer the advantage of larger therapeutic DNA insert, whereas smaller plasmids (>5kb) are of decreased sizes which minimises issues regarding cellular and nuclear uptake. In this section of the chapter a simultaneous comparison of the effect of plasmid size on PLL interaction is presented. Two plasmids were studied; a 3.8kb plasmid and a bacterial artificial chromosome (BAC) displaying a size of 56.5kb (both plasmids studied were in the SC conformation).

3.5.1 The effect of nucleic acid size on polyplex zeta potential

Zeta potentials of polyplexes containing either a 3.8 or 56.5kb nucleic acid of varying charge ratios was measured (Figure 3.18). It is clear that pDNA size affects interaction with PLL in terms of charge, whereby the smaller 3.8kb plasmid displayed a rapid charge neutralisation (at a charge ratio of 0.6) and increase to a more cationic charge. In contrast the BAC exhibited a neutral charge even when the charge ratio increased to +10. This may be due to the larger anionic phosphate backbone of the BAC whereby more positively charged polymer is required to neutralise the charge. This is important and would have important implications for further downstream studies such as cell uptake assays.

3.5.2 Electrophoretic analysis and confirmation of polyplex formation

Binding of PLL to either plasmid, regardless of size, caused a rapid decrease in EtBr fluorescence as shown by gel electrophoresis (Figure 3.19). Fluorescence was reduced rapidly at low charge ratios. Moreover electrophoretic mobility was retarded which is in line with Figure 3.18 in terms of surface charge. Furthermore even though the 56.5kb BAC is

essentially neutralised by PLL, some fluorescence and migration is observed, which may reflect the decrease in positive charge. Both small and large plasmids were subjected to nicking and restriction digestion to confirm analysis (Figure 3.19a and b).

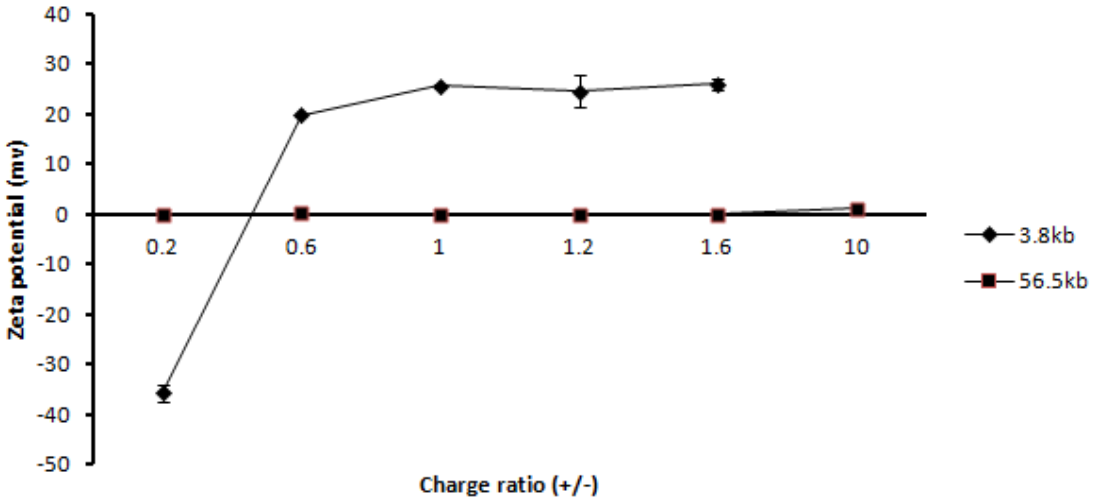

Figure 3.18: **The effect of nucleic acid size on polyplex surface charge.** Polyplexes were prepared in 1mM HEPES, pH 7.5. The figure shows the mean and SE of 5 replicate measurements. The experiment was repeated 3 times independently. One-way ANOVA was employed to deduce levels of statistical significance ($p < 0.05$) between complexes of differing pDNA sizes.

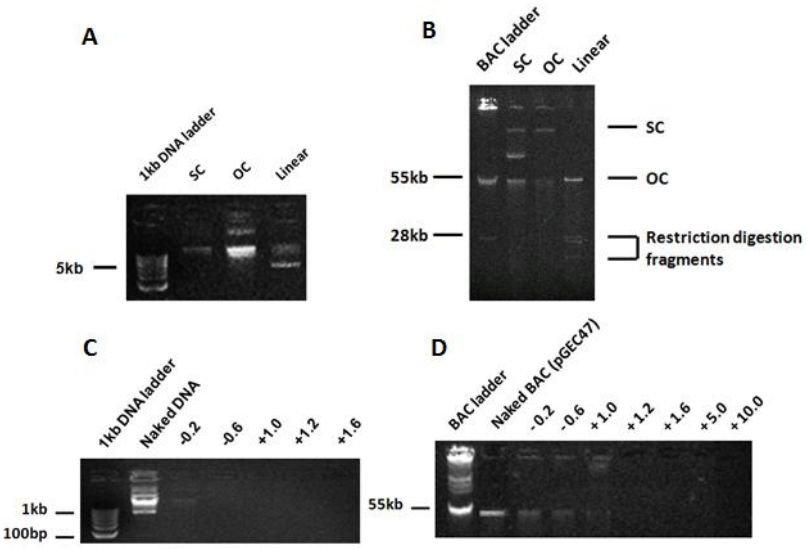

Figure 3.19: **Electrophoretic confirmation of both small and large nucleic acids.** Confirmation achieved via nicking and restriction digestion of the 3.8kb plasmid (A) and 56.5kb (B) BAC. Electrophoretic analysis of PLL/DNA polyplexes containing either the 3.8kb plasmid (C) or the 56.5kb BAC (D).

3.5.3 Polyplex size analysis

DLS was used to measure complex mean diameters and the effect of pDNA size on polyplex size. Polyplex size shows dependence on nucleic acid size (Figure 3.20). Polyplexes containing the 3.8kb plasmid exhibit sizes within the region of 100-137nm. Despite a larger charge ratio of +10 and containing a greater concentration of PLL to facilitate DNA condensation and charge neutralisation, complexes containing the 56.5kb BAC were measured to be approximately <900nm. Such observations may be due to the existing large BAC structure (mean diameter of the naked BAC was 468.14nm), which with the addition of the polymer may form a larger complex. However nucleic acid size clearly affects polyplex size, with smaller plasmids being efficiently condensed by PLL, which is a critical parameter for uptake studies.

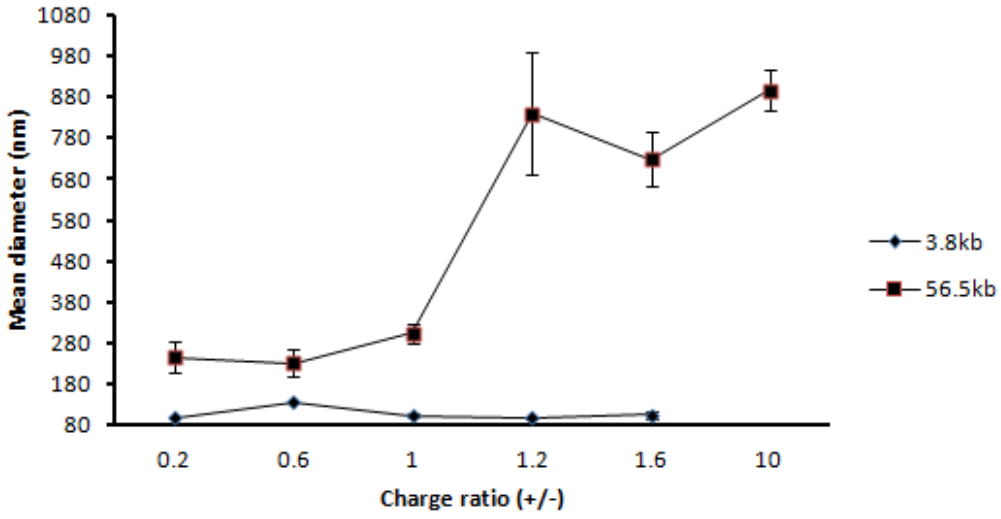

Figure 3.20: **The effect of nucleic acid size on polyplex mean diameter**. Polyplexes were prepared in 1mM HEPES, pH 7.5 for size measurements attained via dynamic light scattering (DLS). Points represent mean and SE for 10 readings. The experiment was repeated 3 times independently. One-way ANOVA was employed to deduce levels of statistical significance ($p < 0.05$) between complexes of differing pDNA sizes.

3.5.4 The effect of nucleic acid size on DNA condensation

An EtBr fluorescence exclusion assay was performed to deduce whether nucleic acid size affects the ability of PLL to condense it and hence exclude EtBr intercalation. Figure 3.21 shows how the 3.8kb plasmid displays a reduced EtBr fluorescence profile than its 52kb counterpart. The 3.8kb plasmid is more efficiently packaged by PLL resulting in reduced EtBr DNA intercalation. The ability of PLL to effectively condense the 3.8kb plasmid is consistent with the smaller sizes observed in Figure 3.20. Although the 3.8kb pDNA polyplex excluded EtBr access, >20% fluorescence was recorded which is greater than previous measurements with the larger 6.8kb pDNA polyplex. This may be due to smaller DNA molecules being bound to larger polymers which may allow DNA access.

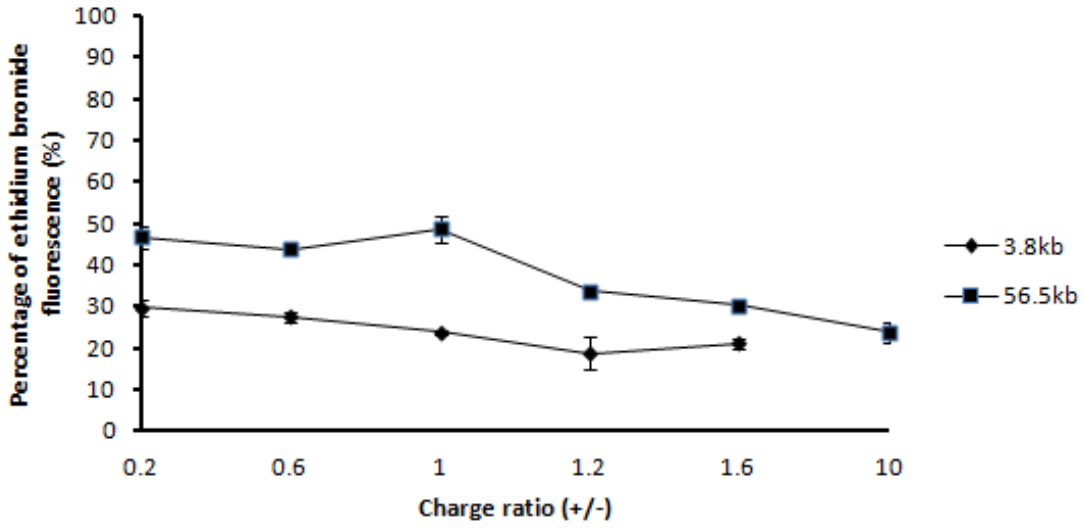

Figure 3.21: **The effect of nucleic acid size on PLL induced DNA condensation.** The figure shows the mean and SE of 3 independent experiments. One-way ANOVA was employed to deduce levels of statistical significance ($p < 0.05$) between complexes of differing pDNA sizes.

3.6 Discussion

Non-viral gene delivery has centred on the use of polycation-based techniques. Polycations are polymer based systems which bind and condense pDNA into smaller particles for gene delivery (Tiera *et al*, 2011). Various types of polycations have been successful in delivering pDNA (Ali and Mooney, 2008; Dutta *et al*, 2008; Liu *et al*, 2011). However gene expression remains low which could be due to the prevalence of host cell nucleases which can degrade pDNA following separation from the polymer within the endosome (polymer becomes protonated to allow DNA to escape from degradative enzymes which operate at a low pH). This is important as sustained expression is necessary for therapeutic purposes. For this to happen gene transfer most overcome various molecular barriers. In order to achieve this, the key factors that affect polycation DNA complexes (polyplexes) must be analysed.

The present chapter focused on the characterisation of pDNA polyplexes and the key factors that affect complex biophysical properties in regards to potential uptake in mammalian cells. Plasmid DNA was complexed with poly-$_L$-lysine (PLL) to form DNA polyplexes. Parameters such as DNA topology, plasmid size, polyplex size, charge ratio and stability amongst others were investigated. Understanding such parameters will improve the design of effective non-viral gene delivery vehicles in bio-processing.

3.6.1 DNA topology

Plasmid DNA (pDNA) can exhibit a variety of topological conformations and such structural discrepancies may affect potential pDNA gene expression. Plasmids usually confer to a supercoiled (SC) compact form (Brown, 2001). A strand breakage leads to open circular (OC)-pDNA (Cherng *et al*, 1999), while restriction digestion of the strand leads to linear-pDNA. Conventional gene delivery studies have long employed SC-pDNA which is

presumed to be more stable than other conformations (Hsu and Uludag, 2008). However OC-pDNA which consists of a single nick may not differ in biological activity and the accessible nature of the linear-pDNA conformation may favour gene expression (Anada *et al*, 2005). Few studies have actually compared DNA of differing topologies in regards to polyplex biophysical analysis and uptake. Reports have produced conflicting results with topology being a major factor (Remaut *et al*, 2006) or having no significant impact (Hsu and Uludag, 2008) (Summarised in Table 3.1).

3.6.1.1 Polyplex confirmation

In this study a 6.8kb plasmid of three differing topologies was complexed with PLL, and analysed in terms of biophysical characterisation. Polyplex formation was confirmed by charge neutralisation which occurred rapidly for SC- and OC-pDNA, whereas linear-pDNA required more PLL to produce a net positive charge. Such observations have been attributed towards the selective affinity of polycations towards DNA of differing topology (Bronich *et al*, 2000). Moreover linear-pDNA display a more open and accessible structure and so may require more PLL to neutralise the exposed phosphate backbone. A study by von Groll *et al*, (2006) required three times the amount of recommended lipofectamine agent for linear-pDNA to produce a lipoplex with a cationic charge necessary for cellular uptake. In that study linear-pDNA lipoplexes displayed necklace-like structures whereas SC-pDNA was more spherical (von Groll *et al*, 2006). Therefore the large surface area of the linear form may require greater charge neutralisation.

3.6.1.2 Polyplex sizes

Polyplex size is important as various physical barriers limit cellular uptake and ultimately gene expression. Size measurements of PLL/DNA complexes were recorded via dynamic

Non-viral gene delivery system	Charge ratio (polymer:DNA)	Size (nm)	Zeta potential (mv)	Duration of nuclease resistance (mins)	Percentage of DNA intercalation exclusion (%)	References
PLL/SC-pDNA PLL/OC-pDNA PLL/Linear-pDNA	+1.6 +1.6 +5	<200 <400 <1000	+13 +23 +27	25 20 5 Exposed to 50 units bezonase	4 (EtBr) 6.75 (EtBr) 19.55 (EtBr)	Dhanoya *et al*, (2011)
P(DMAEMA)/SC-pDNA P(DMAEMA)/OC-pDNA P(DMAEMA)/Linear-pDNA	+3 +3 +3	84 91 98	N/A	N/A	21 (Acridine orange) 24 (Acridine orange) 25 (Acridine orange)	Cherng *et al*, (1999)
Lipid/SC-pDNA Lipid/OC-pDNA Lipid/Linear-pDNA	+2.5 +2.5 +2.5	114 207 117	N/A	Complexes containing SC-pDNA were exposed to 1unit/µl DNase I which displayed resistance for up 15 minutes. After this SC-pDNA was converted to OC and Linear forms.	N/A	Remaut *et al*, (2006)
PEI/SC-pDNA PEI/OC-pDNA PEI/Linear-pDNA	+2.5 N/A +2.5	>100 N/A <400	N/A	N/A	N/A	Hsu and Uludag (2008)

Table 3.1: Summary of the key biophysical characteristics of PLL/DNA polyplexes containing DNA of differing topologies. Biophysical characteristic parameters such as polyplex size, charge, ability to exclude intercalating agents and nuclease resistance are presented. Where fields are denoted 'N/A' the respective study did not report the value.

light scattering (DLS). Regardless of polyplex buffer formulation, complexes containing SC-pDNA were found to be the smallest at just <200nm followed by OC-pDNA and linear-pDNA polyplexes (Figure 3.5 and Table 3.1). The results may be due to the pre-existing dense structure of SC-pDNA, which is then further compacted by PLL. These results are consistent with previous reports which identified larger aggregated complexes in regards to linear-pDNA (Hsu and Uludag, 2008; von Groll *et al*, 2006). This is shown in Table 3.1 whereby studies focusing on DNA topology identified smaller complex sizes for those containing SC-pDNA. However as the charge ratio increased polyplex sizes increased which may be due to excess amounts of polymer added which could lead to aggregation rather than further DNA condensation.

Despite reporting smaller complex sizes for those containing SC-pDNA, Cherng *et al*, (1999) (Table 3.1) reported how polyplex size was independent of DNA topology with all three DNA forms displaying reduced mean diameters (>100nm for each topology when formulated in HEPES buffer, pH 7). Those results differed to the present study whereby a significant difference in size was recorded, particularly regarding linear-pDNA polyplexes. The large size of the linear-pDNA polyplex (>1000nm at high charge ratio [PLL to DNA] of +5) may be due to the greater amounts of PLL added to the nucleic acid leading to an increase in size and polydispersity (large size range detected). The high charge ratio necessary for charge neutralisation for linear-pDNA polyplexes may also be a hindrance in regards to uptake, whereby excess polycation has been found to cause aggregation due to interaction with negatively charged blood molecules (Christie *et al*, 2010).

Nucleic acid condensation by polycations has been credited with the reduction in pDNA size. Detailed knowledge and exploitation of this process would improve future analysis. Nucleic acid condensation is important whereby the existing compact structure must be relaxed and

made accessible to the polymer, which then results in further bending and coiling (Eisenberg, 1987). Recent studies which produced PLL/DNA complexes, used atomic force microscopy (AFM) to identify how condensed pDNA display rod and torroid structures (Osada *et al*, 2010). The authors proposed a quantized folding model to explain the mechanism of DNA condensation. Osada and colleagues reported how condensed pDNA rod structure folds upon itself multiple times in a regulated manner. This may occur more readily for SC-pDNA which may account for the topology dependent size profiles identified in the present analysis. However from this study it is clear that polyplexes containing SC-pDNA display smaller sizes than OC- and linear-pDNA in a topology dependent manner.

3.6.1.3 DNA condensation assays

DNA polyplexes were treated with fluorescent intercalating dyes to quantify the degree to which PLL condenses pDNA. Complexes containing SC-pDNA were found to reduce intercalation much more efficiently than OC- and linear-pDNA polyplexes. The cationic PLL relaxes the anionic charge of the rigid phosphate backbone causing the structure to bend and coil (Hartmann *et al*, 2008). This seems to occur most effectively for SC-pDNA. In contrast linear-pDNA allows intercalation to occur much more readily. Although employing a different polymer to that of the present study, Cherng *et al*, (1999) reported how SC-pDNA complexes were most efficient at excluding intercalating dyes. Therefore in regards to gene delivery, SC-pDNA polyplexes seem quite efficient due to the effective packaging of DNA.

However despite the inability to effectively restrict EtBr fluorescence in this study, linear-pDNA has been shown to be efficiently condensed. Viral genomes containing DNA in the linear form, can be as large as 1000kb, but can be effectively packaged within a viral particle of ~100nm (Ledley, 1996). In order to carry out such functions, viruses utilise ATP driven

molecular motors to package the high density genomes which could be exploited for non-viral purposes (Ray *et al*, 2010).

3.6.1.4 Stability

For non-viral gene delivery to be applied therapeutically, the gene of interest must stay intact and avoid degradation by nucleases which are prevalent *in vivo*. Polyplexes were exposed to bezonase nuclease. The aim of the nuclease experiments was to analyse the effect of DNA topology on polyplex resistance towards nuclease attack. When exposed to nucleases complexes containing SC-pDNA were found to be the most resistant (Figure 3.11), which is consistent with the results of Remaut *et al*, (2006) (Table 3.1). The half life of transfected SC-pDNA was found to be within 50 minutes (Lechardeur *et al*, 1999). In this study Southern blot detection of SC-pDNA polyplexes persisted up to 20 minutes post nuclease exposure (Figure 3.11). The Southern blot experiment is a more sensitive method of detection than ethidium bromide staining via electrophoresis (Figure 3.8). This is because DNA was biotinylated prior to complex formation and probed after formation and exposure to enzymes, via streptavidin antibodies. However ethidium bromide is unable to intercalate between DNA strands within the polyplex due to PLL induced condensation. As ethidium bromide only fluoresces when bound to DNA, detection is restricted as a result. Polyplexes containing linear-pDNA were most susceptible to nuclease attack (Figure 3.11). DNA condensation studies revealed how the linear form exhibits a more open and accessible structure which may make it prone to nuclease attack. In contrast SC-pDNA complexes are smaller, compact and dense, thereby restricting exposure of the DNA cargo. OC-pDNA polyplexes displayed similar nuclease resistance to that of the SC form, which may be due to similarities in structure (Cherng *et al*, 1999). Therefore nuclease studies highlighted in this chapter

recommend DNA in the SC form for future uptake studies, due to displaying greater nuclease resistance.

3.6.1.4.1 Methods to improve polyplex nuclease resistance

However susceptibility of polyplexes to nuclease cleavage can be improved. For instance incorporation of poly(ethylene glycol) (PEG) which is a non-ionic hydrophilic polymer may increase nuclease resistance. PEG is beneficial as it interacts with DNA to form polyion complex (PIC) micelles. These micelles surround the DNA, thereby shielding it and nuclease resistance was found to be significantly improved (DNA in the intact SC form was observed 2 hours after exposure to DNase I) (Wakebayashi *et al*, 2004). Stabilization by PEG is important, as previous studies found how PLL/DNA complexes lacking PEG degraded within the blood (Mullen *et al*, 2000).

However incorporation of PEG within polyplexes can bring about non-specific interactions with cellular components. This is a problem as it can lead to the premature release of the DNA cargo (Christie *et al*, 2010). Research groups have previously found how oligopeptides can effectively and stably transport nucleic acids (Wadhwa *et al*, 1997; Niidome *et al*, 2000). Oligopeptide/DNA complexes were of 20 nm in size and displayed DNase I resistance for up to 1 hour longer than non-complexed DNA (van Rosenberg *et al*, 2004). Oligopeptides were reported to condense DNA at specific sites which may restrict pDNA exposure to nucleases (van Rosenberg *et al*, 2004). The reduction in size and resistance towards nuclease cleavage identified in van Rosenberg's study may account for the nuclease resistance displayed by SC-pDNA polyplexes in comparison to that of OC- and linear-pDNA complexes.

The condensed and compact structure of SC-pDNA polyplexes may alleviate nuclease digestion. Studies have shown how chemically identical DNA molecules can be distinguished

by structural differences. Less compact DNA underwent type I restriction nuclease digestion which occurs via DNA translocation (Keatch *et al*, 2004). However the translocation mechanism is blocked when the DNA is condensed by a polycation. Nucleotide recognition and cleavage is restricted when the DNA is coiled, unlike that of OC- or linear-pDNA. The uncondensed accessible structure such as the linear form is a suitable substrate for the translocation mechanism leading to restriction digestion (Keatch *et al*, 2004).

Therefore the results of the present chapter indicate the importance of DNA topology in regards to biophysical characterisation of PLL/DNA polyplexes. Parameters such as size, surface charge, charge ratio, DNA condensation and nuclease resistance are heavily influenced by DNA topology which are summarised in Table 3.1. Plasmids in the SC conformation are recommended for non-viral gene delivery studies.

3.6.2 Ionic strength

DNA polyplexes need to overcome various molecular and chemical barriers when transporting the DNA cargo. Nuclease resistance is a key pre-requisite, along with non-specific binding with blood components. However a key requirement of polyplexes is ionic stability (Neu *et al*, 2006). Ionic physiological conditions have been found to disrupt polycation/DNA interactions previously. Guo and Lee (2001) reported how PEI/DNA polyplexes formulated in high salt solutions (150mM NaCl) led to aggregation of particles. This was in agreement with the present study, whereby polyplex formation was perturbed when formed in high salt solutions. Regardless of DNA topology, PLL/DNA polyplex size increased dramatically (>1500nm) when formulated in high salt solutions mimicking physiological conditions (Figure 3.14). Ionic disruption of PLL/DNA formation was confirmed by a reduction in positive zeta potential measurements and DNA condensation

studies (Figures 3.15 and 3.16). If DNA polyplexes are to be employed therapeutically they must overcome changes in pH and salt concentrations. This is important in regards to various cellular and extracellular compartments whereby such parameters vary. A review by Park *et al*, (2010) discusses the use of pH-responsive polymers which allow the safe transport of DNA in compartments sensitive to pH and salt concentration. Another way of tackling ionic disruption is by cross linking polymers with disulphide bonds (Neu *et al*, 2006). Interaction occurs via polymer amine groups which secure the polyplex and maintained particle size and cationic charge during high ionic strength (Neu *et al*, 2006).

Triblock copolymers have been applied for polyplex gene delivery, which are stable towards pH buffering and variable salt concentrations. These systems refer to the combined use of three polymers, each with a specific function aimed to maximise gene delivery (Christie *et al*, 2010). One macromolecule will stabilise the polyplex (such as PEG), a second polycation condenses the DNA cargo, and finally a hydrophobic segment allows for ionic stabilisation. An example is that of Oishi *et al*, (2006) whose polyplex consisted of PEG-*block*poly(silamine) (PSAO)-*block*-poly{2-(N, N-dimethylamino)ethyl methacrylate] (PAMA). By incorporating various polymers to simultaneously resist nuclease cleavage, condense DNA and stabilise in physiological ionic conditions, gene delivery is enhanced and such complexes have yielded higher gene expression (Oishi *et al*, 2006). However such systems are highly polydisperse and cytotoxic to host cells.

3.6.3 Plasmid size

Conventional gene delivery studies analyse plasmids that are <15kb in size (Baker and Cotten, 1997). However in regards to gene therapy a large DNA insert is advantageous, particularly for therapeutic purposes where long term gene expression is vital. Recent studies

have analysed bacterial artificial chromosomes (BACs) expressing a 135kb genomic DNA insert for Friedreich's ataxia (FRDA) (Gimenez-Cassina *et al*, 2011). The BAC was formulated within a herpes simplex virus type 1 (HSV-1) vector and injected within mice. Gimenez-Cassina's team reported high vector transduction along with sustained gene expression for almost 75 days. Baker and Cotten, (1997) formulated BAC plasmids of up to 170kb, which were condensed with PEI (polyethylenimine) and conjugated to an adenovirus. Their combined viral/polycation approach yielded a tenfold increase in delivery compared to conventional methods. This provided the motivation for the present study whereby a 56.5kb BAC plasmid was complexed with PLL to form DNA polyplexes and analysed along with a smaller plasmid (3.8kb) undergoing the same procedure. When bound to PLL, the BAC polyplexes were both large (>900nm in diameter) and polydisperse. This was similar to the results of Baker and Cotten (1997), whose complexes were >500nm in size when formulated within HEPES buffer. The major disadvantage of the PLL/BAC polyplex was its inability to undergo charge neutralisation, even at extremely high charge ratios (Figure 3.18). In contrast the 3.8kb pDNA polyplexes (of varying charge ratios) displayed cationic charges, were >100nm in size and this compactness was reflected in EtBr fluorescence exclusion studies (Figures 3.20 and 3.21). Therefore in regards to the present study, PLL/BAC polyplexes seem unfeasible for gene delivery due to their large size, inability to be effectively condensed, and its failure to display a strong cationic charge. Moreover large BACs grown in *E.coli* are laborious to purify due to low copy numbers. Therefore in terms of bio-processing gene delivery through such means is extremely limited.

Therefore this chapter reveals how DNA topology clearly affects PLL/DNA polyplex characterisation. Parameters such as charge, size, DNA condensation and nuclease resistance are all affected by topology with the SC form displaying the most favourable characteristics.

Therefore in line with current FDA guidelines, plasmids in the SC conformation should be employed for non-viral gene delivery studies. Parameters such as ionic strength and plasmid vector size should be considered in order to maximise uptake and gene expression into host cells.

3.7 Chapter Summary

- Biophysical characterisation of PLL/DNA polyplexes was affected by DNA vector topology. The SC is recommended for uptake studies as complexes displayed:
    - Charge neutralisation at lower charge ratio of 0.6 (ratio of PLL to DNA), unlike that of linear-pDNA polyplexes which required a charge ratio of at least +2 to display a neutral charge.
    - Smaller sizes when measured by dynamic light scattering (DLS). SC-pDNA polyplexes were found to be approximately <200nm, whereas OC- and linear-pDNA complexes were larger at <400nm and <1000nm respectively.
    - Efficiently condensed by PLL as measured by ethidium bromide (EtBr) and TOTO-3 intercalating dye fluorescence studies. Complexes containing SC-pDNA reduced EtBr fluorescence to only 4%, unlike linear-pDNA at 20%.
    - Greater nuclease resistance as shown by Southern blot detection of the remaining amounts of DNA post exposure which was more sustained than OC- and linear-pDNA complexes.
- When produced in high salt solution the PLL/DNA interaction was disrupted. This led to increased sizes and a decrease in DNA condensation and cationic charge. This is important in terms of considerations for mimicking the vesicular ionic environment.
- Plasmid vector size affected polyplex characterisation with smaller plasmids complexed with PLL displaying smaller sizes (>100nm), charge neutralisation at lower charge ratios and effective DNA condensation, unlike that of larger DNA vectors (>1000nm mean diameter).

Chapter 4.
Visualising DNA and poly-L-lysine (PLL) by fluorescent labeling

4. Visualising DNA and poly-L-lysine (PLL) by fluorescent labelling

Bio-processing of non-viral gene delivery vehicles requires monitoring of the DNA cargo. Labelling of polyplexes is a critical procedure that allows tracking of its intracellular fate. In this chapter fluorescent labelling of DNA and the polycation vector; poly-$_L$-lysine (PLL) was studied. Fluorescent labelling is important as it can be monitored by a variety of techniques such as fluorescent confocal microscopy, spectrophotometry analysis, flow cytometry and live cell imaging amongst others. Polyplex labelling is important in regards to transfection studies, as it can reveal the path taken by DNA and enable greater understanding of the cellular mechanisms involved (Godbey *et al*, 1999).

In this study a dual labelling technique was employed whereby PLL and the DNA cargo were individually stained. This labelling strategy was employed in order to deduce whether DNA and PLL share the same intracellular fate or whether their paths are independent post transfection. Both direct and indirect methods of DNA labelling were explored in this chapter. Indirect labelling entailed fluorescent antibody detection of biotinylated DNA, whereas direct labelling involved staining through intercalating agents. Validation of labelling through fluorescent tagging was addressed in this chapter.

4.1 Labelling of PLL

4.1.1 Fluorometry analysis

Previous analyses focusing on polycation mediated gene delivery have employed various fluorophores and/or antibodies specific for the polymer of interest. The current study dual

labelled the polyplex which first entailed labelling the PLL. The polycation was labelled with a green fluorescent tag; Oregon Green-488 (Invitrogen) in a procedure similar to that of Godbey *et al*, (1999) (succinimidyl ester linkage). Unbound dye was removed by spin column purification in accordance to the manufacturer's protocol (Invitrogen) (refer to Chapter 2, section 2.4.1). The fluorescent signal of the labelled PLL was measured by fluorescent spectrophotometry (Figure 4.1). Tagged PLL showed dose-dependent emission at 521nm, while native PLL gave no signal. The labelling efficiency was found to be 1.21 Oregon Green dyes per PLL molecule.

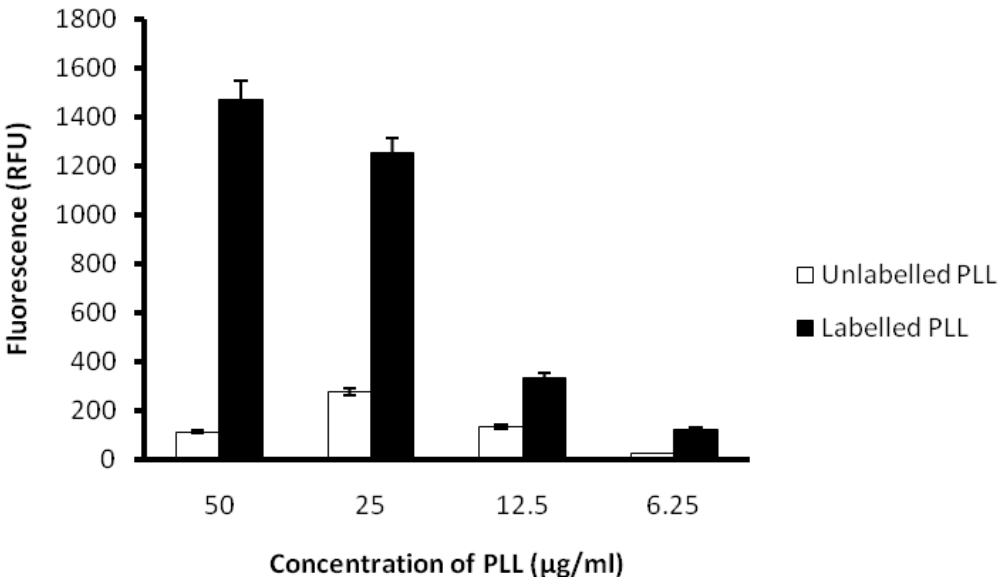

Figure 4.1: **Fluorometry analysis of labelled PLL.** Detection of labelled PLL at an excitation and emission spectra of 488 and 521nm respectively. The figure shows the mean and standard error (SE) of 3 independent experiments. One-way ANOVA was employed to deduce levels of statistical significance ($p < 0.05$) between unlabelled and labelled PLL.

4.1.2 Confocal microscopy analysis of labelled PLL

In order to confirm successful labelling of PLL that would enable fluorescent detection via confocal microscopy a number of experiments were conducted. Firstly coverslips were coated with fluorescently labelled PLL (50µg/ml) to immobilise the polycation on the glass surface. Labelled PLL could be detected on the coverslips through the Oregon Green fluorescence. PLL distribution was non-uniform, with aggregates of PLL at specific areas upon the coverslip. In contrast unlabelled PLL-coated coverslips displays no fluorescence (Figure 4.2).

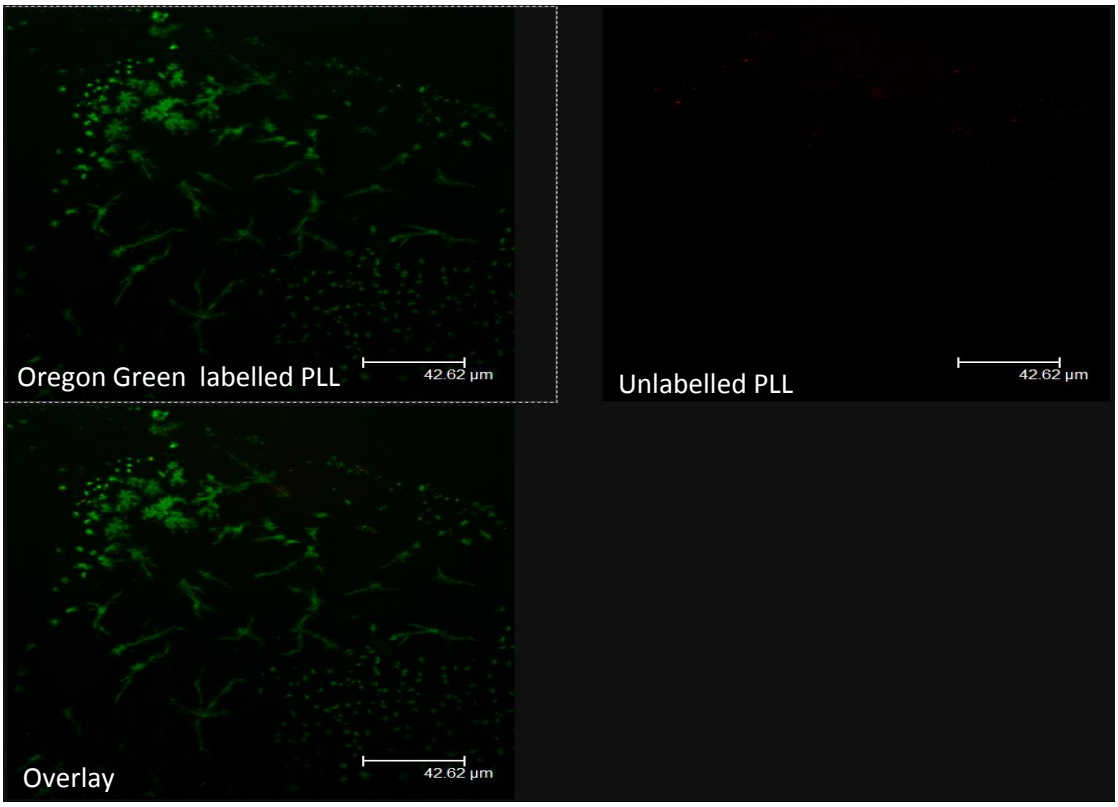

Figure 4.2: **Confocal microscopy detection of Oregon Green labelled PLL**. PLL (50µg/ml) was coated on coverslips, mounted on slides and analysed via fluorescent confocal microscopy.

4.1.3 Identification of labelled PLL when 'mock transfected' within Chinese hamster ovary (CHO) cells

To deduce whether PLL labelling can be detected in mammalian cells, Chinese hamster ovary (CHO) cells were 'mock' transfected with Oregon Green labelled PLL for one hour. Cells were fixed with paraformaldehyde and stained with DAPI (nuclear stain) and HCS CellMask^{TM} (cytosolic stain) and observed by confocal microscopy (Figure 4.3). Aggregates of PLL were observed at the periphery of the CHO cell (presumably the aggregated native PLL exhibiting a large size to readily enter the cell). Importantly the PLL retains the Oregon Green label through the 'transfection', fixation and staining protocols and can therefore be used to localise the PLL for confocal microscopy studies.

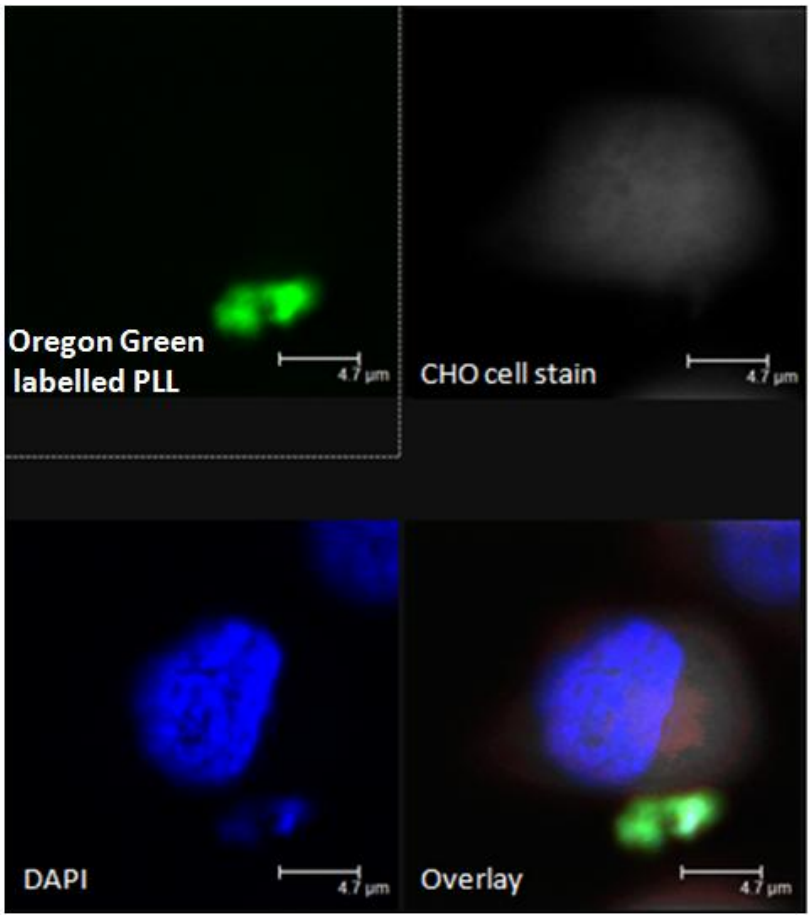

Figure 4.3: **Confocal microscopy observation of labelled PLL when 'mock' transfected in CHO cells**. Coverslips were mounted on microscope slides using DAPI (4',6-diamidino-2-phenylindole) mounting medium which is a nuclear blue stain displaying excitation and emission spectra of 358 and 461nm respectively. CHO cells were stained using the HCS CellMask™ Stains (Invitrogen) at an excitation and emission spectra of 556nm and 572nm respectively. Cells were fixed with paraformaldehyde, permeabilised and stained, followed by mounting with DAPI.

4.2 DNA labelling

Stable labelling of the nucleic acid cargo is critical in order to track transfected polyplexes. Labelling should be maintained and not jeopardise function.

4.2.1 Indirect labelling of DNA - biotinylation

Initially the pDNA was biotinylated and probed with a labelled streptavidin fluorophore. The biotinylation procedure incorporated a DNA precipitation step in order to remove any unbound biotin from the nucleic acid with the aim of reducing false positive signals. DNA was labelled at a 0.25:1 v:w ratio of reagent per µg of DNA (Chapter 2, section 2.4.2). Biotinylation of pDNA was confirmed by Southern blot (Figure 4.4). As shown the detection of the biotin/avidin DNA signal via chemiluminescence clearly corresponded to the nucleic acid samples run via agarose gel electrophoresis. This signal increases with DNA concentration upon the membrane.

In addition to the Sothern blot, a dot blot procedure was carried out whereby biotinylated DNA of differing concentrations (serial dilutions) were spotted directly onto a nitrocellulose membrane and probed as before (Figure 4.5). Clear intense signals are detected, which are in line with that of the positive control, suggesting that the nucleic acid has successfully been biotinylated. Dot blots provide a simple and quick assay to detect successful biotinylated samples; however such a procedure does not provide information about the size of the labelled product to which the conventional Southern blot does.

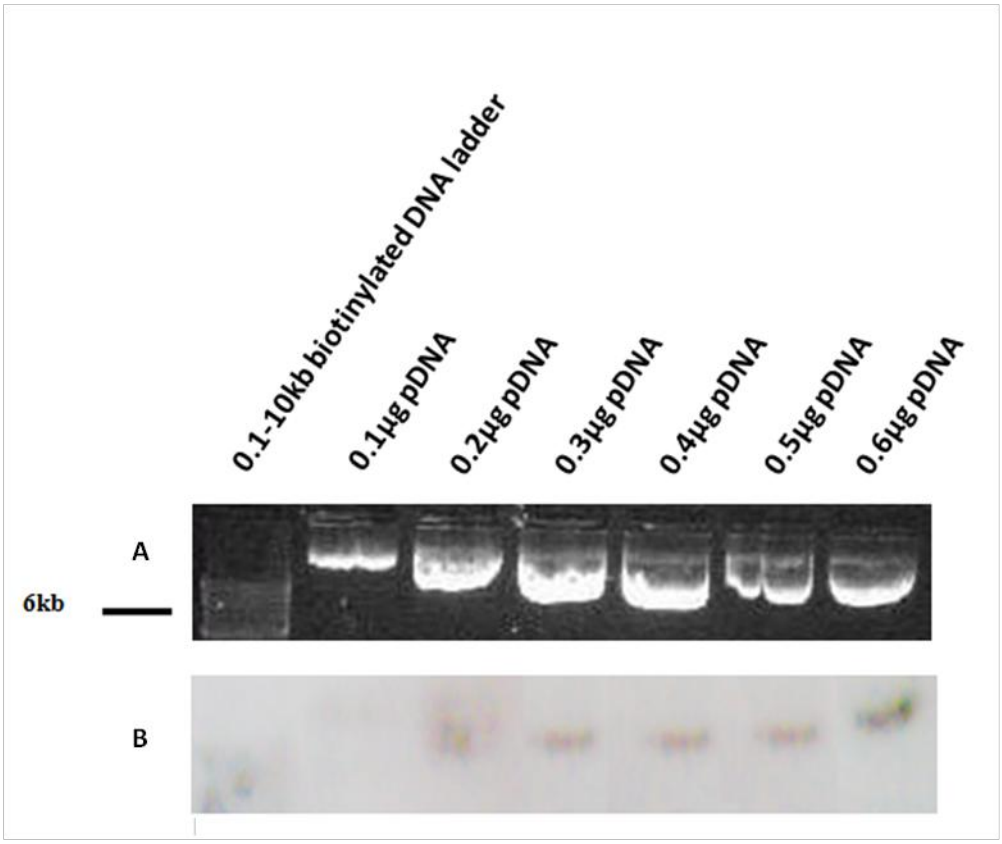

Figure 4.4: **Southern blot detection of biotinylated DNA**. Transfer of biotinylated DNA from the agarose gel (A) to the nitrocellulose membrane (B). The biotinylated DNA upon the membrane was detected by probing with a streptavidin-HRP (horse radish peroxidase) antibody which was confirmed via chemiluminescence.

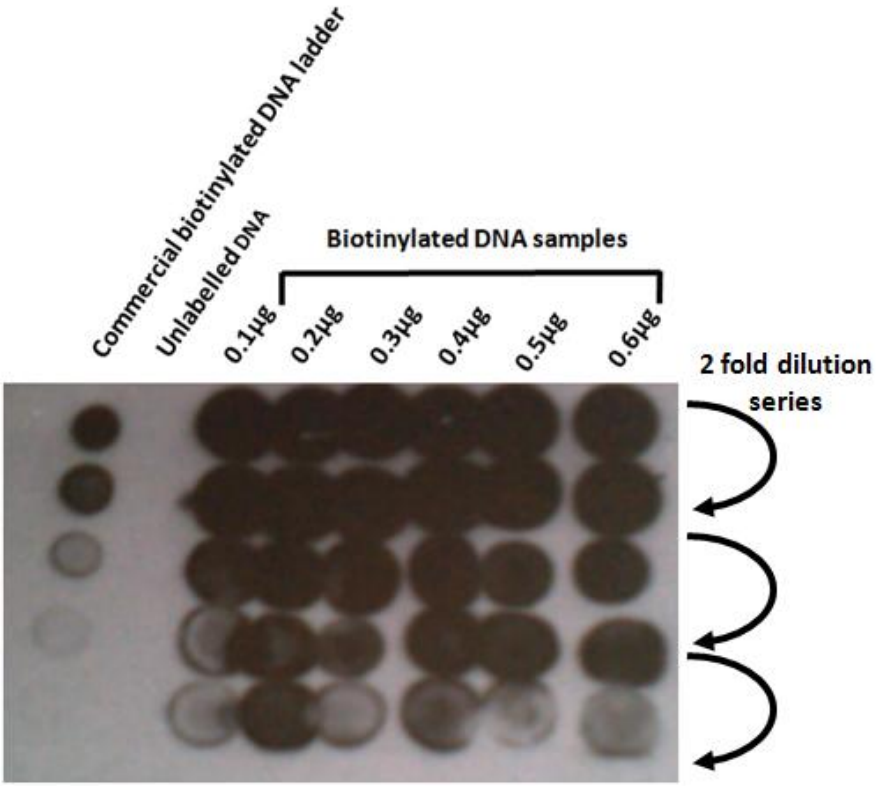

Figure 4.5: **Dot blot confirmation of biotinylated DNA**. Labelled DNA was spotted directly upon the membrane. Membrane was blocked with 1% BSA/PBS for 1 hour, followed by probing with streptavidin-HRP antibody and detection via chemiluminescence.

However as PLL condenses the pDNA, it is important to analyse whether PLL binding with biotinylated DNA jeopardises streptavidin probing (hence detection of DNA). In order to address this biotinylated DNA (SC-form) was complexed with PLL at a high charge ratio (ratio of PLL to DNA) of +1.6. The biotinylated DNA complex was then detected via dot blot

analysis (Figure 4.6). PLL binding and induced condensation does restrict streptaavidin access towards the biotin, reducing the signal intensity in comparison to naked biotinylated DNA. The limits of detection of biotinylated DNA within complexes was 0.1µg, at least ten fold higher than that of free uncomplexed biotinylated DNA (lane 2, Figure 4.6). This is consistent with previous studies showing that biotinylation of DNA complexes did not affect streptavidin binding and retained biological function (Leahy *et al*, 1996). However the condensation induced by PLL may limit the sensitivity of detection of complexes within the cell.

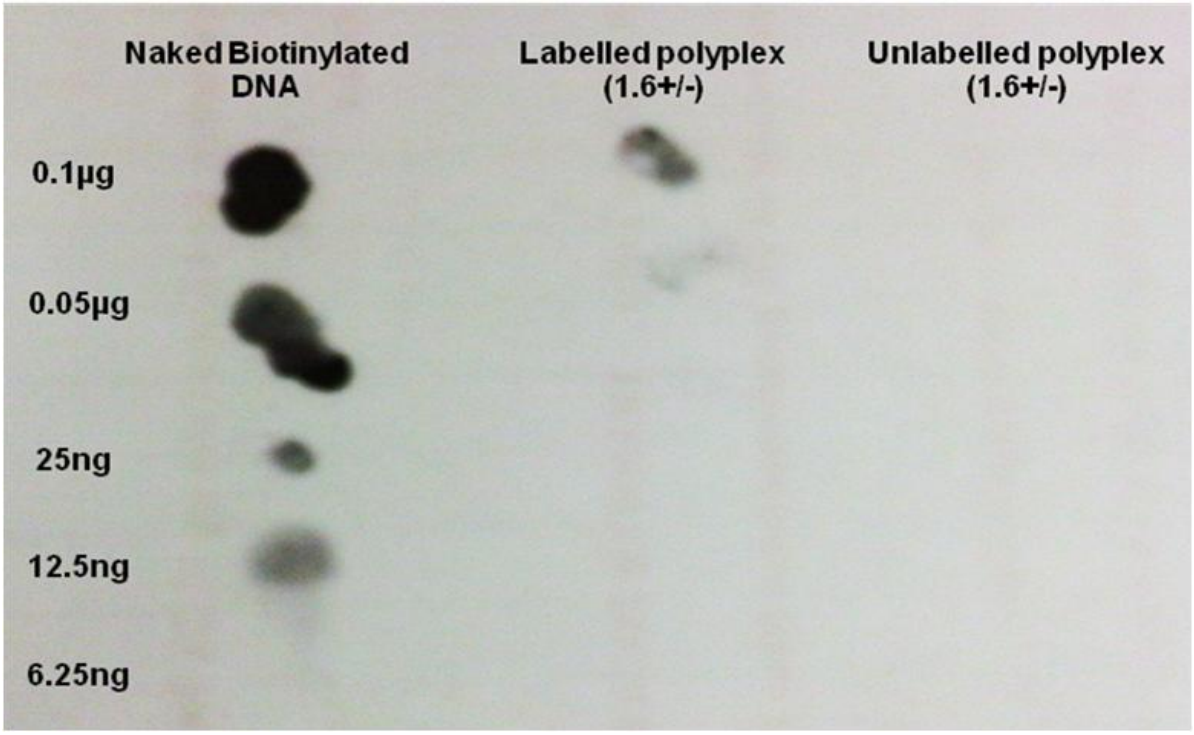

Figure 4.6: **Dot-blot displaying the effect of PLL condensation on the ability to probe the nucleic acid with streptavidin-HRP antibody**. SC-pDNA was formulated at a charge ratio of +1.6.

To study whether labelling is maintained post transfection, labelled complexes were transfected within CHO cells and observed via confocal microscopy. Figure 4.7 displays confocal microscopy images which show labelled DNA polyplexes (biotinylated DNA complexed with PLL) at one hour. CHO cells were also stained (with HCS CellMask^{TM} – cytosol) to show passage of complexes. For all three major topologies (SC-, OC- and linear-pDNA) DNA observation (far red channel) is quite restricted. Complexes containing biotinylated SC-pDNA exhibit limited fluorescence which may be due to the dense structure of the topological form, coupled with PLL induced condensation (Figure 4.7a). This may culminate in restricted access for the streptavidin probe. A similar observation is also true for complexes containing biotinylated OC-pDNA. However linear-pDNA exhibited a much more improved signal (Figure 4.7c).

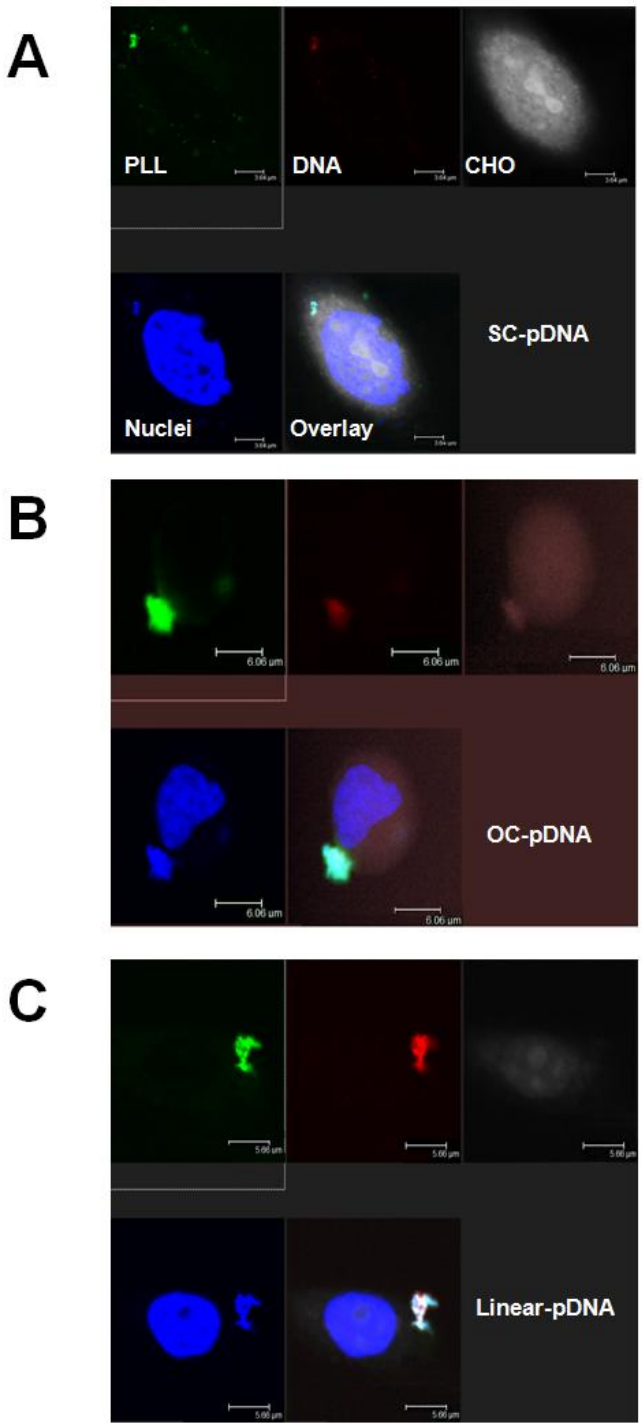

Figure 4.7: **Fluorescent confocal microscopy imaging of biotinylated DNA complexes when transfected within CHO cells.** The far red colour was selected in order to distinguish from the Oregon Green labelled PLL. SC-pDNA complexes (A), OC-pDNA complexes, (B) and linear-pDNA complexes (C). Polyplexes (containing 2μg) were produced at charge ratios of +1.6 (SC and OC-pDNA) and +5 (linear-pDNA). The biotinylated DNA was probed with a Texas Red labelled streptavidin antibody. CHO cells were stained with HCS CellMask^{TM}, while nuclei were stained with DAPI. Images show polyplexes at 1 hour post transfection.

4.2.2 Direct labelling of DNA – intercalating fluorescent dyes

Although labelling via biotinylation enabled detection of pDNA in the cell, the sensitivity of the method was poor. Furthermore the method required permeabilisation and staining of the cell with streptavidin conjugates. An alternative direct method of identifying the nucleic acid was analysed. Various studies have employed families of fluorescent intercalating dyes, major examples of which are the Dimeric Cyanine Nucleic Acid Stains (Invitrogen). These dyes are potent intercalating agents which offer great specificity and stability upon DNA binding (up to 1000 fold increase in fluorescence when interwoven between DNA strands) (Rye *et al*, 1992). Such dyes offer far more stability (approximately 50 fold greater) than that of ethidium bromide, a fellow intercalating agent (Rye *et al*, 1992). In this study the Dimeric Cyanine Nucleic Acid stain; TOTO-3 (excitation: 642nm, emission: 660nm) was employed to label the pDNA (Chapter 2, section 2.4.2). This particular far red stain was selected as it can be combined with existing dyes employed for other components. Experiments were undertaken to test whether such a stain firstly bound to the nucleic acid and also whether fluorescent intensity can allow direct detection of DNA for confocal microscopy studies.

2µg of naked pDNA was treated with 4µM TOTO-3 according to the manufacturer's protocol. In order to detect the stained DNA, samples were spotted onto coverslips coated with fluorescently labelled PLL (Figure 4.8). DNA immobilised to the bound PLL and was identified by co-localisation of the red (DNA) and green (PLL) fluorescence. Unlike biotinylated labelling steps, intercalating dyes bypass probing and washing procedures due to their specific affinity.

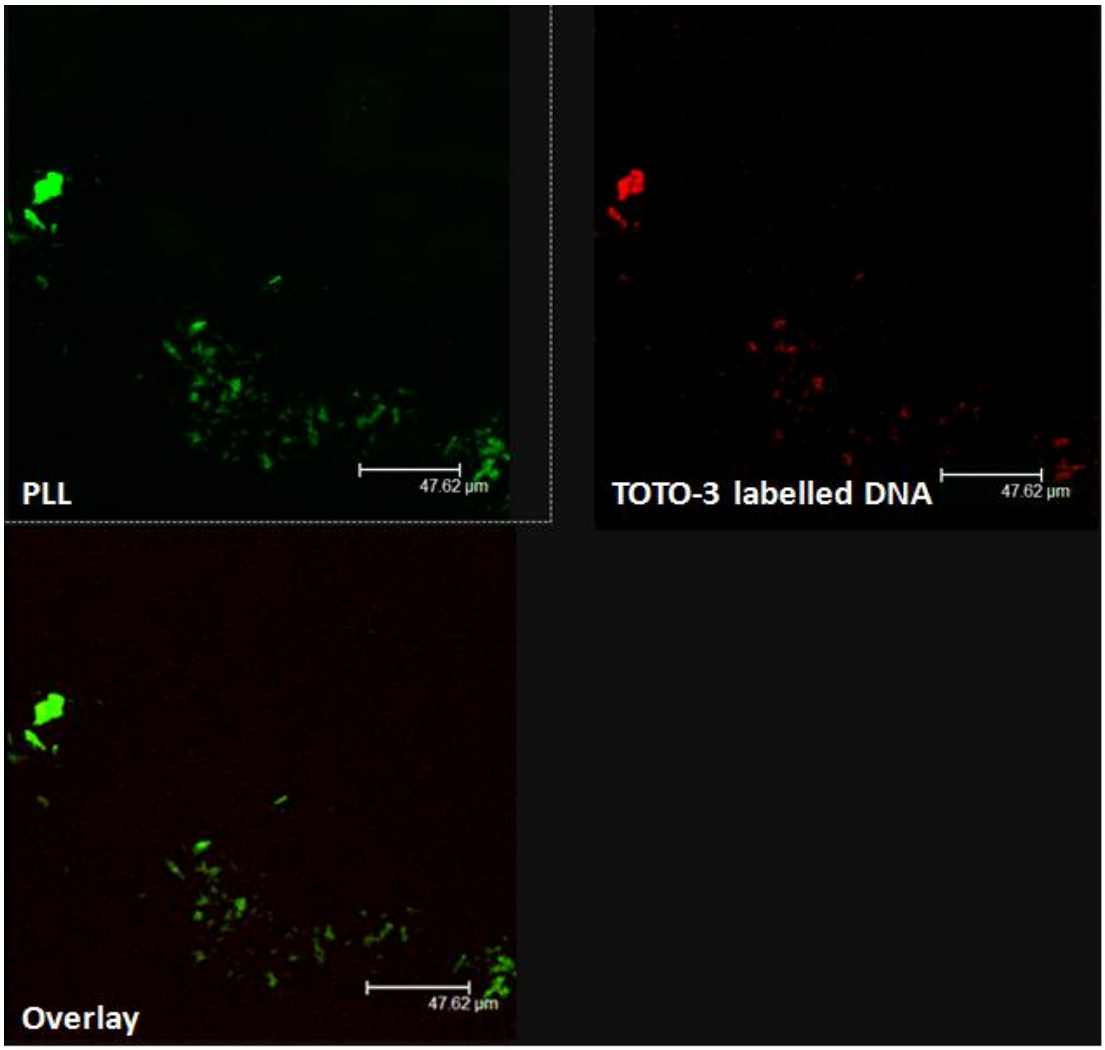

Figure 4.8: **Confocal microscopy observation of TOTO-3 stained DNA**. DNA (2µg) was stained with TOTO-3 at a final concentration of 4µM. Labelled DNA was spotted onto a PLL (50µg/ml) coated coverslip and mounted on a slide for fluorescent confocal microscopy analysis.

Another method was also employed to visualise the stained DNA. TOTO-3 labelled DNA was spotted on coverslips coated with fluorescent beads. These particular beads fluoresce at various wavelengths (can be visualised under green, red and blue filters). Figure 4.9 shows how the DNA binds to the beads allowing identification of the nucleic acid. Although the

beads can be observed at different fluorescent filters, the DNA is only visualised within the far red filter, showing no leakage at differing channels.

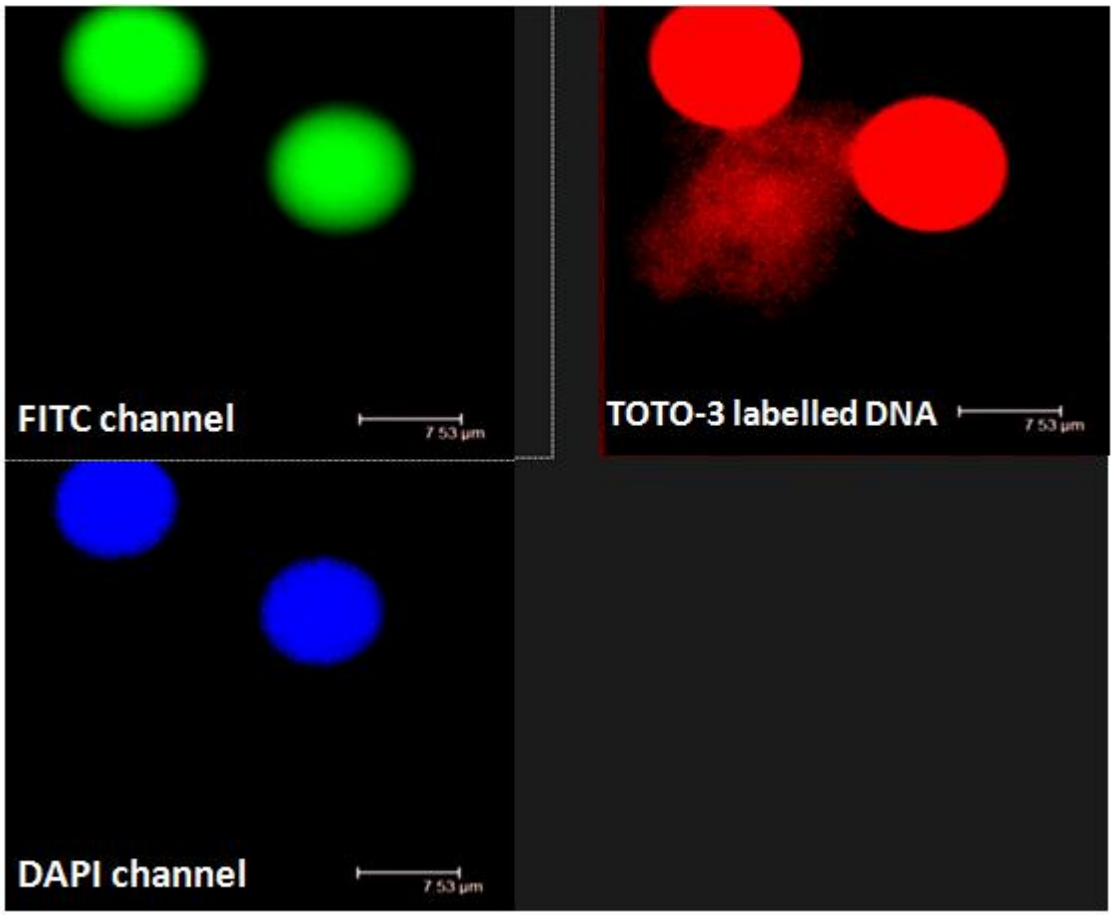

Figure 4.9: **Confocal microscopy observation of TOTO-3 stained DNA via fluorescent bead detection.** DNA (2µg) was bound to fluorescent beads and is exclusively identified in the far red channel. No fluorescence is leaked into other channels.

In order to further validate the results of Figure 4.9, TOTO-3 labelled DNA was visualised in the near red filter which is used to observe the HCS CellMask^{TM} stain. This experiment is important as fluorescence spectra of TOTO-3 and HCS CellMask^{TM} are quite similar. Importantly Figure 4.10 shows no leakage of fluorescence between the different channels

when analysing labelled polyplex DNA and CHO cells which were fluorescently stained. TOTO-3 stained DNA is exclusively visualised in the far red filter (TOTO-3 excitation: 642nm and emission: 660nm) rather than the near red filter used to visualise the HCS CellMask™ stain (excitation 556nm and emission: 572nm). The aim of this particular experiment was to analyse whether fluorescent leakage occurs between the channels, not the study of uptake (which is analysed in subsequent chapters). The key take home message from this particular experiment is that TOTO-3 labelled DNA fluorescence is not observed when viewing the CellMask™ labelled CHO cells (and vice versa).

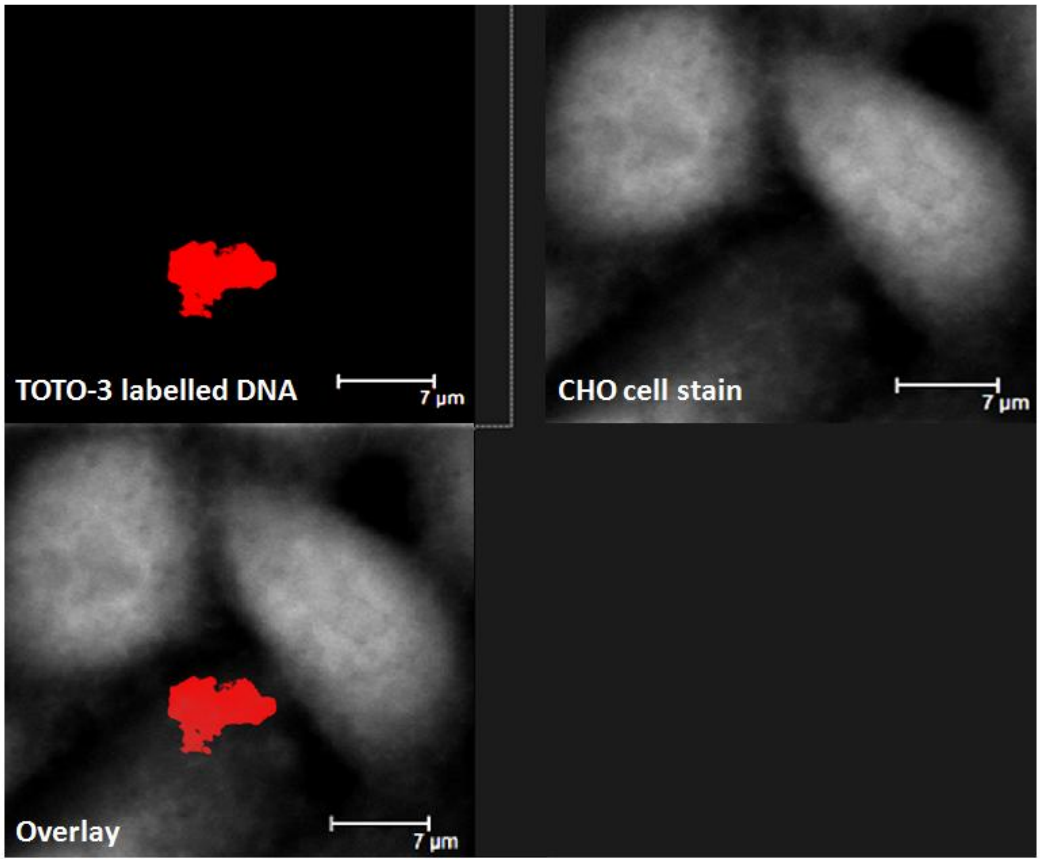

Figure 4.10: **Confocal microscopy observation of TOTO-3 stained DNA in far and near red channels.** Polyplexes containing TOTO-3 stained DNA (2µg) was transfected into CHO cells which were stained with HCS CellMask™ . DNA is exclusively identified in the far red channel. No fluorescence is leaked into other

A control microscope slide was prepared whereby PLL itself (no DNA) was spotted on the coverslip mounted on a slide. Separate images of the same slide were taken in both the FITC (Oregon Green labelled PLL settings) and far red (TOTO-3 stained DNA) channels (Figure 4.11). There was no evidence of any spillover of the Oregon Green signal into the TOTO-3 channel confirming that the signal observed in this channel in Figure 4.8 and Figure 4.9 was due to TOTO-3 stained DNA.

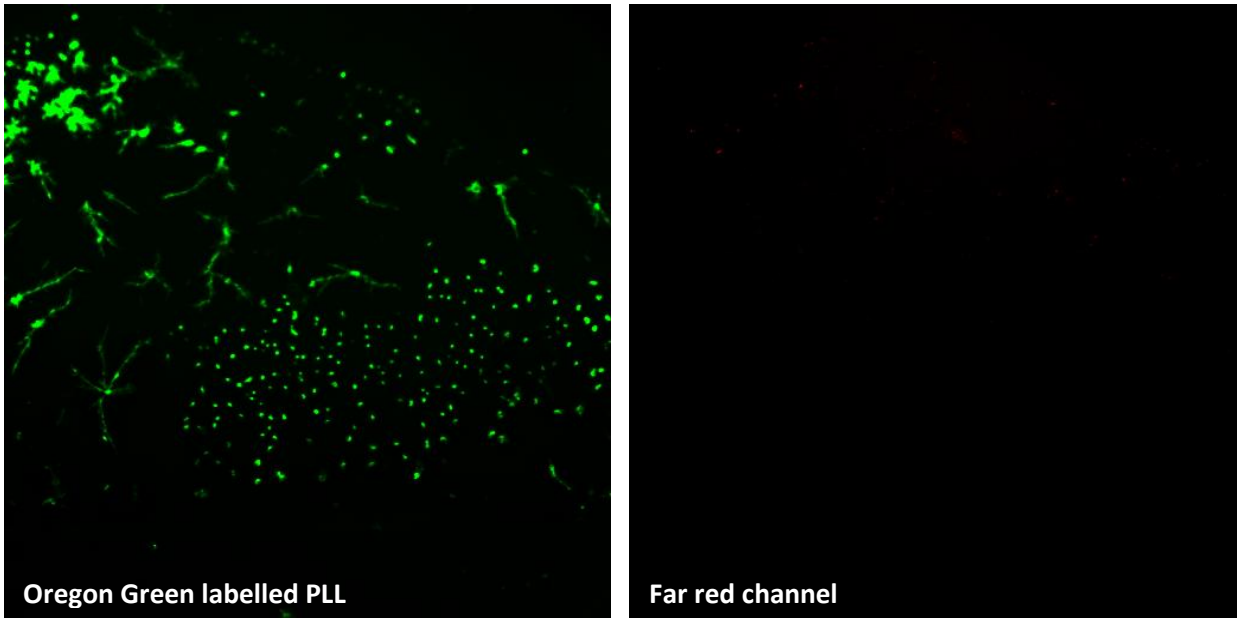

Figure 4.11: **No spill over of PLL fluorescence in DNA fluorescent channel**. Detection of labelled PLL (50µg/ml) demonstrating that fluorescence does not spill over into the far red channel when the same image is captured under the far red channel thereby confirming no false positive images.

4.2.2.1 Identification of TOTO-3 labelled DNA polyplexes post transfection

Plasmids were labelled with TOTO-3 (4μM) and complexed with PLL. Polyplexes were analysed by fluorescent confocal microscopy (Figure 4.12). Regardless of topology the DNA is very visible and can be tracked quite quickly, which is critical for further studies. Polyplexes were prepared at charge ratios of +1.6 (SC- or OC-pDNA) and +5 (linear-pDNA) as these complexes are of equal surface charge and will be employed for further transfection studies.

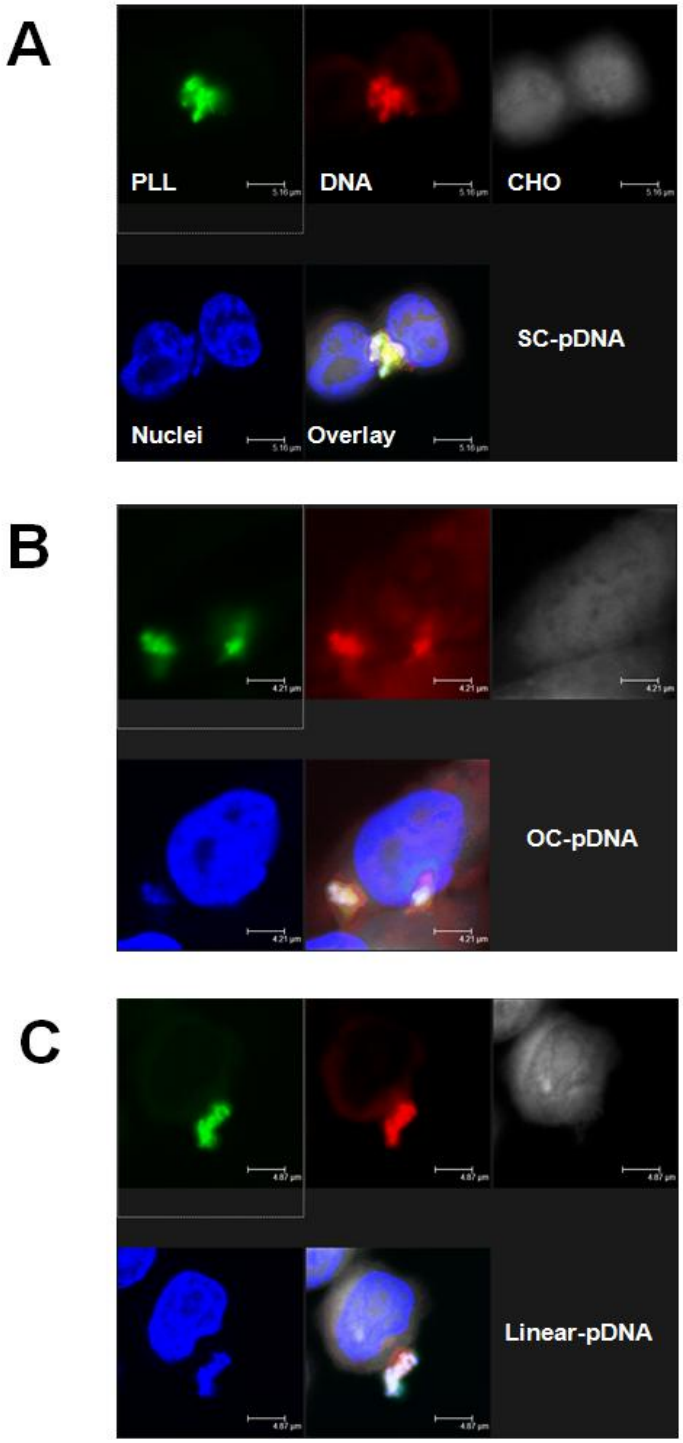

Figure 4.12: **Fluorescent confocal microscopy imaging of TOTO-3 labelled DNA complexes when transfected within CHO cells.** SC-pDNA complexes (A), OC-pDNA complexes, (B) and linear-pDNA complexes (C). Polyplexes (containing 2µg) were produced at charge ratios of +1.6 (SC and OC-pDNA) and +5 (linear-pDNA). CHO cells were stained with HCS CellMask^{TM}, while nuclei were stained with DAPI. Images show polyplexes at 1 hour post transfection.

4.3 Characterisation of labelled polyplexes

Labelling the nucleic acid, either through biotinylation or a DNA intercalating agent coupled with PLL binding, which is also labelled, brings up the question as to whether such labelling alters the structure of the polyplex or its biophysical characteristics. In order to address this issue labelled polyplexes were analysed through a variety of characterisation assays. Polyplexes were prepared at charge ratios of +1.6 (for SC- and OC-pDNA) and +5 (for linear-pDNA), as deduced from the previous chapter (Chapter 3).

4.3.1 Size measurements

The sizes of labelled and unlabelled complexes were measured via dynamic light scattering (DLS) (Figure 4.13). Labelling of DNA or polycation (irrespective of DNA topology) does not affect size measurements. Regardless of the method of labelling; polyplex size shows dependence on DNA topology. The observation that polyplex size is independent of method of labelling is important considering its employment as a delivery vehicle. Slight aggregation was detected for OC-pDNA complexes (when the DNA was stained with TOTO-3) with diameters peaking at 695nm. Mean diameters were larger than those of biotinylated and unlabelled samples. This is similar to that of linear-pDNA polyplexes stained with TOTO-3. Severe aggregation was recorded for all three linear-pDNA polyplex samples.

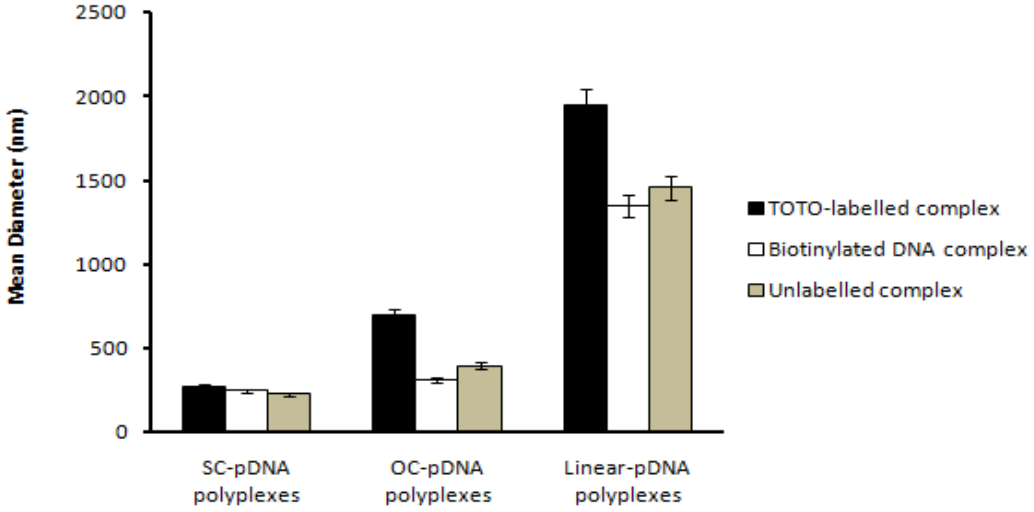

Figure 4.13: DLS measurements of labelled polyplexes. 2µg pDNA was stained with 4µM TOTO-3. 2µg DNA was biotinylated at a 0.25:1 v:w ratio of reagent per µg of DNA. Polyplexes were prepared at charge ratios of; +1.6 for SC- and OC-pDNA, and +5 for linear-pDNA. The figure shows the mean and SE for 10 readings. The figure shows the mean and SE of 5 replicate measurements. The experiment was repeated 3 times independently. One-way ANOVA was employed to deduce levels of statistical significance ($p < 0.05$) between labelled and unlabelled complexes of differing DNA topologies.

4.3.2 TOTO-3 fluorescence assay

The Dimeric Cyanine Nucleic Acid Stain; TOTO-3 is a potent nucleic acid stain, which was shown to label DNA to a high degree. One approach to quantifying the level of fluorescence of the labelled DNA, was a via a fluorometry assay (Figure 4.14). Labelled and unlabelled DNA samples, along with naked and complexed DNA were analysed. The RFU (relative fluorescence units) were greatest for naked DNA samples that were stained with the dye (regardless of DNA topology). Fluorescence decreased when pre-stained DNA was complexed with PLL. This may be due to DNA condensation induced by PLL, which restricts DNA intercalation and fluorescence. Unlabelled naked DNA displayed moderate RFU which is presumably due to autofluorescence.

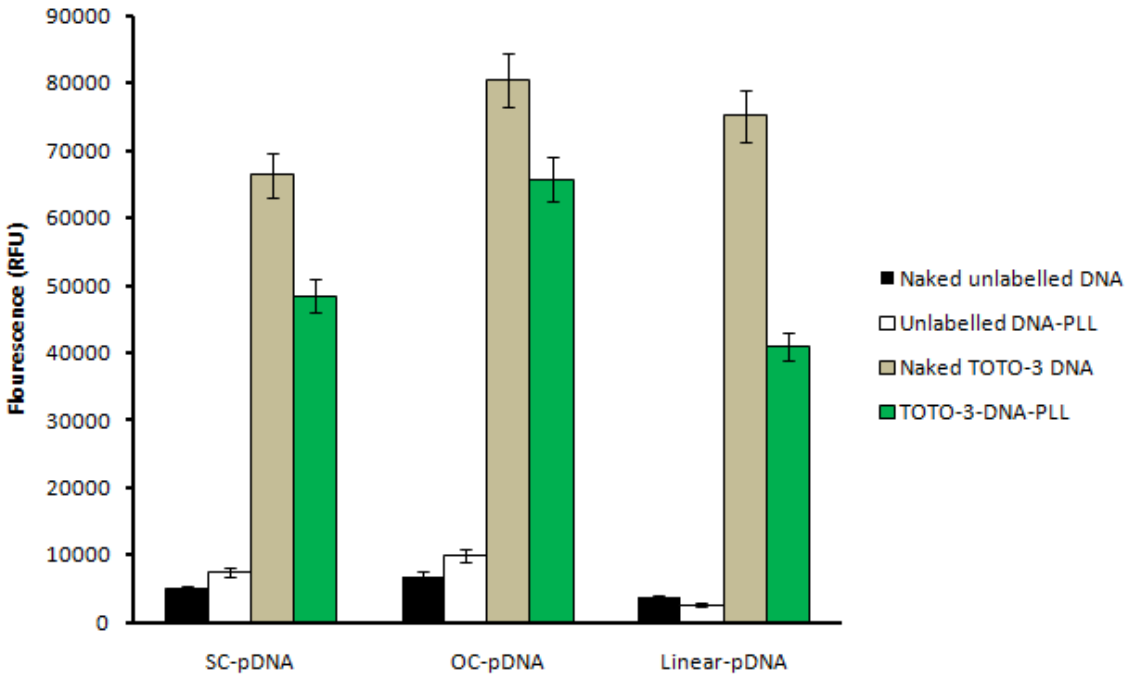

Figure 4.14: **Fluorometry assay of TOTO-3 labelled DNA complexes along with unlabelled controls at an excitation and emission spectra of 642 and 660nm respectively**. 2µg pDNA was labelled with 4µM TOTO-3 dye. Polyplexes were prepared at charge ratios of; +1.6 for SC- and OC-pDNA, and +5 for linear-pDNA. The figure shows the mean and SE of 3 independent experiments. One-way ANOVA was employed to deduce levels of statistical significance ($p < 0.05$) between unlabelled and TOTO-3 stained samples.

4.3.3 Electrophoretic analysis

Agarose gel electrophoresis was employed to analyse the electrophoretic mobility and ethidium bromide (EtBr) fluorescence, and whether labelling affected such parameters. Labelling of naked DNA with either TOTO-3 or biotin does not hinder electrophoretic mobility pDNA (regardless of topology) (Figure 4.15). As expected electrophoretic mobility and EtBr fluorescence is reduced for polyplexes (regardless of labelling) due to PLL induced DNA condensation and change in surface charge. EtBr fluorescence is limited for naked DNA stained with TOTO-3 (Figure 4.15, lane 1C). This may be due to the pre-existing

TOTO-3/DNA intertwined strands which may restrict and compete with EtBr for access. The results from Figure 4.15 demonstrate that labelling (through biotin or TOTO-3 staining) does not alter electrophoretic mobility, and indicates no major disruption to the physical nature of polyplexes that could jeopardize the aim of attaining mammalian cell entry.

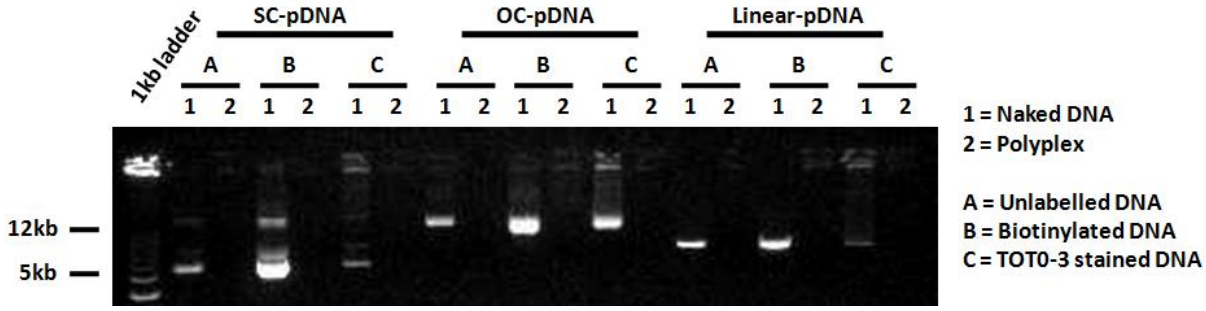

Figure 4.15: **Agarose gel electrophoresis of labelled and unlabelled pDNA (naked and complexed).** 2µg pDNA was stained with 4µM TOTO-3. 2µg DNA was biotinylated at a 0.25:1 v:w ratio of reagent per µg of DNA. Polyplexes were prepared at charge ratios of; +1.6 for SC- and OC-pDNA, and +5 for linear-pDNA.

4.4 Discussion

In this chapter fluorescent labelling was analysed in regards to visualising both DNA and polymer. This is important in terms of monitoring the path taken by the pDNA and PLL and whether they share the same intracellular fate post transfection. Moreover in terms of bio-processing it is important to monitor the DNA cargo and whether it remains intact. This is important from regulatory viewpoints and allows greater understanding of the pathway undertaken by polyplexes following potential uptake.

4.4.1 PLL Labelling

PLL was labelled with a green fluorescent tag which bound via a succinimidyl ester linkage. This was done in accordance to Godbey *et al*, (1999), who observed efficient and sustained labelling of PEI. In this study quantitative analysis revealed how PLL was effectively labelled (Figure 4.1) and qualitative studies showed how fluorescence can be detected when 'mock transfected' into CHO cells (Figure 4.3). This is important in terms of tracking the polymer and its association with DNA through dual labelling. Fluorescent labelling plays a central role in studies monitoring the trafficking of complexes and gives an insight into the mechanism of cellular entry. By fluorescently labelling PEI, endocytic mechanisms of DNA polyplex uptake was recorded (Godbey *et al*, 1999). PLL like many polymers can be covalently attached to many fluorophores, allowing effective labelling whilst maintaining native function.

However despite fluorescently labelling PLL via succinimidyl ester linkage, unbound polymer can arise which can limit labelling. This requires an additional step to remove unbound PLL. Alternative polymer labelling methods include the use of water soluble fluorescent dyes such as Cy5, which have been found to effectively label PLL (Lucas *et al*,

2002). The benefits of such dyes include sensitivity which allowed analysis of PLL/DNA binding kinetics (Lucas *et al*, 2002). Polar sensitive fluorescent labels (covalently attached to PLL) have recently been employed. These dyes change colour on the basis of the environmental polarity and their application has enabled analysis of membrane binding of PLL (Postupalenko *et al*, 2011).

4.4.2 DNA labelling

Labelling of nucleic acids is critical in order to follow potential uptake of pDNA. Direct and indirect methods of DNA labelling were explored. Indirect labelling was brought about via biotinylation and probed by fluorescent streptavidin conjugates. Although detection of DNA occurred, the sensitivity of the method was weak (Figure 4.7). In contrast direct labelling of DNA was found to be more effective through the use of DNA intercalating agents and labelling was maintained during the transfection process (Figure 4.12). Intercalating dyes such as TOTO-3 fluoresce only when interwoven between DNA strands. This offers specificity and bypasses antibody probing and permeabilisation stages. Moreover such dyes have been found to be extremely stable when bound to DNA (Rye *et al*, 1992). The ability to label DNA with TOTO-3 in live and fixed cell analysis was reported previously. TOTO-3 staining was found to be most effective in samples probed with other fluorophores (Suzuki *et al*, 1997). Using 3-D confocal microscopy fluorescent intercalating dyes have been found to be extremely useful in determining DNA ploidy (Ploeger *et al*, 2008). The TOTO-3 dye employed in the present study is part of the Dimeric Cyanine Nucleic Acid Stains family (Invitrogen). Fluorophore members of this family exhibit such a strong affinity for DNA that studies have employed such dyes to assess structural changes in DNA polyplexes (Wang *et al*, 2001). When polyplexes are produced at high charge ratios, EtBr fluorescence is

restricted. However the sensitivity of TOTO-3 allows complexes to be viewed via confocal microscopy.

Although DNA staining through intercalating dyes has led to stable, effective and persistent labelling, there are drawbacks. These include safety issues regarding the use of intercalating agents, such as handling and disposal (Hardy *et al*, 1996). Secondly, intercalating dyes such as TOTO-3 and EtBr bind non-discriminately to double stranded nucleic acids. Whilst this is a benefit, this can also lead to unspecific binding with host cell nucleic acids. These are key points to consider for future analyses.

4.4.3 Alternative methods of labelling

To track potential uptake of DNA complexes, DNA and PLL were individually labelled to observe whether fluorescence co-localises. Although this facilitates dual tracking, there are alternative labelling strategies. Specific alternative labelling methods are available which are designed to highlight minute amounts of nucleic acids and polymer. These labelling strategies have been used to study the kinetics of DNA/polymer interactions. For instance anthraquinone dyes (which intercalate and bind to specific DNA regions) have been used to distinguish cytoplasmic and nuclear regions within the cell (Edward, 2009). Such dyes have previously been used to show via fluorescence correlation spectroscopy (FCS), how nucleosome core particles diffuse through high concentrations of DNA to mimic nuclear transport (Margenot *et al*, 2003).

Semiconductor quantum dots (QDs) have also been used to monitor uptake of pDNA. QDs are nanocrystal structures of minute sizes that facilitate labelling and cellular uptake (van Driel *et al*, 2008). Fluorescent QD labelling of pDNA is widely used and offers benefits such as displaying high fluorescence and photostability (Srinivasan *et al*, 2006). QD labelling of

pDNA is brought about through linkers that are covalently attached to the plasmid which allow binding of multiple QDs. Such methods have facilitated the analysis of CHO cell uptake of DNA (Srinivasan *et al*, 2006). QD attachment to pDNA has been found to increase plasmid folding, leading to a decrease in nucleic acid diameter (Zhang and Liu, 2010). Further advantages of QD attachment include sustained labelling, thereby allowing long term analysis, in which attachment does not jeopardise functionality (Srinivasan *et al*, 2006). QD labelling in uptake studies has proven extremely useful in monitoring chitosan complexes. In that particular study attachment of QDs to DNA did not affect gene expression nor increase cytotoxicity (Xiang *et al*, 2007).

Fluorescence resonance energy transfer (FRET) is the transfer of energy through the emission of fluorescence between two close proximity related fluorophores (Haugland *et al*, 1969). Fluorescence emitted on the basis of proximity allows sensitive and very specific detection. This proximity dependent mechanism has been exploited for a wide range of applications. For instance FRET has been used to study DNA decondensation when separated from its respective polymer (Thibault *et al*, 2010). Often co-localisation of fluorescence may not be adequate to confirm interaction and so the sensitive detection offered by FRET is important in regards to polyplex dissociation kinetics (Thibault *et al*, 2010). FRET has also recently been applied to study physical compositions of DNA polyplexes. By using FRET, Ko *et al*, (2011) revealed how fractions of polymer remain unbound to pDNA following complexion. FRET has been combined with QD labelling to optimise labelling of endosomes to enhance knowledge of uptake mechanisms (Delehanty *et al*, 2011).

Chemical and molecular biology techniques have been applied to fluorescently dual label a single plasmid. Srinivasan *et al*, (2009) conjugated rhodamine (red) and fluorescein (green) to a single plasmid via peptide nucleic acid linkers (similar to the attachment method of QDs).

By dual labelling a single plasmid the authors could monitor any cleavage that occurs following uptake through separation of fluorescent signals. This is critically important in terms of monitoring intact DNA cargo. This could also allow potential observation of any incomplete polymer binding.

Fluorescent labelling of host cells is also important in highlighting the passage of uptake regarding DNA complexes. In this study the host cell and cytoplasm were fluorescently labelled with a high content screening (HCS) stain to highlight uptake of polyplexes. This staining protocol allowed detection of cells following fixation. Cell staining is important as nuclear staining alone is not adequate for uptake studies. Cell staining should be non-invasive and allow detection of the cell and its contents in its native form. A major advantage of the HCS stain is that labelling masks the cells allowing the uptake of complexes to be monitored. However a drawback of this stain is its susceptibility to photo bleaching during confocal microscopy analysis. Therefore other forms of cellular labelling are of interest. Antibody detection of cells has been applied although probing may affect cell functionality. However disadvantages do include permeablisation and probing of cells. Aptamers have been applied to detect and reversibly label cells (Herr *et al*, 2006). Aptamers are biotinylated single stranded nucleic acids that interact with cell surface markers (Terazono *et al*, 2010). Populations of cells have been successfully identified via fluorescent QD-linked aptamers, which allowed for quantification via flow cytometry. This process is advantageous in that it avoids invasive probing and labels can be removed via nuclease treatment (Terazono *et al*, 2010).

4.4.4 Functionality and characterisation

Retaining biological function is critical post labelling when monitoring uptake of DNA complexes. In this chapter labelling through direct or indirect means did not affect characteristic features such as polyplex size (Figure 4.13). Electrophoretic analysis revealed observation of labelled complexes (by EtBr staining) was similar to unlabelled controls. Direct labelling with TOTO-3 was confirmed by reduced EtBr fluorescence, which competed with the dye to intercalate within free DNA strands. These findings are consistent with that of Slattum *et al*, (2003) whereby biotinylation and streptavidin labelling of pDNA did not hinder polyplex characteristics (such as size and DNA binding). In fact the study by Slattum *et al*, (2003) recorded how gene expression was not affected by DNA biotinylation. Retention of transcriptional activity may be due to the ability of RNA polymerase II to maintain recognition of modified bases thereby allowing further translational steps to proceed (Leahy *et al*, 1996).

Therefore in conclusion PLL labelling via Oregon Green labelling proved to be sufficient in terms of detecting the polymer via fluorescent confocal microscopy when 'mock transfected' into CHO cells. Direct labelling of DNA through fluorescent intercalating dyes was more effective than indirect methods such as biotinylation in terms of confocal microscopy analysis. Intercalating dyes are more photostable and bypass probing steps. These labelling methods are suitable to monitor and study potential uptake of polyplexes for gene delivery studies.

4.5 Chapter Summary

- The PLL component of polyplexes was efficiently labelled with Oregon Green and was detected by fluorescent microscopy.
- DNA topology did not affect labelling through either biotinylation or intercalating dyes.
- TOTO-3 was a more sensitive fluorescent stain for polyplex DNA than biotin/avidin detection systems and can be used to observe DNA via confocal microscopy. Detection of TOTO-3 stained DNA was clearer allowing more sensitive detection for confocal microscopy imaging. Confocal microscopy detection of biotinylated DNA was restricted.
- Labelling in the form of either biotinylation (indirect labelling) or TOTO-3 staining (direct labelling) did not affect polyplex size.
- Labelling (direct or indirect) did not affect electrophoretic mobility or ability to be detected by ethidium bromide staining. Although pre-stained TOTO-3 naked DNA did exclude ethidium bromide intercalation.

Chapter 5.
Polyplex uptake within CHO cells

5. Polyplex uptake within CHO cells

Non-viral gene delivery into mammalian cells is widely used in the biotechnology industry for the production of recombinant proteins requiring post translational modifications as well as considered for clinical trials in gene therapy vaccination. Gene transfer through such means often entails delivery of nucleic acids that are bound to a cationic polymer (polycations) resulting in plasmid DNA (pDNA) – polymer products, often referred to as polyplexes (Elouahabi and Ruysschaert 2005). Non-viral methods have been tested within mammalian cells such as Chinese hamster ovary (CHO) cells, as these cells allow high protein expression and can be successfully scaled up in culture (Liu *et al*, 2008 and Derouazi *et al*, 2004). Short term transient transfection of CHO cells using polycation polyplexes has been reported to result in high protein yields (Reisinger *et al*, 2009, and Schlaeger and Christensen, 1999) and successfully scaled up.

The current study systematically compares the biophysical properties of supercoiled (SC), open circular (OC) and linear forms of the same plasmid complexed with poly-$_L$-lysine (PLL), focusing on the intracellular uptake of the three types of polyplexes by CHO cells. PLL was specifically selected as a gene carrier due to its effective ability to transfect cells and recommendation by key studies (Tsai *et al*, 1999). Advantages of using PLL over other polymers include its ease of DNA binding and condensation (Luo and Saltzman, 2000). By labeling both nucleic acid and polycation components of the polyplexes, uptake could be followed by confocal microscopy.

In this chapter polyplexes were transfected into CHO cells. This refers to the process of introducing foreign nucleic acids into host cells, often with the aim of expressing a desired

protein product (Liu *et al*, 2008). Uptake (defined as the intake of materials by a cell or tissue leading to its permanent or temporary retention) of complexes was monitored qualitatively and quantitatively.

5.1 Observation of polyplex uptake

5.1.1 Confocal microscopy analysis of DNA polyplexes

Qualitative analysis of polyplex uptake is important. In this experiment fluorescent confocal microscopy was used as a tool to monitor polyplex uptake (Figure 5.1). To confirm whether polyplex uptake has occurred, images were taken as 3-D sections. Ten sections of each image, each of 0.2µm in thickness were taken. Mid section images were taken to confirm true polyplex uptake along with projection images of all sections (referred to as z-stack projection images). Details are provided in Chapter 2, section 2.6.7.1. DNA polyplexes (containing 2µg of pDNA) were transfected into a population of approximately 1 x 10^6 CHO cells. In order to view whether the DNA and PLL share the same cellular fate, the plasmid was pre-stained with a far red fluorophore (TOTO-3) while PLL was tagged with a green dye. The cytosol of the CHO cells was stained to show the outline of the cell. This was achieved by using HCS CellMask™ (Chapter 2, section 2.6.4), a high content screening fluorescent stain which specifically stains the cell cytoplasm. The DNA was stained with an intercalating dye; TOTO-3, however unlike ethidium bromide clear fluorescence is observed as TOTO-3 is approximately 50 fold more sensitive (Rye *et al*, 1992). DNA polyplexes were classified on the basis of their cellular location (through fluorescent co-localisation). Polyplexes were classified as to either being within the periphery of the cell (Figure 5.1a), cytosol (Figure 5.1b) or nucleus (Figure 5.1c). If no fluorescent overlap between the polyplex and the CellMask™ occurs, complexes are defined as being at the cell periphery. If some overlap between the polyplex and the CellMask™ occurs, complexes are classified as located within

the cytosol. Complete overlap between polyplex and nuclear stain is classified as nuclear association. Classification of polyplex location was confirmed as it was consistent in both stack and mid section images as shown in Figure 5.1.

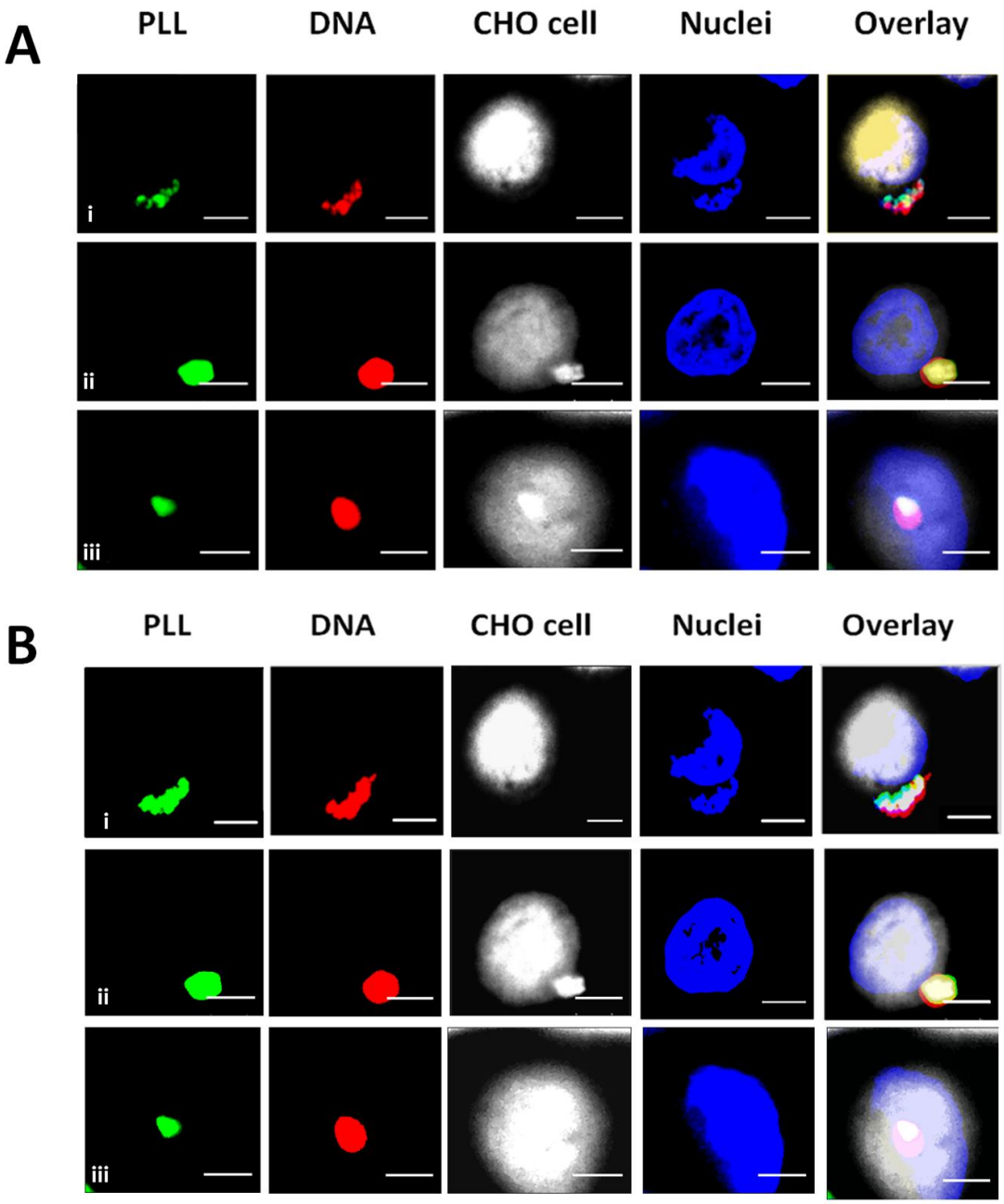

Figure 5.1: **Classification of polyplex cellular location in CHO cells**. Mid section (A) and stack projection images (B). Confocal microscopy analysis showing the location of polyplexes; cell periphery (linear-pDNA polyplexes) (i), cytosol (OC-pDNA polyplexes) (ii) and nucleus (SC-pDNA polyplexes) (iii). Complexes were prepared at charge ratios (ratio of PLL to DNA) of +1.6 (for SC- and OC-pDNA) and +5 for linear-pDNA. Scale bar represents 5μm. CHO cells were fixed with paraformaldehyde, stained and coverslips were mounted on slides.

5.1.2 Short time course

Polyplex uptake within CHO cells was monitored for periods up to 60 minutes. Uptake was analysed via confocal microscopy (Figure 5.2). No obvious difference was observed in the appearance of polyplexes of different topologies. All polyplexes showed dual staining for DNA and PLL, suggesting that the PLL remains closely associated with the DNA during passage though the cell (Figure 5.2). The route taken by the polyplexes begins at the cellular periphery (Figure 5.2a) and culminates with nuclear association (complete overlap between polyplex fluorescence and nuclear stain) by 1 hour (Figure 5.2c). At 60 minutes SC-pDNA polyplexes associate with the nuclei (Figure 5.2c). This is in contrast to linear-pDNA polyplexes whereby at the same time point, are situated at the cell periphery (Figure 5.2a). Complexes appear larger than suggested by initial size measurements (Chapter 3, Figure 3.5), which may be due to the cellular ionic environment, an observation in line with size measurements in high salt solutions (Chapter 3, Figure 3.14).

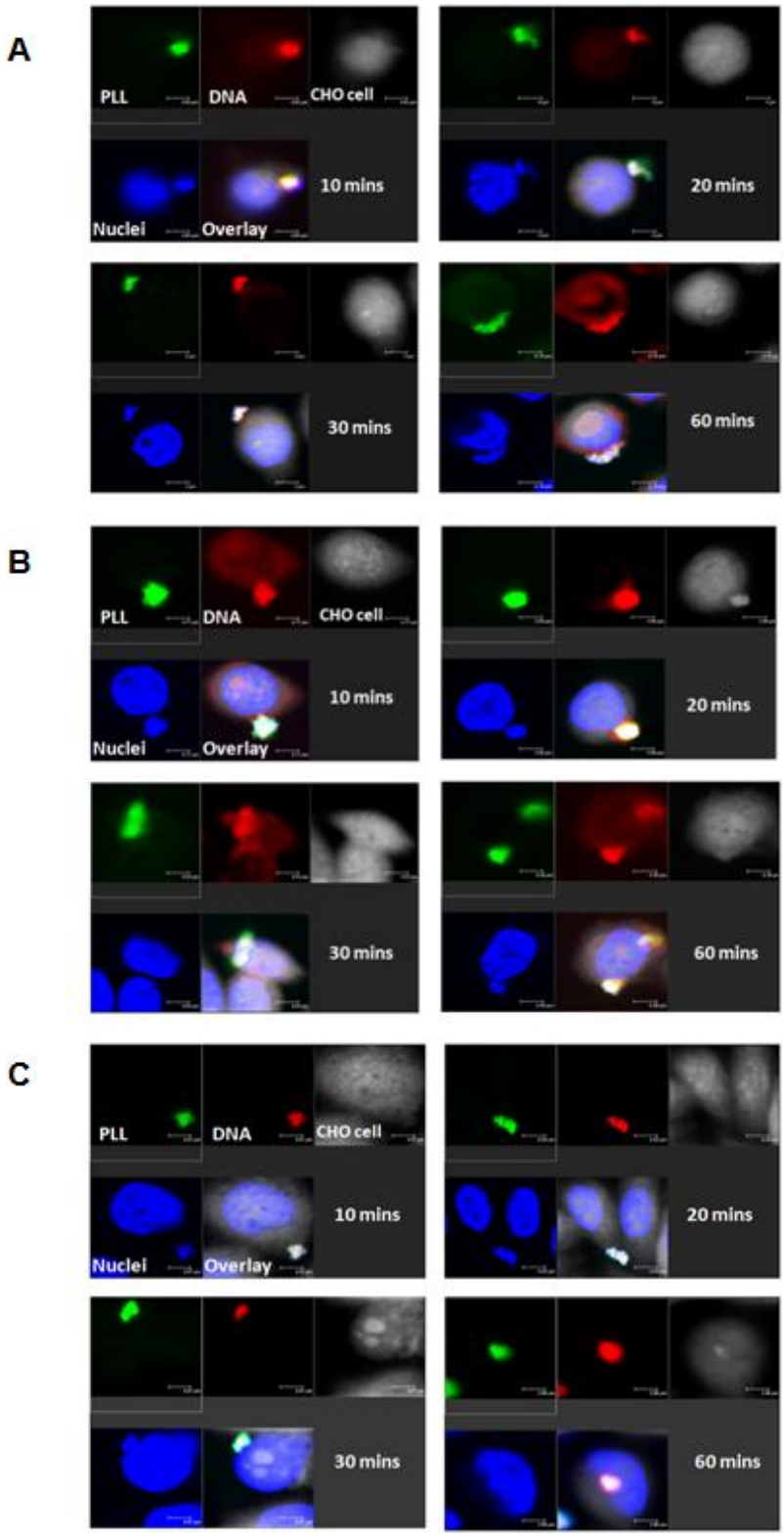

Figure 5.2: **Time course of polyplex uptake in CHO cells as observed via confocal microscopy.** Polyplexes containing linear- (A), OC- (B), and SC- (C) pDNA (2µg). Polyplexes were prepared at charge ratios of +1.6 (for SC- and OC-pDNA) and +5 for linear pDNA. Figure shows mid section images.

Naked DNA controls showed no fluorescence, even by 60 minutes (Figure 5.3). A large number of cells were analysed but no fluorescence corresponding to DNA was observed, presumably nucleic acids required PLL to gain cellular entry.

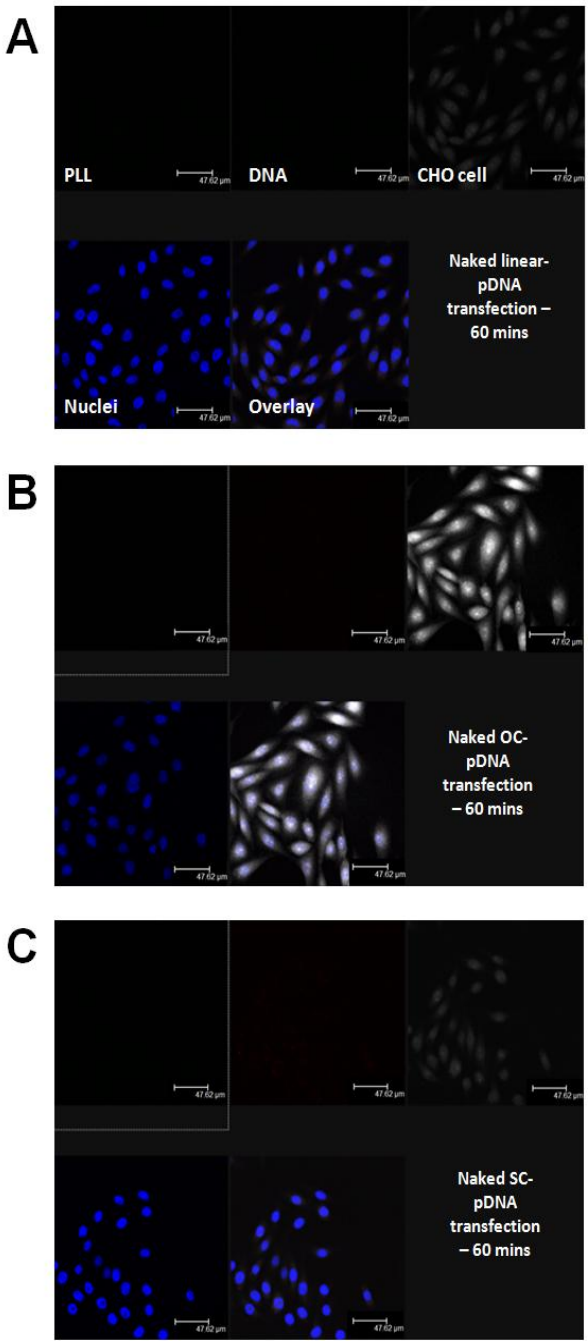

Figure 5.3: **Transfection of naked pDNA in CHO cells as observed via confocal microscopy.** Naked linear- (A), OC- (B), and SC- (C) pDNA (2µg). Figure shows mid section images.

Although previous figures showed low magnification images of cells (to monitor potential polyplex uptake), approximately 30% of cells were transfected with polyplexes. Figure 5.4 shows a low magnification image of transfected CHO cells. The image displays CHO cells transfected with SC-pDNA polyplexes but the proportion of cells transfected is representative for complexes of all DNA topologies. However it must be noted although the proportion of cells transfected may be similar for all DNA topologies, uptake into different cell compartments and gene expression (as shown later in the chapter) can vary between different DNA topologies.

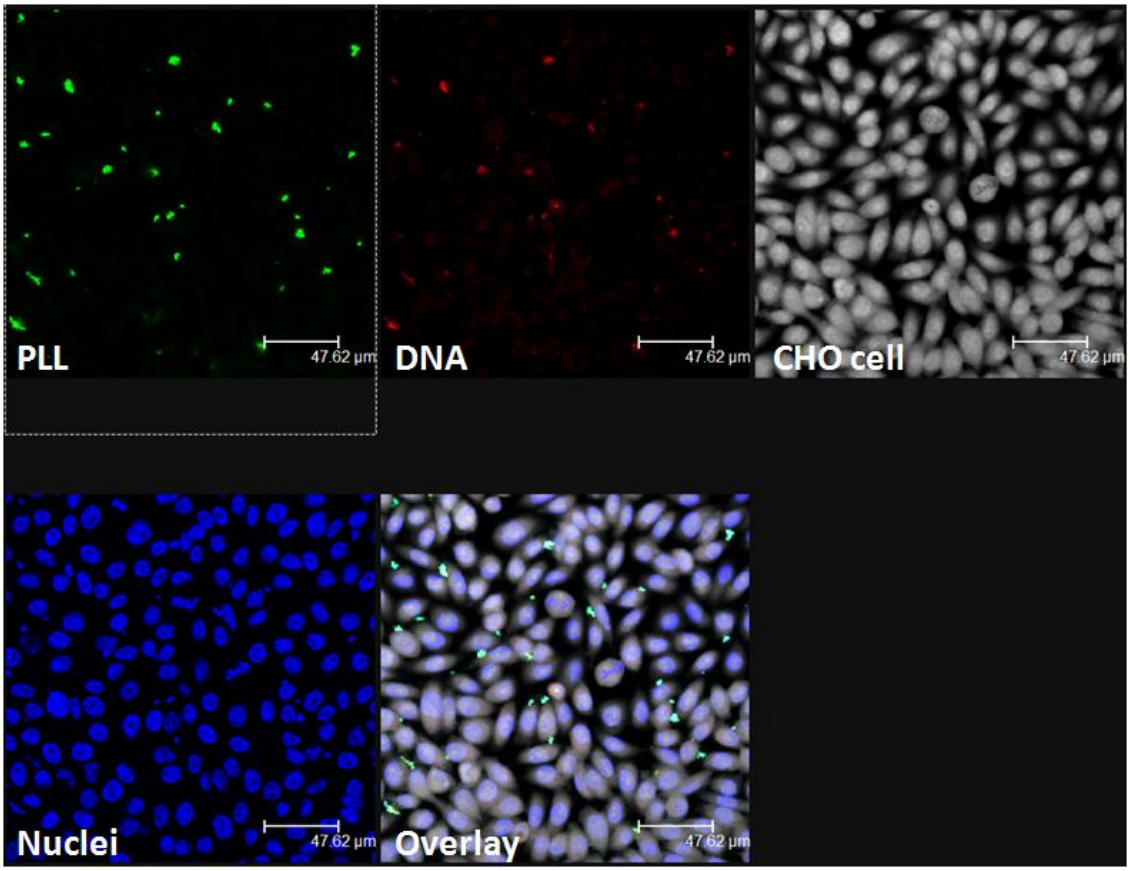

Figure 5.4: Low magnification image showing the proportion of CHO cells transfected. Cells were transfected for 30 minutes with complexes containing SC-pDNA (2µg) at charge ratio of +1.6. Figure shows mid section images.

5.1.3 Extended time course

An extended time course was studied whereby complexes were transfected within CHO cells for a period of 48 hours and analysed via confocal microscopy (Figure 5.5). SC-pDNA polyplexes associated with the nucleus (fluorescence co-localised with nuclear fluorescent stain; DAPI), whereas OC- and linear-pDNA polyplexes were located within the cytosol and periphery respectively. This indicates uptake shows dependence on DNA topology. Also unlike Figure 5.2, DNA and PLL fluorescence are independent of each other, indicating possible dissociation and degradation of PLL over the extended course.

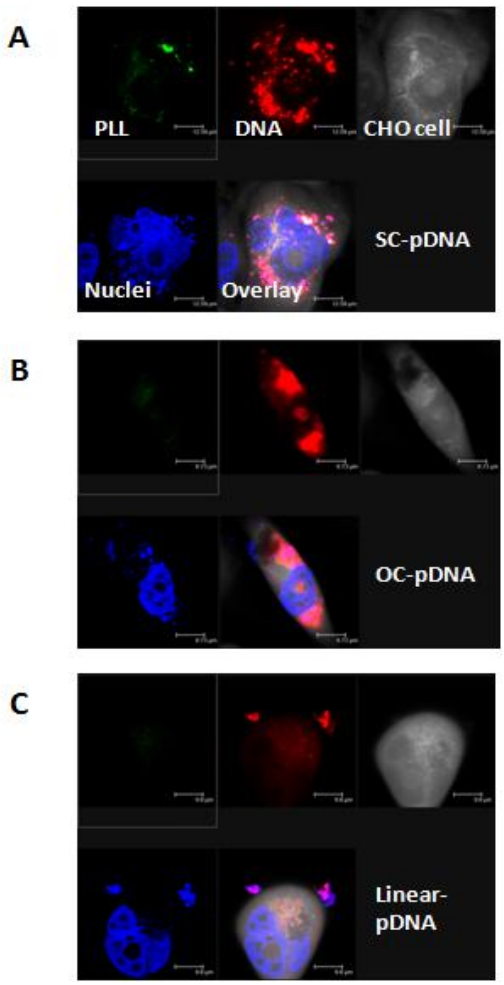

Figure 5.5: **Extended time course of polyplex uptake in CHO cells as observed via confocal microscopy.** Polyplexes containing linear- (A), OC- (B), and SC- (C) pDNA (2μg). Polyplexes were prepared at charge ratios of +1.6 (for SC- and OC-pDNA) and +5 for linear pDNA. Figure shows mid section images.

5.1.4 Reverse transfection

The CHO cells employed in the present study were adherent cells, i.e. they were attached to the tissue culture surface. Transfection of cells involves addition of polyplexes to the cell culture media, which is a conventional method of transient transfection referred to as the bolus procedure (Bengali *et al*, 2009). However many immunological and therapeutic target cells are non-adherent. Therefore polyplex uptake must be tested through alternative transfection methods. One technique is reverse transfection (RT) which involves immobilisation of DNA complexes on a cell adhesive substrate followed by the addition of cells (Bengali *et al*, 2009). This method is advantageous in terms of promoting internalisation (uptake in cells) and reducing aggregation (Bailey *et al*, 2002; Bengali *et al*, 2005).

Uptake of DNA polyplexes in CHO cells was analysed via RT and visualised by confocal microscopy (Figure 5.6). Labelled polyplexes were spotted onto PLL coated coverslips for 1 hour at room temperature and protected from light. Adherent CHO cells were trypsinized to detach from the surface (the trypsin was inactivated by the addition of media), and added to the immobilised polyplexes and incubated for the desired period. Co-localisation of fluorescence corresponding to PLL and DNA was not well defined indicating partial segregation of the components. Uptake of polyplexes via RT was monitored by confocal microscopy, whereby at 60 minutes complexes containing SC-pDNA, were beginning to associate with the nucleus (Figure 5.6a). At 60 minutes post transfection OC- and linear-pDNA complexes were located within the cytosol (Figure 5.6b and 5.6c).

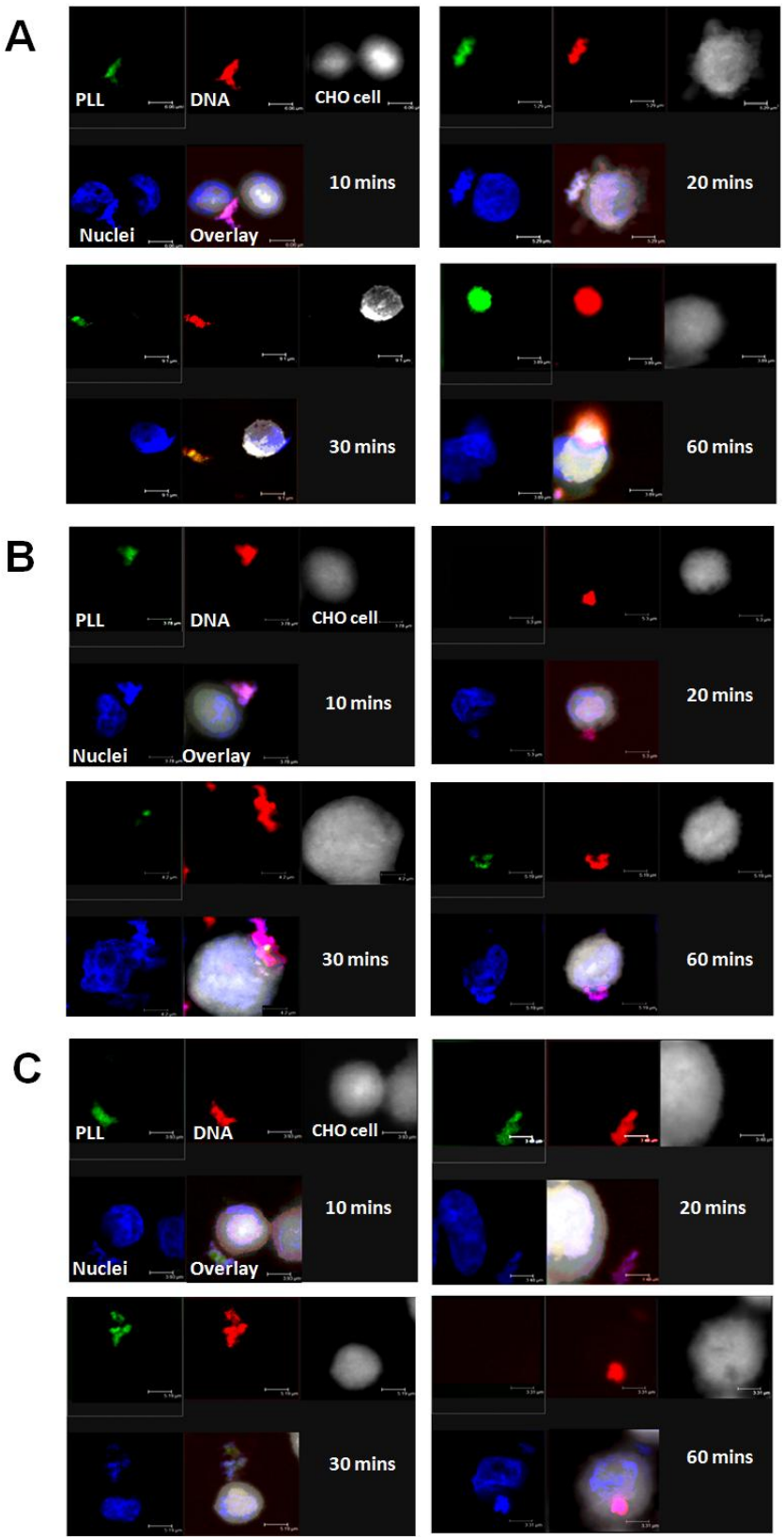

Figure 5.6: **Time course of polyplex uptake in CHO cells via reverse transfection (RT).** Confocal microscopy analysis of polyplexes containing SC- (A), OC- (B) and linear- (C) pDNA within CHO cells at varying time points. Polyplexes containing 2µg pDNA were spotted onto PLL coated coverslips for 1 hour at room temperature in the dark. CHO cells were trypsinised and loosened, and then added to complexes. Cells were incubated at 37°C for the desired period. Subsequently cells were fixed, stained and mounted upon slides. Figure shows mid section images.

DNA polyplexes were reverse transfected for an extended period of 48 hours (Figure 5.7). Complexes containing SC-pDNA were found to be associated with the nuclei (Figure 5.7a), whereas those containing OC- and linear-pDNA were situated at the cell periphery respectively. This indicates polyplex uptake may be dependent on DNA topology.

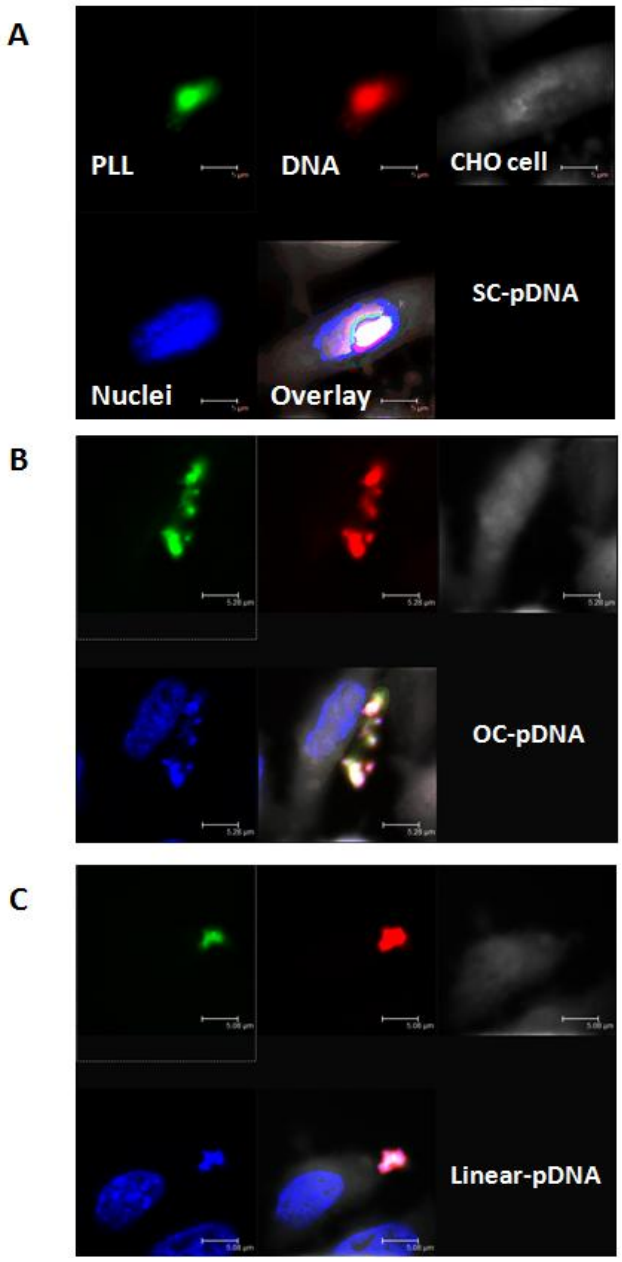

Figure 5.7: **Extended time course of polyplex uptake in CHO cells via reverse transfection (RT).** Confocal microscopy analysis of polyplexes containing SC- (A), OC- (B) and linear- (C) pDNA within CHO cells at varying time points. Polyplexes contained 2µg pDNA. Figure shows mid section images.

5.2 Quantification of polyplex uptake and gene expression

The previous figures identified the uptake of polyplexes within CHO cells at various time points. However such results required quantification in order to deduce the efficiency of polyplexes to gain CHO cell access and induce gene expression (transcription of plasmid encoded gene).

5.2.1 Quantification of DNA polyplex uptake within CHO cells

The findings from Figure 5.2 were quantified, whereby polyplexes which were transfected (via bolus procedure) into CHO cells were analysed via confocal microscopy and the number of cell associated complexes were counted and classified on the basis of their intracellular location (Figure 5.1). The percentage of complexes within each cellular compartment is shown in Figure 5.8. At 10 minutes post transfection, majority of polyplexes regardless of DNA topology are situated at the outer periphery of the cell (Figure 5.8). SC-pDNA polyplexes enter the cell cytosol by 20-30 minutes and can be observed within the nucleus by 60 minutes. OC-pDNA complexes display a similar pattern, although uptake and nuclear association were less efficient. In contrast entry of linear-pDNA polyplexes is much less efficient with very few nuclear associated complexes compared to that of the SC form. Details of quantification methodology are provided in Chapter 2, section 2.6.7.3.

Quantification of polyplex uptake and classification of intracellular location was also deduced for polyplexes transfected into CHO cells for an extended time period of 48 hours (Figure 5.9). Half of all polyplexes containing SC-pDNA were associated with the nuclei with the remainder of complexes predominantly situated within the cytosol. The percentage of nuclear associated polyplexes decreased for complexes containing OC- and linear-pDNA emphasising the influence of pDNA topology on the efficiency of polyplex cellular uptake. It

must be noted though, that nuclear association does not necessarily correspond to gene expression due to various molecular barriers and presence of nucleases.

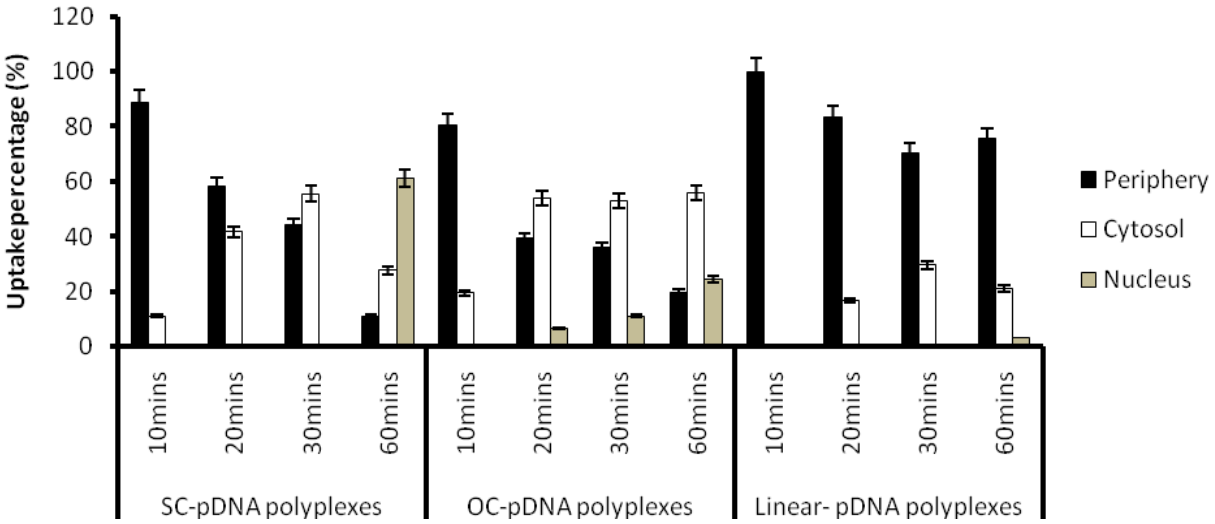

Figure 5.8: **Quantification of polyplex uptake in CHO cells for up to 1 hour**. Polyplexes (containing 2µg DNA) were prepared at charge ratios of +1.6 (for SC- and OC-pDNA) and +5 for linear pDNA. The figure shows the mean and standard error (SE) of 3 independent experiments. One-way ANOVA was employed to deduce levels of statistical significance ($p < 0.05$) between complexes of differing DNA topologies in different cell compartments.

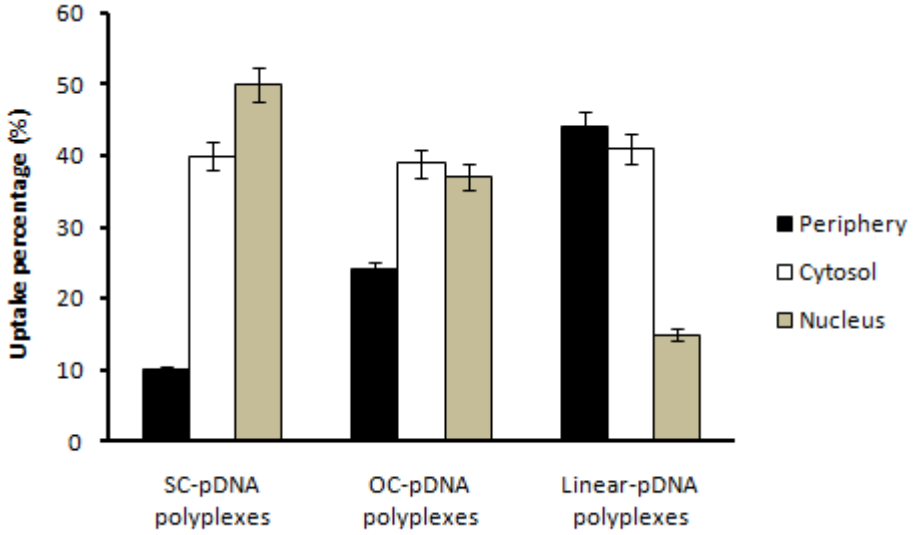

Figure 5.9: **Quantification of polyplex uptake in CHO cells at 48 hours**. Polyplexes (containing 2µg DNA) were prepared at charge ratios of +1.6 (for SC- and OC-pDNA) and +5 for linear pDNA. The figure shows the mean and SE of 3 independent experiments. One-way ANOVA was employed to deduce levels of statistical significance ($p < 0.05$) between complexes of differing DNA topologies in different cell compartments.

5.2.2 CHO cell polyplex gene expression studies

In this study PLL/DNA polyplex uptake was analysed and quantified by confocal image analysis. Non-viral gene delivery and gene expression within CHO cells is important particularly in the biopharmaceutical industry whereby CHO cells are often employed for recombinant protein production. To analyse the efficiency of PLL/DNA polyplex uptake efficiency, polyplex gene expression was measured. The pDNA encodes a *lacZ* reporter gene for β-galactosidase which was measured by X-Gal staining via light microscopy (Chapter 2, section 2.6.3). Figure 5.10 shows light microscopy images of β-galactosidase positive cells (following X-gal staining) after transfection and gene expression of SC-pDNA polyplexes.

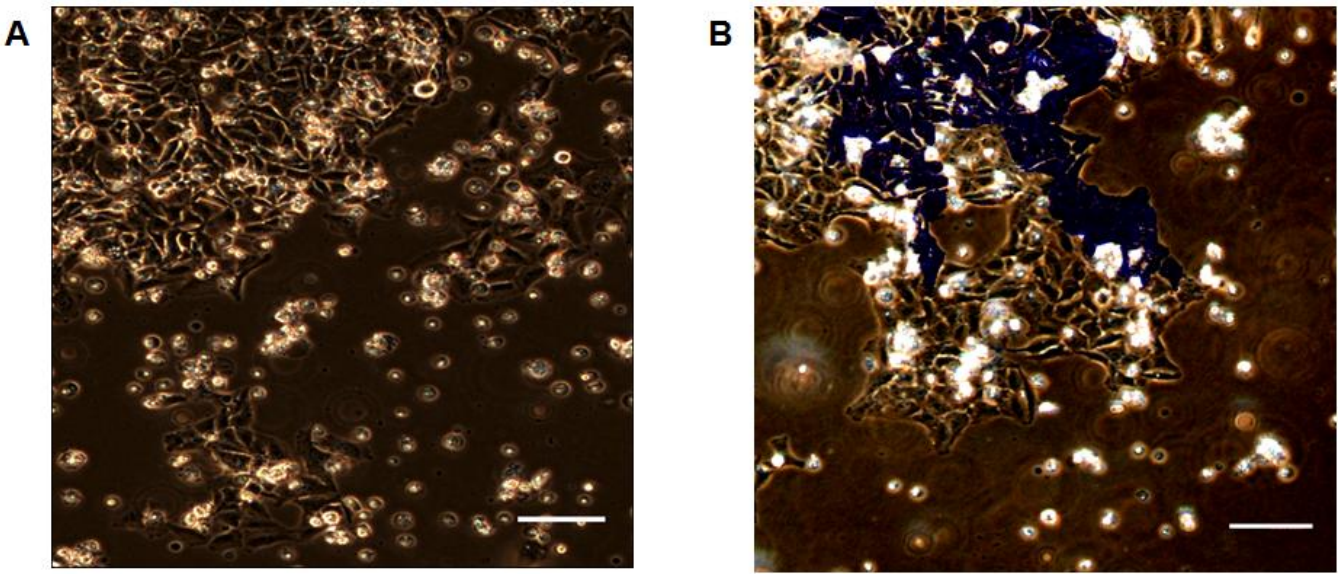

Figure 5.10: **β-galactosidase detection following staining with X-gal**. SC-pDNA polyplexes (containing 20µg DNA) were transfected into CHO cells for a period of 48 hours to induce gene expression. The figure shows non-transfected cells (A) and transfected cells (B) when stained with X-gal. Complexes were prepared at charge ratios of +1.6. Scale bar represents 20µm. Images were taken on a Ti-E light microscope (Nikon) connected with a Fi-1 CCD camera (Nikon) as described in Chapter 2, section 2.6.3.

5.2.2.1 Dose and time dependent course

To deduce the optimal conditions for gene expression, polyplexes containing DNA of varying concentrations were transfected into CHO cells. Gene expression (plasmid encodes a *lacZ* β-galactosidase reporter gene) was measured at various time points. Gene expression was found to be dependent on dose and DNA topology with complexes containing SC-pDNA displaying increased gene expression (Figure 5.11). Optimal gene expression occurs at 48 hours post transfection which is concentration dependent. These conditions can then be applied for further gene expression analysis.

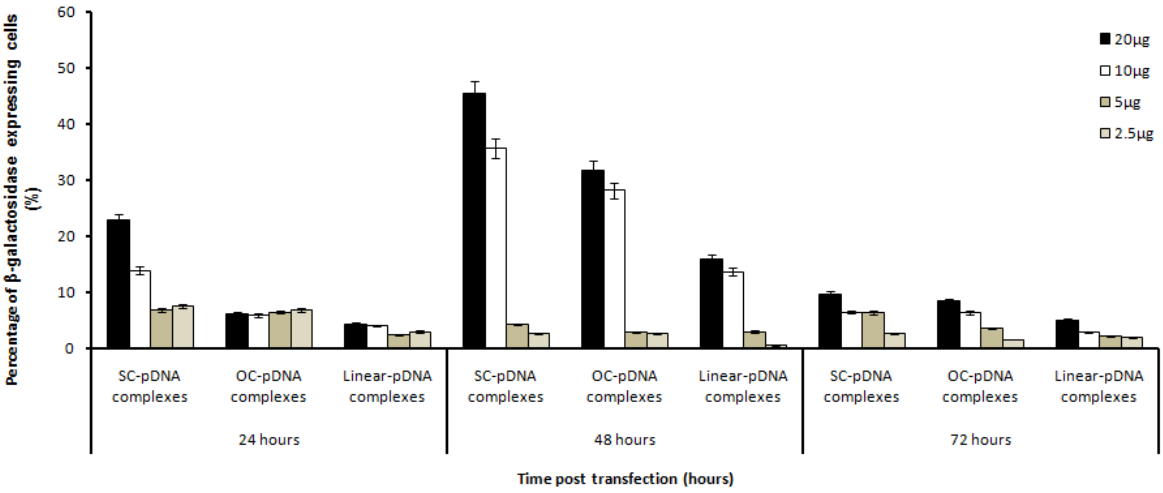

Figure 5.11: **Time and dose dependent gene expression preliminary assay**. Polyplexes were prepared in 1mM HEPES (pH 7.5). The figure shows the mean and SE of 3 independent experiments. One-way ANOVA was employed to deduce levels of statistical significance ($p < 0.05$) between complexes of differing DNA topologies.

5.2.2.2 CHO cell polyplex gene expression

Gene expression of polyplexes of equal surface charge in CHO cells was measured (Figure 5.10). Gene expression was topology dependent which was highest for that of SC- and OC-pDNA polyplexes (which were not significantly different to each other $p > 0.05$). However polyplexes containing linear-pDNA were much less efficient in inducing gene expression. Complexes containing linear-pDNA were not significantly different to that of naked DNA controls highlighting topology dependent gene expression.

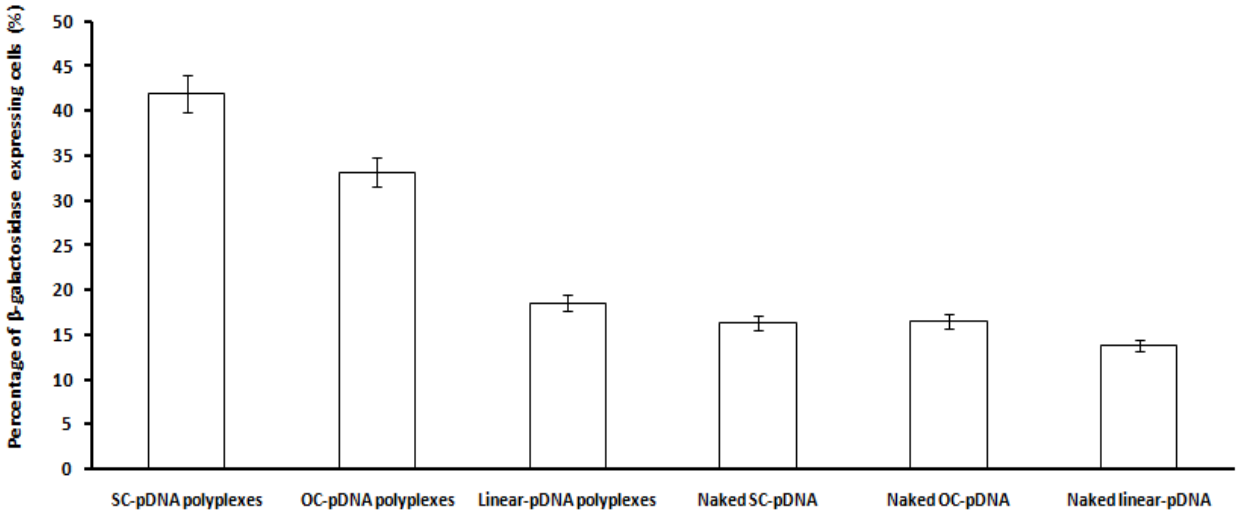

Figure 5.12: **Polyplex gene expression within CHO cells**. 10µg polyplex DNA was transfected into CHO cells for 48 hours. Polyplexes were prepared at charge ratios of +1.6 for SC- and OC-pDNA polyplexes and +5 for linear-pDNA polyplexes (1mM HEPES [pH 7.5]). The figure shows the mean and SE of 3 independent experiments. One-way ANOVA was employed to deduce levels of statistical significance ($p < 0.05$) between complexes of differing DNA topologies. Student's t-test was employed to deduce levels of statistical significance ($p < 0.05$) between SC- and OC-pDNA polyplexes.

5.2.2.3 Gene expression at a short time course

Polyplexes were transfected into CHO cells for shorter times and analysed for gene expression (Figure 5.13). By 10 minutes complexes containing SC-pDNA were able to induce β-galactosidase gene expression and even more so by 1 hour. Rapid gene expression as early as 1 hour was also reported by Stechschulte *et al*, (2001) when administering pDNA, highlighting the potential of pDNA to be rapidly transcribed. Expression remains topology dependent indicating the effective nature of complexes to gain cellular and nuclear access.

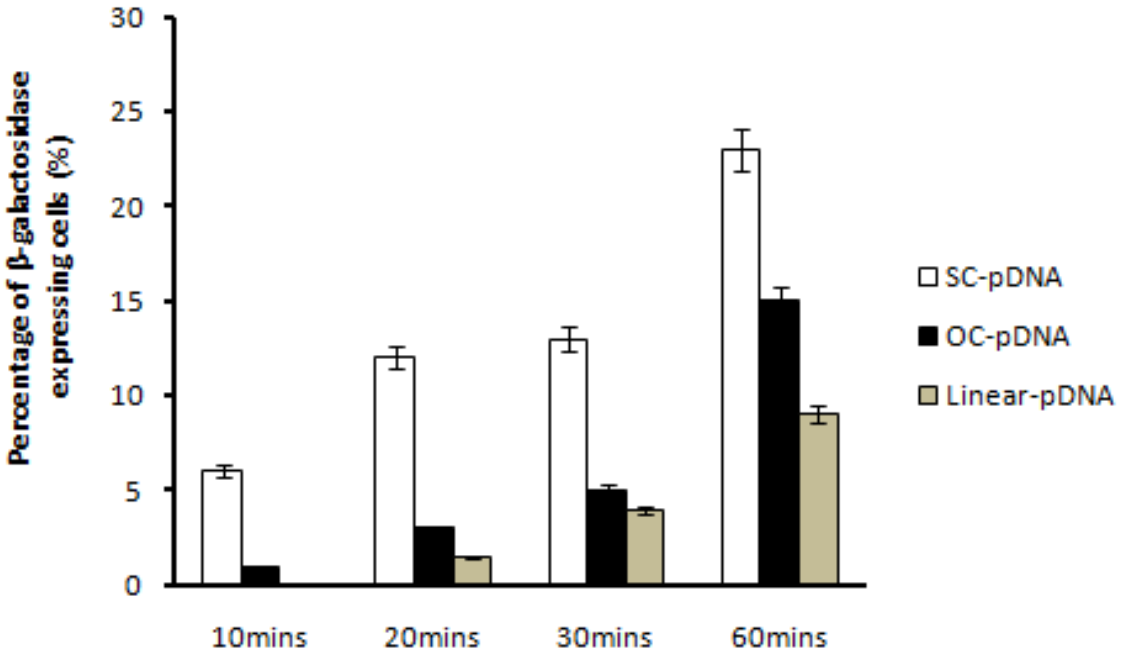

Figure 5.13: **Polyplex gene expression within CHO cells for time periods of up to 1 hour**. 10μg polyplex DNA was transfected into CHO cells. Polyplexes were prepared at charge ratios of +1.6 for SC- and OC-pDNA polyplexes and +5 for linear-pDNA polyplexes (1mM HEPES [pH 7.5]). The figure shows the mean and SE of 3 independent experiments. One-way ANOVA was employed to deduce levels of statistical significance ($p < 0.05$) between complexes of differing DNA topologies.

5.2.2.4 Gene expression at an equal charge ratio

Polyplex charge ratio (ratio of polymer to DNA) is important in terms of converting the negative charge of DNA to a positive charge to facilitate cellular entry. In agreement with previous studies (Cherng *et al*, 1999), SC- and OC-pDNA gives enhanced gene expression when the charge for all three complexes are similar; +1.6 for SC- and OC-pDNA, and +5 for linear-pDNA (Figure 5.12). However even when the charge ratio for all three complexes are the same, gene expression remained topology dependent, which was highest for complexes containing SC-pDNA (Figure 5.14). High charge ratio complexes (+5) resulted in lower gene expression, whereby at charge ratios of +1.6, gene expression increased twofold.

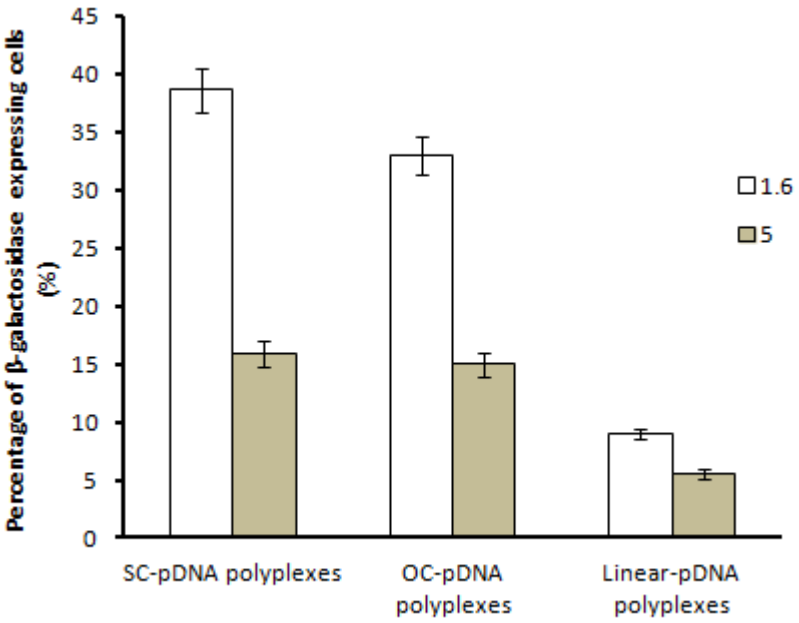

Figure 5.14: **Gene expression of polyplexes at equal charge ratios.** 10µg polyplex DNA was transfected into CHO cells. Polyplexes were formulated at charge ratios of either +1.6 or +5 (1mM HEPES [pH 7.5]). The figure shows the mean and SE of 3 independent experiments. One-way ANOVA was employed to deduce levels of statistical significance ($p < 0.05$) between complexes of differing DNA topologies at different charge ratios.

5.3 Mechanisms of uptake

In order to study the cellular uptake of polyplexes and its intracellular fate, it is important to analyse the mechanisms by which DNA polyplexes are taken up by mammalian cells. The literature widely credits the mechanism of endocytosis as means of polyplex cellular entry (Pichon *et al*, 2010). Endocytosis refers to the means by which extracellular molecules enter cells (Gould and Lippincott-Schwartz, 2009; Pinchon *et al*, 2010). Endocytosis can generally be subdivided into two branches; the clathrin mediated endocytic (CME) pathway and the clathrin independent pathway, such as the caveolae pathway (Rejman *et al*, 2005). The CME pathway involves the formation of clathrin coated pits upon the host cell membrane which acts as a docking site for foreign materials (Rejman *et al*, 2005). These pits eventually form into small vesicles which fuse with early endosomes. In contrast the caveolae pathway involves the formation of lipid raft structures that interact with incoming complexes, and pinch off the membrane to yield vesicle like structures referred to as caveosomes which link with early endosomes (Khalil *et al*, 2006). To deduce the mechanism by which DNA polyplexes gain cellular access, known chemical inhibitors of each pathway were employed to knock out respective pathways. Quantitative analysis of fluorescent confocal localisation and gene expression studies were carried out.

5.3.1 Gene expression of polyplexes within endocytic inhibitor treated CHO cells

Gene expression of polyplexes within CHO cells, which were treated with endocytic inhibitors was measured (Figure 5.15). Two endocytic inhibitors were employed; chloropromazine (CMZ), which blocks Rab5 early endosome development of the CME pathway, and genistein which blocks the recruitment of dynamin-1, which is important for lipid raft formation of the caveolae pathway (Khalil *et al*, 2006). The amount of CMZ and genistein applied were 10µg/ml and 400µM respectively as deduced from Vercauteren *et al*,

(2010). Addition of both chemical inhibitors significantly reduced gene expression when compared to non-treated controls ($p < 0.05$). Gene expression remained topology dependent and despite the addition of both inhibitors the percentage of cells expressing the reporter gene remained >15% for SC-pDNA polyplexes (Figure 5.15).

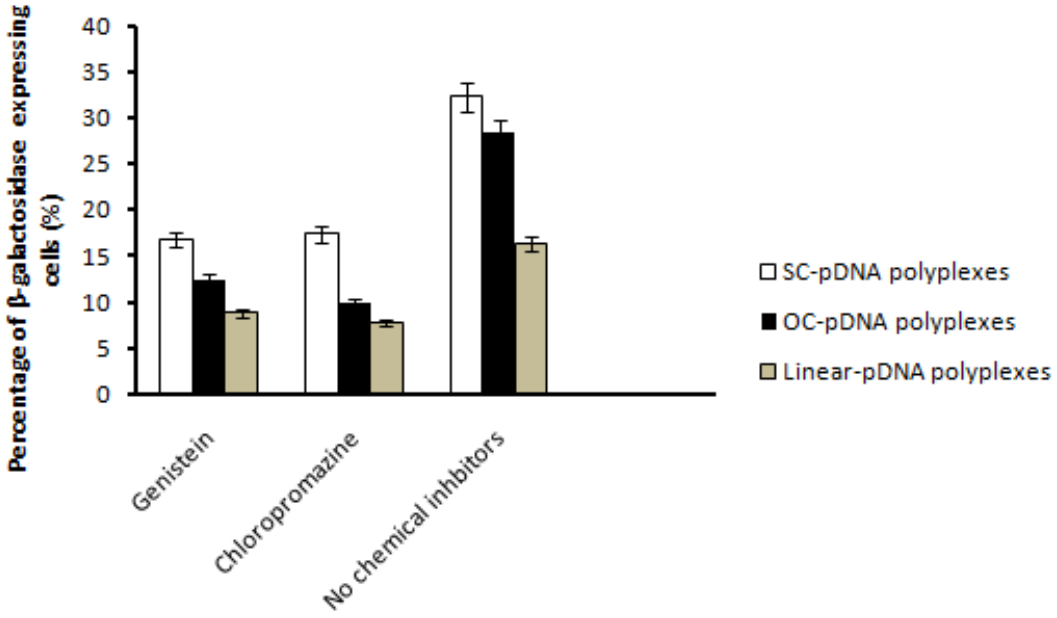

Figure 5.15: **Polyplex gene expression in CHO cells treated with endocytic inhibitors.** 10µg polyplex DNA was transfected into CHO cells treated with either 10µg/ml chloropromazine (CMZ) or 400µM genistein. The figure shows the mean and SE of 3 independent experiments. The figure shows the mean and SE of 3 independent experiments. One-way ANOVA was employed to deduce levels of statistical significance ($p < 0.05$) between inhibitor treated cells transfected with polyplexes and untreated controls.

5.3.2 Confocal image analysis and quantification

Fluorescent confocal microscopy analysis was carried out in order to quantify polyplex uptake in cells treated with endocytic inhibitors. Throughout the time course and regardless of DNA topology, the majority of DNA polyplexes were located on the cellular periphery in cells treated with either CMZ or genistein (Figure 5.16). By 60 minutes SC-pDNA polyplex

nuclear association was <30% in CMZ treated cells (Figure 5.16a). In regards to cells treated with genistein, polyplex nuclear association was not recorded (Figure 5.16b). However by 1 hour complexes containing OC- and SC-pDNA were predominantly located within the cytosol unlike that of linear-pDNA complexes (Figure 5.16b).

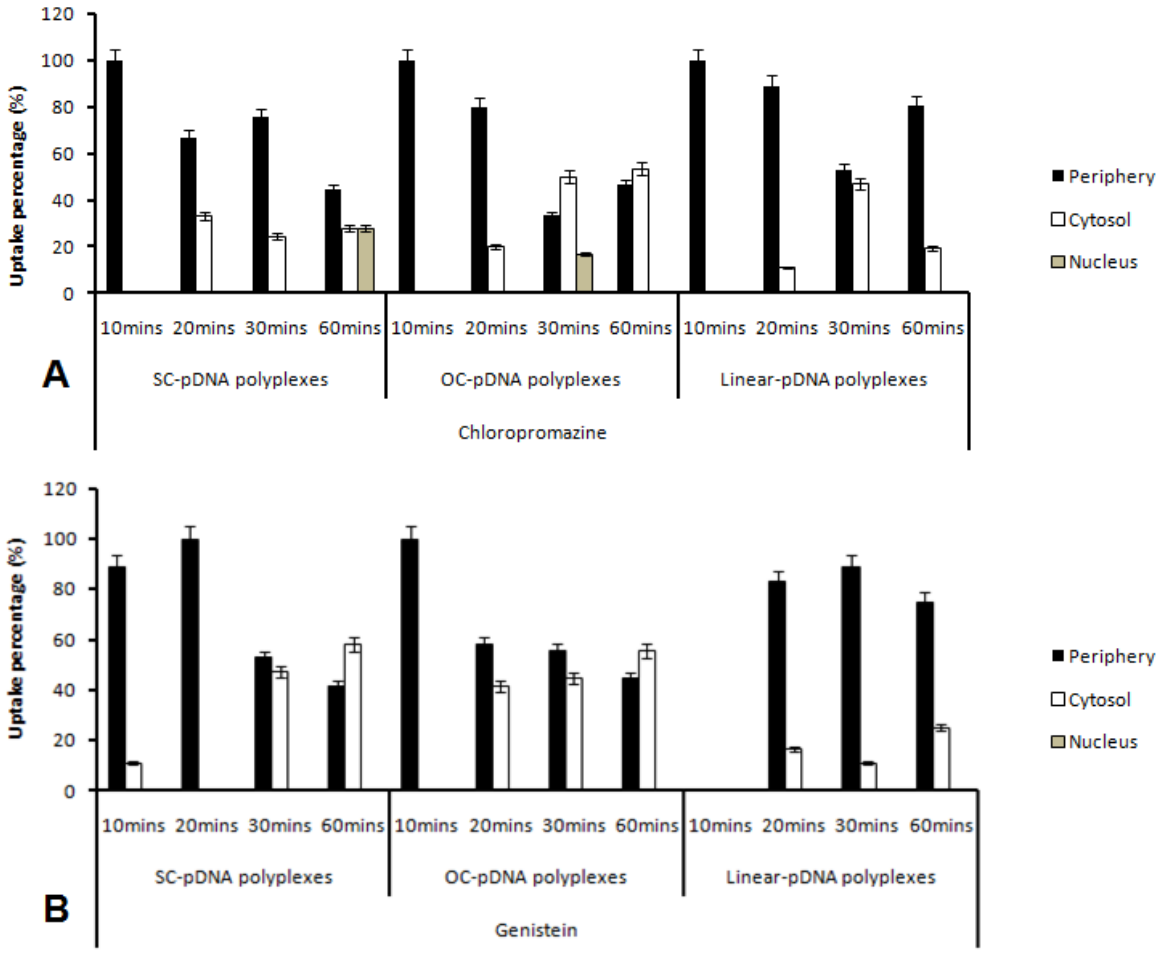

Figure 5.16: **Quantification of polyplex uptake in CHO cells treated with endocytic inhibitors.** Polyplex (containing 2µg pDNA) uptake in cells treated with either chloropromazine (A) and genistein (B). The figure shows the mean and SE of 3 independent experiments. The figure shows the mean and SE of 3 independent experiments. One-way ANOVA was employed to deduce levels of statistical significance ($p < 0.05$) between complexes of differing DNA topologies in different cell compartments.

5.3.3 Control experiments to validate endocytic inhibitors

The previous experiments used endocytic inhibitors to gain insight into the mechanism of polyplex uptake. The addition of inhibitors to cells reduced both uptake and gene expression. However it is important to deduce whether chemical treatment to cells could cause indirect effects leading to a decrease in uptake and gene expression, or specifically block the pathway of interest. A series of control experiments were carried out whereby CHO cells were treated with known characterised markers of both the CME and caveolae pathway, and whether uptake is reduced when the inhibitor of interest is added.

5.3.3.1 Confocal microscopy analysis

To deduce the specificity of CMZ in terms of only inhibiting the CME pathway, a well characterised marker; transferrin (Tran) (Nagabushana *et al*, 2010) conjugates were added to CHO cells. Cells were also treated with cholera toxin subunit B (CTB) conjugates which is a marker for the caveolae pathway. Tran is a glycoprotein that binds and delivers iron atoms via the CME pathway (Nagabushana *et al*, 2010). CTB is marker for lipid raft formation of the caveolae pathway (Skretting *et al*, 1999). Endocytic markers were added to CHO cells according to the protocols of Nagabushana *et al*, (2010) and Skretting *et al*, (1999) (Chapter 2, section 2.6.6). Uptake was observed via confocal microscopy and the addition of chemical inhibitors reduces fluorescence corresponding to the respective endocytic marker (Figure 5.17). Both Tran (Texas red) and CTB (FITC-green) fluorescence is reduced when the appropriate inhibitor is added suggesting possible knockdown of the endocytic pathway of interest. Importantly despite the addition of inhibitors, uptake of other markers corresponding to alternative pathways was not jeopardised. For example addition of CMZ (CME inhibitor) to cells did not hinder CTB uptake (caveolae marker) (Figure 5.17b).

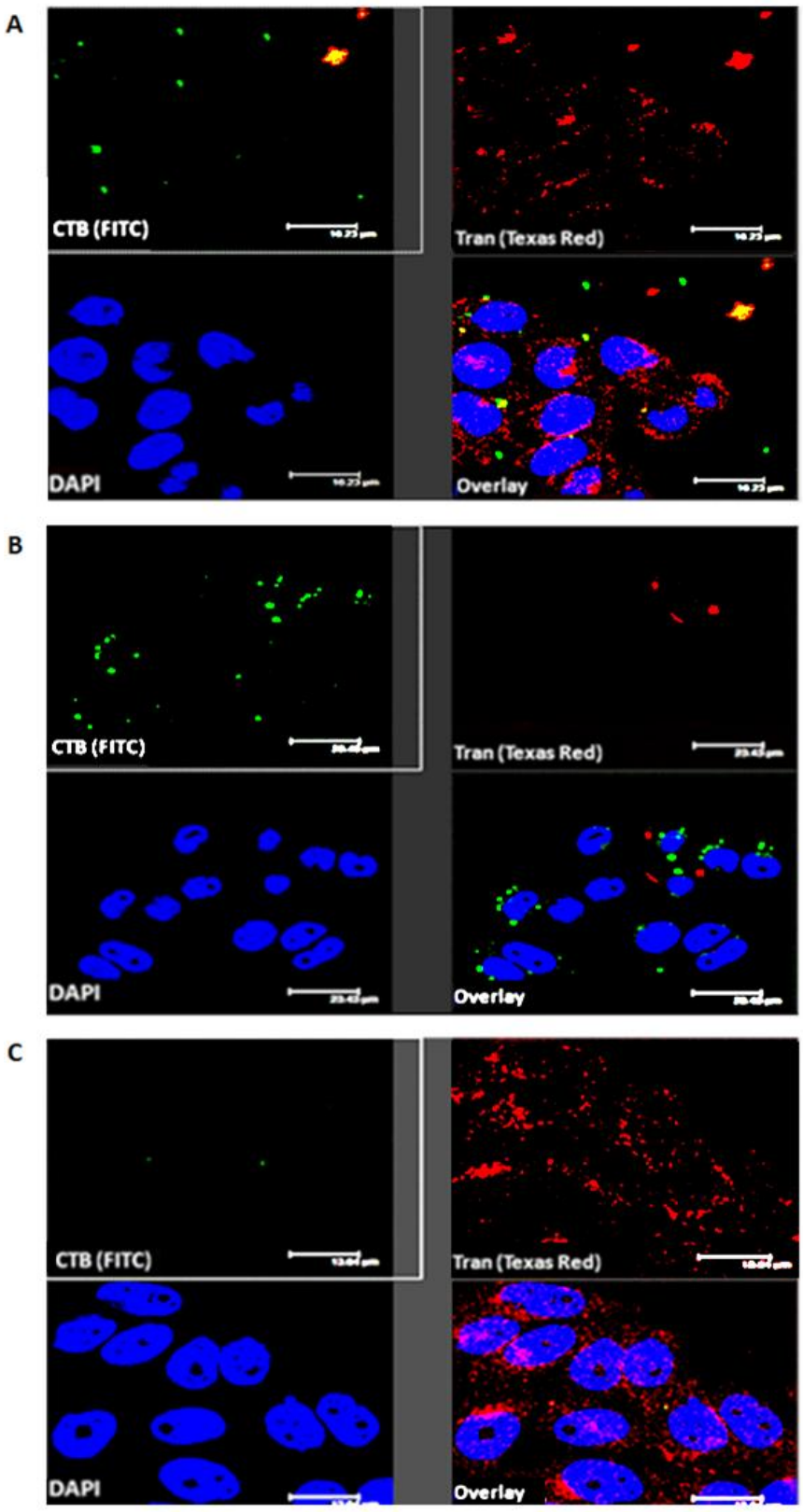

Figure 5.17: **Addition of commercial endocytic markers to CHO cells in the presence of endocytic pathway inhibitors**. Confocal microscopy images displaying uptake of endocytic markers; Transferrin (Tran) (red) and cholera toxin subunit B (CTB) (FITC-green) without any inhibitors (A), in the presence of chloropromazine (CMZ) only (B) and genistein only (C). Endocytic markers were added at a final concentration of 10µg/ml. DAPI was used to stain the nuclei. Markers were added to CHO cells for 20 minutes at 37°C. Cells were then fixed and mounted upon slides. Figure shows mid section images.

5.3.3.2 Flow cytometry analysis

The fluorescent signal intensities corresponding to the endocytic markers were measured in cells treated with the respective inhibitor (Figure 5.18). Flow cytometry was used to measure this against a set of control CHO cells (with no inhibitors) that were treated with the respective markers. Treatment with inhibitors did reduce uptake of the respective markers as shown by the negative shift in fluorescent signals, and did not jeopardise uptake of markers exploiting differing endocytic pathways (positive fluorescent signal shift). For instance the addition of CMZ which inhibits the CME pathway, reduces transferrin fluorescence (marker for the CME pathway), while that of CTB (caveolae pathway marker) is not compromised. This is important in terms of validating the previous inhibition studies.

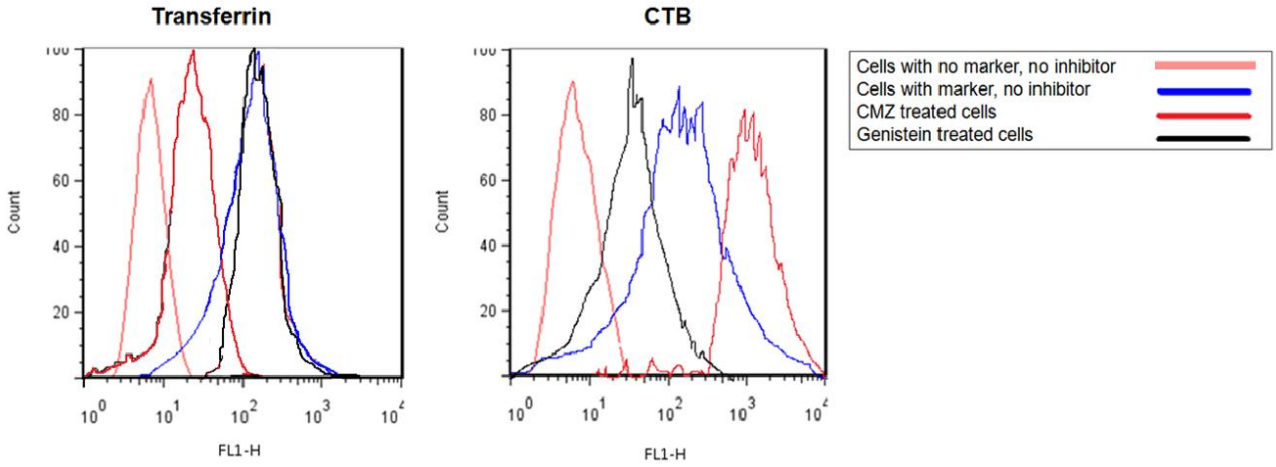

Figure 5.18: **Flow cytometry validation of commercial endocytic markers**. Known commercial fluorescent endocytic markers (Transferrin - Tran, and cholera toxin subunit B - CTB) were added to CHO cells and analysed as to whether chemical inhibitors could reduce uptake, hence fluorescent intensity. CHO cells were treated with either 10µg/ml chloropromazine (CME inhibitor) or 400µM genistein (caveolae inhibitor) prior to addition of markers.

5.3.4 Tracking of polyplexes and endocytic markers

5.3.4.1 Uptake of polyplexes and markers

Both uptake and gene expression of DNA polyplexes were perturbed when CHO cells were pre-treated with either CMZ or genistein. These results suggest polyplexes regardless of DNA topology, may be exploiting both endocytic pathways (CME and caveolae). To further investigate, DNA polyplexes were transfected into CHO cells along with known endocytic markers to observe if uptake is parallel. DNA polyplexes were prepared whereby only the DNA itself was fluorescently labelled (PLL was not tagged to avoid confusion with fluorescently labelled markers). Figure 5.19 shows uptake of DNA polyplexes along with the addition of CTB and transferrin. DNA fluorescence co-localises with that of the fluorescently labelled markers, particularly in the case of the caveolae marker; CTB. The figure displays co-localisation of endocytic markers with DNA polyplexes, containing SC-pDNA, although it must be noted such observations were representative for other DNA topologies.

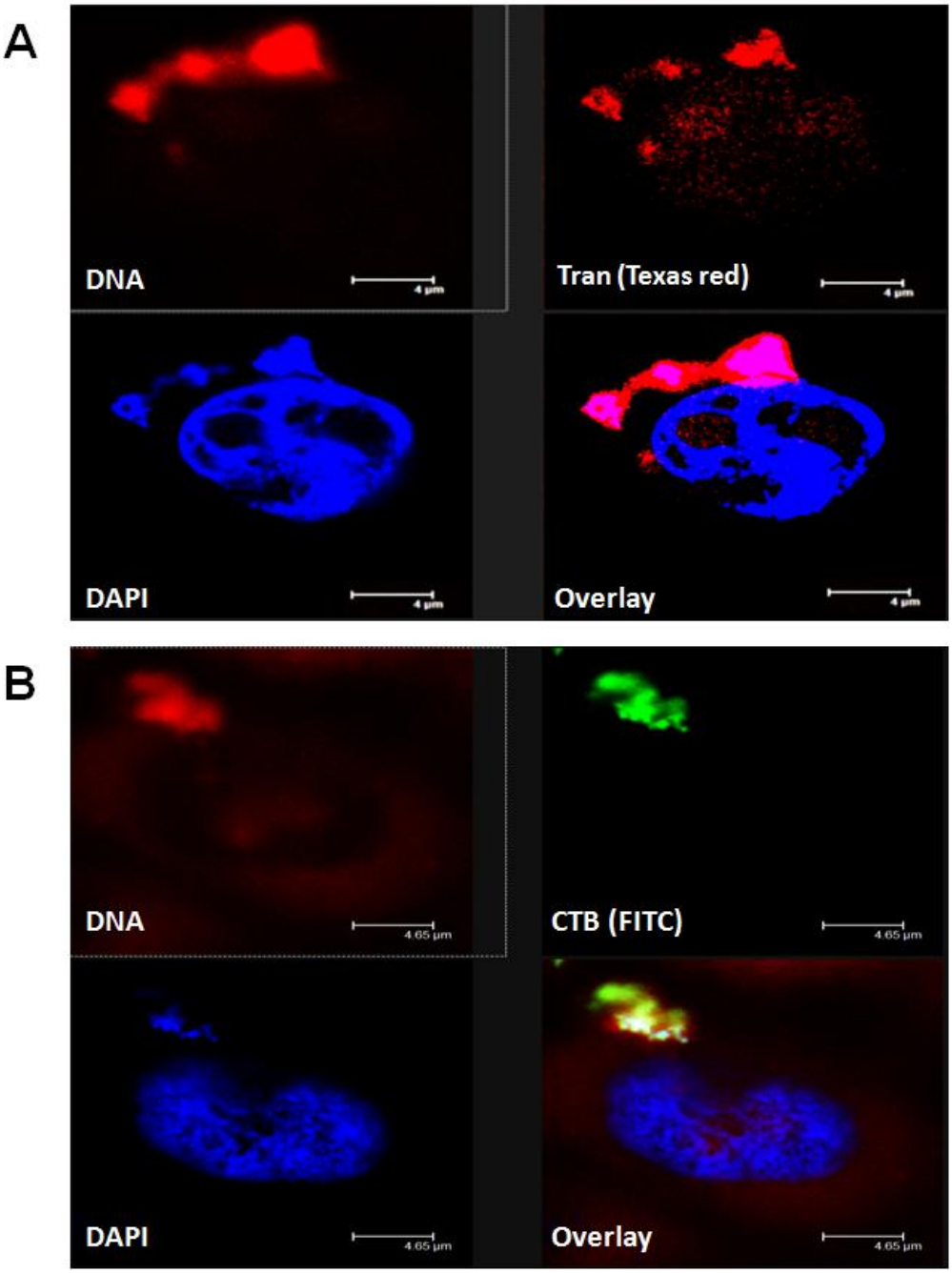

Figure 5.19: Co-transfection of polyplexes and endocytic markers within CHO cells. Polyplexes (containing 2µg pDNA) with: Transferrin - Tran (A) and cholera toxin subunit B - CTB (B). Both markers were added at a final concentration of 10µg/ml. DAPI was used to stain the nuclei. Polyplexes and endocytic markers were transfected for a period of 20 minutes. Figure shows mid section images.

5.3.4.2 Caveolin-1

To further validate the results of Figure 5.19, DNA polyplexes (of various DNA topologies) were transfected into CHO cells which were fluorescently stained with anti-caveolin-1 antibodies. Caveolin-1 has been reported to play a critical role in membrane invagination which ultimately leads to the formation of caveosomes (Liu *et al*, 2002). Polyplex uptake was monitored over a short time course via confocal microscopy (Figure 5.20). Unlike previous results clear co-localisation is not observed between DNA and anti-caveolin antibody fluorescence at early stages of transfection. This could suggest other pathways of uptake may be exploited.

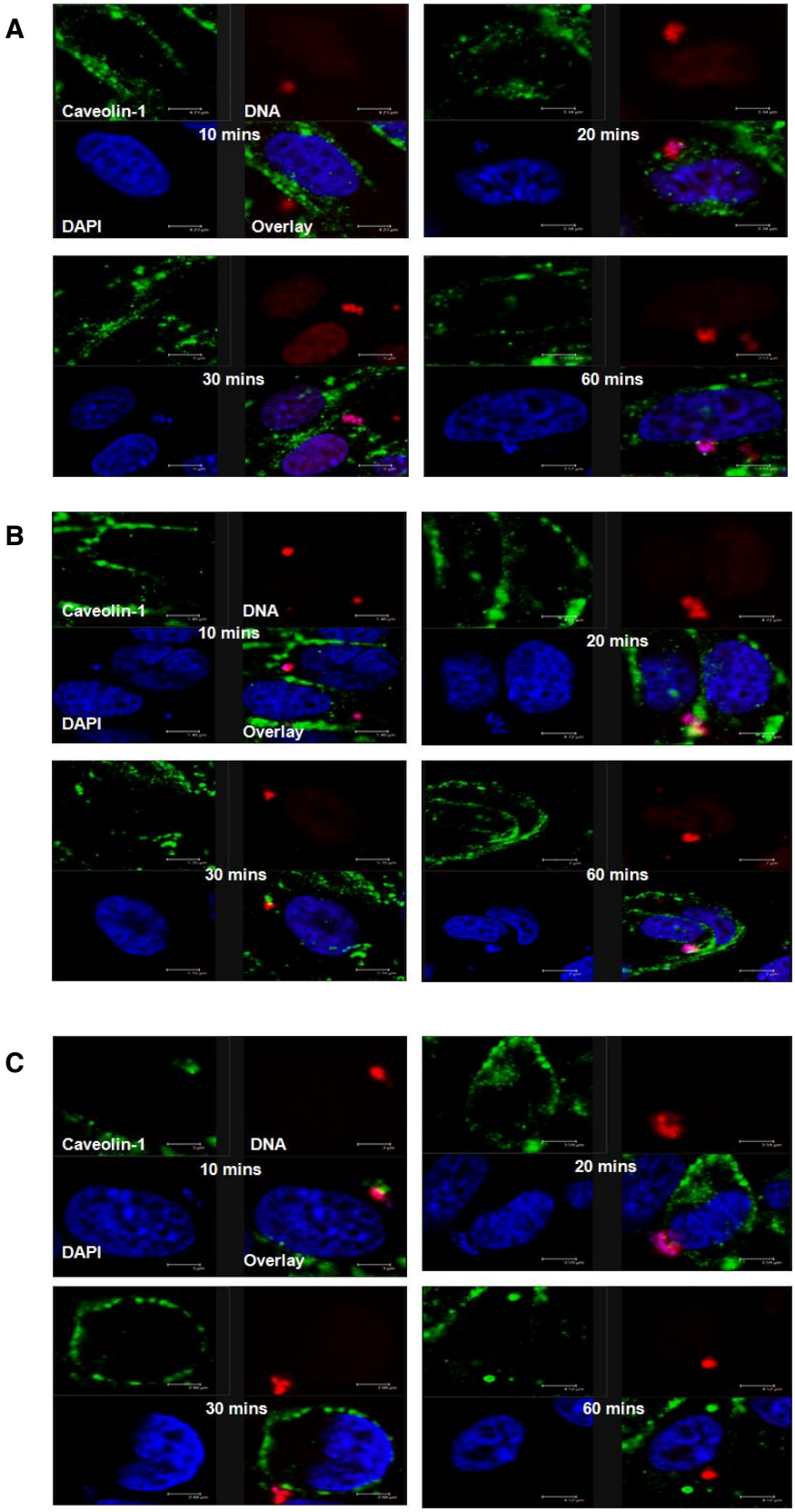

Figure 5.20: **Transfection of polyplexes in cells stained with fluorescent anti-caveolin-1 antibodies**. Uptake of SC- (A), OC- (B), and linear- (C) pDNA polyplexes (containing 2µg pDNA) within cells stained with anti-caveolin-1 antibodies. Primary caveolin-1 antibody (20µg/ml) was added to cells overnight at 4°C and then probed with an anti rabbit IgG (H+L) secondary FITC conjugated antibody. Figure shows mid section of images.

5.3.4.3 Rab5 early endosome tracking

To confirm whether polyplexes exploit the CME pathway, complex uptake was studied in cells stained with anti-Rab5 antibodies. Rab5 is a small GTPase that mediates the fusion of cellular vesicles with early endosomes which is a key step of the CME pathway (Zerial and McBride, 2001). Figure 5.21 shows fluorescently labelled polyplexes when transfected in cells stained with anti-Rab5 antibodies. No clear definitive co-localisation between secondary anti-Rab5 and DNA fluorescence was observed. DNA polyplexes seem to be much larger than that of endosomes suggesting alternative routes of cellular transportation following initial entry. Rab5 fluorescence is very sporadic whereas polyplex DNA is quite defined and larger.

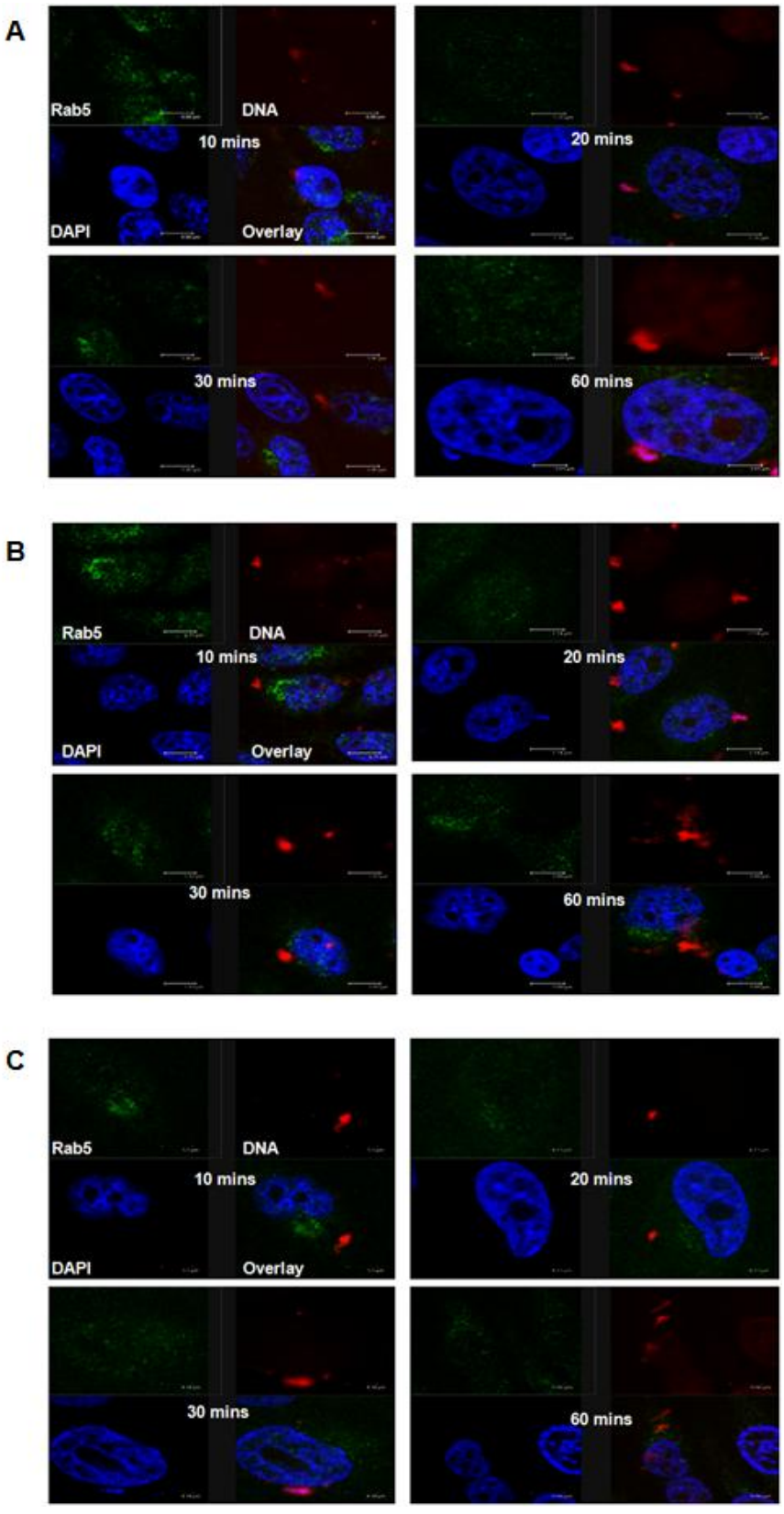

Figure 5.21: **Transfection of polyplexes in cells stained with fluorescent anti-Rab5 antibodies**. Uptake of SC- (A), OC- (B), and linear- (C) pDNA polyplexes (containing 2µg pDNA) within cells stained with anti-Rab5 antibodies. Primary Rab5 antibody (10µg/ml) was added to cells overnight at 4°C and then probed with an anti rabbit IgG (H+L), $F(ab')_2$ fragment FITC conjugated antibody. Figure shows mid section images.

5.4 Discussion

The present chapter focused on the potential uptake of DNA polyplexes within CHO cells and analysed the key factors that affect cellular uptake and gene expression. Understanding the key parameters that affect polyplex uptake along with the molecular mechanisms utilised to gain cellular entry is critical. This is important as CHO cells are widely employed for recombinant protein production (Liu *et al*, 2008). Polyplex uptake was monitored at various time points, qualitatively tracked, quantitatively analysed in terms of confocal image analysis and gene expression. Finally the mechanisms responsible for polyplex uptake are reported. If the detailed parameters of polyplex CHO cell uptake are understood, gene delivery for therapeutic purposes can be significantly enhanced.

5.4.1 Polyplex uptake within CHO cells

In this study PLL/DNA polyplex uptake in CHO cells was monitored qualitatively and quantitatively. Parameters such as DNA topology, charge ratio and uptake mechanisms were studied. The PLL polymer and DNA were individually labelled to track cellular uptake via fluorescent confocal microscopy. Polyplexes were classified on the basis of their cellular location as to being located within the cellular periphery, cytosol or nucleus (Figure 5.1). This was confirmed by identification in both mid section and stack projection images by fluorescent confocal microscopy in order to identify true polyplex uptake. DNA and PLL fluorescence remained co-localised following uptake for periods up to 1 hour (Figure 5.2). Following an extended time period co-localisation was not definitive (Figure 5.5). This may be due to polymer separation or degradation over the course of uptake. Complexes appear larger than initial size measurements (Chapter 3, Figure 3.5), presumably due to the cellular ionic environment, an observation in line with size measurements when polyplexes were formed in high salt solutions (Chapter 3, Figure 3.14). Therefore it is intriguing to speculate

how complexes of such large sizes enter the nuclei to induce gene expression. Studies have shown how large viral DNAs attain nuclear access through the exploitation of importin-7, which is a key nuclear transport receptor (Zaitseva *et al*, 2009). Polyplexes have been observed to associate with various importin proteins in a manner similar to large viral DNA structures (Breuzard *et al*, 2008).

Although both TOTO-3 and DAPI bind to DNA, TOTO-3 labelled DNA did not stain with DAPI which could be due to the difference in fluorescent spectra. In this study pDNA was pre-stained with TOTO-3 prior to PLL binding. TOTO-3 only fluoresces when bound to nucleic acids and DNA condensation by PLL may restrict detection within the fluorescent spectra corresponding to DAPI. Furthermore TOTO-3 is a more sensitive fluorescent stain than DAPI which could lead to increased detection for TOTO-3 than DAPI.

Qualitative (Figure 5.2) and quantitative (Figure 5.8) analysis of confocal microscopy images show topology dependent uptake whereby complexes containing SC-pDNA were most efficient in associating with the nuclei. Although Figure 5.8 shows approximately 60% of SC-pDNA polyplexes associated with the nucleus, this does not immediately correspond to gene expression whereby the percentage of SC-pDNA complex gene expression was <40% (Figure 5.12). Following nuclear association and uptake, gene expression can still be hindered through nuclease cleavage and DNA retention of the polycation which could restrict transcriptional access (Ko *et al*, 2011). Polyplexes containing OC- and linear-pDNA were often situated on the outer periphery of the cells (Figure 5.8). This uptake pattern may be due to a variety of reasons:

- The increased stability of the SC-pDNA polyplex within the cytosol of the cells may facilitate rapid diffusion towards the nuclei (Remaut *et al*, 2006).

- This was also observed when polyplexes were transfected for extended periods (Figure 5.9).
- Findings in Chapter 3 revealed how SC-pDNA polyplexes were smaller in size (<200nm) in comparison to OC- (>300nm) and linear-pDNA complexes (<1000nm), and displayed greater nuclease resistance, which collectively may enhance cellular uptake and subsequent *in vivo* passage.
- Xie and Tsong (1993) reported the increased susceptibility of linear-pDNA towards cytosolic nucleases than SC-pDNA, which ultimately led to reduced gene expression.

The observation of a rapid and efficient cellular uptake pattern for SC-pDNA polyplexes is consistent with that of Shen *et al*, (2006). In that study the authors found how DNA diffusion was both size and topology dependent. Complex sizes of 181nm (radius) were reported which may aid cellular uptake (Shen *et al*, 2006). The present study revealed how SC-pDNA polyplexes displayed the smallest diameters, greatest nuclease resistance and effective DNA packaging (Chapter 3) which could all contribute towards the uptake results observed. The small and compact size of the SC-pDNA polyplex could facilitate entry across the plasma membrane (Zhang *et al*, 2008). Few studies have analysed the effect of DNA topology on polyplex characterisation and uptake in mammalian cells, but those that have concluded SC-pDNA displays beneficial characteristics that enhance uptake and gene expression which are summarised in Table 5.1. For example studies analysing DNA topology have reported smaller complex sizes for those containing SC-pDNA, which may enhance cellular uptake (Table 5.1). Therefore results of the current chapter strongly suggest uptake is dependent on DNA topology with SC-pDNA displaying characteristics that would favour non-viral gene delivery.

Non-viral gene delivery system	Size (nm)	Dose (µg)	Zeta potential (mv)	Nuclear association at 48 hours (%)	Optimal Gene expression	References
P(DMAEMA)/DNA	84 – SC-pDNA 91 – OC-pDNA 98 – Linear-pDNA	5-20 5-20 5-20	N/A	N/A	>0.75 relative transfection efficiency >0.5 relative transfection efficiency >0.1 relative transfection efficiency (β-galactosidase expression) at 48 hours	Cheng *et al*, (1999)
Lipid/DNA	114 – SC-pDNA 207 – OC-pDNA 117 – Linear-pDNA	350 350 350	N/A	N/A	>55 AU GFP Fluorescence <10 AU GFP Fluorescence >10 AU GFP Fluorescence at 24 hours	Remaut *et al*, (2006)
PEI/DNA	>100 – SC-pDNA N/A – OC-pDNA <400 – Linear-pDNA	20 20 20	N/A	N/A	>90% EGFP expression N/A >60% EGFP expression at 24 hours	Hsu and Uludag (2008)
PLL/DNA	<200 – SC-pDNA <400 – OC-pDNA <1000 – Linear-pDNA	10 10 10	+13 +23 +27	50 37 15	41% β-galactosidase expression 33% β-galactosidase expression 18% β-galactosidase expression at 48 hours	Dhanoya *et al*, (2011)

Table 5.1: Summary of studies focusing on the parameters affecting non-viral gene delivery within CHO and other mammalian cell types. Previous findings were compared with that of the present study. Where fields are denoted 'N/A' the respective study did not report the value. Nuclear association was quantified via confocal microscopy image analysis. Nuclear association was defined by complete overlap between polyplex fluorescence and nuclear stain.

However when analysing lipoplex uptake, cell association was most efficient for OC-pDNA (Chancham and Hughes, 2001). Therefore other factors could play a role in cellular uptake and should not be discounted. Also DNA uptake was also found to be independent of DNA topology in another previous study (Hsu and Uludag, 2008). Polyplexes of differing DNA topologies were significantly different in terms of size and so each may exploit specific independent uptake mechanisms leading to different uptake patterns (Hsu and Uludag, 2008).

5.4.2 CHO cell polyplex gene expression

For polyplex gene delivery to be viable tool in bio-processing, complexes must induce strong and sustained gene expression. The current chapter analysed gene expression under a range of conditions and parameters to deduce the ability of DNA polyplexes to undergo gene transcription.

5.4.2.1 Gene expression is dependent on DNA topology

PLL/DNA polyplexes were transfected into CHO cells for a period of 48 hours and plasmid reporter gene expression was highest for complexes containing SC-pDNA (Figure 5.12). OC-pDNA polyplex gene expression was slightly lower followed by linear-pDNA polyplexes, which was significantly lower than that of the SC form ($p < 0.05$). The topology dependent results provide key insights in regards to polyplex gene expression. Firstly the data indicates that DNA in the SC conformation is more readily transcribed than OC- or linear-pDNA. Secondly the ability of SC-pDNA polyplexes to be efficiently taken up in CHO cells and transported from cell periphery to the nucleus will enhance the likelihood of gene expression to occur, unlike that of linear-pDNA complexes (Figure 5.8). Thirdly, the effectiveness of SC-pDNA complexes to diffuse through the cell could lead to higher intracellular concentrations that increase the probability of attaining nuclear entry (Remaut *et al*, 2006).

Complexes containing SC-pDNA were found to be significantly smaller than OC- and linear-pDNA polyplexes, and this may facilitate nuclear pore entry (Kreiss *et al*, 1999). Previous reports found how transient gene expression and long term integration was greater for SC-pDNA, than linear-pDNA (Xie and Tsong, 1993). The SC and OC forms only differ by a nicked strand rather than a double stranded break (Remaut *et al*, 2006). Both SC- and OC-pDNA complexes were quite resistant to nuclease attack (Chapter 3, Figure 3.11) which may ultimately aid preservation of the DNA cargo, and hence enhance gene expression (Quaak *et al*, 2009 and Shen *et al*, 2006). The topology dependent gene expression data reported in this study in addition to further uptake studies are in line with previous results and summarised in Table 5.1. Previous reports such as Cherng *et al*, (1999) reported topology dependent gene expression. Interestingly Hsu and Uludag (2008) reported just over 90% EGFP positive cells following uptake of PEI/DNA complexes. This indicates that uptake may be due to topology although Hsu and Uludag (2008) reported no significant difference in expression when transfection time increased. Therefore uptake and expression could be due to DNA dose which could increase the DNA concentration entering the nuclei.

Although linear-pDNA complexes were susceptible to nuclease cleavage, its open and accessible structure does make it available for transcription factors to induce gene expression (Hsu and Uludag, 2008). This may account for the modest gene expression detected. Linear-pDNA may also self ligate leading to formation of structures similar to OC-pDNA, which may improve gene expression (Cherng *et al*, 1999). Despite reporting superior gene expression for complexes containing SC-pDNA, DNA topology did not significantly affect complex uptake, with more emphasis placed on other factors such as size (Hsu and Uludag, 2008).

To understand why the SC form is more successful at inducing gene expression, the degradative pathways of pDNA must be considered. Maintenance of the plasmid phosphodiester bond is important as cleavage of this can lead to the conversion of different pDNA forms (Middaugh *et al*, 1998). Depurination and β-elimination (cleavage of nucleotide backbone) have been cited as the main cause of pDNA degradation *in viv*o causing breakage of the phosphodiester chain (Lindhal and Karlstrom, 1993). These events are accelerated at low pH environments *in vivo*, and so protection of the pDNA backbone is vital. It may be that the compact nature of the SC form coupled with PLL induced condensation protects against this, thereby maintaining structural integrity.

5.4.2.2 Polyplex charge ratio

Polyplex charge ratio (ratio of polymer to DNA) is important in terms of converting the negative charge of DNA to a positive charge to facilitate cellular entry. In the present study, polyplexes containing SC- and OC-pDNA were produced at charge ratios of +1.6. This particular charge ratio was recommended by previous biophysical polyplex studies (Tsai *et al*, 1999). In that study the authors reported efficient DNA condensation, reduced sizes and strong cationic charge for the given charge ratio, which are characteristics favourable for gene delivery (Tsai *et al*, 1999). Previous studies formulated PEI complexes at a charge ratio of +1.6, and reported complex sizes of only 20nm, which contributed to effective uptake and gene expression (Dunlap *et al*, 1997). Linear-pDNA required a higher charge ratio (greater concentration of PLL) to undergo charge neutralisation and even when the charge ratio was equal, gene expression remained highest for SC-pDNA polyplexes (Figure 5.14). In fact when the charge ratio increased to +5 for all three DNA forms, gene expression decreased by approximately 50%, suggesting greater amounts of PLL may jeopardise DNA uptake. Although experiments were identical to that of Figure 5.12, linear-pDNA polyplexes

displayed approximately 10% reduction in gene expression. This may highlight how such complexes are susceptible to degradation and unstable. Furthermore at high charge ratios it has been shown that increasing the amount of polymer leads to a rise in complex aggregation, which hinders gene expression (Christie *et al*, 2010). Despite displaying similar gene expression profiles to that of SC-pDNA, OC-pDNA polyplexes were much larger in size (>300nm) (Chapter 3, Figure 3.5). This indicates that other factors, along with complex size may contribute towards gene expression such as nuclease resistance and stability. Therefore when formulating DNA polyplexes it is essential to compromise between the amount of polymer and DNA in order to avoid hindering uptake.

5.4.2.3 Short term gene expression

Polyplex gene expression was rapid and was detected within 20-60 minutes (Figure 5.13). Although administered by pressure injection, Stechschulte *et al*, (2001) reported gene expression as early as one hour with naked pDNA. A recent study revealed how a large population of enhancers can be stimulated to induce gene expression programmes. These gene expression programmes have been found to elicit rapid sequential gene expression during cell development, differentiation and stress (Wang *et al*, 2011). Such events may be triggered during uptake of DNA. Furthermore studies have reported rapid gene expression whereby PEI/DNA polyplex gene expression was measured as early as 30 minutes post transfection (Koyama *et al*, 2010). Although the early detection could also be due to background staining for β-galactosidase, this is unlikely to impact on studies as gene expression clearly shows dependence on DNA topology. Moreover staining with X-gal shows a clear difference between cells positive and negative for β-galactosidase (Figure 5.10).

5.4.2.4 Bolus transfection vs. reverse transfection

Polyplex uptake and gene expression were measured in CHO cells that were adherent to the tissue culture surface. Adherent CHO cells in culture media were supplemented with DNA polyplexes (referred to as bolus transfection). However CHO cells employed for recombinant protein production and other key primary cell lines are also non-adherent. Alternative transfection techniques are required. Using confocal microscopy this chapter revealed successful uptake of polyplexes within CHO cells suspended in culture. This occurred via reverse transfection (RT), which involves immobilisation of the polyplex to the culture surface for a given period, and supplementing with suspended cells (Bengali *et al*, 2009). Polyplexes uptake was monitored for periods of up to 1 (Figure 5.6) and 48 hours (Figure 5.7). Uptake of complexes seemed to occur in a topology dependent manner with SC- and OC-pDNA complexes associating with the nuclei. RT has advantages in that direct addition of cells enhances uptake and reduces aggregation (Shea *et al*, 1999). The conventional bolus transfection procedure, although widely employed for reliable gene uptake studies does fall short in the direct delivery of polyplexes to cells (Bengali *et al*, 2009). RT operates by surface binding of complexes and therefore transfection is more controlled, which is a key parameter of biotechnology (Bengali *et al*, 2005).

However although RT promotes immediate uptake of DNA, it does not offer superior gene expression to that of bolus transfection. In fact the study that compared both methods reported no significant differences (Bengali *et al*, 2009).

5.4.2.5 Improvements to current protocols and alternative methods

Although staining and detection by confocal microscopy allowed polyplexes to be tracked and in some experiments revealed co-localisation of fluorescence (PLL and DNA), alternative techniques to study polyplex uptake should also be considered. Fluorescence resonance energy transfer (FRET) is a useful tool that can detect subtle changes in

fluorescence. FRET detects energy transfer in the form of fluorescence between two fluorophores in close proximity (Haugland *et al*, 1969). FRET has been used to study polyplex dissociation kinetics. Recent studies employing FRET revealed incomplete binding of polymer and DNA (Ko *et al*, 2011). Therefore FRET can be used to improve interpretation and confirm DNA/polymer association.

For polyplexes to achieve initial uptake, electrostatic interaction occurs between the positively charged complex and negatively charged plasma membrane (Elouahabi and Ruysschaert, 2005). More specifically polyplexes have been found to associate with negatively charged protein regions of the membrane referred to as proteoglycans. Proteoglycans are negatively charged membrane proteins that are involved in binding with cations (Kopatz *et al*, 2004; Tros de Ilarduya *et al*, 2010). Chenevier *et al*, (2000) reported a two step mechanism of cationic complex association with the cell surface. Firstly acidic glycoproteins within the membrane interact with cationic complexes, followed by anionic matrix components which facilitate complex recognition and entry (Chenevier *et al*, 2000). In regards to CHO cells, Labat-Moieur *et al*, (1996) revealed knock down of heparin sulphate proteoglycans reduced PLL complex cell binding and gene expression. Enzymatic inhibition confirmed such results (Mislick and Baldeschwieler, 1996). Therefore non-viral gene delivery vectors should be designed to target and maximise interactions with cell surface components to facilitate cellular entry.

In regards to future analysis concerning complex uptake, the PLL/DNA polyplexes used in this study can be improved through the incorporation of components that maximise membrane association. Specific peptide nanoparticles have been synthesised which enhance cellular delivery and membrane association, particularly proteoglycan regions (Sun *et al*,

2010). Incorporation of such components could potentially enhance uptake and possibly gene expression.

5.4.3 Mechanism of polyplex uptake

Understanding the mechanisms exploited by DNA polyplexes to gain cellular access will aid in the design of gene delivery vehicles. Polyplex uptake in mammalian cells has been attributed towards endocytosis (Rejman *et al*, 2005). Endocytosis refers to the process of internalisation of extracellular material (Gould and Lippincott-Schwartz, 2009; Pinchon *et al*, 2010). There are two main endocytic pathways to which polyplexes have been reported to exploit. The clathrin mediated endocytic (CME) pathway entails the entry of foreign materials via clathrin coated pits which form into vesicles that transport the internalised cargo (Rejman *et al*, 2005). The vesicles fuse with early endosomes for further trafficking. The second endocytic route of entry is via the caveolae pathway. This involves lipid raft structures that bind and dock with incoming cargo. These structures invaginate off the membrane transporting its contents (Khalil *et al*, 2006).

5.4.3.1 Endocytic uptake of polyplexes

Quantitative analysis was carried out to identify whether polyplexes utilise endocytosis as means of CHO cell entry, and any particular pathway of interest. Known chemical inhibitors of the CME (choloropromazine [CMZ]) and caveolae pathway (genistein) were added to CHO cells and the effect on gene expression was reported. Addition of CMZ and genistein significantly reduced gene expression (Figure 5.15). Furthermore experiments showed reduced uptake and nuclear association of polyplexes regardless of DNA topology in cells treated with endocytic inhibitors (Figure 5.16). The reduction in polyplex uptake when treated with chemical inhibitors is in line with that of Luhmann *et al*, (2008). Previous studies

showed caveolae pathway inhibition did reduce uptake in CHO cells by over 75% in regards to chitosan complexes (Douglas *et al*, 2008). Polyplexes have been reported to utilise various endocytic pathways for cellular uptake. For example PEI/DNA polyplex uptake was reported to occur via both the CME and caveolae pathway (Rejman *et al*, 2005).

Validation of the chemical inhibitors was carried out to confirm specific pathway inhibition. Genistein blocks ATPase function and is involved in hormone induction (Kuiper *et al*, 1998) and such actions may limit complex uptake rather than specific pathway inhibition. To test whether chemical treatment leads to specific pathway inhibition, commercial markers of the CME and caveolae pathway were added to cells treated with the respective inhibitors. Confocal microscopy and flow cytometry studies revealed chemical treatment did lead to specific inhibition of the pathway of interest and did not jeopardise uptake of markers corresponding to alternative pathways (Figures 5.17 and 5.18).

5.4.3.2 Analysis with commercial endocytic markers

To analyse further whether PLL/DNA polyplexes may exploit both CME and caveolae pathways, characterised commercial markers of the CME and caveolae were co-transfected with DNA polyplexes. Fluorescent confocal microscopy analysis revealed co-localisation of polyplex DNA with transferrin (CME marker) and cholera toxin subunit (CTB) (caveolae marker) (Figure 5.19). However polyplexes (regardless of DNA topology) did not show fluorescent co-localisation when transfected in cells treated with an alternative commercial antibody stain specific for markers of the caveolae pathway (Figures 5.20). Furthermore no fluorescent co-localisation was observed in cells treated with fluorescently labelled antibodies specific for the CME marker (Figure 5.21). Therefore the collective results suggest that PLL/DNA polyplexes may exploit both CME and caveolae pathways according to gene expression and quantitative experiments, however antibody staining experiments suggests

otherwise. Therefore alternative endocytic routes may be employed. Endocytic pathways such as these have size criteria for their incoming cargo to which polyplexes may meet (100-300nm) allowing the possible entry through both pathways. (Douglas *et al*, 2008).

Despite uptake and gene expression studies indicating both CME and caveolae pathways of endocytosis could potentially be exploited by DNA polyplexes, no clear fluorescent co-localisation was identified in transfected cells stained with anti-Rab5 (marker of CME pathway) antibodies (Figure 5.21). Knockdown of Rab5 through RNA gene silencing is an alternative method that can be used to specify polyplex CME entry. This method has recently been used to decipher the role of early endosomes (Kageyama-Yahara *et al*, 2011). In addition to the CME and caveolae pathway, there are alternative endocytic pathways. For example macropinocytosis is a form of endocytic entry which involves the formation of large vesicles which pinch off the membrane (Khalil *et al*, 2006). This form of entry could be used by complexes in this study particularly as macropinocytosis entails the entry of foreign cargo as large as 5µm (Khalil *et al*, 2006). Recent studies have developed new methods to track internalised cargo (labelled with MRI agents), in which endosome internalisation corresponds to photochemical activation allowing researchers to identify the location of transfected cargo (Gianolio *et al*, 2011).

5.4.3.3 Enhancing endocytic uptake

Understanding the mechanism of polyplex uptake will lead to improvements in the transportation of DNA, which will ultimately serve to enhance gene expression for therapeutic purposes. The present study revealed how PLL/DNA polyplexes may exploit both the CME and caveolae pathways. This could allow for optimisation. A recent study incorporated transmembrane receptor domains within PEI polyplexes which significantly enhanced cellular uptake and endosomal transportation within CHO cells (Kakimoto *et al*,

2010). Improved cellular uptake and endosomal trafficking also led to increased gene expression (Kakimoto *et al*, 2010). Knowledge of the CME pathway and the role of endosomes as trafficking vesicles, led to Kulkarni *et al*, (2006) to emphasise the importance of the microtubule network for endosomal transport. In that particular study biophysical analysis revealed how motor proteins mediate the active transport of polyplex loaded endosomes towards the nucleus (Kulkarni *et al*, 2006).

Although generally regarded to occur via endocytosis, polyplex uptake varies, depends on various parameters and is very specific. Douglas *et al*, (2008) reported nanoparticle vector uptake is dependent upon the cell line. Qi *et al*, (2010) reported how dendrimer non-viral gene delivery does not occur via the caveolae pathway whereas others report PEI based complexes use the CME pathway (Ma and Lim, 2003). Moreover there are reports that show utilisation of both endocytic pathways by polyplexes (Luhmann *et al*, 2008; Sahay *et al*, 2010). Alternatively pathways independent to that of the CME and caveolae have been used by PEI polyplexes (Hufnagel *et al*, 2009). Therefore from these reports and the findings of the present chapter, endocytosis could be utilised by DNA polyplexes, however antibody staining for specific markers suggest otherwise and factors such as vector type, size and cell type seem to determine pathway of entry.

In this chapter uptake and gene expression of PLL/DNA polyplexes showed dependence on DNA topology. These two parameters were greatest for SC-pDNA polyplexes. Regardless of DNA topology polyplex gene expression was reduced when transfected into cells treated with endocytic inhibitors suggesting possible exploitation of endocytic pathways. Modification or incorporation of elements that target these pathways within complexes, could potentially improve cell uptake. However antibody staining for endocytic markers showed no fluorescent co-localisation indicating other routes of cellular entry may be exploited by DNA polyplexes.

5.5 Chapter Summary

- Polyplex uptake showed dependence on DNA topology whereby approximately 60% of complexes containing SC-pDNA associated with the nuclei by one hour.
- PLL and DNA exhibited close association following uptake as shown by co-localisation in fluorescent confocal microscopy studies. However co-localisation decreased at extended time periods in which PLL may be separated from DNA or degraded.
- CHO cell polyplex gene expression (*lacZ* plasmid reporter gene) was dependent on DNA topology, which was highest for SC-pDNA polyplexes at >40%. This occurred regardless of charge ratio.
- PLL/DNA polyplexes can also be transfected into CHO cells via reverse transfection (RT) as shown by fluorescent confocal microscopy.
- Polyplex (regardless of DNA topology) gene expression was reduced in cells treated with endocytic inhibitors and showed co-localisation when transfected with markers of the caveolae and CME pathways.
- However no fluorescent co-localisation was observed between DNA polyplexes and fluorescently labelled antibodies specific for alternative endocytic markers.

Chapter 6.
Polyplex uptake within dendritic cells

6. Polyplex uptake within dendritic cells

Dendritic cells (DCs) are key components of the immune system which function by binding and collecting antigens. They bridge both arms of immunity; the innate and adaptive response. The innate response refers to the recognition of microbial agents, foreign antigens and pathogens via pathogen recognition receptors (PRRs) (Stevenson *et al*, 2010). The adaptive arm of immunity is primed into response when exposed to a foreign antigen leading to recognition and targeting of the antigen culminating in immunological memory for future attacks (Marieb, 2004). To achieve this DCs present the antigen of interest through selective surface markers to T cells (Ueno *et al*, 2011; Stevenson *et al*, 2010). T-cells are blood cells which recognise antigens presented by DC surface markers and become activated. When activated, T-cells function by releasing small proteins referred to as cytokines which aid in the immune response (Ueno *et al*, 2011). Following antigen presentation T-cells differentiate into effector cells (Finkleman *et al*, 1996). It is these functions that researchers aim to exploit and why polyplex gene delivery to DCs is a key area of study for the design of DNA vaccines.

The chapter investigated non-viral gene delivery within human monocyte derived DCs. Polyplex uptake (defined as the intake of materials by a cell or tissue leading to its permanent or temporary retention) and gene expression (transcription of pDNA reporter gene) is reported. DCs express various cell surface markers which contribute towards antigen presentation (Stevenson *et al*, 2010). In this study polyplex gene expression was measured and whether this impacts on DC surface marker expression and hence activation of DCs.

6.1 Observation of polyplex uptake in DCs

6.1.1 Classification of polyplex location

Polyplexes were transfected into DCs (Chapter 2, section 2.6.2). Polyplexes were dual labelled whereby DNA was fluorescently labelled red, while PLL was tagged green. Dual staining was maintained indicating both DNA and PLL remained associated following uptake (Figure 6.1). DC cytosol was also stained light grey to highlight uptake and location of polyplexes. Polyplexes in each cell were then classified as being at the periphery (Figure 6.1a), in the cytosol (Figure 6.1b) or inside the nucleus (Figure 6.1c). This criterion is applied throughout the chapter as in Chapter 5 (refer to Chapter 5, Figure 5.1). As in Chapter 5, 3-D images were taken (as sections) to confirm polyplex uptake when analysing via fluorescent confocal microscopy. Ten sections of each image, each of 0.2μm in thickness were taken. Mid section images were taken to confirm true polyplex uptake along with projection images of all sections (referred to as z-stack projection images). Details are provided in Chapter 2, section 2.6.7.1.

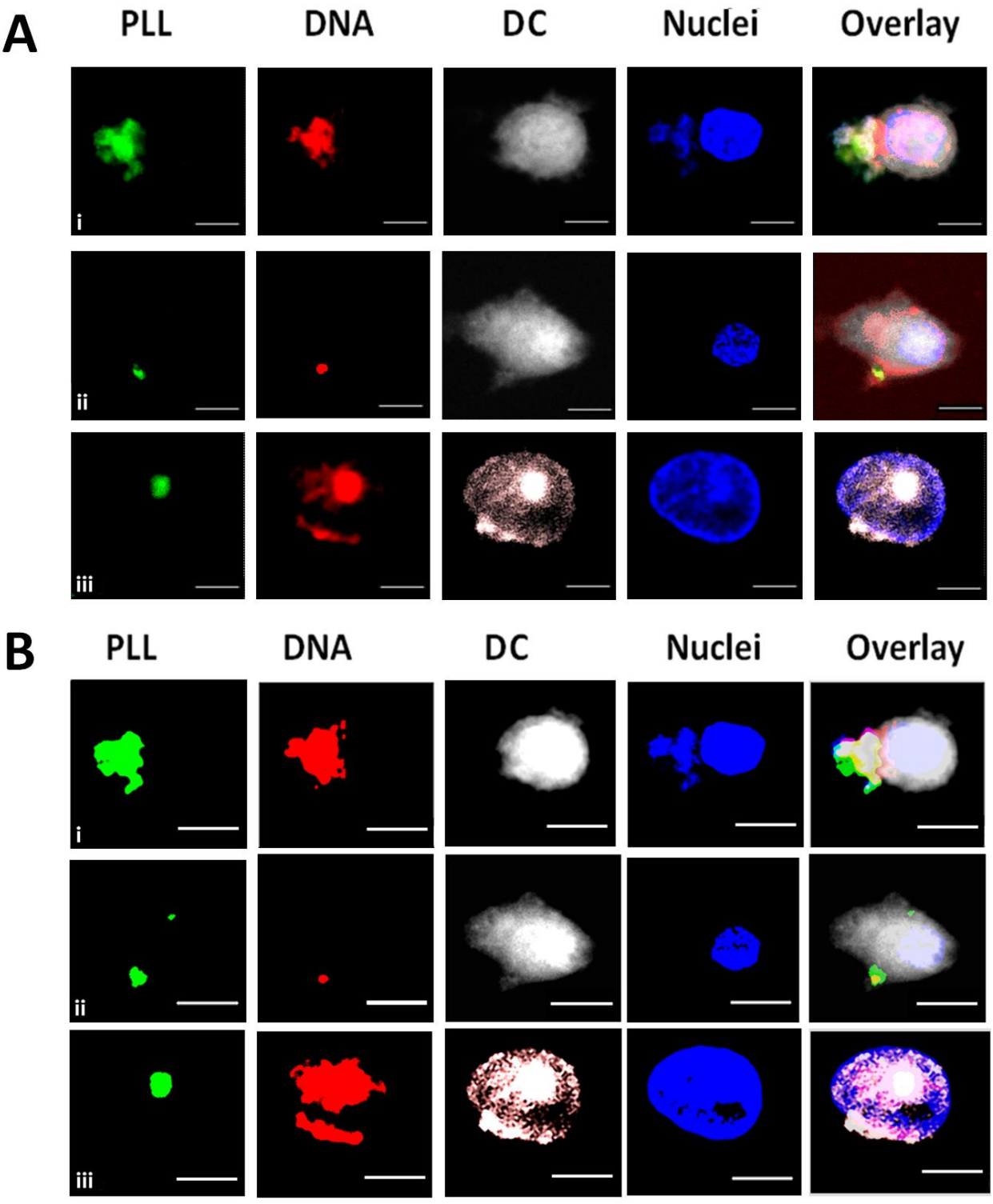

Figure 6.1: **Classification of polyplex cellular location in DCs**. Mid section (A) and stack projection images (B). Confocal microscopy analysis showing the location of polyplexes; cell periphery (linear-pDNA polyplexes) (i), cytosol (OC-pDNA polyplexes) (ii) and nucleus (SC-pDNA polyplexes) (iii). Complexes were prepared at charge ratios (ratio of PLL to DNA) of +1.6 (for SC- and OC-pDNA) and +5 for linear-pDNA. Scale bar represents 5µm. DCs were fixed with paraformaldehyde, stained and coverslips were mounted on slides.

6.1.2 Short time course

Polyplexes containing 2µg pDNA were transfected into approximately $1x10^6$ DCs and analysed via fluorescent confocal microscopy. Complexes were often located on the cell periphery and in the case of SC-pDNA polyplexes, migrated to the cytosol by 30-60 minutes (Figure 6.2). Complexes containing OC- and linear-pDNA were predominately located on the periphery of the cell between 10-30 minutes and cytosol by 60 minutes.

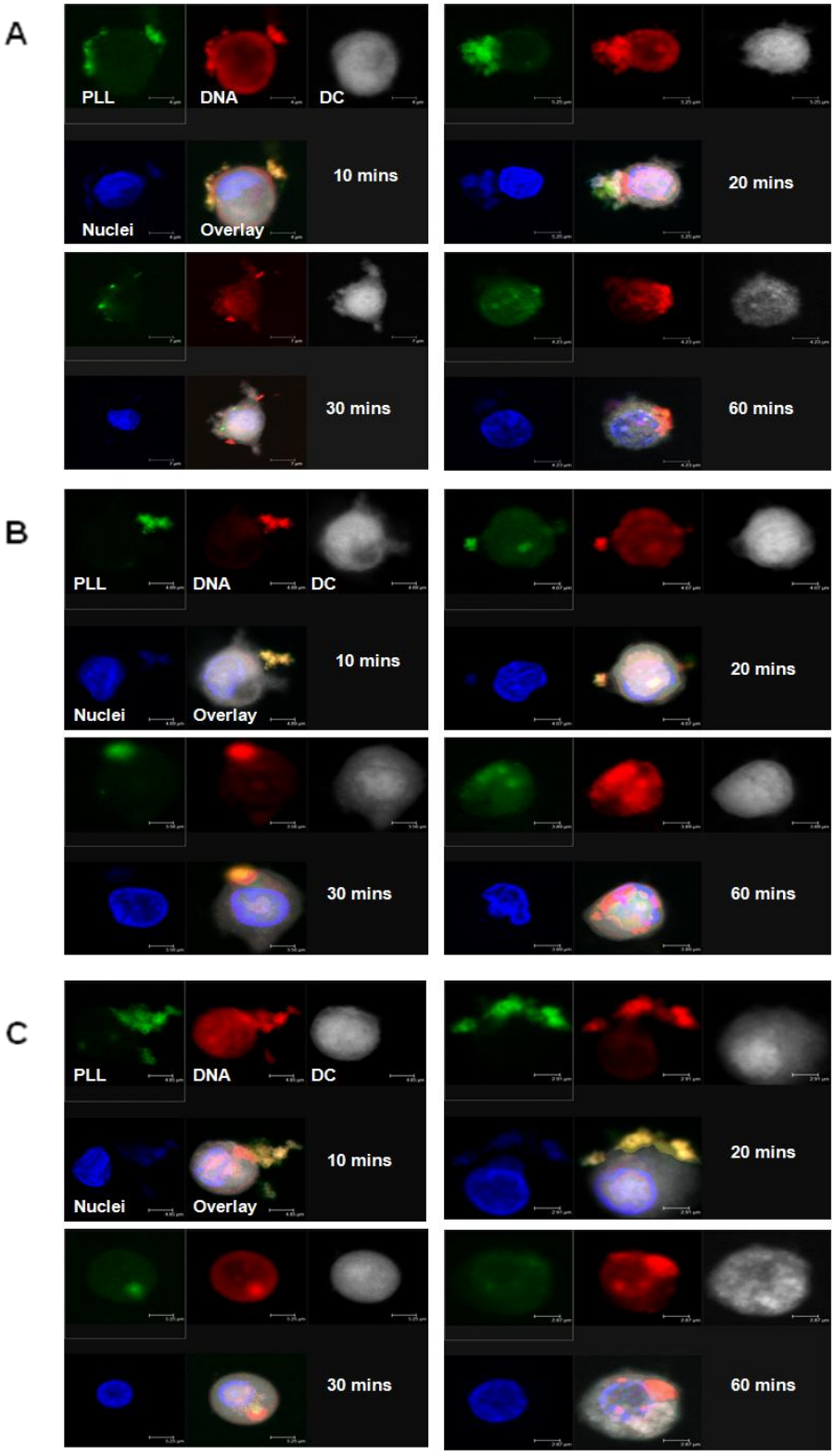

Figure 6.2: **Time course of polyplex uptake in DCs as observed via confocal microscopy.** Polyplexes containing linear- (A), OC- (B), and SC- (C) pDNA (2µg). Polyplexes were prepared at charge ratios of +1.6 (for SC- and OC-pDNA) and +5 for linear pDNA. Polyplexes were spotted onto PLL coated coverslips for 1 hour at room temperature (protected from light). DCs were then added to complexes and incubated at 37°C for the desired period. Figure shows mid section images.

Naked DNA displayed no fluorescence, throughout the time course, presumably requiring PLL to enter cells (Figure 6.3).

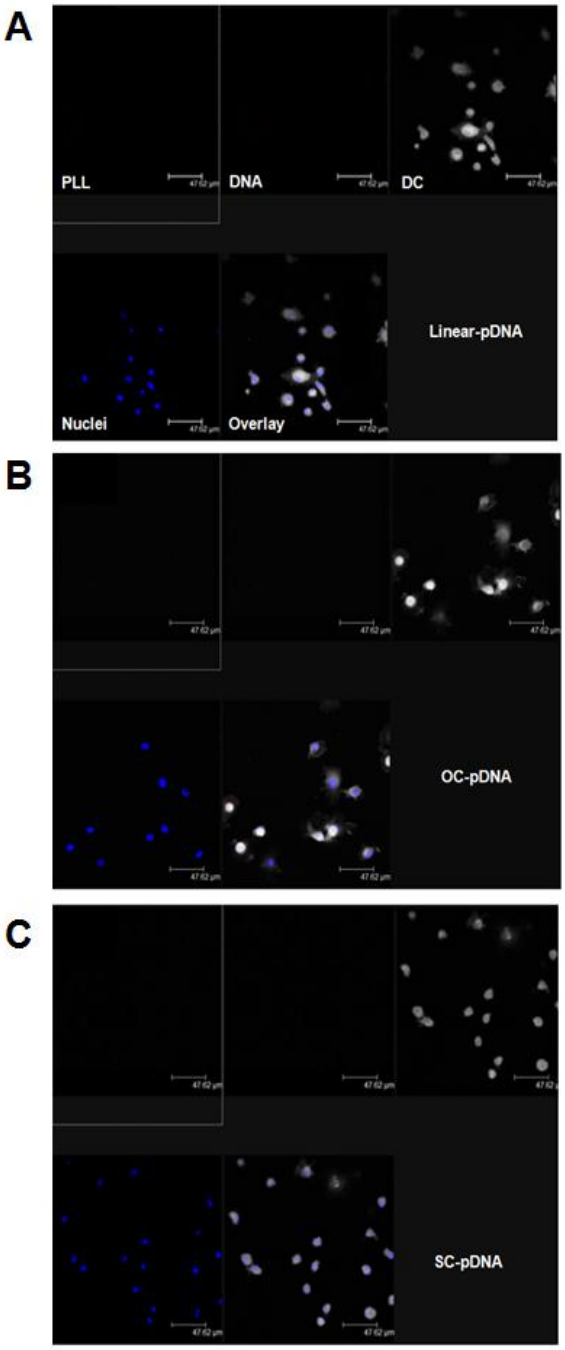

Figure 6.3: **Transfection of naked pDNA in DCs as observed via confocal microscopy.** Naked linear- (A), OC- (B), and SC- (C) pDNA (2μg).

6.1.3 Extended time course

Polyplex uptake was studied at an extended time period of 48 hours (Figure 6.4). Polyplexes were often situated within the periphery (linear-pDNA) or the cytosol (SC- and OC-pDNA) of the cell, with low nuclear association. Unlike what was observed for CHO cells (Chapter 5, 5.1.3) the polyplexes exhibited dual staining. No dissociation of DNA from PLL was noted which may be due to differing uptake mechanisms within the two cell lines.

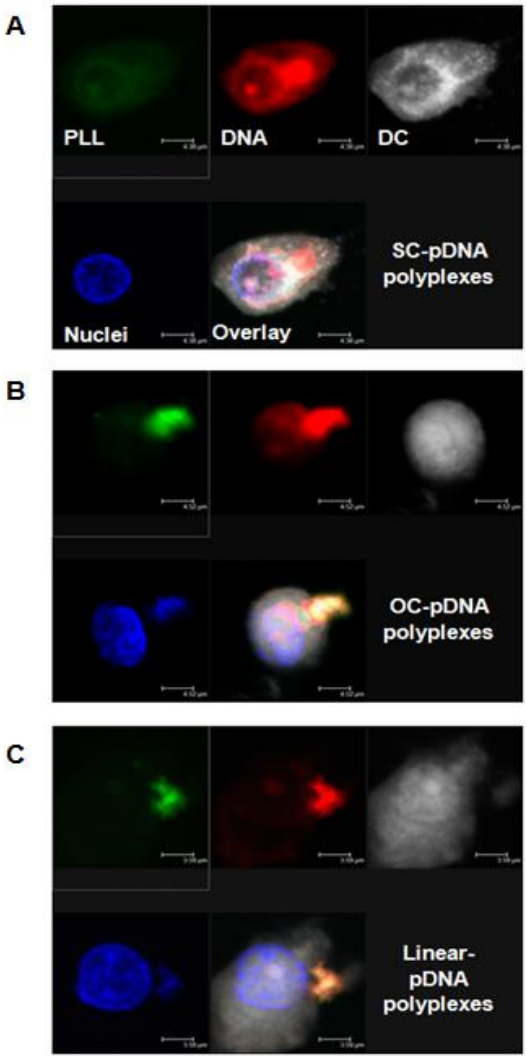

Figure 6.4: **Extended time course of polyplex uptake in DCs as observed via confocal microscopy.** Polyplexes containing linear- (A), OC- (B), and SC- (C) pDNA (2µg). Polyplexes were prepared at charge ratios of +1.6 (for SC- and OC-pDNA) and +5 for linear pDNA. Figure shows mid stack images.

6.2 Quantification of polyplex uptake and gene expression within DCs

Confocal image quantification of polyplex uptake was carried out along with gene expression measurements. As in Chapter 5 (Figure 5.8) polyplexes were classified on the basis of their intracellular location.

6.2.1 Efficiency of polyplex uptake within DCs

The number of cell associated polyplexes was counted and classified according to the basis of their location (as in Figure 6.1). By 10-30 minutes, the majority of polyplexes regardless of DNA topology were often situated within the periphery of DCs (Figure 6.5). However by 1 hour 15% of SC-pDNA complexes associated with the nuclei (complete overlap between polyplex fluorescence and nuclear stain). In contrast, no nuclear association was observed for OC- and linear-pDNA polyplexes, emphasising topology dependent uptake.

Polyplexes were transfected in DCs for an extended period of 48 hours and were also quantified (Figure 6.6). Uptake was topology dependent whereby 30% of SC-pDNA polyplexes associated with the DC nuclei, which was greater than OC- and linear-pDNA polyplexes. Therefore SC-pDNA polyplexes seem more efficient in terms of attaining nuclear association within DCs than its counterparts. It is important to note that while compartment association is a useful indicator for polyplex uptake, nuclear association does not directly correspond to gene expression due to various molecular barriers and presence of nucleases within the nucleus. Details of quantification methodology are provided in Chapter 2, section 2.6.7.3.

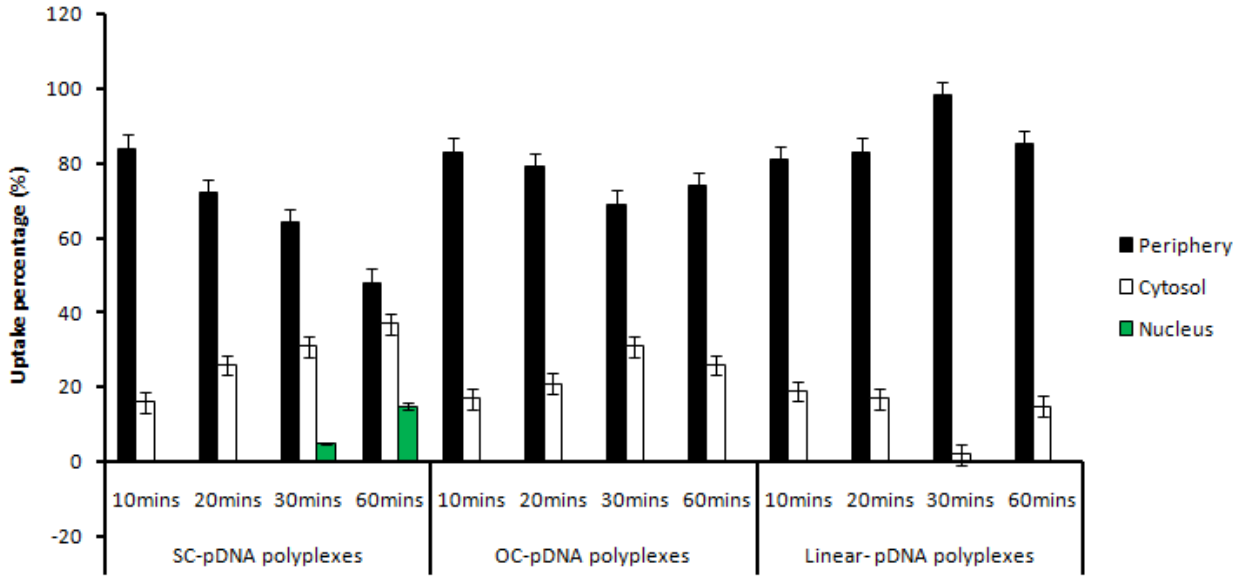

Figure 6.5: **Quantification of polyplex uptake in DCs for up to 1 hour**. Polyplexes (containing 2µg DNA) were prepared at charge ratios of +1.6 (for SC- and OC-pDNA) and +5 for linear pDNA. The figure shows the mean and standard error (SE) of 3 independent experiments. One-way ANOVA was employed to deduce levels of statistical significance ($p < 0.05$) between complexes of differing DNA topologies in different cell compartments.

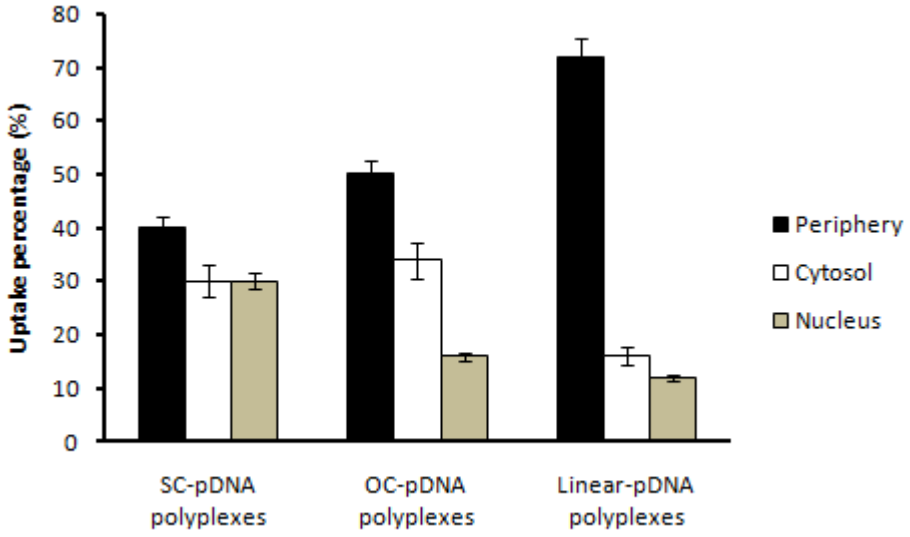

Figure 6.6: **Quantification of polyplex uptake in DCs at 48 hours**. Polyplexes (containing 2µg DNA) were prepared at charge ratios of +1.6 (for SC- and OC-pDNA) and +5 for linear pDNA. The figure shows the mean and SE of 3 independent experiments. One-way ANOVA was employed to deduce levels of statistical significance ($p < 0.05$) between complexes of differing DNA topologies in different cell compartments.

6.2.2 DC polyplex gene expression studies

In this study PLL/DNA polyplex uptake and gene expression was measured in human monocyte derived DCs. The pDNA encodes a *lacZ* reporter gene for β-galactosidase which was measured by X-Gal staining via light microscopy (refer to Chapter 2, section 2.6.3 for details and also shown in Chapter 5, Figure 5.10). Gene expression measurements are important in terms of deducing the efficiency of polyplex uptake and the ability of polyplexes to gain nuclear access and undergo gene transcription. In this study complexes containing 20µg pDNA were transfected into DCs to induce gene expression. This is important in regards to gene expression within DCs as such cells express nucleases (Chain, 2003). Although 2µg pDNA was used for confocal image uptake studies, there was no significant difference between uptake profiles of complexes containing 2 and 20µg.

6.2.2.1 48 hour time course

DCs were transfected for a period of 48 hours. This time period was selected due to optimal expression of the *lacZ* reporter gene identified from previous studies regarding DCs (Nakamura *et al*, 2002). Gene expression showed dependence on DNA topology which was highest for SC-pDNA polyplexes at 14% when the charge for all three complexes are similar; +1.6 for SC- and OC-pDNA, and +5 for linear-pDNA (Figure 6.7). This was significantly greater than OC- and linear-pDNA polyplexes ($p < 0.05$). OC- and linear-pDNA complex gene expressions were not significantly different to naked pDNA controls (with the exception of naked linear-pDNA) (Figure 6.7).

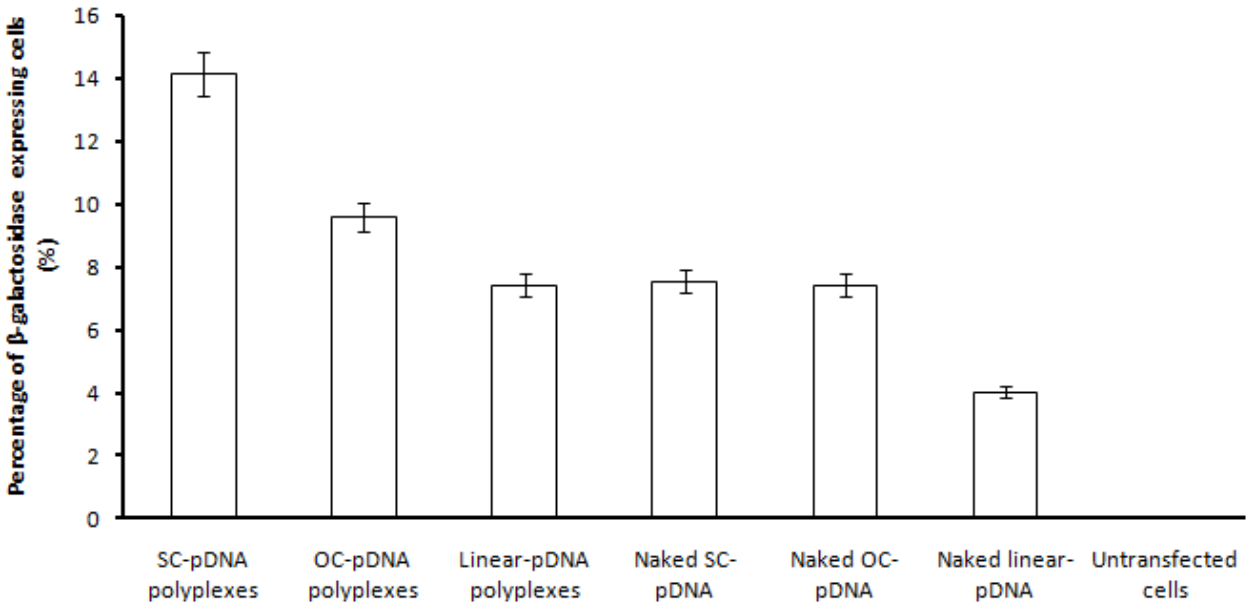

Figure 6.7: **Polyplex gene expression within DCs**. 20µg polyplex DNA was transfected into DCs. Polyplexes were prepared at charge ratios of +1.6 for SC- and OC-pDNA polyplexes and +5 for linear-pDNA polyplexes (1mM HEPES [pH 7.5]). The figure shows the mean and SE of 3 independent experiments. One-way ANOVA was employed to deduce levels of statistical significance ($p < 0.05$) between complexes of differing DNA topologies.

6.2.2.2 Polyplex gene expression at an equal charge ratio

Polyplex charge ratio (ratio of PLL to DNA) is important in terms of converting the negative charge of DNA to a positive charge to facilitate cellular entry (across negatively charged membrane). In the present study, polyplexes containing SC- and OC-pDNA were produced at charge ratios of +1.6. This was due to the equal positive surface charge displayed (zeta potentials). This particular charge ratio was recommended for future gene delivery analysis by previous biophysical polyplex studies (Tsai *et al*, 1999).

The previous figure showed the transfection efficiency when the charge of all three polyplexes was similar (although at differing charge ratios). When DCs were transfected at

equal charge ratios, gene expression still remained highest for the SC-form (Figure 6.8). When the charge ratio increased to +5, transfection efficiency was not significantly different, however gene expression decreased slightly. This observation is consistent with that of CHO cells (Chapter 5, Figure 5.14), suggesting greater concentrations of PLL may jeopardise uptake. When the charge ratio increased polyplex sizes have also been measured to rise (with the exception of SC-pDNA) (Chapter 3, section 3.2.4) and the increase in size may hinder uptake and gene expression for complexes formulated at charge ratios of +5. Furthermore at high charge ratios it has been shown that increasing the amount of polymer leads to a rise in complex aggregation, which hinders gene expression (Christie *et al*, 2010).

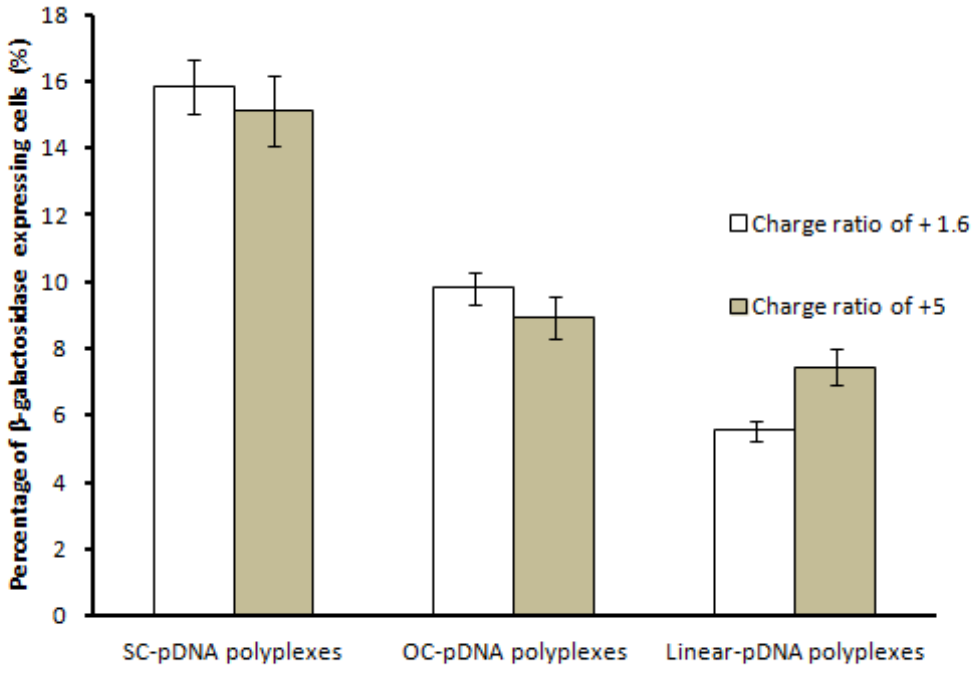

Figure 6.8: **Polyplex gene expression within DCs when the charge ratio is equal.** 20µg polyplex DNA was transfected into DCs. Polyplexes were produced at charge ratios of +1.6 and +5 (1mM HEPES [pH 7.5]). The figure shows the mean and SE of 3 independent experiments. One-way ANOVA was employed to deduce levels of statistical significance ($p < 0.05$) between complexes of differing DNA topologies at different charge ratios.

6.3 Impact of polyplex gene expression on DC phenotype

DCs express various cell surface markers which generally function by presenting foreign antigens to T cells (summarised in Table 6.1). DC surface marker expression has been reported to be upregulated when cells are exposed to chemical allergens. Therefore changes in DC surface marker expression provide a measure of DC activation (Hulette *et al*, 2002). In this study DNA polyplexes were transfected into DCs (approximately 1.9 $x10^6$ cells) to analyse whether polyplex gene expression activates DCs. Polyplex gene expression and the level of DC surface marker expression was measured by flow cytometry.

Unlike previous gene expression studies which entailed X-Gal staining and detection via light microscopy, β-galactosidase activity was probed by a fluorescein stained substrate which allowed for flow cytometric analysis (Chapter 2, section 2.8). Following uptake cells were exposed to fluorescently labelled antibodies specific for various DC surface markers. These antibodies were labelled with far red fluorophores (to distinguish from the green labelled transfected cell population positive for β-galactosidase). Cells were analysed by flow cytometry, whereby fluorescein was measured under the FL-1 filter, while the far red antibody stains were detected under FL-2 or FL-4 filters.

Surface Marker	Function	Reference
CD1a	Recognises foreign lipid antigens and presents to T cells for specific recognition	Hulette *et al*, 2001
DC-SIGN	C-type lectin which regulates activation of CD4+ T cells	Curtis *et al*, 1992
CD11c	Expressed on DCs and involved in a variety of roles including phagocytosis and T cell proliferation.	Sadhu *et al*, 2007
MHC-I	Presents peptides generated by the proteosome. The MHC-I-peptide complex is positioned within the plasma membrane to present the peptide to T cells.	Ueno *et al*, 2011
MHC-II	Complexes which present extracellular derived peptides. MHC-II complex recognises foreign pathogens and bacteria, and presents to CD4+ T cells	Stvenson *et al*, 2010
CD40	Member of the tumour necrosis factor receptor family which is involved in IL-12 synthesis in DCs.	Tone *et al*, 2001
CD80	Expressed on B cells and upregulated during infection.	Suvas *et al*, 2006
CD83	Expressed on mature DCs and expression coincides with MHC-II antigen expression.	Prazma andTedder, 2002
CD86	Widely expressed on DCs and an important costimulator of T cell activation.	Zheng *et al*, 2004

Table 6.1: A selection of the key DC surface markers that play an important role in induction of immunity. These surface markers were studied in subsequent flow cytometry studies.

6.3.1 Flow cytometry analysis

Figure 6.9 shows scatter plots which display the population of DCs and the level of expression of the 9 surface markers following uptake of DNA polyplexes. SC-pDNA polyplexes were analysed, as these gave clear distinguishable population of cells positive for β-galactosidase expression as detected by flow cytometry. Isotype controls (IgG1 and IgG2b) were employed to compensate for non-specific antibody binding. A comparison of the bulk transfected and nontransfected populations showed no evidence of increased expression of any of the markers. DCs expressing β-galactosidase (FL-1 filter) displayed a negative fluorescent shift for surface marker expression detected in the FL-2 or FL-4 filter (such as DC-SIGN [dendritic cell-specific intercellular adhesion molecule-3-grabbing non-integrin]) (Figure 6.9).

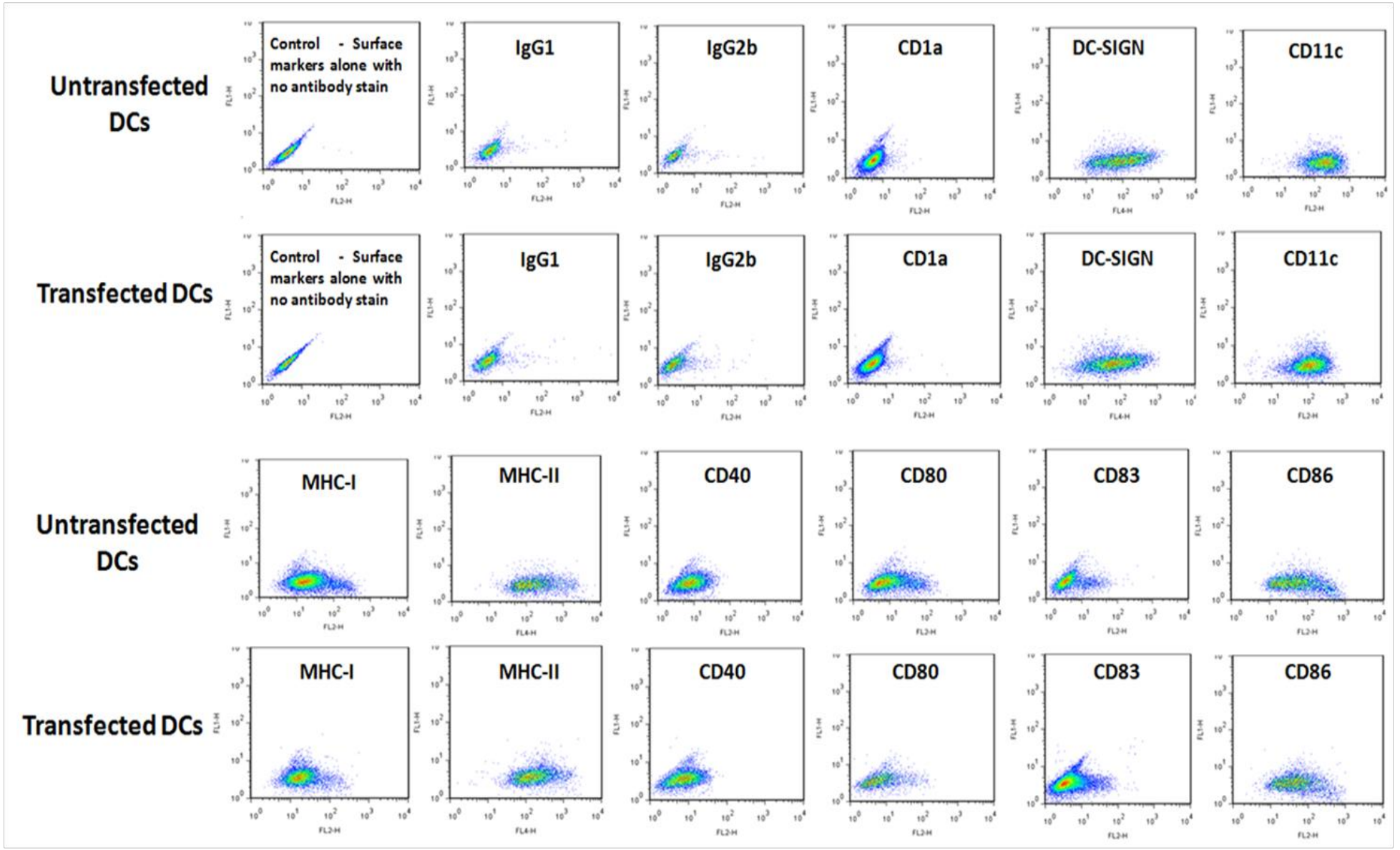

Figure 6.9: Scatter plot analysis displaying effect of polyplex gene expression on DC surface marker expression. DCs were analysed by flow cytometry. Polyplex (containing 20µg DNA) gene expression was measured under the FL-1 filter, while DC surface marker expression was measured under the FL-2 or FL-4 filters

6.3.2 The effect of gene expression on DC surface marker expression

Healthy DC populations were gated in order to avoid analysis of debris and dead cells (Figure 6.10a). The level of polyplex gene expression within DCs was measured (in the fluorescein, FL-1 filter) (Figure 6.10b) and its effect on surface marker expression was compared with untransfected controls (Figure 10c). Gene expression within DCs was detected with a slight positive shift for transfected cells. The level of DC surface marker expression in transfected cells did not change and in some cases was less (e.g. CD80 and CD83) than untransfected controls (Figure 6.10c). These findings are consistent with Figure 6.9 whereby polyplex DNA uptake did not activate DCs through surface marker expression.

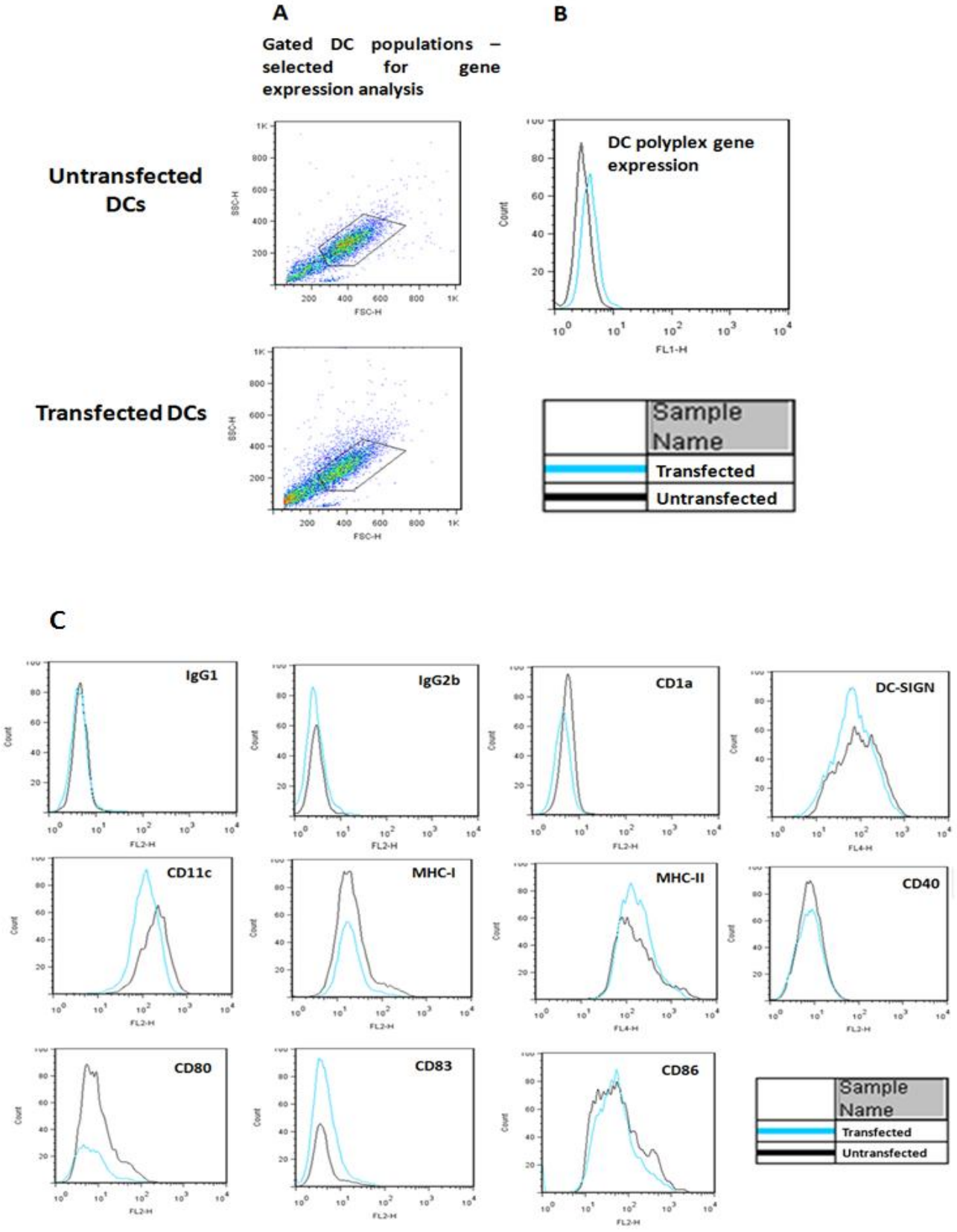

Figure 6.10: **Histogram analysis displaying effect of polyplex gene expression on DC surface marker expression**. DCs were analysed by flow cytometry. Polyplex (containing 20µg DNA) gene expression was measured under the FL-1 filter, while DC surface marker expression was measured under the FL-2 or FL-4 filters. Healthy DCs were gated and selected for analysis (A). DC polyplex gene expression was measured (B) and the effect on surface marker expression was recorded (C).

6.4 Discussion

The current chapter investigated polyplex uptake within dendritic cells (DCs). DCs are important components of the immune system, which function by binding and presenting antigens to T-cells (Ueno *et al*, 2011). DCs express various cell surface markers which contribute towards antigen presentation to T-cells (Landi *et al*, 2007). T-cells are blood cells which recognise antigens presented by DC surface markers and become activated. When activated, T-cells function by releasing small proteins referred to as cytokines which aid in the immune response (Ueno *et al*, 2011). Such cells are unique in that they bridge both arms of immunity; innate and adaptive responses. The innate response refers to the recognition of microbial agents and pathogens via pathogen recognition receptors (PRRs) (Stevenson *et al*, 2010). The adaptive response entails the activation of T cells to trigger antigen specific responses, brought about by the release of specific antibodies (Marieb, 2004).

DCs have important therapeutic applications. One DC based immunotherapy product has gained FDA approval (April 2010) and is available on the market. This refers to the cancer vaccine Sipuleucel-T by the company Dendreon for the treatment of prostate cancer. The vaccine is prepared specifically using patient's own DCs which are then fused with a protein termed; antigen prostatic acid phosphatase (PAP) which is present in approximately over 90% of prostate cancer cells. Patients are treated with the vaccine which is designed to stimulate an immune response towards cancer cells harbouring the antigen.

In this study PLL/DNA complexes were transfected into monocyte-derived human DCs. Polyplex uptake was monitored qualitatively and quantified through confocal image analysis and gene expression studies. Additionally, the effect of polyplex gene expression on DC surface marker expression was studied. This is important in terms of analysing whether

PLL/DNA polyplexes stimulate expression of surface markers involved in antigen presentation, which is a key function of DCs.

6.4.1 DC polyplex uptake

Polyplexes containing different DNA topologies (SC, OC, and linear-pDNA) were transfected into DCs and uptake was monitored qualitatively by confocal microscopy. Polyplex uptake was classified on the basis of intracellular location (periphery, cytosol or nucleus) (Figure 6.1). This was confirmed by identification in both mid section and stack projection images by fluorescent confocal microscopy in order to identify true polyplex uptake. Unlike that of CHO cells (Chapter 5, Figure 5.2), polyplex uptake in DCs was gradual with low nuclear association (Figure 6.2). Regardless of topology, DNA showed co-localisation with PLL (Figure 6.2). By one hour SC-pDNA polyplexes were located in the cytosol (polyplex fluorescence overlaid with cytosol stain) which continued by 48 hours (Figure 6.4). OC- and linear-pDNA polyplexes were observed to be within the cytosol and periphery of the cell respectively. Confocal image quantification studies revealed uptake of complexes was progressive and topology dependent (Figures 6.5 and 6.6). SC-pDNA complexes associated most efficiently and rapidly with the nuclei whereby 15% of complexes associated with the nucleus by 1 hour in comparison to 0% for OC- and linear-pDNA. This may be due to various biophysical factors such as polyplex charge. Moffatt and Cristiano (2006) formulated PEI complexes displaying charges of approximately +45mv and recorded reduced gene expression within DCs. In this study SC- and OC-pDNA complexes displayed zeta potentials of +13.7 and +23mv respectively (Chapter 3, Figure 3.2) and displayed markedly higher percentage nuclear association than linear-pDNA complexes (Table 6.2), which displayed a greater cationic charge of +27mv when formulated at a greater charge ratio (ratio of PLL to DNA) of +5. This suggests increased zeta potentials of strong cationic

Non-viral gene delivery system (plasmids employed 5-9kb)	Size (μm)	Total dose (μg)	Zeta potential (mv)	Nuclear association at 48 hours (%)	Optimal non-viral gene expression in DCs	pDNA topology (% content)	Change in DC phenotype? (Y/N)	References
Lipid/DNA	N/A	5	N/A	N/A	20% GFP expression at 48 hours	SC (N/A)	N	Landi *et al*, (2007)
PLL/SC-pDNA	<0.2	20	+13	30	14% β-galactosidase expression	SC – 100%	N	This study
PLL/OC-pDNA	<0.4	20	+23	16	9% β-galactosidase expression	OC – 100%	N	
PLL/Linear-pDNA	<1.0	20	+27	12	7% β-galactosidase expression at 48 hours	Linear – 100%	N	
Lipid/DNA	N/A	200	N/A	N/A	>1.6% EGFP expression at 24 hours	SC (N/A)	Y	Faham *et al*, (2011)
Lipid /DNA	N/A	4	N/A	N/A	<1% GFP expression at 24 hours	SC (NA)	N	Van Tendeloo *et al*, (1998)
PEI/DNA encapsulated within PLGA particles	0.120	<5	+40	N/A	<0.05% GFP expression at 24 hours	SC (N/A)	N/A	Kanazawa *et al*, (2009)
PEI/DNA encapsulated within PLGA particles	7.82-11.6	10	N/A	N/A	0.005% GFP expression at 48 hours	SC (N/A)	N/A	Jilek *et al*, (2004)
Studies quantifying DC gene expression via luminescence:								
PEI/DNA	<0.3	10	N/A	N/A	<1 x 10^6 RLU/mg protein (luciferase) at 24 hours	SC (N/A)	N	Tang *et al*, (2010)
PEI/DNA/PEG	0.125-0.132	6	+45.8	N/A	<10^4 RLU/mg protein (β-galactosidase) at 28 days	SC (N/A)	N	Moffatt and Cristiano (2006)
Lipid/DNA	0.128	5	+46.7	N/A	< 1ng/mg protein (luciferase) at 24 hours	SC (N/A)	N	Un *et al*, (2010)

Table 6.2: Summary of studies focusing on the parameters affecting non-viral gene delivery into DCs. Previous findings were compared with that of the present study. Where fields are denoted 'N/A' the respective study did not report the value. Nuclear association was quantified via confocal microscopy image analysis. Nuclear association was defined by complete overlap between polyplex fluorescence and nuclear stain.

charges may not necessarily correspond with enhanced DC uptake. The increased cationic charges could lead to non specific binding with protein components culminating in reduced cell uptake (Moffatt and Cristiano, 2006).

DCs are key sentinels of the immune system in which foreign components are recognised and engulfed in a process referred to as phagocytosis (Ishimoto *et al*, 2008). DCs represent the first line of defence of the immune system and so recognition of foreign materials is important. Polyplexes are likely to be engulfed, as they display similar sizes to readily up taken molecules by DCs (Thiele *et al*, 2001; Moffatt and Cristiano, 2006; Jilek *et al*, 2004). Polyplex size is a key parameter that affects uptake and subsequent gene expression. SC-pDNA polyplexes were found to display the smallest mean diameters at <200nm which may facilitate cellular uptake. In contrast OC-pDNA polyplexes were larger at just over 300nm, while linear-pDNA complexes had diameters of approximately 840nm (Chapter 3, Figure 3.14). One study revealed how PEI/DNA complexes with sizes of up to 11µm were engulfed by DCs. However gene expression for these particular complexes was very low which may be due to the large size which may hinder nuclear uptake (Table 6.2) (Jilek *et al*, 2004). These reports along with the findings of the present study indicate smaller complexes favour potential gene expression.

Although DCs are key cells of the immune system their ability to recognise foreign components can lead to unspecific binding. To counter this polyplex cationic charge can be masked and this can be brought about by polyethylene glycol (PEG) which has been found to enhance cellular uptake and gene expression (Ulasov *et al*, 2011). PEG operates by forming a hydrophilic shield around the polycation/DNA complex which masks the cationic charge (Ulasov *et al*, 2011). Further improvements regarding polyplex uptake include the conjugation of DC-specific antibodies which enhance cellular recognition and uptake (Reddy

et al, 2006). One study employed anti-Dec205 antibodies bound to conjugates which significantly increased DC uptake. The antibody bound conjugate was recorded to be <1μm in size which facilitated recognition by DCs (Kwon *et al*, 2005).

6.4.2 DC polyplex gene expression

In this study complexes containing 20μg pDNA were transfected into DCs to induce gene expression. This is important in regards to gene expression within DCs as such cells express nuclear nucleases (Chain, 2003). Although 2μg pDNA was used for confocal image qualitative and quantitative studies, there was no significant difference between uptake profiles of complexes containing 2 and 20μg (data not shown). Non-viral gene expression within DCs is notoriously sensitive. Poor gene transfer has led to reduced gene expression (Landi *et al*, 2007). To date, comparison of PLL/DNA polyplex (containing differing pDNA forms) gene expression within DCs has not been reported. Gene expression (*lacZ* reporter gene encoding β-galactosidase) was highest for SC-pDNA polyplexes at 14% when the charge for all three complexes was similar, (when the charge ratio was +1.6 for SC- and OC-pDNA and +5 for linear-pDNA) (Figure 6.7). This was significantly greater than OC- and linear-pDNA polyplexes. When the charge ratio was equal DC polyplex gene expression still showed dependence on DNA topology (Figure 6.8). The ability of SC-pDNA polyplexes to diffuse through cells more efficiently than the other pDNA forms may contribute towards higher gene expression. As mentioned previously SC-pDNA polyplexes displayed smaller sizes which may facilitate nuclear entry and expression. Importantly this study showed that SC-pDNA polyplexes displayed greater nuclease resistance than other DNA forms which were more susceptible towards nuclease degradation (Chapter 3, Figure 3.11). This is pivotal as DCs have been found to express various nucleases (Chain, 2003). Modest polyplex gene expression has been reported previously and summarised in Table 6.2 in conjunction with the

findings of the current study (Landi *et al*, 2007; Van Tendeloo *et a*l, 1998; Moffatt and Cristiano, 2006). With the exception of Landi *et al*, (2007) and Faham *et al*, (2011), findings from Table 6.2 indicate non-viral gene expression is dependent on DNA dose and complex size. Although Jilek *et al* (2004) employed pDNA doses of up to 10µg gene expression was only 0.005%. This may be due to the size of such complexes which ranged between 7-11.6µm (Table 6.2). Despite polyplexes displaying similar sizes to the present study Kanazawa *et al*, (2009) employed pDNA doses of >5µg and reported <0.05% unlike the present study whereby a dose of 20µg led to up to 14% gene expression. Therefore size and dosage are key parameters. Zeta potentials of SC-pDNA complexes were low in comparison to previous results but displayed greater expression which may be due to a reduction in non-specific binding (Moffatt and Cristiano, 2006) (Table 6.2). As shown in this study DNA topology is a key factor in regards to polyplex DC uptake. Polyplexes containing pDNA in the SC form display smaller sizes, greater nuclease resistance, enhanced nuclear association and greater gene expression than other topologies which is critical for gene delivery to immune cells. Overall DC gene expression was quite low and so techniques to enhance gene expression should be considered (mentioned further in this section).

6.4.3 The effect of polyplex gene expression on DC phenotype

DCs are characteristic through the expression of various cell surface markers. These markers generally contribute towards antigen presentation and changes in expression are a hallmark of DC activation (Stevenson *et al*, 2010). In this study DCs were transfected with DNA polyplexes to observe whether gene expression affects DC phenotype through changes in surface marker expression. Flow cytometry studies (Figures 6.9 and 6.10) revealed no change in DC surface marker expression following uptake of SC-pDNA polyplexes. This may be due to the low DNA dose transfected into DCs, which may not be enough to pass a specific

threshold to elicit phenotypic changes. Table 6.2 summarises how the majority of non-viral gene delivery studies employed doses ranging from 5-20µg pDNA, failed to induce DC phenotypic changes. Plasmid DNA vaccine clinical trials which aim to stimulate immune cells through phenotypic changes employed greater doses. One study administered pDNA doses as high as 1mg/ml, whereas another employed doses of up to 0.5mg (Doukas *et al*, 2011; ClinicalTrials.gov Identifier: NCT00709800; Cebere *et al*, 2006; ClinicalTrials.gov Identifier: NCT00301184). The dose employed in this study (20µg or 0.02mg pDNA) may be insufficient to alter DC phenotype which is in line with previous reports employing similar does, with the exception of Faham *et al*, (2011) who identified DC phenotypic changes following administration of 200µg DNA (Table 6.2). An increased DNA dosage may be required to induce phenotypic changes as DCs predominantly express nucleases (Chain, 2003). Expression of surface markers such as DC-SIGN (dendritic cell-specific intercellular adhesion molecule-3-grabbing non-integrin), which mediates T-cell activation (Curtis *et al*, 1992) did not change with polyplex gene expression (Figure 6.10).

Measuring such parameters is important in regards to clinical applications. Vaccines targeting DCs incorporate adjuvants (enhances recipient's immune response) that are designed to elicit phenotypic changes that activate DCs to induce antigen specific T-cell responses (Tang *et al*, 2010). Therefore the findings from Figures 6.9 and 6.10 reveal how PLL/DNA complexes containing greater DNA dosage (>0.2mg) must incorporate components (adjuvants) to induce DC activation. This is important as DCs predominately express nucleases which are likely to degrade the DNA, thereby preventing DC phenotypic changes. Alternatively by not activating DCs, PLL/DNA polyplexes display biocompatibility allowing safe and effective nucleic acid delivery (Tang *et al*, 2010).

Knowledge of DC surface markers has led researchers to exploit such receptors for targeted delivery. Anderson *et al*, (2010) developed a polyacridine glycopeptide as means of targeted gene delivery. The glycopeptide DNA polyplex consisted of a mannose-glycan that allows recognition by DC-SIGN and led to improved gene expression (Anderson *et al*, 2010).

Although flow cytometry does provide benefits of rapid high throughput analysis, alternative techniques can be used to measure minute changes in DC surface marker expression. Quantitative polymerase chain reaction (Q-PCR) can be used to measure subtle changes in DC surface marker gene expression following transfection. DC activation through changes in DC surface marker gene expression following allergen exposure was recorded by Ryan *et al*, (2004).

6.4.4 Improvement of current protocols to enhance DC polyplex gene expression

In this study DCs were transiently transfected with PLL/DNA polyplexes. However it is important to consider alternative methods to the current protocol which have been shown to enhance DC gene expression. Various groups have attempted techniques to shield the DNA and protect against unspecific binding. One study revealed significantly improved gene expression when immature DCs (iDCs) were used (Landi *et al*, 2007). Monocyte-derived DCs are a common source of DCs which are generated within 5 days. However Landi *et al*, (2007) used iDCs (generated after only 3 days) for transfection studies and revealed improved gene expression of up to 20% (Table 6.2). This was attributed towards higher cell viability allowing gene expression to increase when induced via electroporation (Landi *et al*, 2007).

DCs incorporate mannose cell surface receptors, and uptake of lipid/DNA complexes increased when complexes were mannosylated (Un *et al*, 2010). This increased DC interaction and bypassed non-specific protein binding. The authors reported enhanced gene expression when the DNA dose increased (500µg/200µl). Gene expression corresponding to approximately >1ng/mg protein within DCs was recorded which was not significantly different to commercial gene delivery systems (Un *et al*, 2010). In this study 20µg DNA was used for gene expressions studies which lead to 14% expression for SC-pDNA polyplexes. Therefore an increase in dose could enhance gene expression.

Block copolymer systems consisting of a polycation (for DNA binding) and PEG (steric stabilisation) lead to improved DC uptake and gene expression particularly for long chain polymers. The long polymer chain coupled with an endosomolytic compound (hydroxychloroquine) allowed endosomal escape and reduced clearance (Tang *et al*, 2010). However drawbacks of copolymers include polydispersity and have been found to be quite cytotoxic for primary cell lines.

Overall it is clear that uptake and gene expression of PLL/DNA polyplexes is dependent on DNA topology. Complexes containing SC-pDNA were most efficient in associating with the nucleus as observed by confocal microscopy studies. Complexes containing SC-pDNA displayed significantly higher gene expression than other topological forms, although expression was modest at approximately 14% in comparison to that reported for CHO cells (Chapter 5, section 5.2.2.2). This may be due to DCs predominately expressing nucleases which restrict uptake and gene expression. The modest gene expression and low dose may also explain the inability of complexes to activate DCs through changes in surface marker expression. In terms of bio-processing and vaccine production, the application of SC-pDNA is a key pre-requisite. The findings of this study show how pDNA in the SC conformation is

more efficient in terms of both uptake and gene expression than OC- and linear-pDNA. This is important as very few studies have systematically compared plasmids of different DNA topologies in regards to biophysical characterisation, mammalian cell uptake and potential nuclear import. Therefore DNA topology does impact on processing and vaccine manufacture. This is in agreement with current regulatory bodies such as the FDA which require 80% SC content (Guidance for Industry: Considerations for Plasmid DNA Vaccines for Infectious Disease Indications – FDA, 2007).

6.5 Chapter Summary

- Polyplex uptake in DCs showed dependence on DNA topology.
    - SC-pDNA polyplexes displayed efficient uptake within 60 minutes.
    - SC-pDNA polyplexes associated most with nucleus as shown by confocal microscopy. 15% of SC-pDNA polyplexes associated with the nuclei at 60 minutes.
    - No nuclear association was recorded for OC- and linear-pDNA polyplexes which remained within the cytosol and periphery of cells by 60 minutes.
    - DNA and PLL displayed dual labelling indicating plasmid and polymer remain closely associated.
- DC polyplex gene expression showed dependence on DNA topology, size and dose. Gene expression was highest for SC-pDNA polyplexes at approximately 14%, which was independent of charge ratio (ratio of PLL to DNA).
- OC-pDNA and linear-pDNA polyplex gene expression was not significantly different to each other. Gene expression was not significantly different to naked DNA controls (with the exception of naked linear-pDNA). This may be due to lack of uptake and/or nuclease degradation.
- Transfection of SC-pDNA polyplexes did not alter DC phenotype as shown through flow cytometry analysis. Gene expression did not activate DCs to express key cell surface markers that are involved in antigen presentation. A pDNA dosage of 20µg failed to elicit phenotypic changes unlike previous clinical trials which used in excess of 1mg pDNA (Doukas *et al*, 2011).

Chapter 7.
Role of importin-7 in nuclear import of polyplex molecules by HeLa cells

7. Role of importin-7 in nuclear import of polyplex molecules by HeLa cells

Over the course of this investigation polyplex uptake and gene expression have been extensively studied in CHO cells and DCs. Polyplex uptake was analysed in both CHO cells (Chapter 5) and DCs (Chapter 6). However if DNA polyplexes are to be employed for therapeutic purposes, understanding nuclear uptake is important. The following chapter addressed the mechanism of polyplex nuclear import (defined as the transportation of foreign material into the nucleus) and the factors involved. Very little has been reported on the detailed mechanism of nuclear import of DNA polyplexes. DNA polyplex uptake was analysed in cells deficient in importin-7 (Imp7). Imp7 is a key nucleocytoplasmic transport protein which has been identified to facilitate nuclear import of viral DNA (Zaitseva *et al*, 2009).

To observe whether DNA polyplexes exploit Imp7 and enter the nuclei in a manner similar to viral DNA, complexes were transfected within HeLa cells deficient (knockdown [KD]) in Imp7 and analysed with the appropriate controls. Qualitative and quantitative analysis was carried out. Finally to observe whether DNA polyplexes are taken up in a similar manner to viral DNA, anti-viral innate immune responses was measured and whether Imp7 KD has an effect.

7.1 Qualitative and quantitative analysis of polyplex nuclear import

7.1.1 Confocal microscopy analysis

Polyplex nuclear import was monitored in HeLa cells with a stable Imp7 KD (generated via shRNA [small hairpin RNA] gene silencing) for which two clones were available; clone 2 (Cl2) and clone 4 (Cl4). Control cells containing an shRNA targeting a different mRNA sequence (*Discosoma corallimorpharian* DsRed [DxR]) was used along with cells that were previously Imp7 KD, but were back complemented with an Imp7 cDNA containing two mutations that confer resistance towards gene silencing, thereby restoring Imp7 function (Back Imp7) (Chapter 2, section 2.5.3). Cells were kindly provided by Dr Ari Fassati (Wohl Virion Centre, UCL). Stable KD of cells was via puromycin (1μg/ml) selection (Chapter 2, section 2.5.3). Polyplex uptake was monitored for a period of 1 hour, as uptake and nuclear association has been found to occur quite rapidly. Analysis was carried out by fluorescent confocal microscopy (Figure 7.1). As in previous chapters, mid section images were taken to confirm true polyplex uptake along with projection images of all sections (referred to as z-stack projection images). Polyplex nuclear association (polyplex fluorescence completely overlaid with nuclear stain) did not occur in KD cells. The majority of polyplexes were situated on the outer periphery of the cell or in the cytosol. In contrast nuclear association did occur in the DxR and Back Imp7 controls as in the case of SC-pDNA polyplexes.

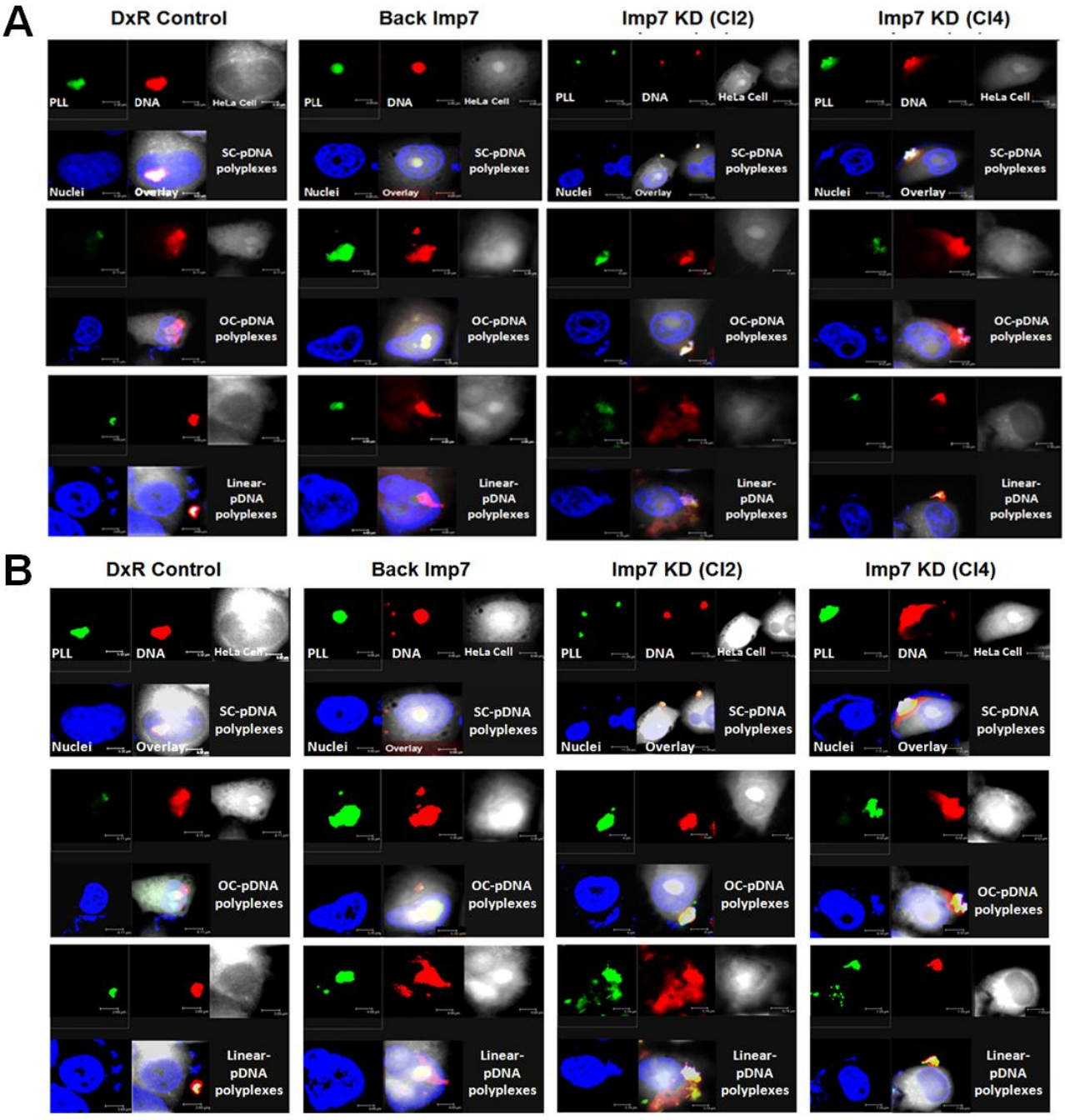

Figure 7.1: **Observation of polyplex uptake in HeLa cells.** Confocal microscopy mid section (A) and stack projection images (B). Figure shows polyplex (containing 2µg DNA) uptake at 1 hour post transfection in HeLa cells whose importin-7 (Imp7) function is knocked down through gene silencing. Two Imp7 KD clones were studied; clone 2 (Cl2) and clone 4 (Cl4). Uptake was also analysed in the appropriate controls; control HeLa cells containing a DxR mRNA target and KD cells whose Imp7 function is restored (Back Imp7).

7.1.2 Quantification of confocal analysis

To quantify the results of Figure 7.1 the number of cell associated polyplexes was counted and classed according to the respective cellular compartment (Figure 7.2). Polyplexes were counted in the DAPI (blue) filter to avoid bias selection of fluorescently labelled complexes (i.e. not selecting complexes in far red or green fluorescent channels). Furthermore sample slides were blinded before analysis. The percentage of nuclear associated polyplexes is significantly reduced in Imp7 KD cells and uptake shows dependence on DNA topology. Polyplexes were often situated and accumulated within the periphery of the cell. However the percentage of nuclear associated polyplexes in control cells (which was greatest for SC-pDNA polyplexes at >20%), where Imp7 function was not hindered, was almost 3 fold greater than KD cells with polyplexes gradually migrating from the periphery through the cytosol, culminating in nuclear access. Details of quantification methodology are provided in Chapter 2, section 2.6.7.3.

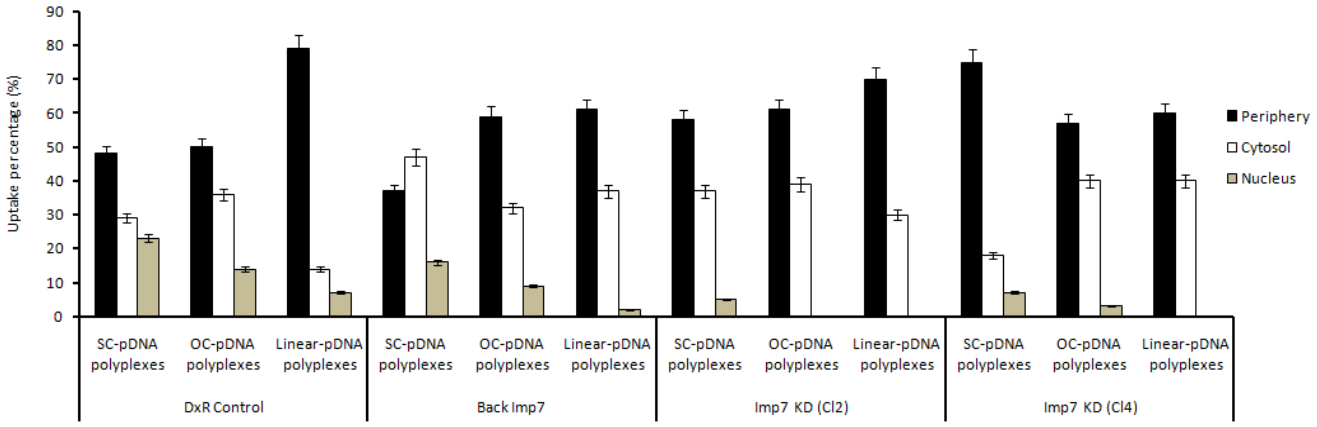

Figure 7.2: **Quantification of polyplex uptake in HeLa cells at 1 hour**. Polyplexes (containing 2µg DNA) were prepared at charge ratios of +1.6 (for SC- and OC-pDNA) and +5 for linear pDNA. The figure shows the mean and standard error (SE) of 3 independent experiments. One-way ANOVA was employed to deduce levels of statistical significance ($p < 0.05$) of the percentage uptake of complexes within each cellular location between those of the control cells and Imp7 KD cells.

7.1.3 The effect of Imp7 KD on polyplex gene expression

Polyplex gene expression was measured in Imp7 KD and control cells according to optimal conditions of preliminary studies (Figure 7.3a). Gene expression is significantly reduced in Imp7 KD cells, whereas those of the controls (DxR and Back Imp7) are more than 2 fold greater (SC and OC forms) (Figure 7.3b). Polyplex gene expression was not significantly different ($p < 0.05$) between the controls and was highest for SC-pDNA polyplexes in a topology dependent manner.

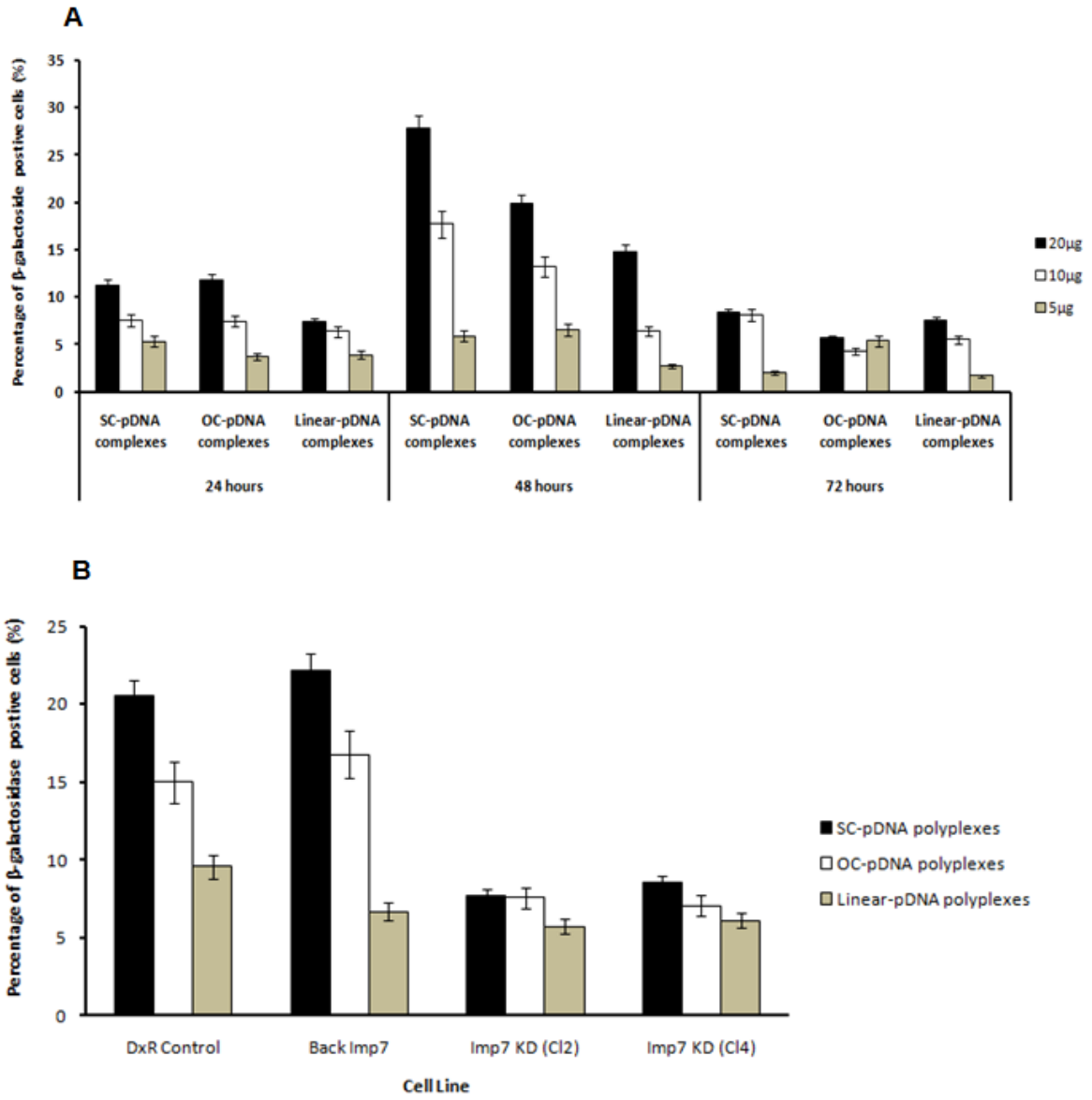

Figure 7.3: **The effect of Imp7 KD on polyplex gene expression.** Time and dose dependent polyplex gene expression within control DxR HeLa cells (A). Polyplex gene expression at optimal conditions (48 hours, 20µg DNA) (B). Polyplexes were prepared at charge ratios of; +1.6 for SC- and OC-pDNA, and +5 for linear-pDNA. The figure shows the mean and SE of 3 independent experiments. One-way ANOVA was employed to deduce levels of statistical significance ($p < 0.05$) of polyplex gene expression between those of the control cells and Imp7 KD cells.

7.2 Live cell confocal microscopy analysis of nuclear uptake

For the first time PLL/DNA polyplex (of differing DNA topologies) uptake was monitored in real time in Imp7 KD cells via live cell confocal microscopy. HeLa cells were seeded (approximately 500,000 cells per well) into chambered glass coverslips and stained for nuclei. Cells were transfected with fluorescently labelled polyplexes (containing 2µg of pDNA) in a chambered confocal microscope (37°C) and immediately imaged. Images were attained as a projection of slices, taken every 2 minutes for 1 hour. A total of 10 slices (each of 0.2µm in thickness) were taken. To accurately deduce whether DNA is truly associated with the nuclei (fluorescence overlay) and gaining nuclear access, individual image slices from the total stack were analysed. Images from the middle of the slice stack (slice number 5 out of 10) were used for image analysis from each time point to deduce if co-localisation of fluorescence, if any, occurs corresponding to DNA nuclear entry. Details of analysis are provided in Chapter 2, section 2.6.7.2.

7.2.1 SC-pDNA polyplex nuclear import

Live cell imaging was used to analyse whether DNA polyplexes utilise Imp7 for nuclear import. The advantage of live cell imaging is that uptake can be monitored in real time *in vivo* and therefore bypasses fixation and probing. In these experiments the polyplex DNA (red) and nuclei (blue) were stained to highlight any possible entry. Uptake of SC-pDNA polyplexes in HeLa DxR control cells (Figure 7.4a) was compared with that of Imp7 KD cells. By 2 minutes, red fluorescence begins to overlay with the blue nuclei. This continues for the remainder of the time course (Figure 7.4a).

In contrast when the experiment was repeated with Imp7 KD cells no fluorescence overlay occurred. Fluorescence corresponding to polyplex DNA was situated on the outside of the nuclei (Figure 7.4b). By residing on the outside of the nucleus, nuclear association seems to be blocked. This is shown in Figure 7.4b by the accumulation of DNA around the nuclei which continues throughout the time course. Imp7 functions by shuttling foreign cargo between the cytosol and nucleus (Fassati *et al*, 2003) and inhibition of this clearly affects polyplex nuclear import.

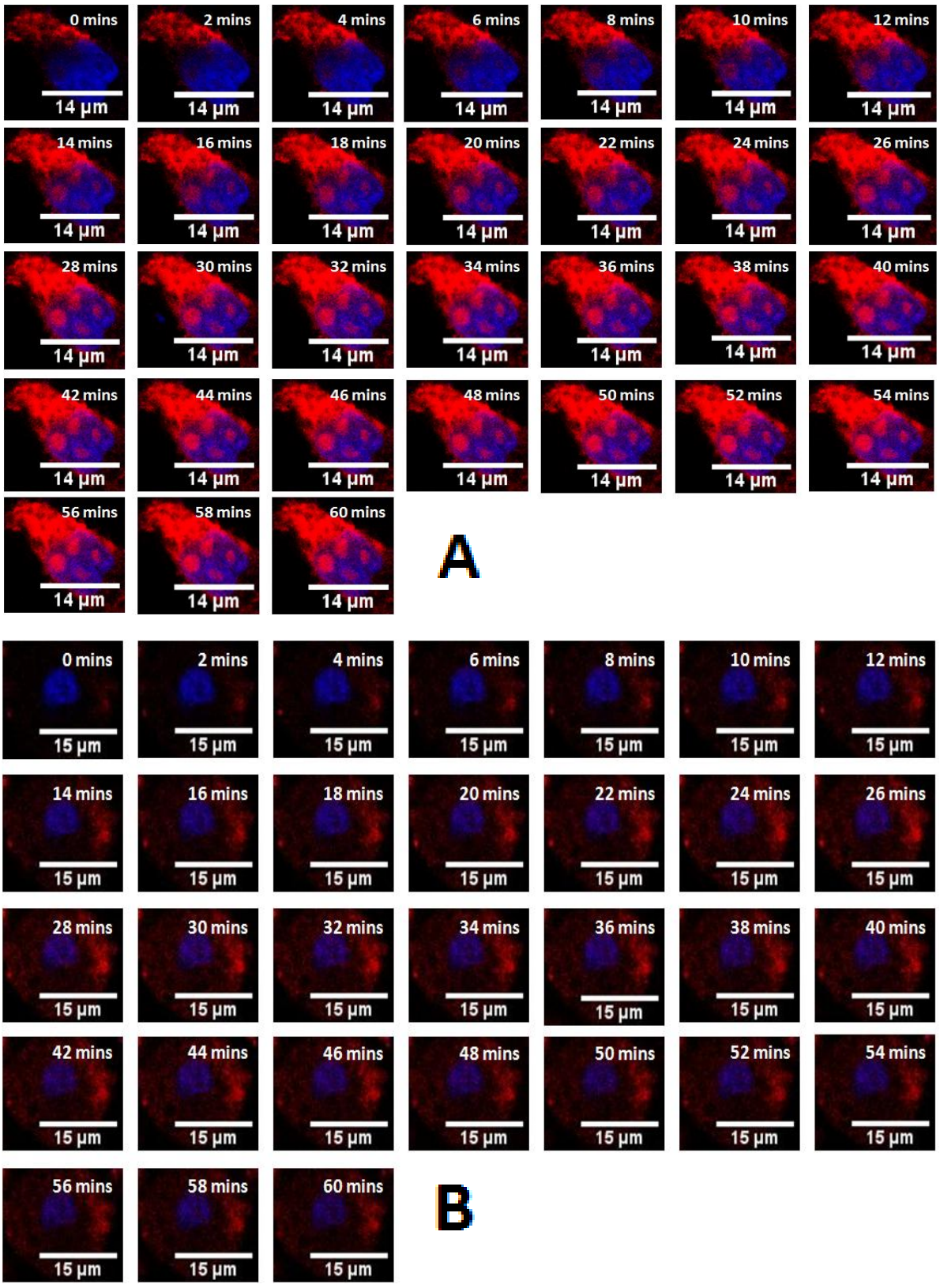

Figure 7.4: **Live cell fluorescent confocal microscopy analysis of SC-pDNA polyplexes in control DxR and Imp7 KD cells.** Images show polyplex (2µg DNA) uptake within control DxR HeLa cells (A) and Imp7 KD cells (Importin-7 function is rendered) (B). Microscope images were collected as a stack of ten image slices. The figure shows the middle slice (slice number 5) spanning a time course of 60 minutes. HeLa cells were stained with Hoechst 34580 and immediately imaged in real time.

7.2.2 OC-pDNA polyplex nuclear import

Polyplexes containing OC-pDNA did show fluorescence overlay with the DxR control cell nuclei by 6 minutes (Figure 7.5a) which continued throughout the time course. DNA fluorescence was also detected in Imp7 KD cells which could be due to residual DNA, although this was much lower than that of the control (Figure 7.5b).

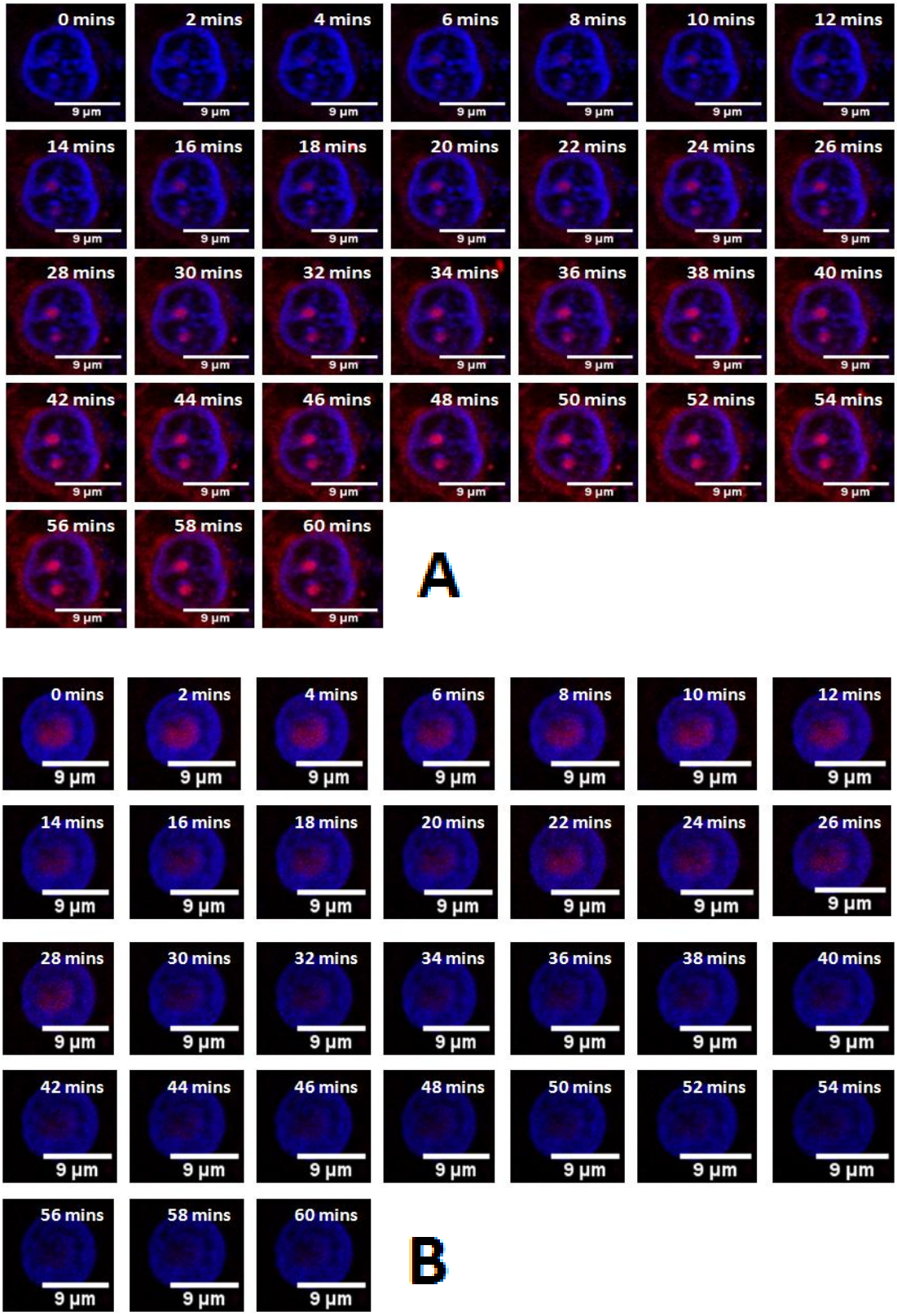

Figure 7.5: **Live cell fluorescent confocal microscopy analysis of OC-pDNA polyplexes in control DxR and Imp7 KD cells.** Images show polyplex (2µg DNA) uptake within control DxR HeLa cells (A) and Imp7 KD cells (Importin-7 function is rendered) (B). Microscope images were collected as a stack of ten image slices. The figure shows the middle slice (slice number 5) spanning a time course of 60 minutes. HeLa cells were stained with Hoechst 34580 and immediately imaged in real time.

7.2.3 Linear-pDNA polyplex nuclear import

Linear-pDNA polyplexes showed fluorescence overlay with the DxR cell nuclei (Figure 7.6a) in contrast to that of the Imp7 KD cell (Figure 7.6b). This could indicate potential use of Imp7 for nuclear access.

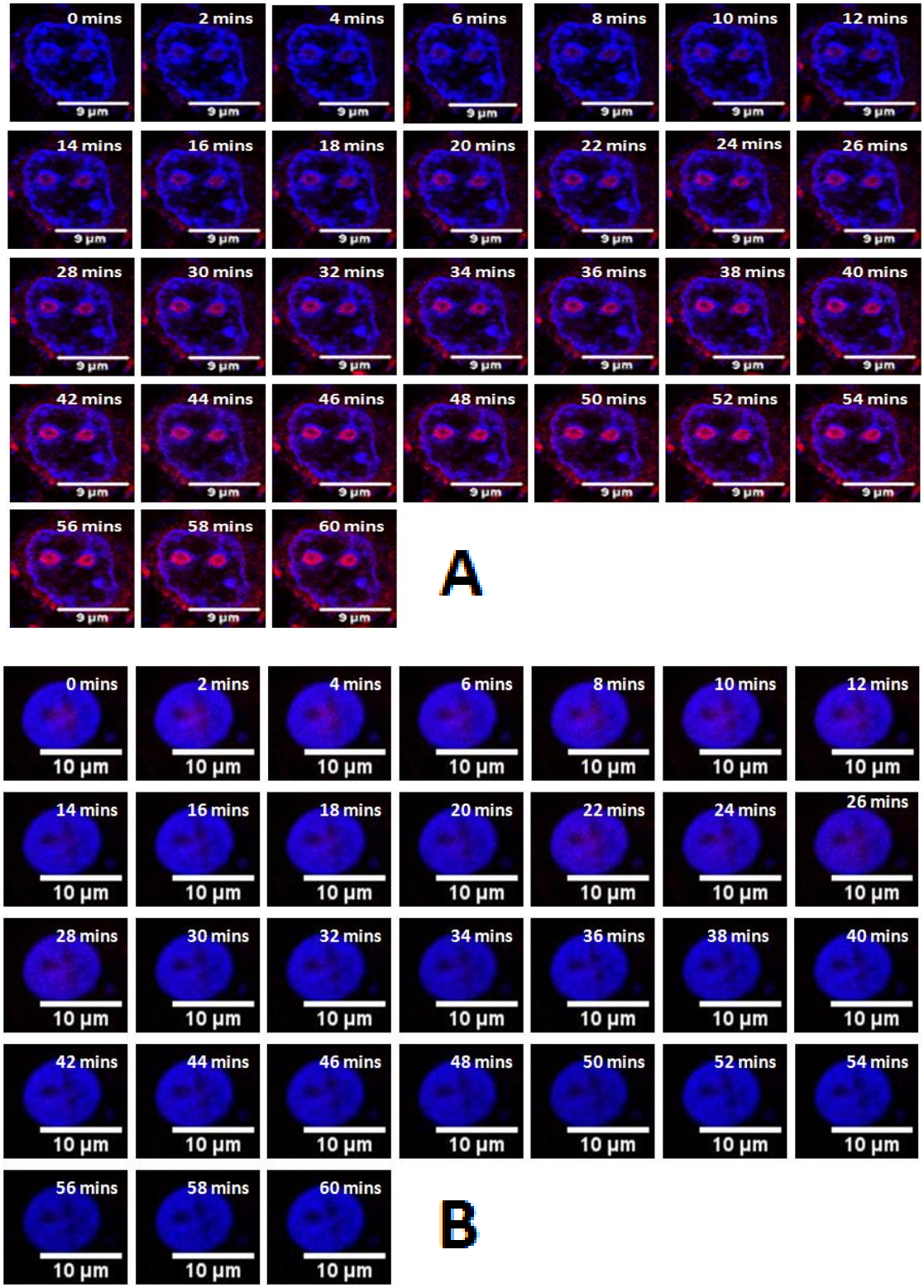

Figure 7.6: **Live cell fluorescent confocal microscopy analysis of linear-pDNA polyplexes in control DxR and Imp7 KD cells.** Images show polyplex (2µg DNA) uptake within control DxR HeLa cells (A) and Imp7 KD cells (Importin-7 function is rendered) (B). Microscope images were collected as a stack of ten image slices. The figure shows the middle slice (slice number 5) spanning a time course of 60 minutes. HeLa cells were stained with Hoechst 34580 and immediately imaged in real time.

7.2.4 Naked DNA controls

To show uptake of DNA was due to association with PLL, fluorescently labelled naked pDNA was transfected into the DxR control cell line.

7.2.4.1 Naked SC-pDNA

SC- (2µg naked DNA) was transfected into DxR control cell line. Throughout the time course of up to 1 hour, no fluorescence is observed. This could be due to DNA degradation by nucleases and also the nucleic acid requiring PLL to enter cells (Figure 7.7)

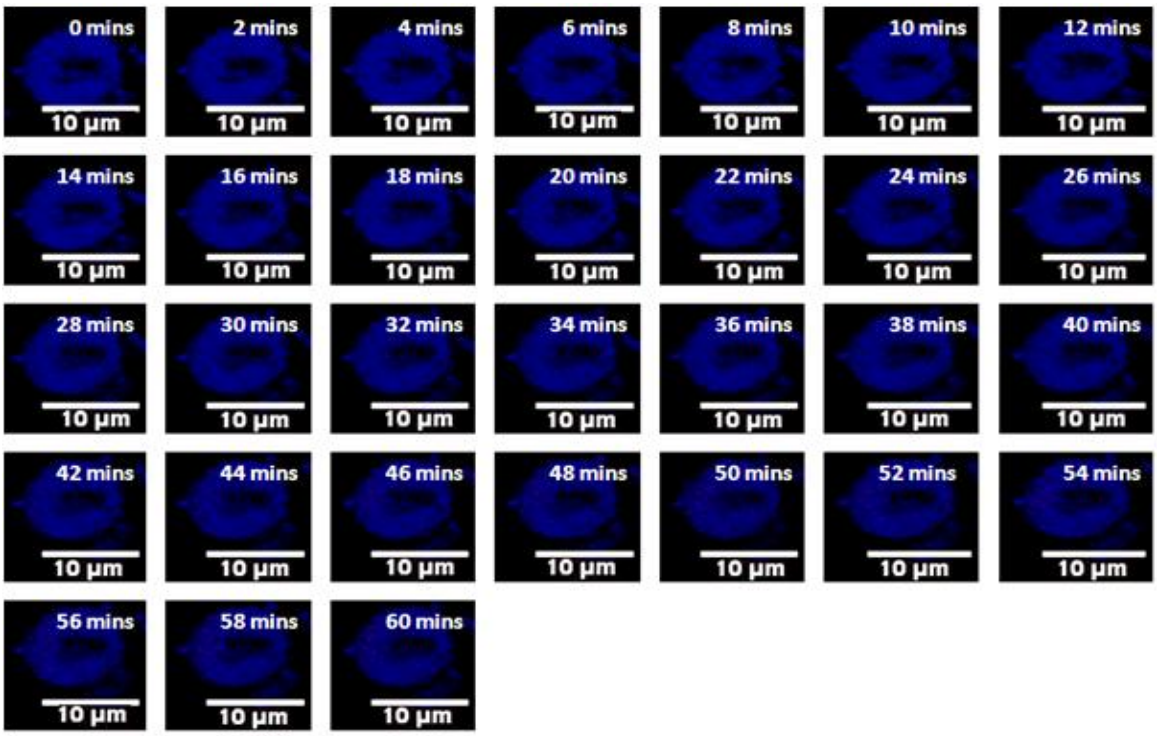

Figure 7.7: **Live cell fluorescent confocal microscopy analysis of naked SC-pDNA (2*µ*g).** Images show uptake within control DxR HeLa cells. Microscope images were collected as a stack of ten image slices. The figure shows the middle slice (slice number 5) spanning a time course of 60 minutes.

7.2.4.2 Naked OC-pDNA

Naked OC-pDNA was transfected in the DxR control cell line and like Figure 7.7 no fluorescence corresponding to DNA is observed (Figure 7.8). Again this could be due to nucleic acids requiring PLL to enter cells.

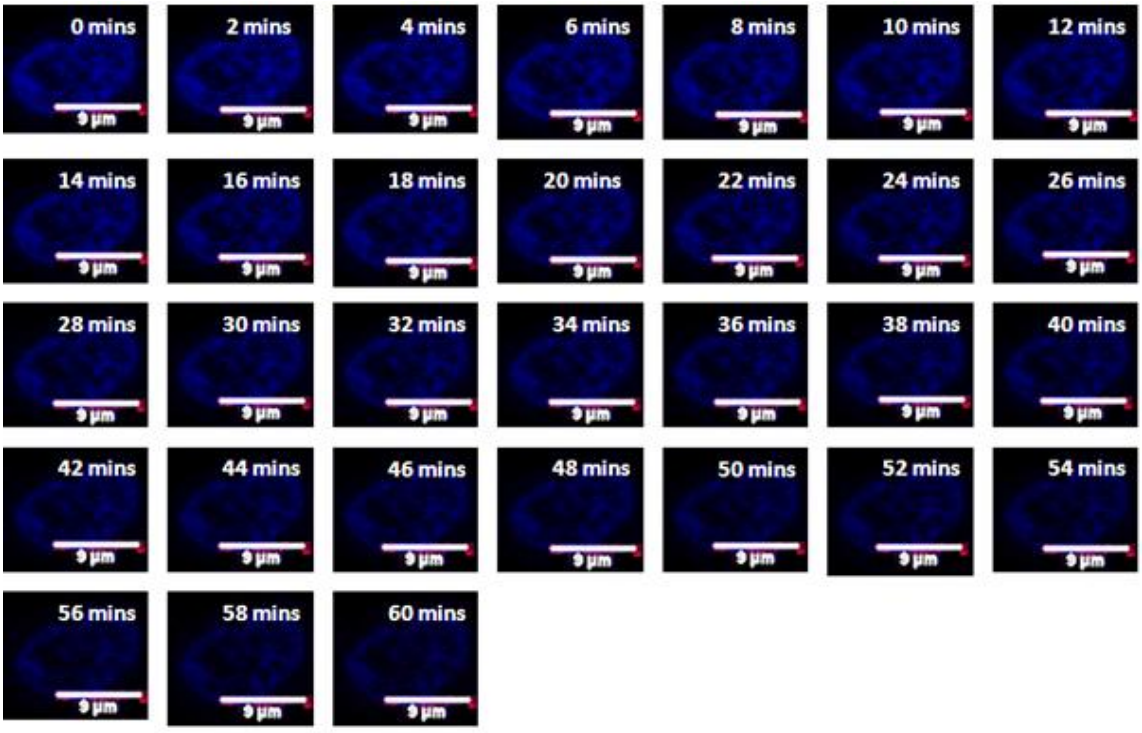

Figure 7.8: **Live cell fluorescent confocal microscopy analysis of naked OC-pDNA (2*µ*g).** Images show uptake within control DxR HeLa cells. Microscope images were collected as a stack of ten image slices. The figure shows the middle slice (slice number 5) spanning a time course of 60 minutes.

7.2.4.3 Naked linear-pDNA

Naked linear-pDNA was transfected into the DxR control cell line and no DNA fluorescence is observed within the nuclei or outside of it (Figure 7.9). This could be due to the pDNA requiring PLL to enter cells. Alternatively DNA may have entered cells but could be readily degraded by host cell nucleases due to lack of protection that is offered by PLL (due to DNA condensation).

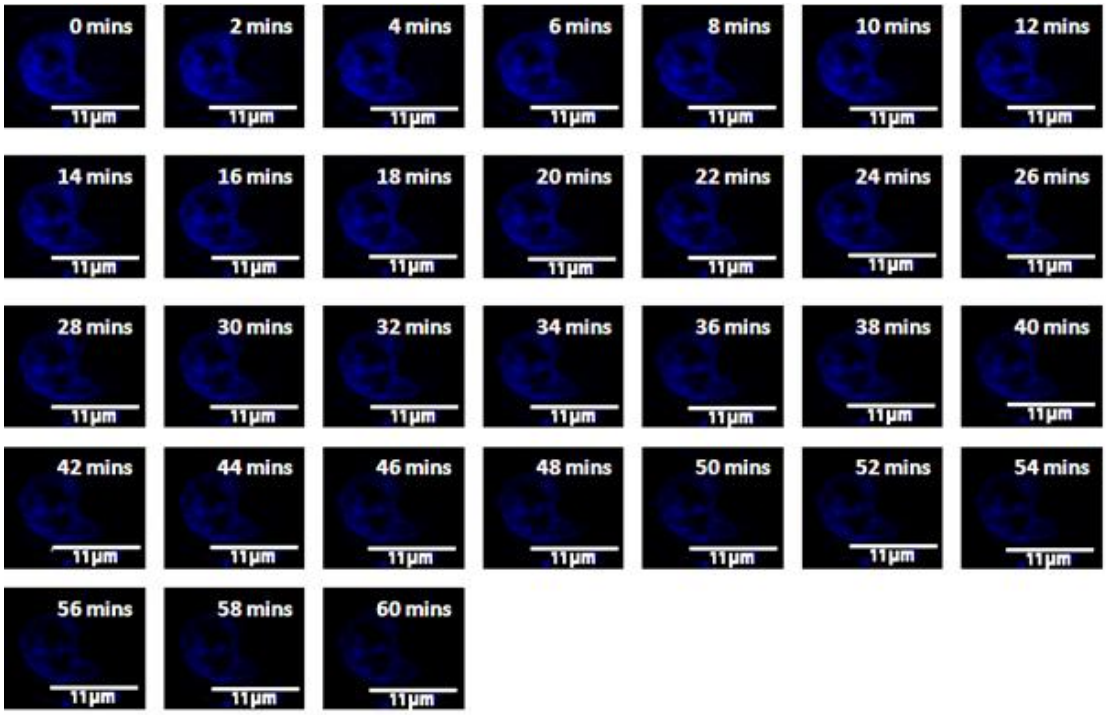

Figure 7.9: **Live cell fluorescent confocal microscopy analysis of naked linear-pDNA (2*µ*g).** Images show uptake within control DxR HeLa cells. Microscope images were collected as a stack of ten image slices. The figure shows the middle slice (slice number 5) spanning a time course of 60 minutes.

Therefore the data provided by the live cell imaging studies highlight how:

- DNA polyplex fluorescent (regardless of DNA topology) co-localisation with host cell nuclei was reduced in Imp7 KD cells.
- Although DNA fluorescent co-localisation with the nuclei occurred in Imp7 KD cells, this was much more pronounced in control cells suggesting a possible role of Imp7 regarding nuclear import. However alternative import mechanism may be utilised.
- Imp7 KD inhibits nuclear import, as shown by the accumulation of DNA fluorescence surrounding the nuclei (Figure 7.4b). This is a key function of Imp7 (Fassati *et al*, 2003).

7.3 DNA polyplexes trigger anti-viral innate immune responses

Imp7 has been found to facilitate viral DNA nuclear import (Zaitseva *et al*, 2009). To observe whether DNA polyplexes are taken up in a similar manner to viral DNA, anti-viral innate immune responses was measured and whether Imp7 KD has an effect. Polyplexes were transfected into HeLa cells for 4 hours (time required to stimulate innate response) and interferon-β (IFN-β) activity was measured. IFN-β is a cytokine protein synthesized by host cells and secreted in response to viral or pathogen infection. They are important in terms of facilitating immune responses to protect against pathogens (Li *et al*, 2010). IFN-β stimulates the production of various proteins in response to viral infection, such as interferon-induced protein with tetratricopeptide repeats-2 (IFIT2). To deduce whether uptake of DNA polyplexes triggers an innate immune response similar to that of viruses, IFIT2 gene expression was measured via quantitative polymerase chain reaction (Q-PCR) (Chapter 2, section 2.7).

7.3.1 Q-PCR analysis of IFIT2 gene expression

Q-PCR was used to measure IFIT2 gene expression following uptake of DNA polyplexes in Imp7 KD and control cells (Figure 7.10). Q-PCR is based on the fluorescent detection of the target nucleic acid sample. The figure displays Ct (cycle threshold) values for each component. The Ct value refers to the number of cycles required for the fluorescent signal to cross the threshold (beyond background fluorescence). Ct values are inversely proportional to the amount of target DNA sample present, hence high Ct values equate to low gene expression. Figure 7.10 shows the Ct values of triplicate data. The highest Ct value regardless of Imp7 KD was that of untransfected cells (lowest IFIT2 gene expression) (Figure 7.10a). IFIT2 gene upregulation was greatest in cells transfected with SC-pDNA polyplexes.

However no significant difference in expression was observed between polyplexes of differing DNA topologies ($p < 0.05$).

To confirm the results of Figure 7.10a, the Ct values were normalized with those of a housekeeping gene (whose expression remains constant) GAPDH (glyceraldehyde 3-phosphate dehydrogenase) to yield delta Ct (dCt) values (Figure 7.10b). Like the Ct component, dCt values are inversely proportional to IFIT2 gene expression (low dCt values correspond to high gene expression). Uptake of DNA polyplexes causes upregulation of IFIT2 gene expression, which was greater than untransfected cells.

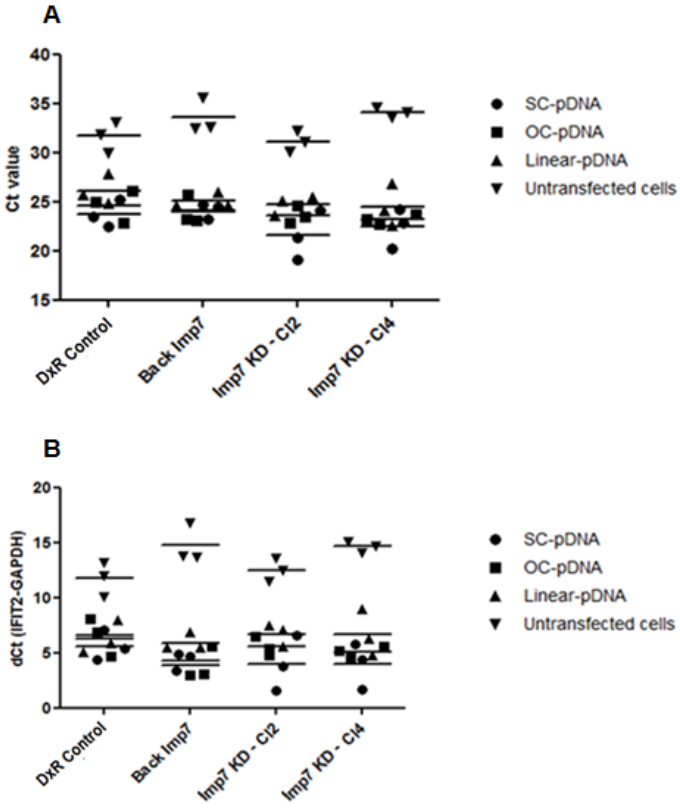

Figure 7.10: **DNA polyplexes stimulated upregulation of IFIT2 gene expression**. Gene expression profiles before (A) and after (B) normalization with GAPDH housekeeping gene. Polyplexes were prepared at charge ratios of; +1.6 for SC- and OC-pDNA, and +5 for linear-pDNA. Error bars represent the SE of triplicate readings. QPCR experiments were performed twice independently. Bonferroni's Multiple Comparison's Test was used to deduce levels of statistical significance ($p < 0.05$) of IFIT2 gene expression between control cells and Imp7 KD cells transfected with polyplexes of differing DNA topologies.

7.3.2 IFIT2 gene upregulation showed dependence on polyplex DNA topology

Figure 7.10 shows uptake of PLL/DNA polyplexes induces IFIT2 gene expression. However these polyplexes were transfected at a high DNA dose (20µg pDNA) which may mask subtle changes in IFIT2 expression between differing DNA topologies. Polyplexes were transfected at a lower dose of 0.2µg pDNA (Figure 7.11). IFIT2 gene expression (normalised against GAPDH) was highest for cells transfected with SC- and OC-pDNA polyplexes, which were not significantly different to each other, but were significantly different to cells transfected with linear-pDNA polyplexes ($p < 0.05$). More specifically IFIT2 upregulation was not significantly different between Imp7 KD Cl2 and Cl4 cells transfected with SC-pDNA ($p < 0.05$). IFIT2 gene expression was highest in Imp7 KD cells transfected with SC-pDNA which may be due to the accumulation of polyplex DNA in the cytosol triggering cytosolic DNA sensing agents. IFIT2 gene expression was slightly lower for cells transfected with linear-pDNA polyplexes. Untransfected cells displayed significantly higher dCt values corresponding to low gene expression, hence no anti-viral response. To deduce whether IFIT2 gene expression was due to DNA and not the transfection process, uncomplexed PLL (at amounts corresponding to a charge ratio of +1.6 and +5) were 'mock transfected' within cells and gene expression was measured. The dCt values for these samples were quite high indicating that only transfected DNA caused an innate response through IFN-β induced IFIT2 synthesis (Figure 7.11). Therefore innate immune response in the form of IFIT2 increased in cells transfected with SC-pDNA polyplexes (topology dependent), particularly Imp7 KD cells. This could be due to the efficiency of SC-pDNA polyplexes gaining cellular access unlike its topological counterparts and activating cytosolic DNA receptors that can trigger innate immune responses due to nuclear access being blocked (Hornung and Latz, 2010).

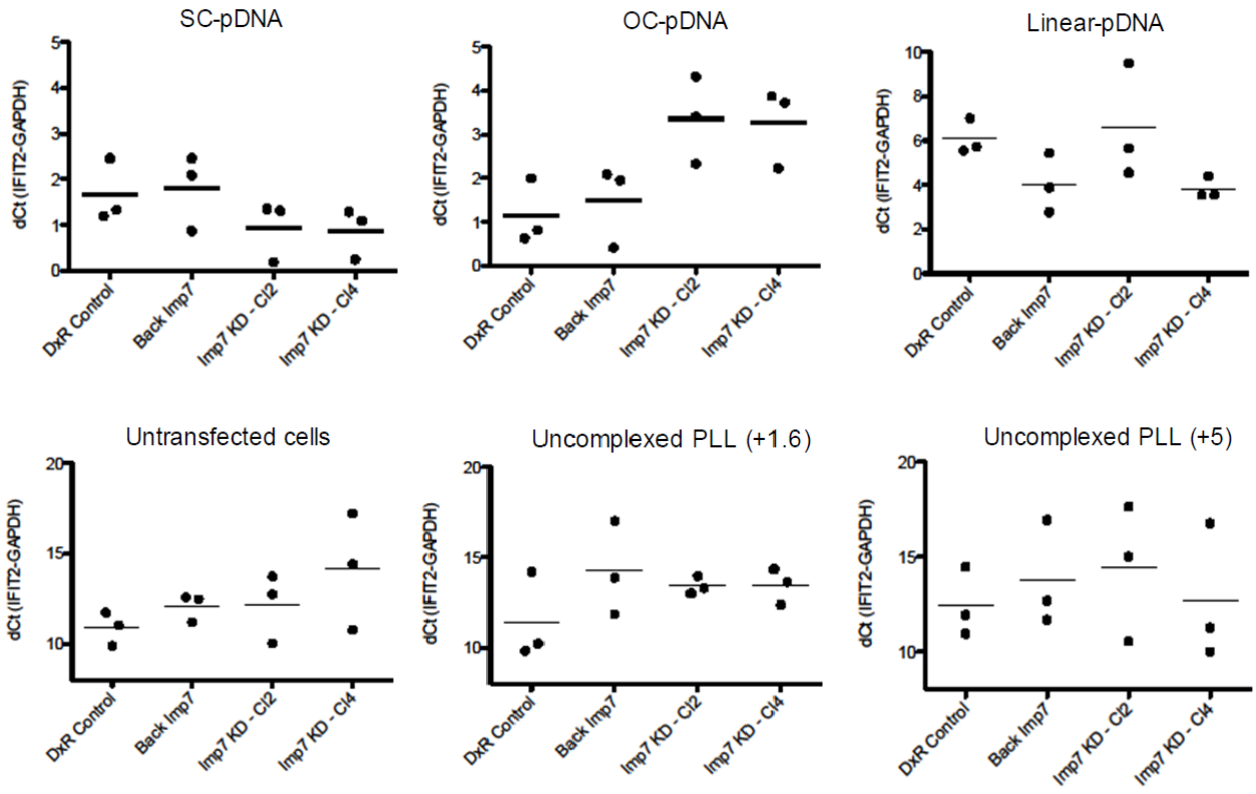

Figure 7.11: **IFIT2 gene upregulation showed dependence on DNA topology.** DNA polyplexes (containing 0.2µg pDNA) were transfected into HeLa cells. Uncomplexed PLL was 'mock transfected' at amounts corresponding to charge ratios of +1.6 and +5. Polyplexes were prepared at charge ratios of; +1.6 for SC- and OC-pDNA, and +5 for linear-pDNA. Error bars represent the SE of triplicate readings. QPCR experiments were performed twice independently. Bonferroni's Multiple Comparison's Test was used to deduce levels of statistical significance ($p < 0.05$) of IFIT2 gene expression between control cells and Imp7 KD cells transfected with polyplexes of differing DNA topologies.

Details of the significant difference provided by the Bonferroni's Multiple Comparison's Test to deduce levels of statistical significance ($p < 0.05$) of IFIT2 gene expression between control cells and Imp7 KD cells transfected with polyplexes of differing DNA topologies, are provided in Table 7.1

A

Bonferroni's Multiple Comparison Test	Significant? P < 0.05?	Summary
SC-pDNA DxR Control vs SC-pDNA Back Imp7	No	ns
SC-pDNA DxR Control vs SC-pDNA Imp7 - Cl2	Yes	****
SC-pDNA DxR Control vs SC-pDNA Imp7 - Cl4	Yes	****
SC-pDNA DxR Control vs OC-pDNA DxR Control	Yes	****
SC-pDNA DxR Control vs OC-pDNA Back Imp7	Yes	*
SC-pDNA DxR Control vs OC-pDNA Imp7 - Cl2	Yes	****
SC-pDNA DxR Control vs OC-pDNA Imp7 - Cl4	Yes	****
SC-pDNA DxR Control vs Linear-pDNA DxR Control	Yes	****
SC-pDNA DxR Control vs Linear-pDNA Back Imp7	Yes	****
SC-pDNA DxR Control vs Linear-pDNA Imp7 - Cl2	Yes	****
SC-pDNA DxR Control vs Linear-pDNA Imp7 - Cl4	Yes	****
SC-pDNA DxR Control vs Untransfected DxR Control	Yes	****
SC-pDNA DxR Control vs Untransfected Back Imp7	Yes	****
SC-pDNA DxR Control vs Untransfected Imp7 - Cl2	Yes	****
SC-pDNA DxR Control vs Untransfected Imp7 - Cl4	Yes	****
SC-pDNA DxR Control vs PLL +1.6 - DxR Control	Yes	****
SC-pDNA DxR Control vs PLL +1.6 - Back Imp7	Yes	****
SC-pDNA DxR Control vs PLL +1.6 - Imp7 KD Cl2	Yes	****
SC-pDNA DxR Control vs PLL +1.6 - Imp7 KD Cl4	Yes	****
SC-pDNA DxR Control vs PLL +5 - DxR Control	Yes	****
SC-pDNA DxR Control vs PLL +5 - Back Imp7	Yes	****
SC-pDNA DxR Control vs PLL +5- Imp7 KD Cl2	Yes	****
SC-pDNA DxR Control vs PLL +5 - Imp7 KD Cl4	Yes	****
SC-pDNA Back Imp7 vs SC-pDNA Imp7 - Cl2	Yes	****

B

SC-pDNA Back Imp7 vs SC-pDNA Imp7 - Cl4	Yes	****
SC-pDNA Back Imp7 vs OC-pDNA DxR Control	Yes	****
SC-pDNA Back Imp7 vs OC-pDNA Back Imp7	Yes	***
SC-pDNA Back Imp7 vs OC-pDNA Imp7 - Cl2	Yes	****
SC-pDNA Back Imp7 vs OC-pDNA Imp7 - Cl4	Yes	****
SC-pDNA Back Imp7 vs Linear-pDNA DxR Control	Yes	****
SC-pDNA Back Imp7 vs Linear-pDNA Back Imp7	Yes	****
SC-pDNA Back Imp7 vs Linear-pDNA Imp7 - Cl2	Yes	****
SC-pDNA Back Imp7 vs Linear-pDNA Imp7 - Cl4	Yes	****
SC-pDNA Back Imp7 vs Untransfected DxR Control	Yes	****
SC-pDNA Back Imp7 vs Untransfected Back Imp7	Yes	****
SC-pDNA Back Imp7 vs Untransfected Imp7 - Cl2	Yes	****
SC-pDNA Back Imp7 vs Untransfected Imp7 - Cl4	Yes	****
SC-pDNA Back Imp7 vs PLL +1.6 - DxR Control	Yes	****
SC-pDNA Back Imp7 vs PLL +1.6 - Back Imp7	Yes	****
SC-pDNA Back Imp7 vs PLL +1.6 - Imp7 KD Cl2	Yes	****
SC-pDNA Back Imp7 vs PLL +1.6 - Imp7 KD Cl4	Yes	****
SC-pDNA Back Imp7 vs PLL +5 - DxR Control	Yes	****
SC-pDNA Back Imp7 vs PLL +5- Imp7 KD Cl2	Yes	****
SC-pDNA Back Imp7 vs PLL +5 - Imp7 KD Cl4	Yes	****
SC-pDNA Imp7 - Cl2 vs SC-pDNA Imp7 - Cl4	No	ns
SC-pDNA Imp7 - Cl2 vs OC-pDNA DxR Control	No	ns
SC-pDNA Imp7 - Cl2 vs OC-pDNA Back Imp7	Yes	****
SC-pDNA Imp7 - Cl2 vs OC-pDNA Imp7 - Cl2	Yes	****

C

SC-pDNA Imp7 - Cl2 vs OC-pDNA Imp7 - Cl4	Yes	****
SC-pDNA Imp7 - Cl2 vs Linear-pDNA DxR Control	Yes	****
SC-pDNA Imp7 - Cl2 vs Linear-pDNA Back Imp7	Yes	****
SC-pDNA Imp7 - Cl2 vs Linear-pDNA Imp7 - Cl2	Yes	****
SC-pDNA Imp7 - Cl2 vs Linear-pDNA Imp7 - Cl4	Yes	****
SC-pDNA Imp7 - Cl2 vs Untransfected DxR Control	Yes	****
SC-pDNA Imp7 - Cl2 vs Untransfected Back Imp7	Yes	****
SC-pDNA Imp7 - Cl2 vs Untransfected Imp7 - Cl2	Yes	****
SC-pDNA Imp7 - Cl2 vs Untransfected Imp7 - Cl4	Yes	****
SC-pDNA Imp7 - Cl2 vs PLL +1.6 - DxR Control	Yes	****
SC-pDNA Imp7 - Cl2 vs PLL +1.6 - Back Imp7	Yes	****
SC-pDNA Imp7 - Cl2 vs PLL +1.6 - Imp7 KD Cl2	Yes	****
SC-pDNA Imp7 - Cl2 vs PLL +1.6 - Imp7 KD Cl4	Yes	****
SC-pDNA Imp7 - Cl2 vs PLL +5 - DxR Control	Yes	****
SC-pDNA Imp7 - Cl2 vs PLL +5 - Back Imp7	Yes	****
SC-pDNA Imp7 - Cl2 vs PLL +5- Imp7 KD Cl2	Yes	****
SC-pDNA Imp7 - Cl2 vs PLL +5 - Imp7 KD Cl4	Yes	****
SC-pDNA Imp7 - Cl4 vs OC-pDNA DxR Control	Yes	**
SC-pDNA Imp7 - Cl4 vs OC-pDNA Back Imp7	Yes	****
SC-pDNA Imp7 - Cl4 vs OC-pDNA Imp7 - Cl2	Yes	****
SC-pDNA Imp7 - Cl4 vs OC-pDNA Imp7 - Cl4	Yes	****
SC-pDNA Imp7 - Cl4 vs Linear-pDNA DxR Control	Yes	****
SC-pDNA Imp7 - Cl4 vs Linear-pDNA Back Imp7	Yes	****
SC-pDNA Imp7 - Cl4 vs Linear-pDNA Imp7 - Cl2	Yes	****
SC-pDNA Imp7 - Cl4 vs Linear-pDNA Imp7 - Cl4	Yes	****

D

SC-pDNA Imp7 - Cl4 vs Untransfected DxR Control	Yes	****
SC-pDNA Imp7 - Cl4 vs Untransfected Back Imp7	Yes	****
SC-pDNA Imp7 - Cl4 vs Untransfected Imp7 - Cl2	Yes	****
SC-pDNA Imp7 - Cl4 vs Untransfected Imp7 - Cl4	Yes	****
SC-pDNA Imp7 - Cl4 vs PLL +1.6 - DxR Control	Yes	****
SC-pDNA Imp7 - Cl4 vs PLL +1.6 - Back Imp7	Yes	****
SC-pDNA Imp7 - Cl4 vs PLL +1.6 - Imp7 KD Cl2	Yes	****
SC-pDNA Imp7 - Cl4 vs PLL +1.6 - Imp7 KD Cl4	Yes	****
SC-pDNA Imp7 - Cl4 vs PLL +5 - DxR Control	Yes	****
SC-pDNA Imp7 - Cl4 vs PLL +5 - Back Imp7	Yes	****
SC-pDNA Imp7 - Cl4 vs PLL +5- Imp7 KD Cl2	Yes	****
SC-pDNA Imp7 - Cl4 vs PLL +5 - Imp7 KD Cl4	Yes	****
OC-pDNA DxR Control vs OC-pDNA Back Imp7	Yes	***
OC-pDNA DxR Control vs OC-pDNA Imp7 - Cl2	Yes	****
OC-pDNA DxR Control vs OC-pDNA Imp7 - Cl4	Yes	****
OC-pDNA DxR Control vs Linear-pDNA DxR Control	Yes	****
OC-pDNA DxR Control vs Linear-pDNA Back Imp7	Yes	****
OC-pDNA DxR Control vs Linear-pDNA Imp7 - Cl2	Yes	****
OC-pDNA DxR Control vs Linear-pDNA Imp7 - Cl4	Yes	****
OC-pDNA DxR Control vs Untransfected DxR Control	Yes	****
OC-pDNA DxR Control vs Untransfected Back Imp7	Yes	****
OC-pDNA DxR Control vs Untransfected Imp7 - Cl2	Yes	****
OC-pDNA DxR Control vs Untransfected Imp7 - Cl4	Yes	****
OC-pDNA DxR Control vs PLL +1.6 - DxR Control	Yes	****
OC-pDNA DxR Control vs PLL +1.6 - Back Imp7	Yes	****

E

OC-pDNA DxR Control vs PLL +1.6 - Imp7 KD Cl2	Yes	****
OC-pDNA DxR Control vs PLL +1.6 - Imp7 KD Cl4	Yes	****
OC-pDNA DxR Control vs PLL +5 - DxR Control	Yes	****
OC-pDNA DxR Control vs PLL +5 - Back Imp7	Yes	****
OC-pDNA DxR Control vs PLL +5- Imp7 KD Cl2	Yes	****
OC-pDNA DxR Control vs PLL +5 - Imp7 KD Cl4	Yes	****
OC-pDNA Back Imp7 vs OC-pDNA Imp7 - Cl2	Yes	****
OC-pDNA Back Imp7 vs OC-pDNA Imp7 - Cl4	Yes	****
OC-pDNA Back Imp7 vs Linear-pDNA DxR Control	Yes	****
OC-pDNA Back Imp7 vs Linear-pDNA Back Imp7	Yes	****
OC-pDNA Back Imp7 vs Linear-pDNA Imp7 - Cl2	Yes	****
OC-pDNA Back Imp7 vs Linear-pDNA Imp7 - Cl4	Yes	****
OC-pDNA Back Imp7 vs Untransfected DxR Control	Yes	****
OC-pDNA Back Imp7 vs Untransfected Back Imp7	Yes	****
OC-pDNA Back Imp7 vs Untransfected Imp7 - Cl2	Yes	****
OC-pDNA Back Imp7 vs Untransfected Imp7 - Cl4	Yes	****
OC-pDNA Back Imp7 vs PLL +1.6 - DxR Control	Yes	****
OC-pDNA Back Imp7 vs PLL +1.6 - Back Imp7	Yes	****
OC-pDNA Back Imp7 vs PLL +1.6 - Imp7 KD Cl2	Yes	****
OC-pDNA Back Imp7 vs PLL +1.6 - Imp7 KD Cl4	Yes	****
OC-pDNA Back Imp7 vs PLL +5 - DxR Control	Yes	****
OC-pDNA Back Imp7 vs PLL +5 - Back Imp7	Yes	****
OC-pDNA Back Imp7 vs PLL +5- Imp7 KD Cl2	Yes	****
OC-pDNA Back Imp7 vs PLL +5 - Imp7 KD Cl4	Yes	****
OC-pDNA Imp7 - Cl2 vs OC-pDNA Imp7 - Cl4	No	ns

F

OC-pDNA Imp7 - Cl2 vs Linear-pDNA DxR Control	Yes	****
OC-pDNA Imp7 - Cl2 vs Linear-pDNA Back Imp7	Yes	****
OC-pDNA Imp7 - Cl2 vs Linear-pDNA Imp7 - Cl2	Yes	****
OC-pDNA Imp7 - Cl2 vs Linear-pDNA Imp7 - Cl4	Yes	****
OC-pDNA Imp7 - Cl2 vs Untransfected DxR Control	Yes	****
OC-pDNA Imp7 - Cl2 vs Untransfected Back Imp7	Yes	****
OC-pDNA Imp7 - Cl2 vs Untransfected Imp7 - Cl2	Yes	****
OC-pDNA Imp7 - Cl2 vs Untransfected Imp7 - Cl4	Yes	****
OC-pDNA Imp7 - Cl2 vs PLL +1.6 - DxR Control	Yes	****
OC-pDNA Imp7 - Cl2 vs PLL +1.6 - Back Imp7	Yes	****
OC-pDNA Imp7 - Cl2 vs PLL +1.6 - Imp7 KD Cl2	Yes	****
OC-pDNA Imp7 - Cl2 vs PLL +1.6 - Imp7 KD Cl4	Yes	****
OC-pDNA Imp7 - Cl2 vs PLL +5 - DxR Control	Yes	****
OC-pDNA Imp7 - Cl2 vs PLL +5 - Back Imp7	Yes	****
OC-pDNA Imp7 - Cl2 vs PLL +5- Imp7 KD Cl2	Yes	****
OC-pDNA Imp7 - Cl2 vs PLL +5 - Imp7 KD Cl4	Yes	****
OC-pDNA Imp7 - Cl4 vs Linear-pDNA DxR Control	Yes	****
OC-pDNA Imp7 - Cl4 vs Linear-pDNA Back Imp7	Yes	****
OC-pDNA Imp7 - Cl4 vs Linear-pDNA Imp7 - Cl2	Yes	****
OC-pDNA Imp7 - Cl4 vs Linear-pDNA Imp7 - Cl4	Yes	****
OC-pDNA Imp7 - Cl4 vs Untransfected DxR Control	Yes	****
OC-pDNA Imp7 - Cl4 vs Untransfected Back Imp7	Yes	****
OC-pDNA Imp7 - Cl4 vs Untransfected Imp7 - Cl2	Yes	****
OC-pDNA Imp7 - Cl4 vs Untransfected Imp7 - Cl4	Yes	****
OC-pDNA Imp7 - Cl4 vs PLL +1.6 - DxR Control	Yes	****

G

OC-pDNA Imp7 - Cl4 vs PLL +1.6 - Back Imp7	Yes	****
OC-pDNA Imp7 - Cl4 vs PLL +1.6 - Imp7 KD Cl2	Yes	****
OC-pDNA Imp7 - Cl4 vs PLL +1.6 - Imp7 KD Cl4	Yes	****
OC-pDNA Imp7 - Cl4 vs PLL +5 - DxR Control	Yes	****
OC-pDNA Imp7 - Cl4 vs PLL +5 - Back Imp7	Yes	****
OC-pDNA Imp7 - Cl4 vs PLL +5- Imp7 KD Cl2	Yes	****
OC-pDNA Imp7 - Cl4 vs PLL +5 - Imp7 KD Cl4	Yes	****
Linear-pDNA DxR Control vs Linear-pDNA Back Imp7	Yes	****
Linear-pDNA DxR Control vs Linear-pDNA Imp7 - Cl2	Yes	****
Linear-pDNA DxR Control vs Linear-pDNA Imp7 - Cl4	Yes	****
Linear-pDNA DxR Control vs Untransfected DxR Control	Yes	****
Linear-pDNA DxR Control vs Untransfected Back Imp7	Yes	****
Linear-pDNA DxR Control vs Untransfected Imp7 - Cl2	Yes	****
Linear-pDNA DxR Control vs Untransfected Imp7 - Cl4	Yes	****
Linear-pDNA DxR Control vs PLL +1.6 - DxR Control	Yes	****
Linear-pDNA DxR Control vs PLL +1.6 - Back Imp7	Yes	****
Linear-pDNA DxR Control vs PLL +1.6 - Imp7 KD Cl2	Yes	****
Linear-pDNA DxR Control vs PLL +1.6 - Imp7 KD Cl4	Yes	****
Linear-pDNA DxR Control vs PLL +5 - DxR Control	Yes	****
Linear-pDNA DxR Control vs PLL +5 - Back Imp7	Yes	****
Linear-pDNA DxR Control vs PLL +5- Imp7 KD Cl2	Yes	****
Linear-pDNA DxR Control vs PLL +5 - Imp7 KD Cl4	Yes	****
Linear-pDNA Back Imp7 vs Linear-pDNA Imp7 - Cl2	Yes	****
Linear-pDNA Back Imp7 vs Linear-pDNA Imp7 - Cl4	No	ns
Linear-pDNA Back Imp7 vs Untransfected DxR Control	Yes	****

H

Linear-pDNA Back Imp7 vs Untransfected Back Imp7	Yes	****
Linear-pDNA Back Imp7 vs Untransfected Imp7 - Cl2	Yes	****
Linear-pDNA Back Imp7 vs Untransfected Imp7 - Cl4	Yes	****
Linear-pDNA Back Imp7 vs PLL +1.6 - DxR Control	Yes	****
Linear-pDNA Back Imp7 vs PLL +1.6 - Back Imp7	Yes	****
Linear-pDNA Back Imp7 vs PLL +1.6 - Imp7 KD Cl2	Yes	****
Linear-pDNA Back Imp7 vs PLL +1.6 - Imp7 KD Cl4	Yes	****
Linear-pDNA Back Imp7 vs PLL +5 - DxR Control	Yes	****
Linear-pDNA Back Imp7 vs PLL +5 - Back Imp7	Yes	****
Linear-pDNA Back Imp7 vs PLL +5- Imp7 KD Cl2	Yes	****
Linear-pDNA Back Imp7 vs PLL +5 - Imp7 KD Cl4	Yes	****
Linear-pDNA Imp7 - Cl2 vs Linear-pDNA Imp7 - Cl4	Yes	****
Linear-pDNA Imp7 - Cl2 vs Untransfected DxR Control	Yes	****
Linear-pDNA Imp7 - Cl2 vs Untransfected Back Imp7	Yes	****
Linear-pDNA Imp7 - Cl2 vs Untransfected Imp7 - Cl2	Yes	****
Linear-pDNA Imp7 - Cl2 vs Untransfected Imp7 - Cl4	Yes	****
Linear-pDNA Imp7 - Cl2 vs PLL +1.6 - DxR Control	Yes	****
Linear-pDNA Imp7 - Cl2 vs PLL +1.6 - Back Imp7	Yes	****
Linear-pDNA Imp7 - Cl2 vs PLL +1.6 - Imp7 KD Cl2	Yes	****
Linear-pDNA Imp7 - Cl2 vs PLL +1.6 - Imp7 KD Cl4	Yes	****
Linear-pDNA Imp7 - Cl2 vs PLL +5 - DxR Control	Yes	****
Linear-pDNA Imp7 - Cl2 vs PLL +5 - Back Imp7	Yes	****
Linear-pDNA Imp7 - Cl2 vs PLL +5- Imp7 KD Cl2	Yes	****
Linear-pDNA Imp7 - Cl2 vs PLL +5 - Imp7 KD Cl4	Yes	****
Linear-pDNA Imp7 - Cl4 vs Untransfected DxR Control	Yes	****

I

Linear-pDNA Imp7 - Cl4 vs Untransfected Back Imp7	Yes	****
Linear-pDNA Imp7 - Cl4 vs Untransfected Imp7 - Cl2	Yes	****
Linear-pDNA Imp7 - Cl4 vs Untransfected Imp7 - Cl4	Yes	****
Linear-pDNA Imp7 - Cl4 vs PLL +1.6 - DxR Control	Yes	****
Linear-pDNA Imp7 - Cl4 vs PLL +1.6 - Back Imp7	Yes	****
Linear-pDNA Imp7 - Cl4 vs PLL +1.6 - Imp7 KD Cl2	Yes	****
Linear-pDNA Imp7 - Cl4 vs PLL +1.6 - Imp7 KD Cl4	Yes	****
Linear-pDNA Imp7 - Cl4 vs PLL +5 - DxR Control	Yes	****
Linear-pDNA Imp7 - Cl4 vs PLL +5 - Back Imp7	Yes	****
Linear-pDNA Imp7 - Cl4 vs PLL +5- Imp7 KD Cl2	Yes	****
Linear-pDNA Imp7 - Cl4 vs PLL +5 - Imp7 KD Cl4	Yes	****
Untransfected DxR Control vs Untransfected Back Imp7	Yes	****
Untransfected DxR Control vs Untransfected Imp7 - Cl2	Yes	****
Untransfected DxR Control vs Untransfected Imp7 - Cl4	Yes	****
Untransfected DxR Control vs PLL +1.6 - DxR Control	Yes	****
Untransfected DxR Control vs PLL +1.6 - Back Imp7	Yes	****
Untransfected DxR Control vs PLL +1.6 - Imp7 KD Cl2	Yes	****
Untransfected DxR Control vs PLL +1.6 - Imp7 KD Cl4	Yes	****
Untransfected DxR Control vs PLL +5 - DxR Control	Yes	****
Untransfected DxR Control vs PLL +5 - Back Imp7	Yes	****
Untransfected DxR Control vs PLL +5- Imp7 KD Cl2	Yes	****
Untransfected DxR Control vs PLL +5 - Imp7 KD Cl4	Yes	****
Untransfected Back Imp7 vs Untransfected Imp7 - Cl2	No	ns
Untransfected Back Imp7 vs Untransfected Imp7 - Cl4	Yes	****

J

Untransfected Back Imp7 vs PLL +1.6 - Back Imp7	Yes	****
Untransfected Back Imp7 vs PLL +1.6 - Imp7 KD Cl2	Yes	****
Untransfected Back Imp7 vs PLL +1.6 - Imp7 KD Cl4	Yes	****
Untransfected Back Imp7 vs PLL +5 - DxR Control	Yes	****
Untransfected Back Imp7 vs PLL +5 - Back Imp7	Yes	****
Untransfected Back Imp7 vs PLL +5- Imp7 KD Cl2	Yes	****
Untransfected Back Imp7 vs PLL +5 - Imp7 KD Cl4	Yes	****
Untransfected Imp7 - Cl2 vs Untransfected Imp7 - Cl4	Yes	****
Untransfected Imp7 - Cl2 vs PLL +1.6 - DxR Control	Yes	****
Untransfected Imp7 - Cl2 vs PLL +1.6 - Back Imp7	Yes	****
Untransfected Imp7 - Cl2 vs PLL +1.6 - Imp7 KD Cl2	Yes	****
Untransfected Imp7 - Cl2 vs PLL +1.6 - Imp7 KD Cl4	Yes	****
Untransfected Imp7 - Cl2 vs PLL +5 - DxR Control	Yes	**
Untransfected Imp7 - Cl2 vs PLL +5 - Back Imp7	Yes	****
Untransfected Imp7 - Cl2 vs PLL +5- Imp7 KD Cl2	Yes	****
Untransfected Imp7 - Cl2 vs PLL +5 - Imp7 KD Cl4	Yes	****
Untransfected Imp7 - Cl4 vs PLL +1.6 - DxR Control	Yes	****
Untransfected Imp7 - Cl4 vs PLL +1.6 - Back Imp7	No	ns
Untransfected Imp7 - Cl4 vs PLL +1.6 - Imp7 KD Cl2	Yes	****
Untransfected Imp7 - Cl4 vs PLL +1.6 - Imp7 KD Cl4	Yes	****
Untransfected Imp7 - Cl4 vs PLL +5 - DxR Control	Yes	****
Untransfected Imp7 - Cl4 vs PLL +5 - Back Imp7	Yes	****
Untransfected Imp7 - Cl4 vs PLL +5- Imp7 KD Cl2	No	ns
Untransfected Imp7 - Cl4 vs PLL +5 - Imp7 KD Cl4	Yes	****

K

PLL +1.6 - DxR Control vs PLL +1.6 - Imp7 KD Cl2	Yes	****
PLL +1.6 - DxR Control vs PLL +1.6 - Imp7 KD Cl4	Yes	****
PLL +1.6 - DxR Control vs PLL +5 - DxR Control	Yes	****
PLL +1.6 - DxR Control vs PLL +5 - Back Imp7	Yes	****
PLL +1.6 - DxR Control vs PLL +5- Imp7 KD Cl2	Yes	****
PLL +1.6 - DxR Control vs PLL +5 - Imp7 KD Cl4	Yes	****
PLL +1.6 - Back Imp7 vs PLL +1.6 - Imp7 KD Cl2	Yes	****
PLL +1.6 - Back Imp7 vs PLL +1.6 - Imp7 KD Cl4	Yes	****
PLL +1.6 - Back Imp7 vs PLL +5 - DxR Control	Yes	****
PLL +1.6 - Back Imp7 vs PLL +5 - Back Imp7	Yes	****
PLL +1.6 - Back Imp7 vs PLL +5- Imp7 KD Cl2	No	ns
PLL +1.6 - Back Imp7 vs PLL +5 - Imp7 KD Cl4	Yes	****
PLL +1.6 - Imp7 KD Cl2 vs PLL +1.6 - Imp7 KD Cl4	No	ns
PLL +1.6 - Imp7 KD Cl2 vs PLL +5 - DxR Control	Yes	****
PLL +1.6 - Imp7 KD Cl2 vs PLL +5 - Back Imp7	Yes	****
PLL +1.6 - Imp7 KD Cl2 vs PLL +5- Imp7 KD Cl2	Yes	****
PLL +1.6 - Imp7 KD Cl2 vs PLL +5 - Imp7 KD Cl4	Yes	****
PLL +1.6 - Imp7 KD Cl4 vs PLL +5 - DxR Control	Yes	****
PLL +1.6 - Imp7 KD Cl4 vs PLL +5 - Back Imp7	Yes	***
PLL +1.6 - Imp7 KD Cl4 vs PLL +5- Imp7 KD Cl2	Yes	****
PLL +1.6 - Imp7 KD Cl4 vs PLL +5 - Imp7 KD Cl4	Yes	****
PLL +5 - DxR Control vs PLL +5 - Back Imp7	Yes	****
PLL +5 - DxR Control vs PLL +5- Imp7 KD Cl2	Yes	****
PLL +5 - DxR Control vs PLL +5 - Imp7 KD Cl4	No	ns
PLL +5 - Back Imp7 vs PLL +5- Imp7 KD Cl2	Yes	**
PLL +5 - Back Imp7 vs PLL +5 - Imp7 KD Cl4	Yes	****

Table 7.1: Bonferroni's Multiple Comparison's Test showing the statistical significance of IFIT2 gene upregulation between Imp7 KD and control cells (DxR and Back Imp7) when transfected with polyplexes (containing 0.2μg) of differing DNA topologies. IFIT2 gene upregulation was also measured in untransfected cells and cells treated with native PLL ($p < 0.05$).

7.4 Discussion

Knowledge of polyplex nuclear import is pivotal if non-viral gene delivery is to be applied therapeutically. Few studies have reported detailed mechanisms of polyplex nuclear entry. Importin-7 (Imp7) is part of a large family of factors involved in the continuous shuttling of cargo between the cytosol and nucleus, and has been specifically implicated in the nuclear import of viral DNA; HIV-I (Zaitseva *et al*, 2009). This could provide some insight into pDNA uptake and expression.

7.4.1 Polyplex nuclear import: qualitative and quantitative analysis

The findings from Chapter 5 revealed PLL/DNA polyplex uptake in CHO cells and how complexes are also taken up by DCs (Chapter 6). However polyplex nuclear import and the mechanisms responsible have not been reported in great depth. The current chapter attempted to address this whereby polyplex uptake in cells lacking importin-7 (Imp7) was studied. Imp7 is a key receptor transport protein reported to aid nuclear import of viral DNA. Uptake of polyplexes within Imp7 knockdown (KD) (which was brought about via shRNA [small hairpin RNA] gene silencing) cells was monitored by confocal microscopy and gene expression studies. Uptake and gene expression was compared with control cells that contained functioning Imp7.

7.4.1.1 Imp7 KD reduces polyplex nuclear association as revealed by confocal microscopy

Imp7 has been reported to facilitate HIV-I viral DNA nuclear import (Zaitseva *et al*, 2009; Fassati *et al*, 2003). To observe whether PLL/DNA complexes exploit such a mechanism, polyplex uptake was studied in HeLa cells containing a stable Imp7 KD via puromycin

selection (two clone cells were used; clone 2 [Cl2] and clone 4 [Cl4]). Uptake was also studied within control HeLa cells containing a shRNA targeting an alternative mRNA sequence (DxR), along with KD cells that had Imp7 function restored (Back Imp7). Confocal microscopy analysis revealed polyplex nuclear association (defined when polyplex fluorescence completely overlaid with nuclear stain) was hindered in Imp7 KD cells (Figure 7.1). This was confirmed in both mid section and stack confocal images. The percentage of nuclear associated polyplexes, which was greatest for SC-pDNA polyplexes at >20%, reduced dramatically when Imp7 function was abolished (<5%) (Figure 7.2). Although infected with viral DNA, Imp7 KD led to DNA accumulation within the cytosol (Zaitseva *et al*, 2009; Miller *et al*, 2009). Imp7 works in conjunction with protein factors and nucleoporins which constitute the nuclear pore complex (NPC) (Gorlich and Kutay, 1999). The nuclear pore import receptor (NIR) in the cytosol has been found to recognise viral DNA. The NIR/DNA complex then interacts with the NPC to gain access within the nucleoplasm (Fassati *et al*, 2003). This mechanism could be responsible for polyplex nuclear import.

7.4.1.2 Imp7 KD decreases polyplex gene expression

Polyplex gene expression was measured to record the effect of Imp7 KD. Gene expression significantly decreased when Imp7 function was silenced. Gene expression reduced by 50% for SC-pDNA polyplexes (Figure 7.3). HIV-I plasmid gene expression was also found to be hindered when Imp7 function was inhibited (Zaitseva *et al*, 2009). However this is the first reported case of Imp7 inhibition affecting PLL/DNA complex gene expression. Fluorescence resonance energy transfer (FRET) has revealed how DNA polyplex nuclear entry occurs via the NPC and binds to various importin proteins (Breuzard *et al*, 2008; Lam and Dean, 2010).

The present study identified DNA topology dependent gene expression for polyplexes within CHO cells, DCs and HeLa cells. Although displaying larger sizes (<1000nm) and susceptibility towards nucleases, linear-pDNA polyplexes still managed to induce gene expression. This may occur via Imp7 mediated NPC nuclear delivery, which readily occurs for large viral DNAs which share the same topological form as linear-pDNA.

7.4.2 Live cell imaging studies

PLL/DNA polyplex (containing different DNA topological forms) uptake in Imp7 KD cells was monitored in real time via live cell confocal microscopy (Figure 7.4). These experiments provided some key insights:

- Polyplex DNA fluorescence and host cell nuclei (of control) fluorescence co-localised.
- However DNA fluorescence also co-localised with host cell nuclei in Imp7 KD cells (Figure 7.5b) indicating alternative import mechanisms may be utilised, although this was much more pronounced in control cells indicating Imp7 may be used by DNA complexes.
- This is important as nuclear import of cargo is a key function of Imp7 (Fassati *et al*, 2003; Nagasaki *et al*, 2005).
- Nuclear import of SC- and OC-pDNA polyplexes is rapid occurring in less than 10 minutes.

However it is clear there is significantly more polyplex DNA in the control cells (Figure 7.4a), than Imp7 KD cells (Figure 7.4b). A possible reason could be due to a reduction in cytoplasmic transport as a result of Imp7 KD. Imp7 is a key nucleocytoplasmic complex that

shuttles foreign components to the nucleus. As Imp7 function is reduced, it is unable to bind to cytoplasmic protein complexes such as Impβ which constitutes a protein complex that hauls foreign components from the cytosol (Ao *et al*, 2007; Zaitseva *et al*, 2009). Therefore Imp7 KD reduces Impβ interaction which could potentially hinder polyplex uptake and transport in the cytosol towards the nuclei. This could account for the reduced DNA fluorescence in Figure 7.4b).

To optimise this strategy and further confirm the role Imp7 in polyplex nuclear import, live cell imaging studies could incorporate fluorescent staining of NPC components. Although Imp7 KD specifically inhibited nuclear import, Imp7 operates in conjunction with various other protein factors which constitute the NPC, and so it would be interesting to analyse how other factors may contribute towards nuclear entry (such as Impβ).

7.4.3 Polyplex uptake triggers anti-viral innate immune responses

To confirm whether DNA polyplexes utilise viral uptake mechanisms such as Imp7, anti-viral responses were measured. Interferon-β (IFN-β) cytokine activity was measured following polyplex uptake. IFN-β is secreted in response to viral or pathogen infection and stimulates the synthesis of interferon-induced protein with tetratricopeptide repeats-2 (IFIT2) (Katsoulidis *et al*, 2008; Li *et al*, 2010).

Following polyplex uptake, IFIT2 gene upregulation was measured by Q-PCR. The protective attributes of IFIT2 as an antiviral protein was reported previously whereby transformation of BCR-ABL (breakpoint cluster region Abelson leukaemia fusion protein) within host cells abolished IFIT2 antileukaemic pathways (Katsoulidis *et al*, 2008). HeLa cells transfected with PLL/DNA polyplexes led to higher IFIT2 gene expression (lower cycle

threshold [Ct]) than untransfected cells (Figure 7.10). Despite normalization with housekeeping genes, the addition of polyplex DNA (regardless of topology) clearly induced an anti-viral response (Figure 7.10b).

Figure 7.10 shows upregulation of IFIT2 following uptake of polyplexes containing 20µg pDNA. The experiment was repeated with polyplexes containing 0.2µg pDNA as a high dose may mask subtle changes in IFIT2 expression between differing DNA topologies. Upregulation of IFIT2 showed dependence on DNA topology which was greatest for Imp7 KD cells transfected with SC-pDNA polyplexes (Figure 7.11). SC-pDNA polyplexes are more efficient than its topological counterparts in regards to gaining cellular access, and cytosolic accumulation of these complexes in Imp7 KD cells (as a result of nuclear import being blocked) may activate cytosolic DNA sensing agents (Hornung and Latz, 2010). IFIT2 gene upregulation was exclusive to transfected DNA as native PLL induced a very low response (presumably protein could not enter the cell) as well as untransfected cells.

Innate responses such as IFN-β upregulation of IFIT2 and cytokine production can occur through various detection pathways which are often located in the cytosol. Kobiyama *et al*, (2010) revealed how histone H2B stimulates innate antiviral immune responses within human cells. Foreign DNA stimulates H2B to interact with interferon-β promoter stimulator 1 (IPS-1) via the adapter protein; CIAO (COOH terminal importin-9 related adaptor organising histone H2B and IPS-1) (Kobiyama *et al*, 2010). The IPS-1/CIAO interaction transmits a signal specifically for dsDNA leading to IFN-β response (Kobiyama *et al*, 2010). Other DNA sensing agents include toll-like receptors (TLRs), which are pathogen recognition receptors (PRRs) that offer immediate protection against viral infection. TLR9 is an example of a PRR that specifically detects DNA (Vilaysane and Muruve, 2009). TLR-9 was shown to recognise

DNA which led to the recruitment of the adaptor protein MyD88 to induce cytokine production (Hemmi *et al*, 2000). DNA detecting agents such as TLR-9 have been found to induce IFN-β transcription (Uematsu *et al*, 2005). Other DNA sensors also include Z-DNA binding protein-1 (ZBP1) which binds to DNA and elicits IFN responses through the recruitment of interferon regulatory factors (IRFs) (Takaoka *et al*, 2007). Absent in melanoma 2 (AIM2) are a family of PRRs that detects cytoplasmic dsDNA which in turn triggers inflammatory responses as well as programmed cell death referred to as pyroptosis (Shao *et al*, 2007; Fernandes-Alnemri *et al*, 2007, Vilaysane and Muruve, 2009). Therefore the induction of IFN-β induced IFIT2 activity can take place through a variety of mechanisms due to the multiple DNA sensing agents available.

7.4.4 Improvements and future analyses

In order to improve the current protocol, fluorescent staining/probing of Imp7 could be applied and co-localisation between the receptor and cargo could be used to confirm interaction (Jäkel *et al*, 1999). Imp7 nuclear shuttling is mediated by GTPases; enzymes which bind to guanosine triphosphate (GTP) and reversibly hydrolyse this to produce guanosine diphosphate (GDP). Conversion of GDP to GTP is mediated by guanine nucleotide exchange factor in which GTP production activates the cell (through conformational changes to the Imp7/cargo complex) to allow nuclear entry and release of the foreign cargo (Zatiseva *et al*, 2009; Ao *et a*l, 2007). Specific knockdown of this GTP/GDP hydrolysis mechanism in regards to nuclear shuttling, could also potentially confirm the role of Imp7 towards the nuclear import of polyplex DNA.

Improvements for future analysis could include the incorporation of nuclear localisation signal (NLS) peptides which interact with importin proteins, and has proven successful with

polymers such as PEI and PLL whereby improved gene expression has been reported (Kim *et al*, 2009).

This chapter focused on the potential exploitation of Imp7 for nuclear import by DNA polyplexes. Confocal qualitative and quantitative studies showed reduced nuclear association in Imp7 KD cells than in control cells with functioning Imp7. Furthermore experiments showed reduced gene expression profiles in Imp7 KD cells. However whilst live cell imaging did show fluorescent co-localisation between DNA and nuclei in Imp7 KD cells, co-localisation was more pronounced in control cells with functioning Imp7. Q-PCR studies revealed higher antiviral responses detected in Imp7 KD cells when transfected with SC-pDNA. Therefore in regards to future therapeutic studies design of polyplexes could incorporate components that could potentially enhance Imp7 interaction and nuclear import.

7.5 Chapter Summary

- PLL/DNA polyplex uptake and gene expression in HeLa cells showed dependence on DNA topology (greatest for SC-pDNA complexes).
- Regardless of DNA topology:
    - Qualitative confocal microscopy analysis showed Imp7 KD reduced nuclear association of complexes.
    - Quantitative confocal image analysis revealed a decrease in the percentage of polyplex nuclear association in Imp 7 KD cells. SC-pDNA polyplexes displayed highest complex nuclear association at >20% in control cells which decreased to <5% in Imp7 KD cells.
    - Reduction in gene expression in Imp7 KD cells. Gene expression (particularly for SC- and OC-pDNA polyplexes) decreased from approximately >20% in DxR and Back Imp7 control cells to >8% in Imp7 KD cells.
- Live cell imaging showed co-localisation of DNA and nucleus in Imp7 KD cells; however co-localisation was more pronounced in cells with functioning Imp7.
- DNA polyplexes stimulate anti-viral responses as shown by the upregulation of IFIT2 (protein synthesised in response to viral infection).
    - Upregulation of IFIT2 showed dependence on DNA topology. IFIT2 gene expression was greatest for Imp7 KD cells transfected with SC-pDNA polyplexes presumably due to cytosolic accumulation of DNA which could activate DNA sensing agents. Responses were exclusive to transfected cells.

Chapter 8.
Conclusions and future work

8. Conclusions and Future Work

In this study plasmid DNA (pDNA) was complexed with poly-$_L$-lysine (PLL) to form DNA complexes (polyplexes). Biophysical analysis revealed how parameters such as DNA topology affect polyplex characterisation (charge, size, nuclease resistance and DNA condensation by PLL). To deduce whether topology and biophysical characteristics impact on cellular uptake (defined as the intake of materials by a cell or tissue leading to its permanent or temporary retention), polyplexes were transiently transfected into mammalian cells. This refers to the process of introducing foreign nucleic acids into host cells, often with the aim of expressing a desired protein product (Liu *et al*, 2008). Polyplexes containing plasmids in the supercoiled (SC) form displayed greatest gene expression (expression of encoded plasmid reporter *lacZ* gene) within Chinese hamster ovary (CHO), HeLa and dendritic cells (DCs). Polyplex uptake was analysed in CHO cells and possible nuclear import by importin-7 (Imp7) in a manner similar to viral DNA was also studied. Polyplexes were found to stimulate anti-viral innate immune responses.

Key points encountered in this study were:

- DNA topology affected polyplex biophysical characteristics which included parameters such as size, surface charge, ability to be condensed by PLL and nuclease resistance amongst others. SC-pDNA polyplexes were smaller and displayed greater nuclease resistance than OC (open circular) - and linear-pDNA complexes. Furthermore linear-pDNA required greater amounts of PLL to neutralise the anionic pDNA charge.

- Plasmid vector size was found to affect polyplex characterisation. A bacterial artificial chromosome (BAC, 56.5kb) was studied in conjunction with a 3.8kb plasmid. The large size of the BAC restricted charge neutralisation and condensation by PLL unlike that of the smaller 3.8kb plasmid.

- Mammalian cell uptake of complexes was monitored qualitatively and quantitatively via fluorescent confocal microscopy. Uptake (which was confirmed by both mid section and stack confocal microscopy images) of SC-pDNA polyplexes was the most efficient in all three cell types studied. A greater percentage of SC-pDNA polyplexes associated with the nuclei (fluorescent co-localisation of polyplex and nuclear stain).

- Confocal microscopy studies revealed plasmids remain associated with PLL post transfection as shown by fluorescent overlay between the individual components.

- SC-pDNA polyplexes displayed highest gene expression in mammalian cells. Gene expression showed dependence on DNA topology regardless of charge ratio (ratio of PLL to DNA).

- PLL/DNA nuclear import (defined as the transportation of foreign material into the nuclei) was studied in importin-7 (Imp7) knockdown (KD) cells. Confocal image qualitative and quantitative analysis showed nuclear association decreased in Imp7 KD cells. Polyplex gene expression decreased in Imp7 KD cells in comparison to control cells with functioning Imp7. However live cell imaging analysis did show co-localisation between DNA and nuclei in Imp7 KD cells suggesting other possible nuclear import mechanisms.

- Uptake of DNA polyplexes stimulated anti-viral innate immune responses. Upregulation of IFIT2 (interferon induced protein with tetratricopeptide repeats-2)

which is produced by IFN-β in response to viral infection was measured. Upregulation of IFIT2 increased in Imp7 KD cells transfected with SC-pDNA indicating possible cytoplasmic accumulation of polyplex DNA stimulates DNA sensing agents that trigger innate responses.

8.1 Biophysical characteristic study of PLL/DNA polyplexes

Biophysical studies were performed on DNA polyplexes. The findings revealed in Chapter 3 show that key parameters such as DNA topology influence polyplex characteristics such as polyplex size, charge, ability of DNA to be condensed by PLL, nuclease resistance, ionic strength and plasmid vector size.

Data from Chapter 3 showed that SC- and OC-pDNA underwent rapid charge neutralisation unlike that of linear-pDNA, which required greater amounts of PLL (Figure 3.2). PLL/DNA complexes containing pDNA in its SC form were the smallest (Figure 3.5), most efficiently condensed by PLL (Figure 3.6) and resistant towards nuclease attack (Figure 3.11). Therefore based on the biophysical data the study highly recommends the use of SC-pDNA for polyplex mediated gene delivery.

Plasmid size is an important consideration for gene delivery as insert size can have important therapeutic implications. This study analysed a 3.8kb plasmid along with a bacterial artificial chromosome (BAC) of 56.5kb in size, when complexed with PLL. The smaller plasmid yielded more favourable characteristics in regards to future gene delivery applications. When bound to PLL, the 3.8kb pDNA complex was much smaller, underwent rapid charge neutralisation and packaged (condensed by PLL) effectively. Despite offering larger gene insert the BAC was much larger and displayed neutral charge (even when formulated at an extremely high charge ratio) unworthy of uptake through the negatively charged mammalian

cell membrane. However it is important to note whether there is a threshold for plasmid vector size whereby binding with polycations is restricted which in turn limits gene delivery. In this study 3.8kb and 6.9kb plasmids complexed efficiently with PLL. The size threshold at which binding and cell uptake is reduced has been found to be approximately 12kb when bound to PEI (Campeau *et al*, 2001). Therefore smaller vector sizes in the SC conformation are recommended for gene delivery studies.

Ionic strength similar to that of the microcellular environment was found to be disruptive of PLL/DNA complexes. When polyplexes were produced in high salt concentration (>150mM NaCl), size, surface charge, and DNA condensation were perturbed. This provides important insights towards the limitations of PLL/DNA interaction and susceptibility of the DNA cargo under such conditions.

8.2 Mechanism of polyplex uptake and nuclear entry

Mammalian cell experiments indicated possible endocytosis of polyplexes in CHO cells. However whilst this was indicative in endocytic inhibitor experiments, co-localisation between DNA fluorescence and antibody fluorescence corresponding to specific endocytic markers were inconclusive. SC-pDNA polyplexes displayed the greatest gene expression within CHO, HeLa, and dendritic cells which may be due to the advantageous biophysical characteristics of this particular DNA topology recorded in Chapter 3. Greater percentage of SC-pDNA associated with the nucleus than complexes containing other DNA forms. Therefore in conjunction with the biophysical data the results of mammalian cell studies show that DNA topology clearly effects polyplex uptake with SC-pDNA being a key pre-requisite

DCs are key cells of the immune system and their targeting and exploitation for therapeutic application is of immense interest. Polyplex uptake within DCs can be restricted due to DCs predominately expressing nucleases. Confocal microscopy analysis revealed the majority of DNA polyplexes were found to be on the cell periphery (no overlay of polyplex fluorescence and cell), with a small percentage of SC-pDNA complexes associated with the nuclei (Figure 6.4). Gene expression was highest for SC-pDNA complexes which may be due to its small size and ability to evade nuclease attack. DCs can trigger antibody responses and so the ability of SC-pDNA polyplexes to induce substantial gene expression over its counterparts is important for further therapeutic applications. However despite uptake of polyplexes containing 20µg SC-pDNA, complexes failed to activate DCs to stimulate antigen presentation. This suggests that future studies should incorporate polyplexes that contain greater DNA dosage and an adjuvant (component that enhances recipient's immune response) to trigger such a response (Tang *et al*, 2010).

Polyplex nuclear import was studied in Chapter 7 particularly in regards to Imp7 for nuclear import. This is interesting as such mechanisms have been observed in regards to viral DNA (Zaitseva *et al*, 2009). Gene expression studies along with qualitative and quantitative confocal microscopy analyses indicated possible exploitation of Imp7. However live cell imaging experiments showed co-localisation between DNA and nuclei fluorescence in Imp7 KD cells which suggests other routes of nuclear import may be employed.

Uptake of PLL/DNA polyplexes stimulated anti-viral innate immune response, particularly in Imp7 KD cells. Upregulation of IFIT2 (which is synthesised in response to viral infection) was greatest in Imp7 KD cells transfected with SC-pDNA. These results indicate that polyplex uptake may occur in a manner similar to viral DNA

Therefore the data regarding the mechanism of polyplex uptake and nuclear import has three important implications for future studies:

- PLL/DNA polyplexes (regardless of DNA topology) could incorporate elements (such as lipid components that interact with cell membrane) that target various endocytic pathways.
- Incorporating components (such Impβ that binds with various importin proteins) within polyplexes that allow specific recognition by Imp7 to maximise nuclear import.
- The ability to activate and stimulate an immune response in DCs may be achieved by increasing DNA dosage and including adjuvants (enhances immune response) within polyplexes.

8.3 Impact on processing

Although the FDA (U.S Food and Drug Administration) has yet to approve any gene therapy products for sale, phase I clinical study of DNA vaccine treatment for diseases such as malaria, hepatitis B and HIV has been undertaken (FDA, 2007). This is a long and stringent process and in order to enter clinical trials FDA guidelines mentioned how gene therapy products must undergo potency tests in order to validate gene therapy products (Guidance for Industry: Potency tests for cellular and gene therapy products – FDA, 2011). More specifically FDA guidelines require gene therapy products to consist of 80% SC content (Guidance for Industry: Considerations for Plasmid DNA Vaccines for Infectious Disease Indications – FDA, 2007). The results presented in this thesis strongly indicate that DNA topology does impact on PLL/DNA complex biophysical characteristics and mammalian cell uptake. In agreement with FDA guidelines the results of the current investigation

recommends the employment of pDNA in the SC confirmation for future gene delivery studies. FDA guidelines require removal of other pDNA conformations in bulk product tests, which is in agreement of the present study whereby OC- and linear-pDNA polyplexes displayed inefficient uptake and gene expression profiles unlike complexes containing SC-pDNA. Therefore in terms of processing this study recommends the focusing on SC-pDNA manufacture for vaccine processing in order to maximise uptake and gene expression profiles.

8.4 Future aspects

This study focused on the characterisation and uptake of pDNA when bound to PLL. The findings presented in this report provide a body of data regarding polyplex biophysical attributes, uptake, nuclear import, gene expression, DC phenotype activation and ability to induce innate responses. To optimise these key parameters, with the aim of improving gene delivery, studies are currently employing multiple polymers. A major advantage of PLL is its versatility whereby it can undergo chemical modification for tailor made transfection studies (Fu *et al*, 2011; von Erlach *et al*, 2011). Modification can take the form of polymers which can perform a variety of functions such as shielding complex from nuclease digestion, preventing aggregation and enhancing cellular uptake. Such modification has recently been applied with DCs. Glycopeptide attachment to enhance interaction with DC surface markers was reported to improve complex uptake (Anderson *et al*, 2010). Therefore the combinational use of DNA condensing agents along with co-polymers to prevent nuclease attack and enhance cellular uptake is paving the way for future polyplex applications.

Appendix I. Plasmid DNA maps

Appendix I: Plasmid DNA maps

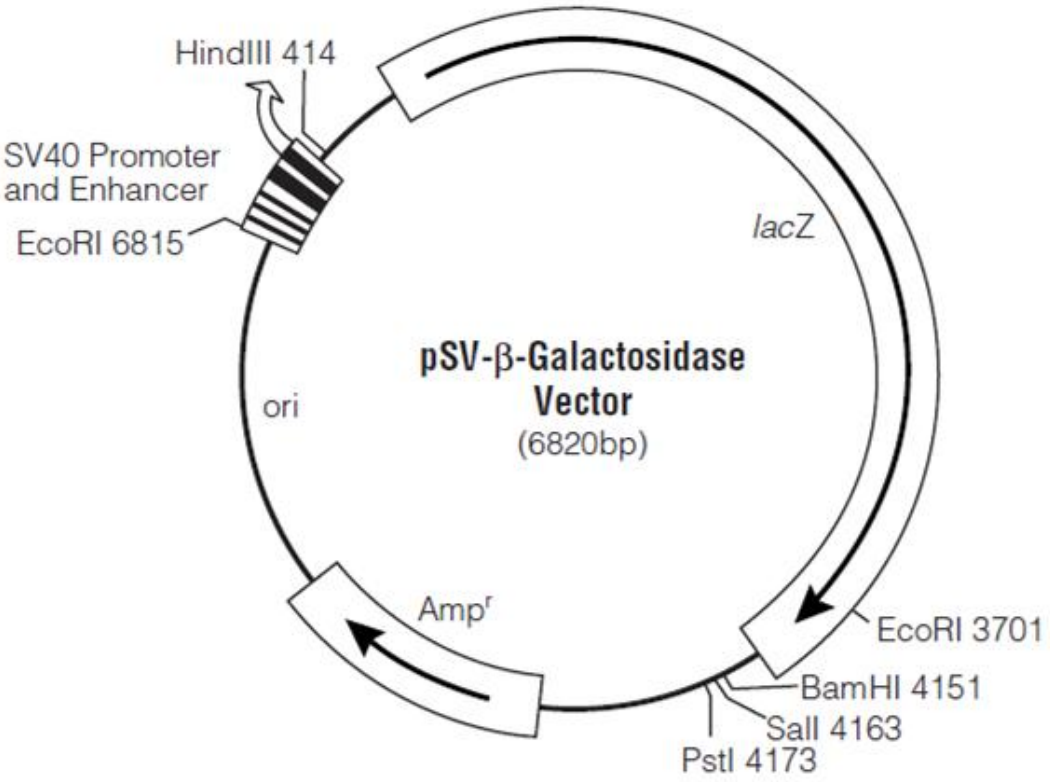

AI i: pSVβ (6.8kb) (Promega, Southampton, UK)

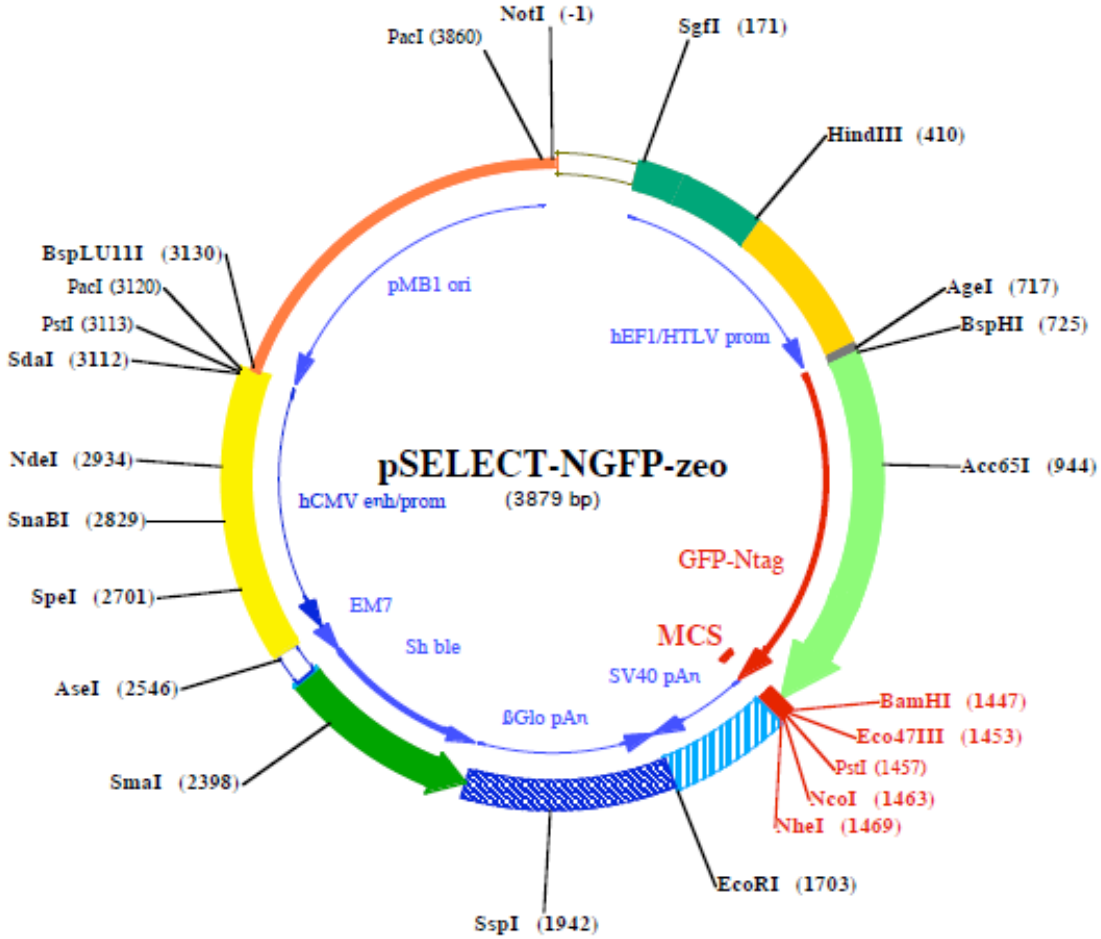

AI ii: pSELECT-NGFP-zeo (3.8kb) (InvivoGen, USA)

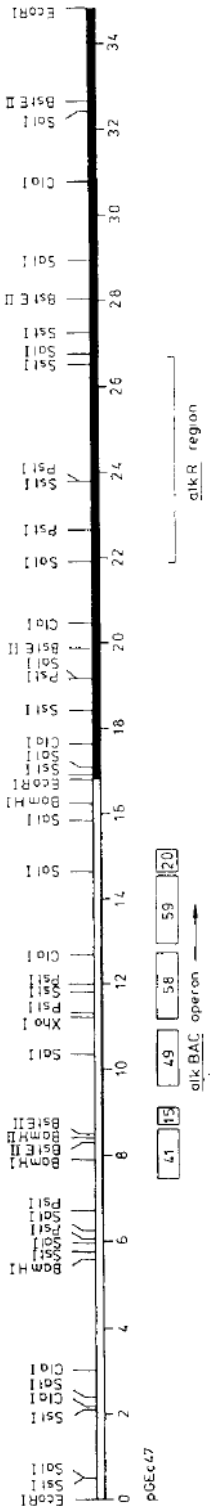

AI iii: pGEc47 (56.5kb) (Deutsche Sammlung von Mikroorganismen und Zellkulturen GmbH, Germany)

Appendix II. Calculation of charge ratio

Appendix II: Charge ratio calculation

The theoretical charge ratio between the DNA and PLL was calculated from the equation below as deduced from Tsai *et al*, (1999) and Lollo *et al*, (2002). The equation is based on several assumptions (Tsai *et al*, 1999):

1. Average molecular weight of 1 DNA nucleotide = 309
2. Average molecular weight of 1 lysine chain = 204
3. Calculation assumes the lysine polymer is protonated to interact and bind with DNA.

$$\textbf{Charge ratio} = \frac{\text{Mass of PLL}}{\text{Mass of DNA}} \times \frac{309}{204}$$

Appendix III. Publication 1

Appendix IV. Publication II

References

Akhtar, S. 2006. *Non-viral cancer gene therapy: beyond delivery*. *Gene Therapy*. May. 13 (9): pp 739-740.

Akita, H., Ito, R., Khalil, I.A., Futaki, S., and Harashima, H. 2004. *Quantitative three-dimensional analysis of the intracellular trafficking of plasmid DNA transfected by a nonviral gene delivery system using confocal laser scanning microscopy*. *Molecular Therapy: the Journal of the American Society of Gene Therapy*. Mach. 9 (3): pp 443-451.

Ali, O.A., and Mooney, D.J. 2008. *Sustained GM-CSF and PEI condensed pDNA presentation increases the level and duration of gene expression in dendritic cells*. *Journal of controlled release*. July 132 (3): pp 273-278.

Allen, T.M. and Chonn, A. 1987. *Large unilamellar liposomes with low uptake into the reticuloendothelial system*. *FEBS Letters*. October. 223 (1): pp 42-46.

Amyere, M., Mettlen, M., Van Der Smissen, P., Platek, A., Payrastre, B., Veithen, A., and Courtoy, P.J. 2002. *Origin, originality, functions, subversions and molecular signalling of macropinocytosis*. *International Journal of Medical Microbiology: IJMM*. February. 291 (6-7): pp 487-494.

Anada, T., Karinaga, R., Koumoto, K., Mizu, M., Nagasaki, T., Kato, Y., Taira, K., Shinkai, S., and Sakurai, K. 2005. *Linear double-stranded DNA that mimics an infective tail of virus genome to enhance transfection*. *Journal of Controlled Release*. November. 108 (2-3): pp 529-539.

Anderson, K., Fernandez, C., and Rice, K.G. 2010. *N-glycan targeted gene delivery to the dendritic cell SIGN receptor*. *Bioconjugate Chemistry*. August. 21 (8): pp 1479-1485.

Ao, Z., Huang, G., Yao, H., Xu, Z., Labine, M., Cochrane, A.W., and Yao, X. 2007. *Interaction of Human Immunodeficiency Virus Type 1 Integrase with Cellular Nuclear Import Receptor Importin 7 and Its Impact on Viral Replication*. *The Journal of Biological Chemistry*. May. 282. (18): pp 13456-13467.

Babiuk, S., van Drunen Littel-van den Hurk, S., and Babiuk, L.A. 2006. *Delivery of DNA vaccines using electroporation*. *Methods in Molecular Medicine*. 127: pp 73-82.

Bailey, S.N., Wu, R.Z., and Sabatini, D.M. 2002. *Applications of transfected cell microarrays in high-throughput drug discovery*. *Drug Discovery Today*. September. 7 (18): S113-118.

Baker, A., and Cotten, M. 1997. *Delivery of bacterial artificial chromosomes into mammalian cells with psoralen-inactivated adenovirus carrier*. *Nucleic Acids Research*. May. 25 (10): pp 1950-1956.

Banchereau, J., Briere, F., Caux, C., Davoust, J., Lebecque, S., Liu, Y.J., Pulendran, B., and Palucka, K. 2000. *Immunobiology of dendritic cells*. *Annual Review of Immunology*. 18: pp 767-811.

Baxby, D. 2002. *Smallpox vaccination techniques; from knives and forks to needles and pins*. *Vaccine*. May. 20 (16): pp 2140-2149.

Beláková, J., Horynová, M., Krupka, M., Weigl, E., and Raska, M. 2007. *DNA vaccines: are they still just a powerful tool for the future?* *Archivum immunologiae et therapiae experimentalis*. November-December. 55 (6): pp 387-398.

Bengali, Z., Pannier, A.K., Segura, T., Anderson, B.C., Jang, J.H., Mustoe, T.A., and Shea, L.D. 2005. *Gene delivery through cell culture substrate adsorbed DNA complexes*. *Biotechnology Bioengineering*. May. 90 (3): pp 290-302.

Bengali, Z., Rea, J.C., Gibly, R.F., and Shea, L.D. 2009. *Efficacy of immobilized polyplexes and lipoplexes for substrate-mediated gene delivery*. *Biotechnology Bioengineering*. April. 102 (6): pp 1679-1691.

Bielinska, A.V., Lataloo, J.F.K., and Baker, Jr J.R. 1997. *The interaction of plasmid DNA with polyamidoamine dendrimers; mechanism of complex formation and analysis of alternations induced in nuclear sensitivity and transcriptional activity of the complexed DNA*. *Biochimica et Biophysica Acta (BBA) - Gene Structure and Expression*. August. 1353 (2): pp 180-190.

Biewenga, J.E., Destrée, O.H., and Schrama, L.H. 1997. *Plasmid-mediated gene transfer in neurons using the biolistics technique*. *Journal of Neuroscience Methods*. January. 71 (1): pp 67-75.

Bivas-Benita, M., Ottenhoff, T.H., Junginger, H.E., and Borchard, G. 2005. *Pulmonary DNA vaccination: concepts, possibilities and perspectives*. *Journal of Controlled Release*. September. 107 (1): pp 1-29.

Blom, H., Bennemo, M., Berg, M., and Lemmens, R. 2010. *Flocculate removal after alkaline lysis in plasmid DNA production*. *Vaccine*. December. 29 (1): pp 6-10.

Bloomfield, V.A. 1996. *DNA condensation*. *Current Opinion in Structural Biology*. 6: pp 334-331.

Boles, T.C., White, J.H., and Cozzarelli, N.R. 1990. *Structure of plectonemically supercoiled DNA*. *Journal of Molecular Biology*. June. 213 (4): pp 931-951.

Brandsma, J.L. 2006. *DNA vaccine design*. *Methods in Molecular Medicine*. 127: pp 3-10.

Bremner, K.H., Seymour, L.W., Logan, A., and Read, M.L. 2004. *Factors influencing the ability of nuclear localization sequence peptides to enhance nonviral gene delivery*. *Bioconjugate chemistry*. January-February. 15 (1): pp 152-161.

Breunig, M., Lungwitz, U,, Liebl, R., Fontanari, C., Klar, J., Kurtz, A., Blunk, T., and Goepferich, A. 2005. *Gene delivery with low molecular weight linear polyethylenimines*. *The journal of gene medicine*. October. 7 (10): pp 1287-1298.

Breuzard, G., Tertil, M., Goncalves, C., Cheradame, H., Geguan, P., Pichon, C., and Midoux, P. 2008. *Nuclear delivery of NFiB-assisted DNA/polymer complexes: plasmid DNA quantitation by confocal laser scanning microscopy and evidence of nuclear polyplexes by FRET imaging*. *Nucleic Acids Research*. July. 36 (12): e71.

Brewer, C., Otto-Duessel, M,, Lykkesfeldt, J,, Nick, H,, and Wood, J. 2012. *Ascorbate status modulates reticuloendothelial iron stores and response to deferasirox iron chelation in ascorbate deficient rats*. *Experimental Hematology*. June 16. [Epub ahead of print].

Bronich, T.K., Nguyen, H.K., Eisenberg, A., and Kabanov, A.V. 2000. *Recognition of DNA topology in reactions between plasmid DNA and cationic copolymers*. Journal of the American Chemical Society. August. 122 (35): pp 8339-8343.

Brown, T.A. 2004. *Gene Cloning and DNA analysis. An Introduction*. 4th Edition. Blackwell Publishing, Oxford, UK.

Buchan, S., Grønevik, E., Mathiesen, I., King, C.A., Stevenson, F.K., and Rice J. 2005. *Electroporation as a "prime/boost" strategy for naked DNA vaccination against a tumor antigen*. *Journal of Immunology*. May. 174 (10): pp 6292-6298.

Campeau, P., Chapdelaine, P., Seigneurin-Venin, S., Massie, B., and Tremblay, J.P. 2001. *Transfection of large plasmids in primary human myoblasts*. *Gene Therapy*. September. 8 (18): pp 1387-1394.

Carnes, A.E., Hodgson, C.P., and Williams, J.A. 2006. *Inducible Escherichia coli fermentation for increased plasmid DNA production*. *Biotechnology and Applied Biochemistry*. November. 45 (3): 155-166.

Cebere, I., Dorrell, L., McShane, H., Simmons, A., McCormack, S., Schmidt, C., Smith, C., Brooks, M., Roberts, J.E., Darwin, S.C., Fast, P.E., Conlon, C., Rowland-Jones, S., McMichael, A.J., and Hanke, T. 2006. *Phase I clinical trial safety of DNA- and modified virus Ankara-vectored human immunodeficiency virus type 1 (HIV-1) vaccines administered alone and in a prime-boost regime to healthy HIV-1-uninfected volunteers*. *Vaccine*. January. 24 (4): pp 417-425.

Chain, B.M. 2003. *Current issues in antigen presentation--focus on the dendritic cell*. *Immunology Letters*. October. 89 (2-3): pp 237-241.

Chakrabarti, A., Sitaric, S., and Ohi, S. 1992. A procedure for large-scale plasmid isolation without using ultracentrifugation. Biotechnology and Applied Biochemistry. October. 16 (2): pp 211-215.

Chancham, P., and Hughes, J.A. 2001. *Relationship between plasmid DNA topological forms and in vitro transfection*. *Journal of Liposome Research*. 11 (2-3): pp 139-152.

Chen, H.H., Ho, Y.P., Jiang, X., Mao, H.Q., Wang, T.H., and Leong, K.W. 2008. *Quantitative comparison of intracellular unpacking kinetics of polyplexes by a model constructed from quantum dot-FRET*. *Molecular Therapy: the Journal of the American Society of Gene Therapy*. February. 16 (2): pp 324-332.

Chenevier, P., Veyret, B., Roux, D., and Henry-Toulmé N. 2000. *Interaction of cationic colloids at the surface of J774 cells: a kinetic analysis*. *Biophysical Journal*. September. 79 (3): pp 1298-1309.

Cherng, J.Y., Schuurmans-Nieuwenbroek, N. M. E., Jiskoot, W., Talsma, H., Zuidam, N. J., Hennink, W. E., and Crommelin, D. J. A. 1999. *Effect of DNA topology on the transfection efficiency of poly((2-dimethylamino)ethyl methacrylate)–plasmid complexes*. *Journal of Controlled Release*. August. 60 (2-3): pp 343-353.

Chiu, Y.H., Macmillan, J.B., and Chen, Z.J. 2009. *RNA polymerase III detects cytosolic DNA and induces type I interferons through the RIG-I pathway*. *Cell*. August. 138 (3): pp 576-591.

Choi, M.J., and Maibach, H.I. 2005. *Elastic vesicles as topical/transdermal drug delivery systems*. *International Journal of Cosmetic Science*. August. 27 (4): pp 211-221.

Choi, Y.H., Liu, F., Kim, J.S., Choi, Y.K., Park, J.S., and Kim, S.W. 1998. *Polyethylene glycol-grafted poly-L-lysine as polymeric gene carrier*. *The Journal of Controlled Release*. June. 54 (1): pp 39-48**.**

Christie, R.J., Nishiyama, N., and Kataoka, K. 2010. *Delivering the code: polyplex carriers for deoxyribonucleic acid and ribonucleic acid interference therapies*. *Endocrinology*. February. 151 (2): pp 466-473.

Ciolina, C., Byk, G., Blanche, F., Thuillier, V., Scherman, D., and Wils, P. 1999. *Coupling of nuclear localization signals to plasmid DNA and specific interaction of the conjugates with importin alpha*. *Bioconjugate chemistry*. January-February. 10 (1): pp 49-55.

Conner, S.D., and Schmid, S.L. 2003. *Regulated portals of entry into the cell*. *Nature*. March. 422 (6927): pp 37-44**.**

Cooke, J.R., McKie, E.A., Ward, J.M., and Keshavarz-Moore, E. 2004. *Impact of intrinsic DNA structure on processing of plasmids for gene therapy and DNA vaccines*. Journal of Biotechnology. November. 114 (3): pp 239-254.

Curtis, B.M., Scharnowske, S., and Watson, A.J. 1992. *Sequence and expression of a membrane-associated C-type lectin that exhibits CD4-independent binding of human immunodeficiency virus envelope glycoprotein gp120*. *Proceedings of the National Academy of Sciences of the United States of America*. September. 89 (17): pp 8356-8360.

Davis, H.L., Whalen, R.G., and Demeneix, B. 1993. *Direct gene transfer in skeletal muscle in vivo: factors influencing efficiency of transfer and stability of expression*. *Human Gene Therapy*. April. 4 (2): pp 151–156.

Delehanty, J.B., Bradburne, C.E., Susumu, K., Boeneman, K., Mei, B.C., Farrell, D., Blanco-Canosa, J.B., Dawson, P.E., Mattoussi, H., and Medintz I.L. 2011. *Spatiotemporal Multicolor Labeling of Individual Cells Using Peptide-Functionalized Quantum Dots and Mixed Delivery Techniques*. *Journal of the American Chemical Society*. May. [Epub ahead of print].

Derouazi, M., Girard, P., Van Tilborgh, F., Iglesias, K., Muller, N., Bertschinger, M., Wurm, F.M. 2004. *Serum-free large-scale transient transfection of CHO cells*. *Biotechnology Bioengineering*. August. 87 (4): pp 537-545.

Dhama, K., Mahendran, M., Gupta, P.K., and Rai, A. 2008. *DNA vaccines and their applications in veterinary practice: current perspectives*. *Veterinary Research Communications*. June. 32 (5): pp 341-356. Epub 2008. April 19th.

Diogo, M.M., Queiroz, J.A., Monteiro, G.A., Martins, S.A., Ferreira, G.N., and Prazeres, D.M. 2000. *Purification of a cystic fibrosis plasmid vector for gene therapy using hydrophobic interaction chromatography*. *Biotechnology Bioengineering*. June. 68 (5): pp 576-583.

Douglas, K.L., Piccirillo, C.A., and Tabrizian, M. 2008. *Cell line-dependent internalization pathways and intracellular trafficking determine transfection efficiency of nanoparticle vectors*. *European journal of pharmaceutics and biopharmaceutics : official journal of Arbeitsgemeinschaft für Pharmazeutische Verfahrenstechnik e.V*. March. 68 (3): pp 676-687.

Doukas, J., Morrow, J., Bellinger, D., Hilgert, T., Martin, T., Jones, D., Mahajan, R., Rusalov, D., Sullivan, S., and Rolland A. 2011. *Nonclinical biodistribution, integration, and toxicology evaluations of an H5N1 pandemic influenza plasmid DNA vaccine formulated with Vaxfectin®*. *Vaccine*. July. 29 (33): pp 5443-5452.

Dunlap, D., Maggi, A., Soria, M.R., and Monaco, L. 1997. *Nanoscopic structure of DNA condensed for gene delivery*. *Nucleic Acids Research*. August. 25 (15) pp 3095-3101.

Dutta, T., Garg, M., and Jain, N.K. 2008. *Poly(propyleneimine) dendrimer and dendrosome mediated genetic immunization against hepatitis B*. *Vaccine*. June. 26 (27-28): pp 3389-3394. Epub 2008. May 12th.

Edward, R. 2009. *Use of DNA-specific anthraquinone dyes to directly reveal cytoplasmic and nuclear boundaries in live and fixed cells*. *Molecules and Cells*. April. 27 (4): pp 391-396.

Eisenberg, H. 1987. *DNA flexing, folding and function*. *Accounts of Chemical Research*. 20 (8): pp 276–282.

Elouahabi, A., and Ruysschaert, J.M., 2005. *Formation and intracellular trafficking of lipoplexes and polyplexes*. Molecular Therapy. March. 11 (3): pp 336-347.

Evans, R.K., Xu, Z., Bohannon, K.E., Wang, B., Bruner, M.W., and Volkin, D.B. 2000. *Evaluation of degradation pathways for plasmid DNA in pharmaceutical formulations via accelerated stability studies*. *Journal of Pharmaceutical Sciences*. January. 89 (1): pp 76-87.

Faham, A., Herringson, T., Parish, C., Suhrbier, A., Khromykh, A.A., and Altin, J.G. 2011. *pDNA-lipoplexes engrafted with flagellin-related peptide induce potent immunity and anti-tumour effects*. *Vaccine*. September. 29 (40): pp 6911-69-19.

Farhood, H., Serbina, N., and Huang, L. 1995. *The role of dioleoyl phosphatidylethanolamine in cationic liposome mediated gene transfer*. *Biochimica et Biophysica Acta*. May. 1235 (2): pp 289-295.

Fassati, A., Görlich, D., Harrison, I., Zaytseva, L., and Mingot, J.M. 2003. *Nuclear import of HIV-1 intracellular reverse transcription complexes is mediated by importin 7*. *The EMBO Journal*. July. 22 (14): pp 3675-3685.

Fernandes-Alnemri, T., Wu, J., Yu, J.W., Datta, P., Miller, B., Jankowski, W., Rosenberg, S., Zhang, J., and Alnemri, E.S. 2007. *The pyroptosome: a supramolecular assembly of ASC dimers mediating inflammatory cell death via caspase-1 activation*. *Cell Death and Differeentiation*. September. 14 (9): pp 1590-1604.
Fernandes-Alnemri, T., Yu, J.W., Datta, P., Wu, J., and Alnemri, E.S. 2009. *AIM2 activates the inflammasome and cell death in response to cytoplasmic DNA*. *Nature*. March. 458 (7237): pp 509-513.

Fernandez, C.A., and Rice, K.G. 2009. *Engineered nanoscaled polyplex gene delivery systems*. *Molecular Pharmaceutics*. September-October. 6 (5): pp 1277-1289.

Ferrari, A., Pellegrini, V., Arcangeli, C., Fittipaldi, A., Giacca, M., and Beltram F. 2003. *Caveolae-mediated internalization of extracellular HIV-1 tat fusion proteins visualized in real time*. *Molecular Therapy: The Journal of the American Society of Gene Therapy*. August. 8 (2): pp 284-294.

Ferreira, G.N.M., Cabral, J.M.S, and Prazeres, D.M.F. 1997. *Comparison of gel filtration chromatographic supports for plasmid purification*. *Biotechnology Techniques*. 11 (6): pp 417-420.

Ferreira, G.N., Cabral, J.M., and Prazeres, D.M. 1999. *Development of process flow sheets for the purification of supercoiled plasmids for gene therapy applications*. *Biotechnology Progress*. July-August. 15 (4): pp 725-731.

Ferreira, G.N., Monteiro, G.A., Prazeres, D.M., and Cabral, J.M. 2000. *Downstream processing of plasmid DNA for gene therapy and DNA vaccine applications*. *Trends in Biotechnology*. September. 18 (9): pp 380-388.

Finkelman, F.D., Lees, A., Birnbaum, R., Gause, W.C., and Morris, S.C. 1996. *Dendritic cells can present antigen in vivo in a tolerogenic or immunogenic fashion*. *Journal of Immunology*. August. 157 (4): pp. 1406–1414.

Fu, C., Sun, X., Liu, D., Chen, Z., Lu, Z., and Zhang, N. 2011. *Biodegradable Tri-Block Copolymer Poly(lactic acid)-poly(ethylene glycol)-poly(l-lysine)(PLA-PEG-PLL) as a Non-Viral Vector to Enhance Gene Transfection*. *International Journal of Molecular Sciences*. February. 12 (2): pp 1371-1388.

Fuller, D.H., Loudon, P., and Schmaljohn, C. 2006. *Preclinical and clinical progress of particle-mediated DNA vaccines for infectious diseases*. *Methods*. September. 40 (1): pp 86-97.

Gersting, S.W., Schillinger, U., Lausier, J., Nicklaus, P., Rudolph, C., Plank, C., Reinhardt, D., and Rosenecker J. 2004. *Gene delivery to respiratory epithelial cells by magnetofection*. Journal of Gene Medicine. 6 (8): pp 913–922.

Gianolio, E., Arena, F., Strijkers, G.J., Nicolay, K., Högset, A., and Aime, S. 2011. *Photochemical activation of endosomal escape of MRI-Gd-agents in tumor cells*. *Magnetic resonance in medicine : official journal of the Society of Magnetic Resonance in Medicine / Society of Magnetic Resonance in Medicine*. January. 65 (1): pp 212-219.

Gimenez-Cassina, A., Wade-Martins, R., Gomez-Sebastian, S., Corona, J.C., Lim, F., and Diaz-Nido, J. 2011. *Infectious delivery and long-term persistence of transgene expression in the brain by a 135-kb iBAC-FXN genomic DNA expression vector*. *Gene Therapy*. April 14. [Epub ahead of print].

Godbey, W.T., Wu, K.K., and Mikos, A.G. 1999. *Tracking the intracellular path of poly (ethylenimine)/DNA complexes for gene delivery*. *Proceedings of the National Academy of Sciences of the USA*. April. 96 (9): pp 5177–5181.

Gomes, A.G., Azevedo, A.M., Aires-Barros, M.R., and Prazeres, D.M. 2010. *Clearance of host cell impurities from plasmid-containing lysates by boronate adsorption*. *Journal of chromatography*. *A*. April. 1217 (15): pp 2262-2266.

Gonçalves, C., Mennesson, E., Fuchs, R., Gorvel, J.P., Midoux, P., and Pichon, C. 2004. *Macropinocytosis of polyplexes and recycling of plasmid via the clathrin-dependent pathway impair the transfection efficiency of human hepatocarcinoma cells*. *Molecular Therapy: The Journal of the American Society of Gene Therapy*. August. 10 (2): pp 373-385.

Gopee, N.V., Cui, Y., Olson, G., Warbritton, A.R., Miller, B.J., Couch, L.H., Wamer, W.G., Howard P.C. 2005. *Response of mouse skin to tattooing: use of SKH-1 mice as a surrogate model for human tattooing*. *Toxicology and Applied Pharmacology*. December. 209 (2): pp 149-158.

Goudy, K.S., Wang, B., and Tisch, R. 2008. *Gene gun-mediated DNA vaccination enhances antigen-specific immunotherapy at a late preclinical stage of type 1 diabetes in nonobese diabetic mice*. *Clinical Immunology*. October. 129 (1): pp 49-57.

Görlich, D., and Kutay, U. 1999. *Transport between the cell nucleus and the cytoplasm*. *Annual Review of Cell and Developmental Biology*. 15: pp 607-660.

Gould, G.W., and Lippincott-Schwartz, J. 2009. *New roles for endosomes: from vesicular carriers to multi-purpose platforms*. *Nature Reviews*. *Molecular Cell Biology*. April. 10 (4): pp 287-292.

Grabski, A., McCormic, M., and Mierendorf, R. 1999. *BugBuster™ and Benzonase®: the clear solutions to simple, efficient extraction of E. coli proteins*. *Innovations*, 10. pp. 17–19.

Greenfield, R.S., Kaneko, T., Daues, A., Edson, M.A., Fitzgerald, K.A., Olech, L.J., Grattan, J.A., Spitalny, G.L., and Braslawsky, G.R. 1990. *Evaluation in vitro of adriamycin immunoconjugates synthesized using an acid-sensitive hydrazone linker*. *Cancer Research*. October. 50 (20): pp 6600-6607.

Gregoriadis G. 1998. *Genetic vaccines: strategies for optimisation*. *Pharmaceutical Research*. May. 15 (5): pp 661–70.

Gregoriadis, G., Saffie, R., and de Souza, J.B. 1997. *Liposome-mediated DNA vaccination*. *FEBS letters*. February. 402 (2-3): pp 107-110.

Guo, W., and Lee, R.J. 2001. *Efficient gene delivery via non-covalent complexes of folic acid and polyethylenimine*. *Journal of Controlled Release*. November. 77 (1-2): pp 131-138.

Hanzlikova, M., Soininen, P., Lampela, P., Männistö, P.T., and Raasmaja, A. 2009. *The role of PEI structure and size in the PEI/liposome-mediated synergism of gene transfection*. *Plasmid*. January. 61 (1): pp 15-21 Epub 2008 Oct 5.

Hardy, E., Pupo, E., Casalvilla, R., Sosa, A.E., Trujillo, L.E., López, E., and Castellanos-Serra, L. 1996. *Negative staining with zinc-imidazole of gel electrophoresis-separated nucleic acids*. *Electrophoresis*. October. 17 (10): pp 1537-1541.

Hartmann, L., Häfele, S., Peschka-Süss, R., Antonietti, M., and Börner, H.G. 2008. *Tailor-made poly(amidoamine)s for controlled complexation and condensation of DNA*. *Chemistry (Weinheim an der Bergstrasse, Germany)*. 14 (7): pp 2025-2033.

Haugland, R.P., Yguerabide, J., and Stryer, L. 1969. *Dependence of the kinetics of singlet-singlet energy transfer on spectral overlap*. *Proceedings of the National Academy of Sciences of the United States of America*. May. 63 (1): pp 23-30.

Hemmi, H., Takeuchi, O., Kawai, T., Kaisho, T., Sato, S., Sanjo, H., Matsumoto, M., Hoshino, K., Wagner, H., Takeda, K., and Akira, S. 2000. *A Toll-like receptor recognizes bacterial DNA*. *Nature*. December. 408 (6813): pp 740-745.

Herr, J.K., Smith, J.E., Medley, C.D., Shangguan, D., and Tan, W. 2006. *Aptamer-conjugated nanoparticles for selective collection and detection of cancer cells*. *Analytical Chemistry*. May. 78 (9): pp 2918-2924.

Hirasaki, T., Sato, T., Tsuboi, T., Nakano, H., Noda, T., Kono, A., Yamaguchi, K., Imada, K., Yamamoto, N., Murakami H., and Manabe, S. 1995. *Permeation mechanism of DNA molecules in solution through cuprammonium regenerated cellulose hollow fiber (BMM™).* *Journal of Membrane Science*. 106 (1-2): pp 123–129.

Hoare, M., Levy, M.S., Bracewell, D.G., Doig, S.D., Kong, S., Titchener-Hooker, N., Ward, J.M., and Dunnill, P. 2005. *Bioprocess engineering issues that would be faced in producing a DNA vaccine at up to 100 m3 fermentation scale for an influenza pandemic*. *Biotechnology Progress*. Novemeber-December. 21 (6): pp 1577-1592.

Horn, N.A., Meek, J.A., Budahazi, G., and Marquet, M. 1995. *Cancer gene therapy using plasmid DNA: purification of DNA for human clinical trials*. *Human Gene Therapy*. May. 6 (5): pp 565-573.

Hornung, V., and Latz, E. 2010. *Intracellular DNA recognition*. *Nature Reviews Immunology*. February. 10: pp 123-130.

Huber, C.G. 1998. *Micropellicular stationary phases for high-performance liquid chromatography of double-stranded DNA*. *Journal of Chromatography*. *A*. May. 806 (1): pp 3-30.

Hufnagel, H., Hakim, P., Lima, A., and Hollfelder, F. 2009. *Fluid phase endocytosis contributes to transfection of DNA by PEI-25*. *Molecular Therapy: the Journal of the American Society of Gene Therapy*. August. 17 (8): pp 1411-1418.

Hulette, B.A., Ryan, C.A., and Gerberick, G.F. 2002. *Elucidating changes in surface marker expression of dendritic cells following chemical allergen treatment*. *Toxicology and Applied Pharmacology*. August. 182 (3): pp 226-233.

Hsu, C.Y., and Uludag, H. 2008. *Effects of size and topology of DNA molecules on intracellular delivery with non-viral gene carriers*. *BMC. Biotechnology*. February. 29 (8): doi: 10.1186/1472-6750-8-23.

Ino, K., Kawasumi, T., Ito, A., and Honda, H. 2008. *Plasmid DNA transfection using magnetite cationic liposomes for construction of multilayered gene-engineered cell sheet*. *Biotechnology Bioengineering*. May. 100 (1): pp 168-176.
Ishikawa, H., Ma, Z., and Barber, G.N. 2009. *STING regulates intracellular DNA-mediated, type I interferon-dependent innate immunity*. *Nature*. October. 461 (7265): pp 788-792.

Ishimoto, H., Yanagihara, K., Araki, N., Mukae, H., Sakamoto, N., Izumikawa, K., Seki, M., Miyazaki, Y., Hirakata, Y., Mizuta, Y., Yasuda, K., and Kohno, S. 2008. *Single-cell observation of phagocytosis by human blood dendritic cells*. *Japanese Journal of Infectious Diseases*. July. 61 (4): pp 294-297.

Ito, A., Hayashida, M., Honda, H., Hata, K., Kagami, H., Ueda, M., and Kobayashi, T. 2004. *Construction and harvest of multilayered keratinocyte sheets using magnetite nanoparticles and magnetic force*. *Tissue Engineering*. May-June. 10 (5-6): pp 873–880.

Ito, A., Hibino, E., Shimizu, K., Kobayashi, T., Yamada, Y., Hibi, H., Ueda, M., and Honda, H. 2005. *Magnetic force-based mesenchymal stem cell expansion using antibody-conjugated magnetoliposomes*. *Journal of Biomedical Materials Research. Part B: Applied Biomaterials*. November. 75 (2): pp 320–327.

Jäkel, S., Albig, W., Kutay, U., Bischoff, F.R., Schwamborn, K., Doenecke, D., and Görlich, D. 1999. *The importin beta/importin 7 heterodimer is a functional nuclear import receptor for histone H1*. *European Molecular Biology Organization*. May. 18 (9): pp 2411-2423.

Jeong, Y., Jin, G.W., Choi, E., Jung, J.H., and Park, J.S. 2011. *Effect of deoxycholate conjugation on stability of pDNA/polyamidoamine-diethylentriamine (PAM-DET) polyplex against ionic strength*. *International journal of pharmaceutics*. November. 420 (2) pp 366-370.

Jilek, S., Zurkaulen, H., Pavlovic, J., Merkle, H.P., and Walter, E. 2004. *Transfection of a mouse dendritic cell line by plasmid DNA-loaded PLGA microparticles in vitro*. *European Journal of Pharmaceutics and Biopharmaceutics*. November. 58 (3): pp 491-499.

Jones, K.S. 2008. *Biomaterials as vaccine adjuvants*. *Biotechnology progress*. July-August. 24 (4): pp 807-814.

Kageyama-Yahara, N., Suehiro, Y., Yamamoto, T., and Kadowaki, M. 2011. *Rab5a regulates surface expression of FcεRI and functional activation in mast cells*. *Biological and pharmaceutical bulletin*. 34 (5): pp 760-763.

Kakimoto, S., Tanabe, T., Azuma, H., and Nagasaki, T. 2010. *Enhanced internalization and endosomal escape of dual-functionalized poly(ethyleneimine)s polyplex with diphtheria toxin T and R domains*. *Biomedicine and Pharmacotherapy*. April. 64 (4): pp 296-301.

Kanazawa, T., Takashima, Y., Murakoshi, M., Nakai, Y., and Okada, H. 2009. *Enhancement of gene transfection into human dendritic cells using cationic PLGA nanospheres with a synthesized nuclear localization signal*. *International journal of pharmaceutics*. September. 379 (1): pp 187-195).

Katsoulidis, E., Sassano, A., Majchrzak-Kita, B., Carayol, N., Yoon, P., Jordan, A., Druker, B.J., Fish, E.N., and Platanias LC. 2008. *Suppression of interferon (IFN)-inducible genes and IFN-mediated functional responses in BCR-ABL-expressing cells*. *The Journal of Biological Chemistry*. April. 283 (16): pp 10793-10803.

Keatch, S.A., Su, T.J., and Dryden, D.T. 2004. *Alleviation of restriction by DNA condensation and non-specific DNA binding ligands*. *Nucleic Acids Research*. November. 32 (19): pp 5841-5850.

Kendall, D., Lye, G.J., and Levy, M.S. 2002. *Purification of plasmid DNA by an integrated operation comprising tangential flow filtration and nitrocellulose adsorption*. *Biotechnology Bioengineering*. September. 79 (7): pp 816-822.

Khalil, I.A., Futaki, S., Niwa, M., Baba, Y., Kaji, N., Kamiya, H., and Harashima, H. 2004. *Mechanism of improved gene transfer by the N-terminal stearylation of octaarginine: enhanced cellular association by hydrophobic core formation*. *Gene Therapy*. April. 11 (7): pp 636-644**.**

Khalil, I.A., Kogure, K., Akita, H., and Harashima, H. 2006. *Uptake pathways and subsequent intracellular trafficking in nonviral gene delivery*. *Pharmacological Reviews*. March. 58 (1): pp 32-45.

Kim, H., Kim, H.A., Bae, Y.M., Choi, J.S., and Lee, M. 2009. *Dexamethasoneconjugated polyethylenimine as an efficient gene carrier with an anti-apoptotic effect to cardiomyocytes*. *The Journal of Gene Medicine*. June. 11 (6): pp 515–522.

Klein, R.M., Wolf, E.D., Wu, R., and Sanford, J.C. 1987. *High-velocity microprojectiles for delivering nucleic acids into living cells*. *Nature*. 327: pp 70-73.

Ko, Y.T., Bickel, U., and Huang, J. 2011. *Polyethylenimine/Oligonucleotide polyplexes investigated by fluorescence resonance energy transfer and fluorescence anisotropy*. *Oligonucleotide*s. April. 21 (2): pp 109-114.

Ko, Y.T., Kale, A., Hartner, W.C., Papahadjopoulos-Sternberg, B., and Torchilin, V.P. 2009. *Self-assembling micelle-like nanoparticles based on phospholipid-polyethyleneimine conjugates for systemic gene delivery*. *Journal of Controlled Release*. January. 133 (2): pp 132-138.

Kobiyama, K., Takeshita, F., Jounai, N., Sakaue-Sawano, A., Miyawaki, A., Ishii, K.J., Kawai, T., Sasaki, S., Hirano, H., Ishii, N., Okuda, K., and Suzuki, K. 2010.

Extrachromosomal Histone H2B Mediates Innate Antiviral Immune Responses Induced by Intracellular Double-Stranded DNA. *Journal of Virology*. January. 84 (2): pp 822-832.

Kogure, K., Moriguchi, R., Sasaki, K., Ueno, M., Futaki, S., and Harashima, H. 2004. *Development of a non-viral multifunctional envelope-type nano device by a novel lipid film hydration method*. *Journal of Controlled Release*. August. 98 (2): pp 317-322.

Kong, S., Titchener-Hooker, N., and Levy, S. 2006. *Plasmid DNA processing for gene therapy and vaccination: Studies on the membrane sterilisation filtration step*. *Journal of Membrane Science*. September. 280 (1-2): pp 834-831.

Kopatz, I., Remy, J.S., and Behr, J.P. 2004. *A model for non-viral gene delivery: through syndecan adhesion molecules and powered by actin*. *The Journal of Gene Medicine*. July. 6 (7): pp 769-767.

Koyama, H., Oba, M., Miura, Y., Koyama, H., Ishii, T., Takato, T., Kataoka K., and Miyata, T. 2010. *Impact of polyplex micelles installed with cyclic RGD peptide as ligand on gene delivery to vascular lesions*. *Nature Proceedings*. hdl:10101/npre.2010.5020.1

Kreiss, P., Cameron, B., Rangara, R., Mailhe, P., Aguerre-Charriol, O., Airiau, M., Scherman, D., Crouzet, J., and Pitard, B. 1999. *Plasmid DNA size does not affect the physicochemical properties of lipoplexes but modulates gene transfer efficiency*. *Nucleic Acids Research*. October. 27 (9): pp 3792-3798.

Krishnamoorthy, G., Duportail, G., and Mely, Y. 2002. *Structure and dynamics of condensed DNA probed by 1,1 '-(4,4,8,8-tetramethyl- 4,8-diazaundecamethylene)bis[4-[[3-methylbenz-1,3 -oxazol-2-yl]methylidine]-1,4-dihydroquinolinium] tetraiodide fluorescence*. *Biochemistry*. 41 (51): pp 15277–15287.

Kuiper, G.G., Lemmen, J.G., Carlsson, B., Corton, J.C., Safe, S.H., van der Saag, P.T., van der Burg, B., and Gustafsson, J.A. 1998. *Interaction of estrogenic chemicals and phytoestrogens with estrogen receptor beta*. *Endocrinology*. October. 139 (10): pp 4252-4263.

Kulkarni, R.P., Castelino, K., Majumdar, A., and Fraser, S.E. 2006. *Intracellular transport dynamics of endosomes containing DNA polyplexes along the microtubule network*. *Biophysical Journal*. March. 90 (5): pp 42- 44.

Kwon, Y.J., James, E., Shastri, N., and Fréchet, J.M. 2005. *In vivo targeting of dendritic cells for activation of cellular immunity using vaccine carriers based on pH-responsive microparticles*. *Proceedings of the National Academy of Sciences of the United States of America*. December. 102 (51): pp 18264-18268.

Labat-Moleur, F., Steffan, A.M., Brisson, C., Perron, H., Feugeas, O., Furstenberger, P., Oberling, F., Brambilla, E, and Behr, J.P. 1996. *An electron microscopy study into the mechanism of gene transfer with lipopolyamines*. *Gene Therapy*. November. 3 (11): pp1010-1017.

Lahijani, R., Hulley, G., Soriano, G., Horn, N.A., and Marquet, M. 1996. *High-yield production of pBR322-derived plasmids intended for human gene therapy by employing a*

temperature-controllable point mutation. *Human Gene Therapy*. October. 7 (16): pp 1971-1980.

Lam, A.P., and Dean, D.A. 2010. *Progress and prospects: nuclear import of nonviral vectors*. *Gene Therapy*. April. 17 (4): pp 439-447.

Landi, A., Babiuk, L.A., and van Drunen Littel-van den Hurk, S. 2007. *High transfection efficiency, gene expression, and viability of monocyte-derived human dendritic cells after nonviral gene transfer*. *Journal of Leukocyte Biology*. October. 82 (4): pp 849-860.

Langevin, C., Gousset, K., Costanzo, M., Richard-Le Goff, O., and Zurzolo, C. 2010. *Characterization of the role of dendritic cells in prion transfer to primary neurons*. *The Biochemical Journal*. September. 431 (2): pp 189-198.

Latulippe, D.R., and Zydney, A.L. 2011. *Separation of plasmid DNA isoforms by highly converging flow through small membrane pores*. *Journal of colloid and interface science*. May. 357 (2): pp 548-553.

Leahy, P., Carmichael, G.G., and Rossomando, E.F. 1996. *Novel biotinylated plasmid expression vectors retain biological function and can bind streptavidin*. *Bioconjugate Chemistry*. September-October. 7 (5): pp 545-551.

Lechardeur, D., Sohn, K.J., Haardt, M., Joshi, P.B., Monek, M., Grahm, R.W., Squire, J., O'Brodovich, H., and Lukacs, G.L. 1999. *Metabolic stability of plasmid DNA in the cytosol: a potential barrier to gene transfer*. *Gene Therapy*. April. 6 (4): pp 482-497.

Ledley, F.D. 1996. *Pharmaceutical approach to somatic gene therapy*. *Pharmaceutical Research*. November. 13 (11): pp 1595-1614.

Lehtinen, J., Hyvönen, Z., Subrizi, A., Bunjes, H., and Urtti, A. 2008. *Glycosaminoglycan-resistant and pH-sensitive lipid-coated DNA complexes produced by detergent removal method*. *The Journal of Controlled Release*. October. 131 (2): pp 145-149.

Lewis, P.J., and Babiuk, L.A. 1999. *DNA vaccines: a review*. *Advances in virus research*. 54: pp 129-188.

Lee, R.J., and Huang, L. 1996. *Folate-targeted, anionic liposome-entrapped polylysine-condensed DNA for tumor cell-specific gene transfer*. *Journal of Biological Chemistry*. April. 271 (14): pp 8481-8487.

Levy, M.S., O'Kennedy, R.D., Ayazi-Shamlou, P., and Dunnill, P. 2000. *Biochemical engineering approaches to the challenges of producing pure plasmid DNA*. *Trends in biotechnology*. July. 18 (7): pp 296-305.

Li, H.T., Su, Y.P., Cheng, T.M., Xu, J.M., Liao, J., Chen, J.C., Ji, C.Y., Ai, G.P., and Wang, J.P. 2010. *The interaction between interferon-induced protein with tetratricopeptide repeats-1 and eukaryotic elongation factor-1A*. *Molecular and Cellular Biochemistry*. April. 337 (1-2): pp 101-110.

Lindhal, T., and Karlstrom, O. 1993. Heat-Induced Depyrimidination of Deoxyribonucleic Acid in Neutral Solution. Biochemistry. December. 12 (25): pp 5151-5154.

Liu, C., Dalby, B., Chen, W., Kilzer, J.M., and Chiou H.C. 2008. *Transient transfection factors for high-level recombinant protein production in suspension cultured mammalian cells*. *Molecular Biotechnology*. June. 39 (2): pp 141-153.

Liu, G., Wang, Z., Lu, J., Xia, C., Gao, F., Gong, Q., Song, B., Zhao, X., Shuai, X., Chen, X., Ai, H., and Gu, Z. 2011. *Low molecular weight alkyl-polycation wrapped magnetite nanoparticle clusters as MRI probes for stem cell labeling and in vivo imaging*. *Biomaterials*. January. 32 (2): pp 528-537.

Liu, P., Rudick, M., and Anderson, R.G. 2002. *Multiple functions of caveolin-1*. *The Journal of Biological Chemistry*. November. 277 (44): pp 1295-1298.

Liu, Y., Fong, S., and Debs, R.J. 2003. *Cationic liposome-mediated gene delivery in vivo*. *Methods in Enzymology*. 373: pp 536-550.

Lollo, C.P., Banaszczyk, M.G., Mullen, P.M., Coffin, C.C., Wu, D., Carlo, A.T., Bassett, D.L., Gouveia, E.K., and Carlo, D.J. 2002. *Poly-L-lysine-based gene delivery systems. Synthesis, purification, and application*. *Methods in molecular medicine*. 69: pp 1-13.

Lowe, C.R., Lowe, A.R., and Gupta, G. 2001. *New developments in affinity chromatography with potential application in the production of biopharmaceuticals*. *Journal of Biochemical and Biophysical Methods*. October. 49 (1-3): pp 561-574.

Lucas, B., Van Rompaey, E., De Smedt, S.C., and Demeester, J. 2002. *Dual-Color Fluorescence Fluctuation Spectroscopy To Study the Complexation between Poly-l-lysine and Oligonucleotides*. *Macromolecules*. 35 (21): pp 8152-8160.

Lühmann, T., Rimann, M., Bittermann, A.G., and Hall, H. 2008. *Cellular uptake and intracellular pathways of PLL-g-PEG-DNA nanoparticles*. *Bioconjugate Chemistry*. September. 19 (9): pp 1907-1916.

Lundqvist, A., Noffz, G., Pavlenko, M., Saebøe-Larssen, S., Fong, T., Maitland, N., and Pisa, P. 2002. *Nonviral and viral gene transfer into different subsets of human dendritic cells yield comparable efficiency of transfection*. *Journal of Immunotherapy*. November-December. 25 (6): pp 445-454.

Luo, D., and Saltzman, W.M. 2000. *Synthetic DNA delivery systems*. *Nature Biotechnology*. January. 18 (1): pp 33-37.

Ma, Z., and Lim, L.Y. 2003. *Uptake of chitosan and associated insulin in Caco-2 cell monolayers: a comparison between chitosan molecules and chitosan nanoparticles*. *Pharmaceutical Research*. November. 20 (11): pp 1812-1819.

Mangenot, S., Keller, S., and Radler, J. 2003. *Transport of Nucleosome Core Particles in Semidilute DNA Solutions*. *Biophysical Journal*. September. 85: pp 1817-1825.

Mann,A., Richa, R., and Ganguli, M. 2008. *DNA condensation by poly-L-lysine at the single molecule level: role of DNA concentration and polymer length*. *Journal of Controlled Release*. February. 125 (3): pp 252-262.

Marieb, E. 2004. *Human Anatomy and Physiology, 6th Edition*.

Margalith, M., and Vilalta, A. 2006. *Sustained protective rabies neutralizing antibody titers after administration of cationic lipid-formulated pDNA vaccine*. *Genetic Vaccines and Therapy*. February. 4:2.

Manosroi, A., Khositsuntiwong, N., Gotz, F., Werner, R.G., and Manosroi, J. 2009. *Transdermal enhancement through rat skin of luciferase plasmid DNA loaded in elastic nanovesicles*. *Journal of Liposome Research*. February. 25: pp 91-98.

Miao, C.H., Thompson, A.R., Loeb, K., and Ye, X. 2001. *Long-term and therapeutic-level hepatic gene expression of human factor IX after naked plasmid transfer in vivo*. *Molecular Therapy*. *The Journal of the American Society of Gene Therapy*. June. 3 (6): pp 947-957.

Middaugh, C.R., Evans, R.K., Montgomery, D.L., and Casimiro, D.R. 1998. *Analysis of plasmid DNA from a pharmaceutical perspective*. *Journal of Pharmaceutical Sciences*. February. 87 (2): pp 130-146.

Miller, A.M., Munkonge, F.M., Alton, E.W., and Dean, D.A. 2009. *Identification of protein cofactors necessary for sequence-specific plasmid DNA nuclear import*. *Molecular Therapy: the Journal of the American Society of Gene Therapy*. November. 17 (11): pp 1897-1903.

Mislick, K.A, and Baldeschwieler, J.D. 1996. *Evidence for the role of proteoglycans in cation-mediated gene transfer*. *Proceedings of the National Academy of Sciences of the United States of America*. October. 93 (22): pp 12349-12354.

Moffatt, S., and Cristiano, R.J. 2006. *Uptake characteristics of NGR-coupled stealth PEI/pDNA nanoparticles loaded with PLGA-PEG-PLGA tri-block copolymer for targeted delivery to human monocyte-derived dendritic cells*. *International Journal of Pharmaceutics*. September. 321 (1-2): pp 143-154.

Monteiro, G.A., Ferreira, G.N., Cabral, J.M, and Prazeres, D.M. 1999. *Analysis and use of endogenous nuclease activities in Escherichia coli lysates during the primary isolation of plasmids for gene therapy*. *Biotechnology Bioengineering*. 66 (3): pp 189-194.

Mullen, P.M., Lollo, C. P., Phan, Q.-C., Amini, A., Banaszczyk, M.G., Fabrycki, J.M., Wu, D., Carlo, A.T., Pezzoli, P., Coffin, C.C., and Carlo, D.J. 2000. *Strength of conjugate binding to plasmid DNA affects degradation rate and expression level in vivo*. *Biochimica et Biophysica Acta*. September. 1523 (1): pp 103-110.

Murthy, N., Campbell, J., Fausto, N., Hoffman, A.S., and Stayton, P.S. 2003. *Design and synthesis of pH-responsive polymeric carriers that target uptake and enhance the intracellular delivery of oligonucleotides*. *The Journal of Controlled Release*. May. 89 (3): pp 365-374.

Nafisi, S., Saboury, A.A., Keramat, N., Neault, J-F., and Tajmir-Riahi, H-A. 2007. *Stability and structural features of DNA intercalation with ethidium bromide, acridine orange and methylene blue*. *Journal of Molecular Structure*. February. 827 (1-3): pp 35-43.

Nagabhushana, A., Chalasani, M.L., Jain, N., Radha, V., Rangaraj, N., Balasubramanian, D., and Swarup, G. 2010. *Regulation of endocytic trafficking of transferrin receptor by*

optineurin and its impairment by a glaucoma-associated mutant. *BMC Cell Biology*. January. 19:11:4.

Nagasaki, T., Kawazu, T., Tachibana, T., Tamagaki, S., and Shinkai, S. 2005. *Enhanced nuclear import and transfection efficiency of plasmid DNA using streptavidin-fused importin-beta*. *Journal of Controlled Release*. March. 103 (1): pp 199-207.

Nagasaki, T., Myohoji, T., Tachibana, T., Futaki, S., and Tamagaki, S. 2003. *Can nuclear localization signals enhance nuclear localization of plasmid DNA? Bioconjugate chemistry*, March-April. 14 (2): pp 282-286.

Nagatani, N., Shinkai, M., Honda, H., and Kobayashi, T. 1998. *Development of a new transformation method using magnetite cationic liposomes and magnetic selection of transformed cells*. *Biotechnology Techniques*. 12 (7): pp 525–528.

Nakamura, M., Iwahashi, M., Nakamori, M., Ueda, K., Matsuura, I., Noguchi, K., and Yamaue, H. 2002. *Dendritic cells genetically engineered to simultaneously express endogenous tumor antigen and granulocyte macrophage colony-stimulating factor elicit potent therapeutic antitumor immunity*. *Clinical cancer research: an official journal of the American Association for Cancer Research*. August. 8 (8): pp 2742-2749.
Neidle, S., 1994. *DNA Structure and Recognition*. IRL Press, Oxford, (47): pp. 34-35.

Neu, M., Fischer, D., and Kissel, T. 2005. *Recent advances in rational gene transfer vector design based on poly(ethylene imine) and its derivatives*. *The Journal of Gene Medicine*. August. 7 (8): pp 992-1009.

Neu, M., Sitterberg, J., Bakowsky, U., and Kissel, T. 2006. *Stabilized nanocarriers for plasmids based upon cross-linked poly(ethylene imine)*. *Biomacromolecules*. December. 7 (12) pp: 3428–3438.

Neugebauer, U., Schmid, U., Baumann, K., Simon, H., Schmitt, M., and Popp, J. 2007. *DNA tertiary structure and changes in DNA supercoiling upon interaction with ethidium bromide and gyrase monitored by UV resonance Raman spectroscopy*. *Journal of Raman Spectroscopy*. 38 (10): pp 1246-1258.

Niidome, T., Urakawa, M., Sato, H., Takahara, Y., Anai, T., Hatakayama, T., Wada, A.,Hirayama, T., and Aoyagi, H. 2000. *Gene transfer into hepatoma cells mediated by galactose-modified alpha-helical peptides*. *Biomaterials*. September. 21 (17): pp 1811-1819.

O'Kennedy, R.D., Ward, J.M., and Keshavarz-Moore, E. 2003. *Effects of fermentation strategy on the characteristics of plasmid DNA production*. *Biotechnology and Applied Biochemistry*. February. 37 (1): pp 83-90.

Ogris, M., Brunner, S., Schüller, S., Kircheis, R., and Wagner, E. 1999. *PEGylated DNA/transferrin-PEI complexes: reduced interaction with blood components, extended circulation in blood and potential for systemic gene delivery*. *Gene Therapy*. April. 6 (4): pp 595-605.

Oishi, M., Kataoka, K., and Nagasaki, Y. 2006 *pH-responsive three-layered PEGylated polyplex micelle based on a lactosylated ABC triblock copolymer as a targetable and*

endosome-disruptive nonviral gene vector. *Bioconjugate Chemistry*. May-June. 17 (3): pp 677–688.

Osada, K., Oshima, H., Kobayashi, D., Doi, M., Enoki, M., Yamasaki, Y., and Kataoka, K. 2010. *Quantized folding of plasmid DNA condensed with block catiomer into characteristic rod structures promoting transgene efficacy*. *Journal of the American Chemical Society*. September. 132 (35): pp 12343-12348.

Otten, G.R., Schaefer, M., Doe, B., Liu, H., Megede, J.Z., Donnelly, J., Rabussay, D., Barnett, S,, and Ulmer, J.B. 2006. *Potent immunogenicity of an HIV-1 gag-pol fusion DNA vaccine delivered by in vivo electroporation*. *Vaccine*. May. 24 (21): pp 4503-4509.

Park, I.K., Singha, K., Arote, R.B., Choi, Y.J., Kim, W.J., and Cho, C.S. 2010. *pH-Responsive Polymers as Gene Carriers*. *Macromolecular Rapid Communications*. July. 31 (13): pp 1122-1133.

Park, Y.M., Shin, B.A., and Oh, I.J. 2008. *Poly(L-lactic acid)/polyethylenimine nanoparticles as plasmid DNA carriers*. *Archives of Pharmacal Research*. January. 31 (1): pp 96-102.

Paschal, B.M. 2002. *Translocation through the nuclear pore complex*. *Trends in biochemical sciences*. December. 27 (12): pp 593-596.

Perrie, Y., Frederik, P.M., and Gregoriadis, G. 2001. *Liposome-mediated DNA vaccination: the effect of vesicle composition*. *Vaccine*. April. 19 (23-24): pp 3301–3310.

Perrie, Y., and Gregoriadis, G. 2000. *Liposome-entrapped plasmid DNA: characterisation studies*. *Biochimica et Biophysica Acta (BBA)*. July. 1475 (2): pp 125–132.

Perry, H.A., Alhaj Saleh, A.F., Aojula, H., and Pluen, A. 2008. *YOYO as a dye to track penetration of LK15 DNA complexes in spheroids: use and limits*. *Journal of Fluorescence*. January. 18 (1): pp 155-161.

Pichon, C., Billiet, L., and Midoux, P. 2010. *Chemical vectors for gene delivery: uptake and intracellular trafficking*. *Current Opinion in Biotechnology*. October. 21 (5): pp 640-645.

Ploeger, L.S., Dullens, H.F., Huisman, A., and van Diest, P.J. 2008. *Fluorescent stains for quantification of DNA by confocal laser scanning microscopy in 3-D*. *Biotechnic & histochemistry : official publication of the Biological Stain Commission*. April. 83 (2): pp 63-69.

Pollard, H., Remy, J.S., Loussouarn, G., Demolombe, S., Behr, J.P., and Escande, D. 1998. *Polyethylenimine but not cationic lipids promotes transgene delivery to the nucleus in mammalian cells*. *The journal of biological chemistry*. March. 273 (13): pp 7507-7511.

Pokorna, D., Rubio, I., and Müller, M. 2008. *DNA-vaccination via tattooing induces stronger humoral and cellular immune responses than intramuscular delivery supported by molecular adjuvants*. *Genetic vaccines and therapy*. February. 7. 6:4.

Postupalenko, V.Y., Shvadchak, V.V., Duportail, G., Pivovarenko, V.G., Klymchenko, A.S., and Mély, Y. 2011. *Monitoring membrane binding and insertion of peptides by two-color fluorescent label*. *Biochimica et biophysica acta*. January. 1808 (1): pp 424-432.

Pouton, C.W., Wagstaff, K.M., Roth, D.M., Moseley, G.W., and Jans, D.A. 2007. *Targeted delivery to the nucleus*. *Advanced drug delivery reviews*. August. 59 (8): pp 698-717.

Prather K.J., Sagar, S., Murphy, J., and Chartrain, M. 2003. *Industrial scale production of plasmid DNA for vaccine and gene therapy: plasmid design, production, and purification*. *Enzyme and Microbial Technology*. 33 (7): pp 865-883.

Prazeres, D.M., Schluep, T., and Cooney, C. 1998. *Preparative purification of supercoiled plasmid DNA using anion-exchange chromatography*. *Journal of Chromatography*. *A*. May. 806 (1): pp 31-45.

Prazma, C.M., and Tedder, T.F. 2008. *Dendritic cell CD83: a therapeutic target or innocent bystander?* *Immunology letters*. January. 115 (1): pp 1-8.

Przybylowski, M., Bartido, S., Borquez-Ojeda, O., Sadelain, M., and Rivière, I. 2007. *Production of clinical-grade plasmid DNA for human Phase I clinical trials and large animal clinical studies*. *Vaccine*. June. 25(27): pp 5013–5024.

Qi, R., Mullen, D.G., Baker, J.R., and Holl, M.M. 2010. *The Mechanism of Polyplex Internalization into Cells: Testing the GM1/Caveolin-1 Lipid Raft Mediated Endocytosis Pathway*. *Molecular Pharmaceutics*. February. 7 (1): pp 267-279.

Quaak, S.G., van den Berg, J.H., Oosterhuis, K., Beijnen, J.H., Haanen, J.B., and Nuijen, B. 2009. DNA tattoo vaccination: *Effect on plasmid purity and transfection efficiency of different topoisoforms*. *The Journal of Controlled Release*. October. 139 (2): pp 153-159.

Ray, K., Sabanayagam, C.R., Lakowicz, J.R., and Black, L.W. 2010. *DNA crunching by a viral packaging motor: Compression of a procapsid-portal stalled Y-DNA substrate*. Virology. March. 398 (2): pp 224-232.

Reddy, S.T., Swartz, M.A., and Hubbell, J.A. 2006. *Targeting dendritic cells with biomaterials: developing the next generation of vaccines*. *Trends in immunology*. December. 27 (12): pp 573-579.

Reisinger, H., Steinfellner, W., Katinger, H., and Kunert, R. 2009. *Serum-free transfection of CHO cells with chemically defined transfection systems and investigation of their potential for transient and stable transfection*. *Cytotechnology*. July. 60 (1-3): pp 115-123.

Rejman, J., Bragonzi, A., and Conese, M. 2005. *Role of clathrin- and caveolae-mediated endocytosis in gene transfer mediated by lipo- and polyplexes*. *Molecular Therapy: the Journal of the American Society of Gene Therapy*. September. 12 (3): pp 468-474.

Rejman, J., Oberle, V., Zuhorn, I.S., and Hoekstra, D. 2004. *Size-dependent internalization of particles via the pathways of clathrin- and caveolae-mediated endocytosis*. *The Biochemical journal*. January. 377 (Pt 1): pp 159-169.

Remaut, K., Sanders, N. N., Fayazpour, F., Demeester, J., and De Smedt, S.C. 2006. *Influence of plasmid DNA topology on the transfection properties of DOTAP/DOPE lipoplexes*. *Journal of Controlled Release*. October. 115 (3): pp 335-343.

Rice, J., Ottensmeier, C.H., and Stevenson, F.K. 2008. *DNA vaccines: precision tools for activating effective immunity against cancer*. *Nature Reviews*. *Cancer*. February. 8 (2): pp 108-120.

Russell, J.A., Roy, M.K., and Sanford, J.C. 1992. *Physical Trauma and Tungsten Toxicity Reduce the Efficiency of Biolistic Transformation*. *Plant Physiology*. March. 98 (3): pp 1050-1056.

Ryan, C.A., Gildea, L.A., Hulette, B.C., Dearman, R.J., Kimber, I., and Gerberick, G.F. 2004. *Gene expression changes in peripheral blood-derived dendritic cells following exposure to a contact allergen*. *Toxicology* Letters. May. 150 (3): pp 301-316.

Rye, H.S., Yue, S., Wemmer, D.E., Quesada, M.A., Haugland, R.P., Mathies, R.A., and Glazer, A.N. 1992. *Stable fluorescent complexes of double-stranded DNA with bis-intercalating asymmetric cyanine dyes: properties and applications*. *Nucleic Acids Research*. June. 20 (11): pp 2803-2812.

Sadhu, C., Ting, H.J., Lipsky, B., Hensley, K., Garcia-Martinez, L.F., Simon, S.I., and Staunton, D.E. 2007. *CD11c/CD18: novel ligands and a role in delayed-type hypersensitivity*. *Journal of leukocyte biology*. June. 81 (6): pp 1395-1403.

Sagar S, Watson M, Lee A. 2003. *Chromatography-based purification of plasmid DNA*. In: Rathore AS, Vella G, editors. *Scale-up and optimization in preprative chromatography: principles and biopharmaceutical applications*. New York: Marcel Dekker; pp 251–272.

Sahay, G., Alakhova, D.Y., and Kabanov, A.V. 2010. *Endocytosis of nanomedicines*. *Journal of Controlled Release*. August. 145 (3): pp182-195.

Sakurada, K., Toida, I., Sakai, I., Sekiguchi, K., Shiraishi, T., and Takatori, T. 2003. *The BCG scar after percutaneous multiple puncture vaccination may help establish the nationalities of unidentified cadavers*. *Journal of Clinical Forensic Medicine*. December. 10 (4): pp 235-241.

Sanford, J.C., Smith, F.D., and Russell, J.A. 1993. *Optimizing the biolistic process for different biological applications*. *Methods in Enzymology*. 217: pp 483-509.

Scherer, F., Anton, M., Schillinger, U., Henke, J., Bergemann, C., Kruger, A., Gansbacher, B., and Plank C. 2002. *Magnetofection: Enhancing and targeting gene delivery by magnetic force in vitro and in vivo*. *Gene Therapy*. January. 9 (2): pp 102–109.

Schlaeger, E.J., and Christensen, K., 1999. *Transient gene expression in mammalian cells grown in serum-free suspension culture*. *Cytotechnology*. July. 30 (1-3): pp 71-83.

Schnitzer, J.E., Oh, P., Pinney, E., and Allard, J. 1994. *Filipin-sensitive caveolae-mediated transport in endothelium: reduced transcytosis, scavenger endocytosis, and capillary permeability of select macromolecules*. *The Journal of Cell Biology*. December. 127 (5): pp 1217-1232.

Shamlou, P.A. 2003. *Scaleable processes for the manufacture of therapeutic quantities of plasmid DNA*. *Biotechnology and Applied Biochemistry*. June. (3): pp 207-218.

Shao, W., Yeretssian, G., Doiron, K., Hussain, S.N., and Saleh, M. 2007. *The caspase-1 digestome identifies the glycolysis pathway as a target during infection and septic shock*. *The Journal of Biological Chemistry*. December. 282 (50): pp 36321-36329.

Shea, L.D., Smiley, E., Bonadio, J., Mooney, D.J. 1999. *DNA delivery from polymer matrices for tissue engineering*. *Nature Biotechnology*. June. 17 (6): pp 551-554.

Shen, H., Hu, Y., and Saltzman, W.M. 2006. *DNA Diffusion in Mucus: Effect of Size, Topology of DNAs, and Transfection Reagents*. *Biophysical Journal*. July. 91: pp 639-644.

Shim, M.S., Wang, X., Ragan, R., and Kwon, Y.J. 2011. *Dynamics of nucleic acid/cationic polymer complexation and disassembly under biologically simulated conditions using in situ atomic force microscopy*. *Microscopy research and technique*. September. 73 (9): pp 845-856.

Shimizu, K., Ito, A., Lee, J.K., Yoshida, T., Miwa, K., Ishiguro, H., Numaguchi, Y., Murohara, T., Kodama, I., and Honda H. 2007. *Construction of multilayered cardiomyocyte sheets using magnetite nanoparticles and magnetic force*. *Biotechnology Bioengineering*. 96 (4): pp 803–809.

Shinkai, M., Yanase, M., Honda, H., Wakabayashi, T., Yoshida, J., and Kobayashi T. 1996. *Intracellular hyperthermia for cancer using magnetite cationic liposomes: In vitro study*. Japanese Journal of Cancer Research. November. 87 (11): pp 1179–1183.

Skretting, G., Torgersen, M.L., van Deurs, B., and Sandvig K. 1999. *Endocytic mechanisms responsible for uptake of GPI-linked diphtheria toxin receptor*. *Journal of Cell Science*. November. 112 (Pt 22): pp 3899-3909.

Slattum, P.S., Loomis, A.G., Machnik, K.J., Watt, M.A., Duzeski, J.L., Budker, V.G., Wolff, J.A., and Hagstrom, J.E. 2003. *Efficient in vitro and in vivo expression of covalently modified plasmid DNA*. *Molecular Therapy: the Journal of the American Society of Gene Therapy*. August. 8 (2): pp 255-263.

Sousa, F., Prazeres, D.M., and Queiroz, J.A. 2008. *Affinity chromatography approaches to overcome the challenges of purifying plasmid DNA*. *Trends in Biotechnology*. September. 26 (9): pp 518-525.

Srinivasan, C., Lee, J., Papadimitrakopoulos, F., Silbart, L.K., Zhao, M., and Burgess, D.J. 2006. *Labeling and intracellular tracking of functionally active plasmid DNA with semiconductor quantum dots*. *Molecular Therapy: the Journal of the American Society of Gene Therapy*. August. 14 (2): pp 192-201.

Srinivasan, C., Siddiqui, S., Silbart, L.K., Papadimitrakopoulos, F., and Burgess, D.J. 2009. *Dual Fluorescent Labeling Method to Visualize Plasmid DNA Degradation*. *Bioconjugate Chemistry*. January. 20 (1): pp 163-169.

Stadler, J., Lemmens, R., and Nyhammar, T. 2004. *Plasmid DNA purification*. *The Journal of Gene Medicine*. February. 6 (1): S54-66.

Stechschulte, S.U., Joussen, A.M., von Recum, H.A., Poulaki, V., Moromizato, Y., Yuan, J., D'Amato, R.J., Kuo, C., and Adamis, A.P. 2001. *Rapid ocular angiogenic control via naked DNA delivery to cornea*. *Investigative Ophthalmology and Visual Science*. August. 42 (9): pp 1975-1979.

Stevenson, F.K., Ottensmeier, C.H., and Rice, J. 2010. *DNA vaccines against cancer come of age*. *Current Opinion in Immunology*. April. 22 (2): pp 264-270.

Sun, L., Wang, J., and Wang, Z. 2010. *Recognition and transmembrane delivery of bioconjugated Fe2O3@Au nanoparticles with living cells*. *Nanoscale*. February. 2 (2): pp 269-276.

Suvas, S., Singh, V., Sahdev, S., Vohra, H., and Agrewala, J.N. 2002. *Distinct role of CD80 and CD86 in the regulation of the activation of B cell and B cell lymphoma*. *The journal of biological chemistry*. March. 277 (10): pp 7766-7775.

Suzuki, R., Yamada, Y., and Harashima, H. 2008. *Development of small, homogeneous pDNA particles condensed with mono-cationic detergents and encapsulated in a multifunctional envelope-type nano device*. *Biological and Pharmaceutical Bulletin*. June. 31 (6): pp 1237-1243.

Suzuki, T., Fujikura, K., Higashiyama, T., and Takata, K. 1997. *DNA staining for fluorescence and laser confocal microscopy*. *The journal of histochemistry and cytochemistry: official journal of the Histochemistry Society*. January. 45 (1): pp 49-53.

Takaoka, A., Wang, Z., Choi, M.K., Yanai, H., Negishi, H., Ban, T., Lu, Y., Miyagishi, M., Kodama, T., Honda, K., Ohba, Y., and Taniguchi, T. 2007. *DAI (DLM-1/ZBP1) is a cytosolic DNA sensor and an activator of innate immune response*. *Nature*. July. 448 (7152): pp 501-505.

Takei, K., and Haucke, V. 2001. *Clathrin-mediated endocytosis: membrane factors pull the trigger*. *Trends in Cell Biology*. September. 11 (9): pp 385-391.

Takeuchi, Y., Dotson, M., and Keen, N.T. 1992. *Plant transformation: a simple particle bombardment device based on flowing helium*. *Plant Molecular Biology*. February. 18 (4): pp 835-839.

Talsma, S.S., Babensee, J.E., Murthy, N., and Williams, I.R. 2006. *Development and in vitro validation of a targeted delivery vehicle for DNA vaccines*. *The Journal of Controlled Release*. May. 112 (2): pp 271-279.

Tang, D.C., DeVit, M., and Johnston, S.A. 1992. *Genetic immunization is a simple method for eliciting an immune response*. *Nature*. March. 356 (6365): pp 152-154.

Tang, R., Palumbo, R.N., Nagarajan, L., Krogstad, E., and Wang C. 2010. *Well-defined block copolymers for gene delivery to dendritic cells: probing the effect of polycation chain-length*. *Journal of Controlled Release*. March. 142 (2): pp 229-237.

Tanghe, A., Denis, O., Lambrecht, B., Motte, V., van den Berg, T., and Huygen, K. 2000. *Tuberculosis DNA vaccine encoding Ag85A is immunogenic and protective when administered by intramuscular needle injection but not by epidermal gene gun bombardment*. *Infection and Immunity*. July. 68 (7): pp 3854-3860.

Terazono, H., Anzai, Y., Soloviev, M., and Yasuda, K. 2010. *Labelling of live cells using fluorescent aptamers: binding reversal with DNA nucleases*. *Journal of Nanobiotechnology*. April. 8: pp 8.

Theodossiou, I., Collins, J., Ward, J.M., Thomas, O.R.T., and Dunnill, P. 1997. *The processing of a plasmid-based gene from E. Coli. Primary recovery by filtration*. *Bioprocess and Biosystems Engineering*. 16 (13): pp 175-183.

Theodossiou, I., Thomas, O.R.T., and Dunnill, P. 1999. *Methods of enhancing the recovery of plasmid genes from neutralised cell lysate*. *Bioprocess and Biosystems Engineering*. 20(2): pp 147–151.

Thibault, M., Nimesh, S., Lavertu, M., and Buschmann, M.D. 2010. *Intracellular trafficking and decondensation kinetics of chitosan-pDNA polyplexes*. *Molecular Therapy: the Journal of the American Society of Gene Therapy*. October. 18 (1): pp 1787-1795.

Thiele, L., Rothen-Rutishauser, B., Jilek, S., Wunderli-Allenspach, H., Merkle, H.P., and Walter, E. 2001. *Evaluation of particle uptake in human blood monocyte-derived cells in vitro. Does phagocytosis activity of dendritic cells measure up with macrophages? Journal of Controlled Release*. September. 76 (1-2): pp 59-71.

Tiera, M.J., Shi, Q., Winnik, F.M., and Fernandes, J.C. 2011. *Polycation-Based Gene Therapy: Current Knowledge and New Perspectives*. *Current Gene Therapy*. April. 1. [Epub ahead of print].

Tisch, R., Wang, B., Weaver, D.J., Liu, B., Bui, T., Arthos, J., and Serreze, D.V. 2001. *Antigen-specific mediated suppression of beta cell autoimmunity by plasmid DNA vaccination*. *Journal of Immunology*. February. 166 (3): pp 2122-2132.

Tomlinson, R., Heller, J., Brocchini, S., and Duncan, R. 2003. *Polyacetal-doxorubicin conjugates designed for pH-dependent degradation*. *Bioconjugate chemistry*. November-December. 14 (6): pp 1096-1106.

Tone, M., Tone, Y., Fairchild, P.J., Wykes, M., and Waldmann, H. 2001. *Regulation of CD40 function by its isoforms generated through alternative splicing*. *Proceedings of the National Academy of Sciences of the United States of America*. February. 98 (4): pp1751-1756.

Touitou, E., Dayan, N,, Bergelson, L., Godin, B., and Eliaz, M. 2000. *Ethosomes - novel vesicular carriers for enhanced delivery: characterization and skin penetration properties*. *The Journal of Controlled Release*. April. 65 (3): pp 403-418.

Trickett, A., and Kwan, Y.L. 2003. *T cell stimulation and expansion using anti-CD3/CD28 beads*. *Journal of Immunological Methods*. April. 275 (1-2): pp 251-255.

Tripathi, P.K., Khopade, A.J., Dutta, T., Umamaheshewari, R.B., Jain, S., Saraf, D.K., 2003. *Dendrimer polycations for delivery of genes*. *Indian Journal of Pharmeacutical Sciences*. 65 (1): pp 15-21.

Tros de Ilarduya, C., Sun, Y., and Düzgünes, N. 2010. *Gene delivery by lipoplexes and polyplexes*. *European Journal of Pharmaceutical Sciences: Official Journal of the European Federation for Pharmaceutical Sciences*. June. 40 (3): pp 159-170.

Tsai J.T., Keshavarz-Moore, E., Ward, J.M., Hoare, M., Shamlou, P.A., and Dunnill, P. 1999. *Characterisation of plasmid DNA conjugates as a basis for their processing*. *Bioprocess and Biosystems Engineering*. September. 21 (3): pp 279-286.

Uematsu, S., Sato, S., Yamamoto, M., Hirotani, T., Kato, H., Takeshita, F., Matsuda, M., Coban, C., Ishii, K.J., Kawai, T., Takeuchi, O., and Akira, S. 2005. *Interleukin-1 receptor-associated kinase-1 plays an essential role for Toll-like receptor (TLR)7- and TLR9-mediated interferon-{alpha} induction*. *The Journal of Experimental Medicine*. March. 201 (6): pp 915-923.

Ueno, H., Klechevsky, E., Schmitt, N., Ni, L., Flamar, A.L., Zurawski, S., Zurawski, G., Palucka, K., Banchereau, J., and Oh, S. 2011. *Targeting human dendritic cell subsets for improved vaccines*. *Seminars in Immunology*. February. 23 (1): pp 21-27.

Ulasov, A.V., Khramtsov, Y.V., Trusov, G.A., Rosenkranz, A.A., Sverdlov, E.D., and Sobolev, A,S. 2011. *Properties of PEI-based polyplex nanoparticles that correlate with their transfection efficacy*. *Molecular Therapy: the Journal of the American Society of Gene Therapy*. January. 19 (1): pp 103-112.

Ulmer, J.B., Wahren, B., and Liu, M.A. 2006. *DNA vaccines: recent technological and clinical advances*. *Discovery Medicine*. June. 6 (33): pp 109-112.

Un, K., Kawakami, S., Suzuki, R., Maruyama, K., Yamashita, F., and Hashida, M. 2010. *Enhanced transfection efficiency into macrophages and dendritic cells by a combination method using mannosylated lipoplexes and bubble liposomes with ultrasound exposure*. *Human Gene Therapy*. January. 21 (1): pp 65-74.

U.S. Department of Health and Human Services Food and Drug Administration Center for Biologics Evaluation and Research. *Guidance for Industry. Considerations for plasmid DNA vaccines for infectious disease indications*. November 2007.

U.S. Department of Health and Human Services Food and Drug Administration Center for Biologics Evaluation and Research. *Guidance for Industry, Potency tests for cellular and gene therapy products*. January 2011.

Valladeau, J., and Saeland, S. 2005. *Cutaneous dendritic cells*. *Seminars in Immunology*. August. 17 (4): pp 273-283.

van Driel, A.F., Allan, G., Delerue, C., Lodahl, P., Vos, W.L., and Vanmaekelbergh, D. 2005. *Frequency-dependent spontaneous emission rate from CdSe and CdTe nanocrystals: influence of dark states*. *Physical Review Letters. December*. 95 (23): pp 236804.

van Reis, R., and Zydney, A., 2007. *Bioprocess membrane technology*. *Journal of Membrane Science*. July. 297 (1-2): pp 16-50.

van Rossenberg, S.M., van Keulen, A.C., Drijfhout, J.W., Vasto, S., Koerten, H.K., Spies, F., van 't Noordende, J.M., van Berkel, T.J., and Biessen, E.A. 2004. *Stable polyplexes based on arginine-containing oligopeptides for in vivo gene delivery*. *Gene Therapy*. March. 11 (5): pp 457-464.

Van Tendeloo, V.F., Snoeck, H.W., Lardon, F., Vanham, G.L., Nijs, G., Lenjou, M., Hendriks, L., Van Broeckhoven, C., Moulijn, A., Rodrigus, I., Verdonk, P., Van Bockstaele, D.R., and Berneman, Z.N. 1998. *Nonviral transfection of distinct types of human dendritic cells: high-efficiency gene transfer by electroporation into hematopoietic progenitor- but not monocyte-derived dendritic cells*. *Gene Therapy*. May. 5 (5): pp 700-707.

Varley, D.L., Hitchcock, A.G., Weiss, A.M., Horler, W.A., Cowell, R., Peddie, L., Sharpe, G.S., Thatcher, D.R., and Hanak, J.A. 1999. *Production of plasmid DNA for human gene therapy using modified alkaline cell lysis and expanded bed anion exchange chromatography*. *Bioseparation*. 8 (1-5): pp 209-217.

Velinova M, Read N, Kirby C, Gregoriadis G. 1996. *Morphological observations on the fate of liposomes in the regional lymph nodes after footpad injection into rats*. *Biochimica et Biophysica Acta*. January. 1299 (2): pp 207–15.

Vercauteren, D., Vandenbroucke, R.E., Jones, A.T., Rejman, J., Demeester, J., De Smedt, S.C., Sanders, N.N., and Braeckmans, K. 2010. *The use of inhibitors to study endocytic pathways of gene carriers: optimization and pitfalls*. *Molecular Therapy: the Journal of the American Society of Gene Therapy*. March. 18 (3): pp 561-569.

Vilaysane, A., and Muruve, D.A. 2009. *The innate immune response to DNA*. *Seminars in Immunology*. August. 21 (4): pp 208-214.

von Erlach, T., Zwicker, S., Pidhatika, B., Konradi, R., Textor, M., Hall, H., and Lühmann, T. 2011. *Formation and characterization of DNA-polymer-condensates based on poly(2-methyl-2-oxazoline) grafted poly(l-lysine) for non-viral delivery of therapeutic DNA*. *Biomaterials*. August. 32 (22): pp 5291-5303.

von Groll, A., Levin, Y., Barbosa, M.C., and Ravazzolo, A.P. 2006. *Linear DNA low efficiency transfection by liposome can be improved by the use of cationic lipid as charge neutralizer*. *Biotechnology Progress*. July-August. 22 (4): pp 1220-1224.

Wadhwa, M.S., Collard, W.T., Adami, R.C., McKenzie, D.L., and Rice, K.G. 1997. *Peptide-mediated gene delivery: influence of peptide structure on gene expression*. *Bioconjugate Chemistry*. January-February. 8 (1): pp 81-88.

Wakebayashi, D., Nishiyama, N., Itaka, K., Miyata, K., Yamasaki, Y., Harada, A., Koyama, H., Nagasaki, Y., and Kataoka, K. 2004. *Polyion complex micelles of pDNA with acetal-poly(ethylene glycol)-poly(2-(dimethylamino)ethyl methacrylate) block copolymer as the gene carrier system: physicochemical properties of micelles relevant to gene transfection efficacy*. *Biomacromolecules*. November-December. 5 (6): pp 2128-2136.

Walker, G.F., Fella, C., Pelisek, J., Fahrmeir, J., Boeckle, S., Ogris, M., and Wagner, E. 2005. *Toward synthetic viruses: endosomal pH-triggered deshielding of targeted polyplexes greatly enhances gene transfer in vitro and in vivo*. *Molecular therapy: The Journal of the American Society of Gene Therapy*. March. 11 (3): pp 418-425.

Wang, D., Garcia-Bassets, I., Benner, C., Li, W., Su, X., Zhou, Y., Qiu, J., Liu, W., Kaikkonen, M.U., Ohgi, K.A., Glass, C.K., Rosenfeld, M.G, and Fu, X.D. 2011. *Reprogramming transcription by distinct classes of enhancers functionally defined by eRNA*. *Nature*. May. [Epub ahead of print].

Ward, C.M., Read, M.L., and Seymour, L.W. 2001. *Systemic circulation of poly(L-lysine)/DNA vectors is influenced by polycation molecular weight and type of DNA: differential circulation in mice and rats and the implications for human gene therapy*. *Blood*. April. 97 (8): pp 2221-2229.

Weaver, D.J. Jr., Liu, B., and Tisch, R. 2001. *Plasmid DNAs encoding insulin and glutamic acid decarboxylase 65 have distinct effects on the progression of autoimmune diabetes in nonobese diabetic mice*. *Journal of Immunology*. July. 167 (1): pp 586-592.

Williams, R.S., Johnston, S.A., Riedy, M., DeVit, M.J., McElligott, S.G., Sanford, J.C. 1991. *Introduction of foreign genes into tissues of living mice by DNA-coated microprojectiles*. *Proceedings of the National Academy of Sciences of the United States of America*. April. 88 (7): pp 2726-2730.

Wojda, U., Goldsmith, P., and Miller, J.L. 1999. *Surface membrane biotinylation efficiently mediates the endocytosis of avidin bioconjugates into nucleated cells*. *Bioconjugate Chemistry*. Novemeber-December. 10 (6): pp 1044-1050.

Wong, M., Kong, S., Dragowska, W.H., and Bally, M.B. 2001. *Oxazole yellow homodimer YOYO-1-labeled DNA: a fluorescent complex that can be used to assess structural changes in DNA following formation and cellular delivery of cationic lipid DNA complexes*. *Biochimica et biophysica acta*. July. 1527 (1-2): pp 61-72.

Wurm, F.M. 2004. *Production of recombinant protein therapeutics in cultivated mammalian cells*. *Nature Biotechnology*. November. 22 (11): pp 1393-1398.
Xiang, Y.I.N., Zhang, Y., Pan, Y., and Chen, J. 2007. *Application of quantum dot labelling in gene transfection with chitosan nanoparticles*. *Nanoscience*. May. 12 (1): pp15-19.

Xie, T-D., and Tsong, .T.Y. 1993. *Study of Mechanisms of Electric Field-induced DNA Transfection.V. Effects of DNA Topology on Surface Binding, Cell Uptake, Expression, and Integration into Host Chromosomes of DNA in the Mammalian Cell*. *Biophysical Journal*. October. 65: pp 1684-1689.

Yamakawa, H., Higashino, K., and Ohara, O. 1996. *Sequence-dependent DNA separation by anion-exchange high-performance liquid chromatography*. *Analytical Biochemistry*. September. 240 (2): pp242-250.

Yanai, H., Ban, T., Wang, Z., Choi, M.K., Kawamura, T., Negishi, H., Nakasato, M., Lu, Y., Hangai, S., Koshiba, R., Savitsky, D., Ronfani, L., Akira, S., Bianchi, M.E., Honda, K., Tamura, T., Kodama, T., and Taniguchi T. 2009. *HMGB proteins function as universal sentinels for nucleic-acid-mediated innate immune responses*. *Nature*. November. 462 (7269): pp 99-103.

Yao, L., Yao, S., Daly, B., Hendry, W., Windebank, A., and Pandit, A. 2012. *Non-viral gene therapy for spinal cord regeneration*. *Drug Discovery Today*. May 24. [Epub ahead of print].

Yau, S.Y., Keshavarz-Moore, E., and Ward, J. 2008. *Host strain influences on supercoiled plasmid DNA production in Escherichia coli: Implications for efficient design of large-scale processes*. *Biotechnology Bioengineering*. October. 101 (3): pp 529-544.

Zaitseva, L., Cherepanov, P., Leyens, L., Wilson, S.J., Rasaiyaah, J., and Fassati, A. 2009. *HIV-1 exploits importin 7 to maximize nuclear import of its DNA genome*. *Retrovirology*. February. 4:6:11.

Zanta, M.A., Belguise-Valladier, P., and Behr, J.P. 1999. *Gene delivery: a single nuclear localization signal peptide is sufficient to carry DNA to the cell nucleus*. *Proceedings of the National Academy of Sciences of the United States of America*. January. 96 (1): pp 91-96.

Zelphati, O., and Szoka, Jr F.C. 1996. *Cationic liposomes as an oligonucleotide carrier:mechanism of action*. *Journal of Liposome Research*. February. 7 (1): pp 31–49.

Zeng, F., and Zimmerman, S.C. 1997. Dendrimers in Supramolecular Chemistry: From Molecular Recognition to Self-Assembly. *Chemical Reviews*. August. 97 (5): pp 1681-1712.

Zerial, M., and McBride H. 2001. *Rab proteins as membrane organizers*. *Nature Reviews*. *Molecular Cell Biology*. February. 2 (2): pp 107-117.

Zhang, H., Mitin, A., and Vinogradov, S.V. 2009. *Efficient transfection of blood-brain barrier endothelial cells by lipoplexes and polyplexes in the presence of nuclear targeting NLS-PEG-acridine conjugates*. *Bioconjugate Chemistry*, January. 20 (1): pp 120-128.

Zhang, K., Fang, H., Chen, Z., Taylor, J.S., and Wooley, K.L. 2008. *Shape effects of nanoparticles conjugated with cell-penetrating peptides (HIV Tat PTD) on CHO cell uptake*. *Bioconjugate Chemistry*. September. 19 (9): pp 1880-1887.

Zhang, P., and Liu, W. 2010. *ZnO QD@PMAA-co-PDMAEMA nonviral vector for plasmid DNA delivery and bioimaging*. *Biomaterials*. April. 31 (11): pp 3087-3094.

Zhang. Y., Wang, Z., Ng, M.K., and Rothberg, L.J. 2007. *Conformational reorganization and solvation dynamics of dendritic oligothiophenes*. *The Journal of Physical Chemistry*. *B*. November. 111 (46): pp 13211-13216.

Zheng, Y., Manzotti, C.N., Liu, M., Burke, F., Mead, K.I., and Sansom, D.M. 2004. *CD86 and CD80 Differentially Modulate the Suppressive Function of Human Regulatory T Cells*. *Journal of immunology*. March. 172 (5): pp 2778-2784.

Zuhorn, I.S., Kalicharan, R., and Hoekstra, D. 2002. *Lipoplex-mediated transfection of mammalian cells occurs through the cholesterol-dependent clathrin-mediated pathway of endocytosis*. *The Journal of Biological Chemistry*. May. 277 (20): pp 18021-18028.

Online Reports:

The Journal of Gene Medicine Clinical Trial site (2011).
<www.wiley.com/legacy/wileychi/genmed/clinical/>